MOUNTAIN-PLAINS CONSORTIUM

MPC 17-339 | N. Wehbe, X Qin, B Tigges, Z Shen and A. Boudaqa

Evaluation and Mitigation of Vehicle Impact Hazards for Overpasses

A University Transportation Center sponsored by the U.S. Department of Transportation serving the Mountain-Plains Region. Consortium members:

Colorado State University
North Dakota State University
South Dakota State University
University of Colorado Denver
University of Denver
University of Utah
Utah State University
University of Wyoming

Evaluation and Mitigation of Vehicle Impact Hazards for Overpasses

Nadim I. Wehbe, Ph.D., PE
Professor and Department Head
Department of Civil and Environmental Engineering
South Dakota State University
Brookings, South Dakota

Xiao Qin, Ph.D., PE
Associate Professor
Department of Civil and Environmental Engineering
University of Wisconsin – Milwaukee
Milwaukee, Wisconsin

Brett Tigges
Structural Engineer
Raker Rhodes Engineering, LLC
Des Moines, Iowa

Zhao Shen
Civil Associate
Michael Baker Associates
Dallas, Texas

Abdullah Boudaqa
Graduate Research Assistant
Department of Civil and Environmental Engineering
South Dakota State University
Brookings, South Dakota

December 2017

Acknowledgments

The authors would like to acknowledge the financial support of the Mountain-Plains Consortium (MPC) and the South Dakota Department of Transportation for funding this study through project MPC-397. The authors also would like to than Dr. Ahmad Ghadban, post-doctoral scholar at South Dakota State University, for his assistance in compiling this report.

ABSTRACT

Crashes of heavy trucks with bridge columns are random events with low probability of occurrence. In spite of the low odds, previous collision events have resulted in catastrophic partial or full collapse of bridges. AASHTO-LRFD Bridge Design Specifications requires bridge columns to be designed for collision loads to prevent bridge collapse under such extreme events. The majority of overpass bridges on the Interstate system and other major highways in South Dakota were designed and constructed prior to the development of the collision load design requirements. This study was performed to develop a risk and mitigation plan for South Dakota bridges under vehicular collision forces.

A risk assessment for truck collisions with bridge columns was performed, and the vulnerability of bridge columns to catastrophic failure under lateral collision forces was evaluated to develop a risk analysis and mitigation strategy for critical bridges on the state's Interstate system and other critical highways. The risk assessment study resulted in the development of a prioritization list for retrofit of bridge bents to mitigate collapse under vehicular collision forces.

An experimental study was conducted on two one-third-scale bent specimens to assess the effectiveness of a retrofit measure for vulnerable bridge bents. The retrofit consisted of a crash strut that spans between the bent columns and acts as a shear wall. Experimental results showed that the retrofitted specimen was capable of resisting 150 percent of the AASHTO vehicular collision force without experiencing any significant distress. A finite element dynamic analysis showed that the AASHTO-specified 600-kip vehicle collision force is reasonable.

TABLE OF CONTENTS

1. INTRODUCTION 1

1.1 Project Description 1

1.2 Objectives 2

2. COLLISION RISK ANALYSIS 3

2.1 Literature Review 3

2.1.1 Crash Risk Analysis 3

2.1.2 Crash Count Models 4

2.1.3 Roadside Design 4

2.1.4 Road User Costs 6

2.1.5 Multi-Criteria Decision Analysis 6

2.2 Study Design 6

2.2.1 Method for Ranking Bridges for Collision Risk 7

2.2.1.1 Quantifying Crash Risk 7
2.2.1.2 Measuring Impact Area 7
2.2.1.3 Determining Collision Risk 7
2.2.1.4 Evaluating Bridge Economic Significance 8
2.2.1.5 Ranking Bridges for Collision Risk 8

2.3 Data Collection and Processing 8

2.3.1 Bridge Survey 9

2.3.2 Data Sources 10

2.3.2.1 Bridge Dimension and Configuration 10
2.3.2.2 Roadway Characteristics 11
2.3.2.3 Traffic Volume 11
2.3.2.4 Weather Conditions 11
2.3.2.5 Crash Data 12

2.3.3 Data Processing 12

2.3.4 Summary 13

2.4 Methodology 14

2.4.1 Truck Run-Off-the-Road Crash Prediction Model 15

2.4.2 Bridge Hazard Envelope Estimation 15

2.4.3 Road User Costs Evaluation 16

2.4.4 Ranking Strategies 17

2.4.4.1 Weighted Sum Model 17

2.5 Analysis of Results 17

2.5.1 Truck ROR Crash Prediction Model Results 18

2.5.2 Ranking Results 18
2.6 Summary 22
3. EVALUATION AND COLLAPSE MITIGATION OF VULNERABLE OVERPASSES 23
3.1 Introduction 23
3.2 Literature Review 24
3.2.1 Recent Cases of Bridge Collapse under Truck Collision Loads 24
3.2.2 Progression of Code Specifications on Vehicular Collision Force 26
3.2.3 Previous Analytical Work on Vehicular Collision Loads 27
3.2.3.1 Tsang and Lam (2008) 27
3.2.3.2 El-Tawil et al. (2005) 27
3.2.4 MnDOT Crash Strut Retrofit 28
3.3 Description of the Bridge Inventory 28
3.3.1 Introduction 28
3.3.2 Column Types 29
3.3.3 Bridge Types 32
3.3.4 Foundation Types 34
3.3.5 Redundancy 34
3.4 Evaluation of South Dakota Bridge Structures for Vehicular Collision Force 35
3.4.1 Dead Load Carried by the Columns 35
3.4.2 Column Shear Capacity 35
3.4.3 Column Flexural Capacity 37
3.4.4 Shear and Flexural Demands 37
3.4.5 Assessment of Bridge Vulnerability under a Vehicular Collision Force 39
3.4.6 Prioritization of Vulnerable Bridge Bents for Collapse Mitigation 40
3.5 Proof Tests of As-Built and Retrofitted Two-Circular Column Bents 41
3.5.1 Selection and Description of the Prototype Bridge 42
3.5.2 Selection and Description of the Retrofit Method 43
3.5.3 Design and Construction of the Test Specimens 43
3.5.4 Instrumentation 46
3.5.5 Test Set Up 47
3.7.6 Experimental Results 48
3.5.6.1 Specimen NCS 49
3.6 Summary 53

4. ESTIMATION OF THE COLLISION FORCE USING COMPUTATIONAL MODELS 55
4.1 Introduction 55
4.2 Vehicle Finite Element Models 55
4.3 Structure Finite Element Model 56
4.4 Simulation Cases and Results 57
4.5 Analysis of the Simulation Results 60
5. FINDINGS AND CONCLUSIONS 64
5.1 Findings 64
5.2 Conclusions 65
6. RECOMMENDATIONS 66
6.1 Recommendation 1 66
6.2 Recommendation 2 66
7. REFERENCES 67
APPENDIX A: MEETING NOTES 70
APPENDIX B: BRIDGE INVENTORY 89
APPENDIX C: COLLISION RISK ANALYSIS RESULTS 95
APPENDIX D: PRIORITIZATION OF BRIDGE BENTS FOR COLLAPSE MITIGATION 100
APPENDIX E: MNDOT CRASH STRUT DESIGN PROCEDURE 108
APPENDIX F: DEAD LOAD 110
APPENDIX G: SHEAR AND FLEXURAL CAPACITIES AND DEMANDS 115
APPENDIX H: MEASURED STRAIN 130
APPENDIX I: STATISTICAL SOFTWARE CODE 135

LIST OF TABLES

Table 2.1 Roadside Barriers and NCHRP Report 500 Approved Test Levels 5

Table 2.2 Truck ROR Crash Frequency 12

Table 2.3 Summary Statistics of Explanatory Variables of Freeway Segments 14

Table 2.4 Distribution of Vehicle Encroachment Angle and Orientation Angle 156

Table 2.5 Negative Binomial Estimation 18

Table 3.1 Distribution of Bridges by Road 28

Table 3.2 High Collision Risk Bents 41

Table 4.1 Peak Collision Force at 1 ms, 10 ms, and 50 ms Moving Average 62

LIST OF FIGURES

Figure 2.1	Bridge Hazard Envelope	5
Figure 2.2	Bridge Collision Risk Index Flowchart	7
Figure 2.3	Data Portal	8
Figure 2.4	Crash Barrier Systems on I-29 and I-90 in South Dakota	9
Figure 2.5	Crash Barrier Combined Systems on Highways in South Dakota	10
Figure 2.6	Weather Station Locations	11
Figure 2.7	The Shortest Detour Route Using ArcGIS	13
Figure 2.8	Bridge Collision Risk Profile	19
Figure 2.9	Bridge Collision Risk/RUC Clusters	19
Figure 2.10	Bridge Ranking by Weighted Sum Z-scores (1:1)	20
Figure 2.11	Bridge Ranking by Weighted Sum Z-scores (1:3)	21
Figure 2.12	Bridge Ranking by Weighted Sum Z-scores (3:1)	21
Figure 3.1	Collision Risk Assessment and Mitigation Strategy	24
Figure 3.2	I-80 Bridge Collapse near Big Springs, NE (NDOR, 2013)	25
Figure 3.3	I-80 Bridge Collapse near Big Springs, TX (Midland Reporter Telegram, 2013)	25
Figure 3.4	I-90 Bridge Collision near Worthington, MN (Courtesy MnDOT)	26
Figure 3.5	I-90 Diagram of Typical Four-Span Bridge	29
Figure 3.6	Column Types	30
Figure 3.7	Number of Bridges by Column Type	31
Figure 3.8	Number of Bridges with Circular Columns	31
Figure 3.9	Partially- and Fully-Flared Columns	32
Figure 3.10	Flared Columns with No Bent Cap	32
Figure 3.11	Bridge Superstructure Types	33
Figure 3.12	Number of Bridges by Superstructure Type	33
Figure 3.13	Number of Bridges by Foundation Type	34
Figure 3.14	Number of Bridges by Redundancy Classification	35
Figure 3.15	SPT Blow Count vs. Depth to Effective Fixity in Clay (Caltrans, 1990)	38
Figure 3.16	Model of a Non-Integral Bent	39
Figure 3.17	Model of an Integral Bent Bridge	39
Figure 3.18	Number of Bridges Based on Sufficiency and Redundancy	40
Figure 3.19	Typical Bridge Bents in Collision Risk Quadrants 4-4, 3-4, and 4-3	41
Figure 3.20	The Prototype Bridge	42
Figure 3.21	Details of the Prototype Bridge Bent (Courtesy SDDOT)	42

Figure 3.22 Crash Strut Retrofit (Courtesy MnDOT) 43
Figure 3.23 Details of the Test Specimen Columns 44
Figure 3.24 Details of the Test Specimen Bent Cap..... 44
Figure 3.25 Details of the Test Specimen Crash Strut..... 45
Figure 3.26 Details of the Test Specimen Footing 45
Figure 3.27 Test Specimens during Construction 46
Figure 3.28 Instrumentation of the Test Specimens 47
Figure 3.29 Test Set Up..... 48
Figure 3.30 Specimen NCS after Set Up..... 48
Figure 3.31 Elastic Analysis Shear and Bending Moment Diagrams 49
Figure 3.32 Measured Actuator Load-Displacement – Specimen NCS 49
Figure 3.33 Specimen NCS at Different Stages of the Test 50
Figure 3.34 Plastic Hinging in Specimen NCS 51
Figure 3.35 Displacement of the Bent Cap Centerline – Specimen NCS..... 51
Figure 3.36 Measured Actuator Load-Displacement – Specimen CSR 52
Figure 3.37 Specimen CSR Different Stages of the Test 52
Figure 3.38 Footing Failure in Specimen CSR..... 53
Figure 3.39 Displacement of the Bent Cap Centerline – Specimen CSR..... 53
Figure 4.1 15,000 lb Single Unit Truck FE Model..... 55
Figure 4.2 80,000 lb Truck-Trailer FE Model..... 56
Figure 4.3 Concrete Stress-Strain Model 56
Figure 4.4 Reinforcing Steel Stress-Strain Model..... 57
Figure 4.5 FE Model of the Bent Structure 57
Figure 4.6 Isometric Views of the Trucks at Impact 58
Figure 4.7 Isometric Views after Impact – 55 mph Approach Speed..... 58
Figure 4.8 Collision Dynamic Force – SUT Simulation 58
Figure 4.9 Collision Dynamic Force – TT Simulation 59
Figure 4.10 Damaged Bent after Collision – SUT Simulation..... 60
Figure 4.11 Damaged Bent after Collision – TT Simulation..... 60
Figure 4.12 1 ms, 10 ms, and 50 ms Moving Average Collision Force – SUT Simulation 61
Figure 4.13 1 ms, 10 ms, and 50 ms Moving Average Collision Force – TT Simulation..... 61
Figure 4.14 1 ms and 50 ms Moving Average Peak Forces – SUT Simulation 62
Figure 4.15 1 ms and 50 ms Moving Average Peak Forces – TT Simulation..... 63

LIST OF ACRONYMS

AADT	Average Annual Daily Traffic
AASHO	American Association of State Highway Officials
AASHTO	American Association of State Highway and Transportation Officials
AC	Accident Costs
ADTT	Average Daily Truck Traffic
AHP	Analytic Hierarchy Process
AIRM	Aggregated Indices Randomization Method
CSR	Crash Strut Retrofit
DOT	Department of Transportation
ESL	Equivalent Static Load
FE	Finite Element
FHWA	Federal Highway Administration
ft	Foot, Feet
GWU	George Washington University
HE	Hazard Envelope
IDW	Inverse Distance Weighting
in.	Inch; Inches
IPV	Inner Product of Vectors
Km/h	Kilometers per hour
kN	Kilo Newton
lb	Pound
LRFD	Load and Resistance Factor Design
MCDA	Multi-Criteria Decision Analysis
MnDOT	Minnesota Department of Transportation
MPC	Mountain Plains Consortium
mph	Miles per Hour
ms	Milli-Second
NB	Negative Binomial
NCAC	National Crash Analysis Center
NCHRP	National Cooperative Highway Research Program
NCS	No Crush Strut
NHSTA	National Highway Safety Traffic Administration
PDL	Peak Dynamic Load
PERT	Project Evaluation and Review Techniques
RMSE	Root Mean Square Error
ROR	Run Off Road
RSAP	Roadside Safety Analysis Program
RUC	Road User Costs
SUT	Single Unit Truck
SDDOT	South Dakota Department of Transportation
SDDPS	South Dakota Department of Public Safety
SPI	Standard Penetration Index

SPT	Standard Penetration Test
TT	Truck-Trailer
VOC	Vehicle Operating Costs
VOT	Value of Time
VMT	Vehicle Miles Traveled
WSS	Weighted Sum Score
ZINB	Zero-Inflated Negative Binomial
ZIP	Zero-Inflated Poisson

EXECUTIVE SUMMARY

The projected economic growth in South Dakota and neighboring states is expected to generate substantial increase in traffic on regional state highways. A significant portion of the increased traffic will be heavy tractor-semitrailer vehicles carrying equipment and goods to meet the needs of a growing economy.

The increase in highway traffic, in general, and heavy truck traffic, in particular, could ultimately lead to an increased number of traffic accidents on highways. Although not commonly occurring, incidents of the collision of heavy vehicles with highway overpass bridge columns have occurred in the past and resulted in catastrophic structural failures that interrupted traffic on the overpass and highway below. Failure of a critical bridge might have significant adverse effects on local, state, and national economy and well-being.

AASHTO LRFD Bridge Design Specifications (2012) require bridge columns be designed for collision loads to prevent bridge collapse under such extreme events. However, the majority of overpass bridges on South Dakota interstate and other major highways were designed and constructed prior to development of the collision load design requirements. South Dakota is located in a non-seismic region where the lateral seismic loads on bridge columns are negligible. In the absence of other significant lateral load requirements, such as ice loads on bridge piers, the majority of bridge columns on South Dakota highways were designed for low lateral load demands that did not govern the design of the columns. Therefore, the confinement/shear reinforcement in such columns was kept at or slightly above the minimum transverse steel requirements specified in prevailing codes at the time. In the case of a heavy truck collision incident, columns that lack sufficient shear strength and ductility capacity due to inadequate transverse reinforcement would be vulnerable to catastrophic failure and may, consequently, lead to bridge collapse.

The South Dakota Department of Transportation (SDDOT) does not have in place risk assessment and mitigation plans for collision loads to bridge columns. Therefore, a study was needed to perform risk assessment for truck collisions with bridge columns, evaluate the vulnerability of bridge columns to catastrophic failure under lateral collision forces, and develop a risk mitigation strategy for critical bridges on the state's Interstate system and other critical highways.

Factors that contribute to a risk of collision include average annual daily traffic (AADT), average daily truck traffic (ADTT), posted speed limit, geometric characteristics in the vicinity of the bridge, distance from the bridge column to the edge of the travel lane, proximity of the bridge to highway ramps, highway winter conditions, protection barriers, and other factors that were identified. After reviewing previous literature and available data, a methodology was developed to assess the risk a truck collision with bridge columns and to rank the bridge substructures based on their collision risk levels. Elastic structural analysis was performed on 175 overpass bridges on I-29, I-90, I-229, I-190, and other miscellaneous roads in South Dakota. The purpose for the analysis was to assess vulnerability of those bridges to vehicular collision forces. The collision risk assessment and vulnerability assessment were used to develop a retrofit prioritization list for mitigating collapse of bridge bents of the bridges included in this study.

Based on collision risk assessment and collapse vulnerability under vehicular collision force of 175 bridges in South Dakota, a high collision risk and vulnerable two-column bent prototype was selected for an experimental study. The study was designed to examine the structural performance of as-built and retrofitted cases under design collision loads. Two one-third-scale bridge bents were tested in the laboratory. One specimen represented the vulnerable prototype bent. The other specimen was retrofitted

with a MnDOT "crash strut" to prevent bridge collapse under collision loads. Test results were analyzed and effectiveness of the crash strut was evaluated. The test results indicated that the as-built bent is severely inadequate if subjected to the design collision force. The specimen failed at less than one-half the scaled design load and the bent cap underwent excessive displacement that could cause unseating of the superstructure's girders. The addition of a concrete crash strut between the columns increased the bent collision load capacity to at least 1.5 times the collision force demand. Thus, the collision strut would be an effective retrofit measure for bent structures that are vulnerable to collapse under the vehicular collision force.

Based on results obtained from this study, the following findings were identified.

- The uncertainties involved in truck collision events lead to a range of outcomes for calculating the hazard envelope—a physical exposure of a bridge to the collision. Therefore, statistical models have been developed to identify statistically significant collision contributing factors as well as their impacts. The model results show that high truck traffic exposure, sharp horizontal curves, high annual snowfall precipitation, and the concrete pavement surface all increase the truck ROR crash frequency. The hazard envelope of each bridge bent was calculated based on measured bent dimensions and default values recommended in NCHRP Report 492. Coupled with the unit crash counts, the collision risk can be estimated for each bridge bent, and the collision risk for a bridge can be determined by the maximum risk of all the bridge bents.
- The importance of a bridge reflects the severity of the socioeconomic impact that would result from a bridge collapse. It is calculated as road user costs (RUC) because of the additional distance that would need to be traveled.
- When the collision risk and the economic importance of a bridge were combined, a decision analysis method was applied to rank the overpass bridges. The quartile distribution, based on collision risk and RUC, resulted in 16 clusters of bridges that can be used to form a prioritization policy for the implementation of risk mitigation procedures. The highest risk cluster (quartile 4-4, i.e. RUC 4 and Collision Risk 4) contained 24 bridge bents. Quartiles 3-4 and 4-3 contained 49 and 25 bridge bents, respectively.
- AASHTO's Standard Specifications for Highway Bridges did not include provisions for truck collision with bridge columns and abutments. The vehicular collision force requirements first appeared in AASHTO's LRFD Bridge Design Specifications first edition in 1994.
- In the early editions of AASHTO-LRFD, the vehicular collision force requirements for bridges without adequate protection for collision consisted of a 400-kip static force applied horizontally to a bridge column at four feet above ground level. In 2012, the vehicular collision force was increased to 600 kips and the point of application was changed to five feet above ground level.
- The vast majority of the 175 bridges included in this study were designed and constructed prior to the development and implementation of the vehicular collision force requirements for unprotected bridge columns. Using elastic structural analysis and code methods for determining structural capacity, the columns of 140 bridges were found to be structurally inadequate in flexure, shear, or both.
- Bents with less than three columns were considered non-redundant. Of the 175 bridges included in this study, 107 had non-redundant bents (61 percent).
- Bridges with circular columns represented the vast majority of the bridge inventory in this study (77 percent). Flared column bridges were the second highest in number (14 percent). Almost 40 percent of bridges in the inventory were non-redundant two-column bents with circular columns.

- Of the 98 bridge bents that fell in quartiles 4-4, 3-4, and 4-3, 59 bents were both non-redundant and structurally inadequate for the design collision load.
- Laboratory testing of one-third-scale of a vulnerable two-circular column bent indicated structural failure at less than one-half of the design collision force and potential for unseating of the edge girder. A similar specimen but with a crash strut retrofit was capable of resisting 1.5 times the design collision force.
- The finite element dynamic analysis performed in this study showed that for the prototype bridge considered in the analysis, the 600-kip vehicle collision force specified by AASHTO is a reasonable estimate for the load demand induced by the collision with the bridge column of an 80,000-pound tractor-trailer traveling at 55 mph.

Based on the research findings, the following conclusions were made.

- Crashes are random events, as they may be affected by several factors that are unknown or observable. The unobserved elements are the main contributor to data dispersion. To account for data dispersion in the crash risk analysis of this study, negative binomial count models can be employed. The model output reveals that high truck traffic exposure, sharp horizontal curves, high annual snowfall precipitation and the concrete pavement surface all increase the truck ROR crash frequency.
- By considering the vulnerable bents in the high collision risk pool, a priority list for protection or retrofit can be generated by SDDOT engineers and planners. The prioritization should take into consideration additional factors such as the remaining useful life of the bridge, bridge replacement schedule, availability of resources, and cost effectiveness of implementing the same retrofit method for a group of bents that share the same features.
- The columns of the vast majority of two- and three-circular column bents are inadequate in shear, flexure, or both under the 600-kip vehicular collision force.
- The crash strut used in this study provides an effective measure for retrofitting high risk and vulnerable bridge bents. The MnDOT method for designing the crash strut seemed to yield adequate results.

The following recommendations are based on the findings of this study.

- The prioritization list generated in this study, coupled with other factors such as the remaining useful life of the bridge, bridge replacement schedule, availability of resources, and cost effectiveness of using the same retrofit method for a group of bents that share the same features, should be adopted by SDDOT for implementing protection or retrofit measures for vehicular collision forces. The collapse risk of inadequate bents that are vulnerable to vehicular collision forces could be mitigated through implementing retrofit measures to enhance the strength of the bent. However, retrofitting all inadequate bents is cost prohibitive. One strategy to prioritize bridge bents for collapse mitigation retrofit would be to consider the pool of bridge bents that fall in the high risk quartiles (4-4, 3-4, and 4-3) and are vulnerable to collapse under the vehicular collision force. A priority list for retrofit can be generated by SDDOT engineers and planners, It would consider additional factors, such as the remaining useful life of the bridge, bridge replacement schedule, availability of resources, and cost effectiveness of implementing the same retrofit method for a group of bents that share the same features.
- A crash strut, similar to the one tested in this study, should be adopted for retrofit of two- and three-column bents. The test results of the one-third-scaled two-column bent indicated that the as-built bent is severely inadequate if subjected to the design collision force. The as-built specimen failed at less than one-half the scaled design load and the bent cap underwent excessive displacement that could cause unseating of the superstructure's girders. The addition of a concrete

crash strut between the columns increased the bent collision load capacity to at least 1.5 times the collision force demand. Thus, the collision strut provides an effective retrofit measure for bent structures that are vulnerable to collapse under the vehicular collision force.

1. INTRODUCTION

1.1 Project Description

In a June 13, 2012, *Wall Street Journal article*, South Dakota was named as one of the top 10 “future booming states.” The article also named two bordering states—North Dakota and Wyoming—in the top 10 list. The projected economic growth in the Dakotas and neighboring states is expected to generate substantial increase in traffic on regional state highways. A significant portion of the increased traffic will be heavy tractor-semitrailer vehicles carrying equipment and goods to meet the needs of a growing economy, and the booming oil and mining industries and their supporting infrastructure.

The increase in highway traffic, in general, and heavy truck traffic, in particular, could ultimately lead to an increased number of traffic accidents on highways. Although not commonly occurring, incidents of the collision of heavy vehicles with highway overpass bridge columns have happened in the past and resulted in catastrophic structural failures that interrupted traffic on the overpass and highway below. On July 27, 1994, a heavy tractor pulling a propane tank semitrailer on Interstate 287 in White Plains, New York, drifted from the main road, struck a guardrail next to a column bent, and then hit a concrete column of the Grant Avenue overpass. Upon impact, propane vapor escaping from the tank ignited into a fireball that caused injuries to individuals within a 400-foot radius from the location of the accident (NTSB, 1995). On May 23, 2003, a tractor-semitrailer crashed into the column of an overpass on I-80 near Big Springs, Nebraska. The I-80 accident resulted in a bridge collapse and halted traffic on that section of the Interstate for three days (ENR, 2003). Similar incidents have happened in other locations across the country (NTSB, 1993). This type of hazard can be categorized as an extreme event that has a low probability of happening, but carries significant socio-economic consequences.

AASHTO LRFD Bridge Design Specifications (2012) require bridge columns be designed for collision loads to prevent bridge collapse under such extreme events. However, the majority of overpass bridges on South Dakota interstate and other major highways were designed and constructed prior to development of the collision load design requirements. South Dakota is located in a non-seismic region where the lateral seismic loads on bridge columns are negligible. In the absence of other significant lateral load requirements such as ice loads on bridge piers, the majority of bridge columns on South Dakota highways were designed for low lateral load demands that did not govern the design of the columns. Therefore, the confinement/shear reinforcement in such columns was kept at or slightly above the minimum transverse steel requirements specified in the prevailing codes at the time. In the case of a heavy truck collision incident, columns that lack sufficient shear strength and ductility capacity due to inadequate transverse reinforcement would be vulnerable to catastrophic failure and may, consequently, lead to bridge collapse.

The South Dakota Department of Transportation (SDDOT) does not have in place risk assessment and mitigation plans for collision loads to bridge columns. Therefore, a study was needed to perform risk assessment for truck collisions with bridge columns, evaluate vulnerability of bridge columns to catastrophic failure under lateral collision forces, and develop a risk mitigation strategy for critical bridges on the state’s Interstate system and other critical highways.

1.2 Objectives

Three main objectives were addressed in this study.

- Develop a risk assessment methodology for heavy truck collisions with columns of overpasses. A methodology was developed to determine a safety performance metric identified in this study as the Collision Risk Index. The Collision Risk Index is a tool that compares the relative risk of different bridges to collision loads. The Collision Risk Index is dependent on the risk of collision and bridge importance. The risk of collision reflects factors that affect the risk of a heavy vehicle colliding with a bridge column, while the bridge importance measures economic impact as a consequence of bridge collapse.
- Evaluate the risk of overhead bridge collapse caused by heavy truck collisions with columns on the South Dakota interstate system and other major roadways. A risk assessment and mitigation strategy for protecting critical and economically essential bridges against collapse under collision loads involves ranking bridges for crash risk and identifying bridge structures vulnerable to collapse, should a truck collision occurs. Bridges found to be at a high-crash risk and vulnerable to collapse would be the top candidates for retrofit. The risk of a bridge collapse resulting from collision loads at the bridge columns requires estimation of the load demand and structural capacity. In this study, elastic structural analysis of 175 bridges was performed to identify bent structures vulnerable to collapse.
- Propose mitigation measures to the SDDOT to reduce the risk of collapse for existing and future bridges. A risk mitigation plan involves prioritizing bridges for retrofit according to their collision risk level and implementing effective retrofit measures to high-risk bridges in order of their risk level. A retrofit method consisting of a “crash strut,” originally implemented by MnDOT, was tested in the laboratory. Test results indicated that the crash strut provides an effective retrofit technique to prevent collapse under the design collision force.

2. COLLISION RISK ANALYSIS

This section covers work done to develop a collision risk assessment methodology and the results obtained from implementing the developed risk assessment method to overpass bridges on I-29, I-90, I-229, I-190 and other miscellaneous roads selected by the technical panel.

This section starts with a review of previous research in the areas of crash risk analysis, crash count models, roadside design elements, road user costs calculation, and multi-criteria decision analysis. Next, the study design and key elements of the study are presented. This is followed by a description of data collection and processing. The methodology is presented in two major modules. The first is the crash prediction module, including the truck Run-off-the-Road (ROR) crash prediction models and collision risk analysis. The second module is the bridge economic significance, including road user cost evaluation. The weighted sum models introduced as a multi-criteria decision-making (MCDA) ranking strategy to rank the bridges at risk. The results of the truck ROR crash prediction model and the bridge ranking are presented and analyzed. Finally, conclusions are drawn and future work is recommended.

2.1 Literature Review

This section introduces the definitions, procedures, methodologies, and applications of vehicle-bridge collision risk from previous studies. The literature review includes risk analysis, crash prediction models, hazard envelope definition, road user costs calculation, and multi-criteria decision analysis.

2.1.1 Crash Risk Analysis

Risk analysis is the systematic use of available information to evaluate likelihood for negative events to occur, as well as their potential consequences. Risk analysis helps to uncover and identify possible undesirable external and internal conditions or situations. According to the *National Cooperative Highway Research Program (NCHRP) Report 492 – Roadside Safety Analysis Program* (*RSAP*) (Mak and Sicking, 2003), roadside collision risk emerges from two primary sources: the risk for a vehicle to encroach the roadside, and the location and dimension of the hazardous object(s). By combining the two primary sources, collision risk can be calculated as the product of the encroachment frequency and the probability of having an object in its trajectory. The risk of vehicle run-off-road (ROR) can be a collective effect of roadway features, weather and environmental conditions, as well as driver characteristics (Miaou, 1997; Shankar et al., 1997; Zegeer et al., 1988). The hazard exposure to an erratic vehicle can be defined as a function of the dimension and orientation of the vehicle, the vehicle encroachment angle, and the size and lateral offset of the hazard. To assess the risk of a vehicle-bridge collision, each component within the crash risk should be carefully examined.

In previous studies, accident- and encroachment-based approaches were commonly used to develop the relationships between roadside crashes and roadside conditions. A roadside encroachment is defined as "an errant vehicle crosses the outside edges of the travel way and encroaches on either the inside or outside shoulder" (Miaou, 1997). *RSAP* (Mak and Sicking, 2003) used the encroachment-based method to elaborate on the process of analyzing collision risk and severity. Daily et al. (1997) applied a series of conditional probabilities to describe the sequence of events that result in a ROR accident. As Miaou (2001) summarized, the sequence of events considered by the encroachment-based approach is: "(1) an errant vehicle leaves the travel lane and encroaches on the shoulder; (2) the location of encroachment is such that the path of travel is directed towards a potentially hazardous roadside object; (3) the hazardous object is sufficiently close to the travel lanes, the control is not regained before encounter or collision between vehicle and the object; and (4) the collision is severe enough to result in an accident of some level of severity." The advantages of using the encroachment-based approach is that it is based on analytical and engineering concepts. However, this approach makes several subjective assumptions that are difficult to validate, such as the travel path of the errant vehicle. Additionally, the effort to validate these assumptions is difficult and cost prohibitive (Miaou, 2001).

The accident-based approach is more prevalent than the encroachment-based approach because crash data are more readily available. Zegeer et al. (1988) elaborated that the accident-based approach is developed through use of statistical regression models to determine the relationship between ROR crash frequency and traffic conditions, roadway mainline designs, roadside designs, and other explanatory variables. A ROR crash is the consequence of a roadside encroachment event, but a roadside encroachment event might not necessarily lead to a crash event. In other words, ROR crashes are just a small fraction of the multitude of roadside encroachments.

2.1.2 Crash Count Models

Accident-based roadside collision models are usually developed through the use of negative binomial (NB) regression models when equality of the mean and variance of the crash data for a Poisson model is violated. Other model variation, such as the zero-inflated Poisson (ZIP) model and the zero-inflated negative binomial (ZINB) model, have also been used when crash data have an excessive number of zero observations. According to a study conducted in Washington State (Shankar et al., 1997), the NB model is the most appropriate model for ROR crash frequency on urban roadway sections, whereas the zero-inflated negative binomial model is the most appropriate model for rural roadway sections.

2.1.3 Roadside Design

Safe roadside design helps mitigate the consequence of a roadway departure event. There are two key elements in roadside design: the placement and dimension of an object in the clear zone, and the protection systems, such as the barriers and guardrails.

A bridge collision occurs if the bridge bent happens to be located in the erratic vehicle's trajectory path. According to *RSAP* (Mak and Sicking, 2003), the hazard envelope is "along the travel way wherein an encroaching vehicle would impact the roadside feature under consideration." The hazard envelope can be determined from a few parameters: a vehicle of size ω, encroachment angle θ, and orientation angle φ. These parameters vary from case to case and their distributions will determine the range and the mean of the hazard envelope. As Miaou (2001) stated, "for a given vehicle of size ω, encroachment angle θ, and orientation φ, a hazard collision will occur if, within the hazard envelope, the vehicle leaves the roadway and is unable to stop." In *RSAP* (Mak and Sicking, 2003), the hazard envelope is formulated according to Equation 1.

$$HE = \left(\frac{1}{5280}\right)\left[L_h + \left(\frac{W_e}{\sin\theta}\right) + W_h \cot\theta\right] \qquad \text{Equation 1}$$

Where

HE = hazard envelope
L_h= length of hazard (ft)
W_e= effective width of vehicle (ft) = $L_v \sin\varphi + W_v \cos\varphi$
L_v, W_v: length and width of vehicle (ft)
W_h= width of hazard (ft)
θ = encroachment angle
φ = orientation angle

The placement of a bent determines its exposure to potential collisions. Figure 2.1 presents a typical layout of a bridge with three bents (B1, B2, B3 represent Bent #1, #2, #3, respectively) and the bridge hazard envelope.

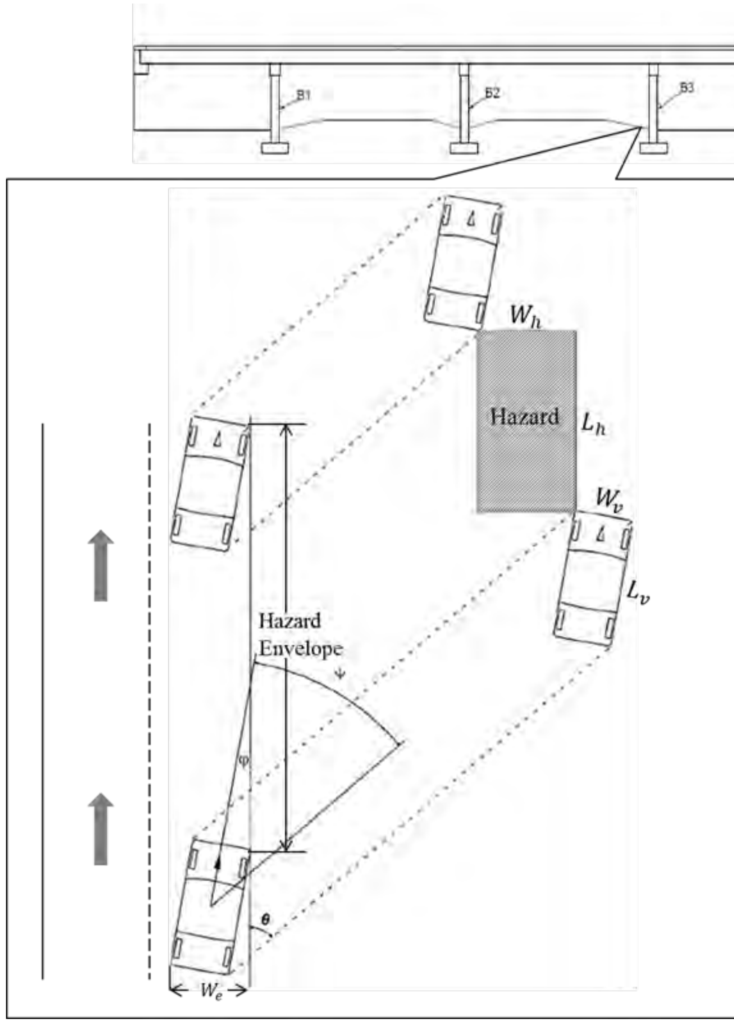

Figure 2.1 Bridge Hazard Envelope

The overpass bridge bents on interstate highways in South Dakota are protected by different types of bridge barrier systems. In NCHRP Report 500 (Neuman et al., 2003), bridge railings are classified into six test levels based on the results of testing impact of different types of vehicles on bridge railings at different speeds and angles. AASHTO MASH (Bligh et al., 2013) updates and supersedes NCHRP Report 500 for the purpose of evaluating new safety hardware devices. Table 2.1, from Roadside Design Guide (AASHTO, 2011), shows approved test levels of roadside barriers installed on South Dakota interstate highways.

Table 2.1 Roadside Barriers and NCHRP Report 500 Approved Test Levels

Roadside Barrier System	Test Level	Vehicle	Containment Capacity (kJ)
W-Beam (Weak Post)	2	2270P	70.5
Three-Strand Cable (Weak Post)	3	2270P	144
Thrie-Beam (Strong Post)	3	2270P	144
Concrete Barrier	5	36000V	548

2.1.4 Road User Costs

According to Daniels et al. (1999), road user costs (RUC) are composed of vehicle operating costs (VOC), value of time (VOT), accident costs (AC) and other indirect costs, such as vehicle emission costs and noise. To improve work zone management, the Federal Highway Administration (FHWA) did a study (Jiang and Adeli, 2003) to evaluate the economic impact of road work to road users. In the FHWA study, input needs and key components of work zone RUC are discussed in detail. The step-by-step procedures and the models have been provided to state DOTs.

A variety of methods have been used by state DOTs to calculate RUC for their own purposes (Jiang, 1999; Collura et al., 2010; Chan et al., 2008). The majority of state DOTs used simplified calculations and spreadsheets. The components included in the calculations range from only vehicle operation costs (VOC) to VOC, value of time (VOT), accident costs (AC) and additional specific components to address safety or emergency relief situations. With respect to South Dakota, Qin and Cutler (2013) conducted a research project for SDDOT to develop the procedure for RUC estimation in South Dakota. In their study, the RUC was calculated as the summation of VOC, VOT and AC. VOT is estimated based on the relationship between wage rates and delays caused by taking a detour route. VOC refers to the costs associated with operating and owning the vehicle over the analysis period. AC is used to measure monetary impacts of possible crashes due to roadway construction or maintenance projects. The unit costs of VOC, VOT and AC were estimated based on South Dakota data.

2.1.5 Multi-Criteria Decision Analysis

To prioritize, select, and recommend bridges for different levels of repair and maintenance budget limitations, a feasible approach is needed to evaluate the multiple criteria involved. Multi-Criteria Decision Analysis (MCDA) is a valuable tool to solve problems such as a choice among alternatives. There are various MCDA methods such as the weighted sum mode (WSM), aggregated indices randomization method (AIRM), inner product of vectors (IPV), and the analytic hierarchy process (AHP). Among these methods, the weighted sum model is the simplest.

2.2 Study Design

Bridge ranking can be determined by combining results from two modules—the truck-bridge collision risk module and the additional road user costs module. The truck-bridge collision risk module aims to develop methods for assessing risk for collisions between trucks and interstate highway overpass bridge bents. It can be calculated in two steps: (a) build truck ROR crash prediction models to calculate the truck ROR crash frequency, and (b) estimate the bridge hazard envelope on the basis of the bridge dimension, vehicle configuration, vehicle orientation angle and encroachment angle.
The road user costs module estimates the additional RUC after a bridge has collapsed. The purpose for introducing this module is to account for the critical location of a bridge. Extra protection may be needed when a bridge is located in an economically vital area, even if the calculated collision risk is low. On the other hand, if the overpass bridge is less important to the community, the bridge may not be considered as high a priority even if the collision risk is higher.

After combining information from the two modules, a composite ranking is provided through the use of a comprehensive ranking strategy. The procedure and factors used to develop a bridge collision risk index are illustrated in Figure 2.2. The rest of this section describes the key components in Figure 2.2.

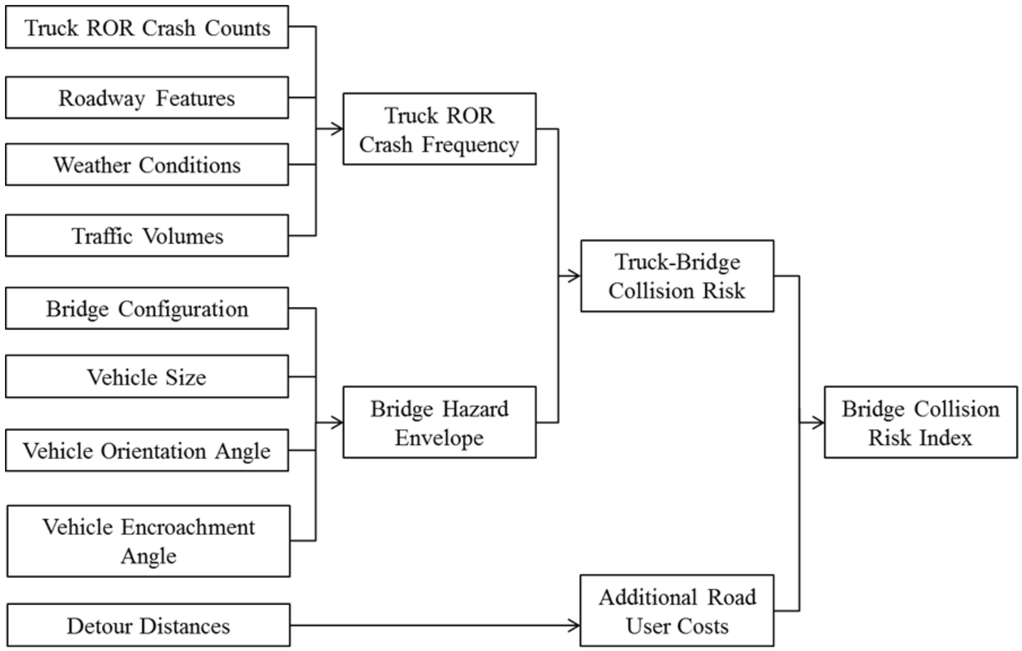

Figure 2.2 Bridge Collision Risk Index Flowchart

2.2.1 Method for Ranking Bridges for Collision Risk

The method used in this study for ranking bridges for collision risk involves the following steps.

2.2.1.1 Quantifying Crash Risk

This step estimates probability of truck run-off-the-road (ROR) crashes ($P\ (N = n_i)$) by using the crash count models. The five-year history of truck ROR crash data, highway geometric data, weather condition data, and traffic information were collected to predict the truck ROR crash frequency for each highway segment. The negative binomial NB model was considered in light of data dispersion. The estimation results are analyzed and compared.

2.2.1.2 Measuring Impact Area

This step estimates the hazard envelope (*HE*) for each bridge bent. The probability for a truck departing the roadway is only related to segment-specific features and environmental factors such as weather and light conditions, and, therefore, is independent of the bridge dimension and location.

2.2.1.3 Determining Collision Risk

The collision risk is specified in Equation 2 as the product of hazard envelop of bridge i and the crash probability density. Crash probability density is defined as the probability of having n crashes at highway segment i divided by the segment length, or the unit length of probability of having n crashes.

$$P(collision\ risk) = \frac{P(N = n_i)}{segment\ length} * HE) \qquad \text{Equation 2}$$

2.2.1.4 Evaluating Bridge Economic Significance

In the event of a bridge collapse, local road users must take a longer detour route to their destination. In this study, all vehicles are assumed to take the shortest available route. The detour costs were measured as the additional RUC from the increased travel distance and increased travel time resulting from the collapse of a bridge. The value of additional RUC can represent the economic significance of a bridge to the local users. The monetary impacts to road users because of new construction, reconstruction, rehabilitation, restoration, resurfacing, and other miscellaneous highway maintenance activities can be estimated from vehicle operating costs, value of road users' time, and accident costs. Because of the limited amount of data, it is assumed that few trucks travel on rural local roads, which means that all vehicles that took the detour route were passenger cars.

2.2.1.5 Ranking Bridges for Collision Risk

The bridges must be prioritized for protection and maintenance after evaluating collision risk and the economic significance of each bridge. Multi-criteria decision analysis (MCDA) was used to prioritize the overpass bridges on I-29, I-90, I-229, I-190, and other miscellaneous roads in South Dakota. MCDA is widely used to help decision-makers deal with multiple criteria associated with objects and make decisions in a technical and systematic manner. The first MCDA method used in this study was a weighted sum of two criteria—bridge collision risk and additional RUC due to the overpass out of service. Because the two criteria have different units and magnitudes, Z-scores were used to represent the significance of the observation. A Z-score measures the standard deviations of an observation away from the mean. This approach can effectively combine the two most important criteria, i.e., bridge collision risk and economic significance.

2.3 Data Collection and Processing

To develop a bridge collision risk index, the truck ROR crash frequency, bridge hazard envelope dimension, and road user costs must be calculated. Figure 2.3 shows the data required for each part of the calculation. Six types of data—bridge dimensions, roadway characteristics, traffic volume, weather conditions, crash counts, and detour distance—were collected in this study. This section is focused on the field survey, data sources, and features, and the procedures of data processing.

Figure 2.3 Data Portal

2.3.1 Bridge Survey

The research team conducted three field surveys to collect data on overpass bridges and site characteristics. The first survey was conducted November 4, 2012, and included overpass bridges on I-29 between Brookings, South Dakota, and the North Dakota state line. The second survey was conducted November 18, 2012, and included overpass bridges on I-29 between Brookings and the Iowa state line at Sioux City, I-90, between Sioux Falls, South Dakota, and the Minnesota state line, and select bridges on I-229, Highway 50 near Vermillion, South Dakota, and Madison Street and 12th Street in Sioux Falls. The third survey was conducted January 5 and 6, 2013, and included overpass bridges on I-90 between Sioux Falls and the Wyoming state line and select bridges on Mt. Rushmore Road and Haines Avenue in Rapid City, South Dakota. The research team focused on the bridge super- and sub-structure types, roadside barrier types, rumble strip condition, clear zones, and the distance between the roadside barrier and the bridge columns. Since this part of the study assesses vehicle-bridge collision risk, only the dimension and configuration of a bridge and site characteristics are of primary interest, as described in the next section.

In general, three types of barrier systems are installed on the state highways in South Dakota: W-Beam (weak post), Three-Strand Cable (weak post), and Thrie-Beam (strong post). Most of the W-Beams on I-29 and I-90 are 27.7 inches high and are supported by wood or steel posts. Three-Strand Cables are composed of three cables and supported by steel posts. Three-Strand Cables are commonly used as median barriers, as they can effectively reduce the number of median crossover crashes. Thrie-Beams consist of two pieces of W-Beams that are formed into one single shape and are supported by wood or steel posts. In general, Thrie-Beams have better performance than W-Beams in terms of preventing vehicles from running off the road. Figure 2.4 shows the three barrier systems.

(a) W-Beam **(b)** Three-Strand Cable **(c)** Thrie Beam

Figure 2.4 Crash Barrier Systems on I-29 and I-90 in South Dakota

Some combinations of these barrier systems are in place, such as transition from Three-Strand Cable to W-Beam, from W-Beam to Thrie-Beam, or from Three-Strand Cable to W-Beam and to Thrie-Beam. Figure 2.5 shows combined barrier systems.

(a) Cable to W-Beam **(b)** W- to Thrie Beam **(c)** Three-Strand Cable to W-Beam to Thrie Beam

Figure 2.5 Crash Barrier Combined Systems on Highways in South Dakota

According to Table 2.1, only the barrier systems passing Test Level 4 or above—such as a concrete barrier—can stop trucks heavier than 10,000 kg from penetrating the barrier system. However, most of the current bridge barrier systems on I-29 and I-90 in South Dakota are below Test Level 4 and, consequently, are unable to protect bridge columns from being hit by heavy trucks. In most cases, the observed clear spacing between the bridge barrier and the column ranges from three inches to five inches. In a few cases, the bridge barrier is located very close to or very far away from the bridge column.

Most highway segments under the overpass bridges have continuous or intermittent rumble strips on the roadside shoulders. A few highway segments located in the proximity of urban areas, such as Sioux Falls and Rapid City, have no rumble strips on the highway shoulders. According to the Road Design Guide (AASHTO, 2011), a clear zone is “an unobstructed, traversable roadside area that allows a driver to stop safely, or regain control of a vehicle that has left the roadway.” Except for a few roadway segments located in the urban areas that have light posts on roadsides, most roadway segments have clear zones in good condition, which means that the edge of roadway is free of obstacles such as trees, light posts, utility poles, rocks, and signs.

2.3.2 Data Sources

2.3.2.1 Bridge Dimension and Configuration

The overpass bridge dimension data were collected from “Bridge Construction Plan Sets” provided by SDDOT. There is a detailed description about configuration of each bridge and roadway features under the bridge. In this study, deck width and column width of each bridge were collected for estimation of the bridge hazard envelope. Deck width is the outside-to-outside width that includes road width, shoulder width and individual elements, such as bridge rails t required to make up the desired bridge cross-section. Column width is measured as width of the column’s cross section. The widths of the columns for multi-column bridges are almost identical. Therefore, a single value was used to represent the column width for those bridges. The bridge deck width was measured in feet, while column width was measured in inches.

2.3.2.2 Roadway Characteristics

Roadway characteristics data were collected from the "State_Road" shape file provided by SDDOT. This database was set up in 2008 and provides a comprehensive description about the roadway and roadside cross-sectional features of all state highways in South Dakota. The roadway characteristics include, but are not limited to, mile marker, number of lanes, lane width, shoulder width, median width, surface type, shoulder type, rumble strips, and vertical and horizontal alignment.

2.3.2.3 Traffic Volume

The traffic volume data were collected from the Highway Needs and Project Analysis Report (SDDOT, 2012) recorded by SDDOT in 2011. This report recorded surface condition, roughness, and asphalt and concrete indexes; three-year average maintenance costs; traffic volume, including the annual average daily traffic (ADT); average daily truck traffic (ADTT); and crash information including crash rate and the number of fatal/injury/property damage crashes, for the major highways in South Dakota. In this study, the traffic volume information was extracted to help develop the truck ROR crash prediction models. The five-year (2004-2008) million truck vehicle miles traveled (VMT) was estimated using Equation 3:

$$Truck\ VMT = (ADTT * 365 * 5 * segment\ length)/1{,}000{,}000 \qquad \text{Equation 3}$$

2.3.2.4 Weather Conditions

Weather condition data were provided by Dr. Dennis Todey, a professor from the SDSU Agriculture and Biosystems Engineering department. The data were collected from 21 weather stations located in South Dakota as shown in Figure 2.6.

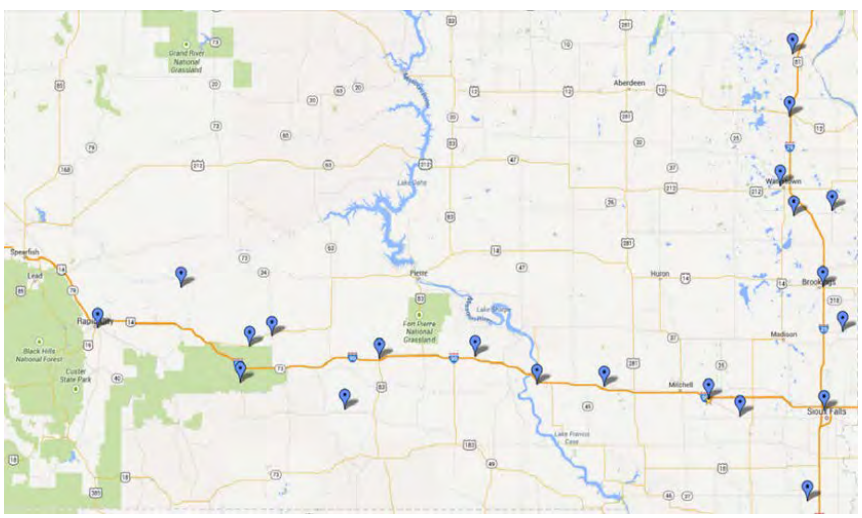

Figure 2.6 Weather Station Locations

The weather conditions provided by weather stations include the annual average rainfall, snowfall, and days of frost—days in which the temperature was equal to or less than 32 °F—for the last 30 years. In this study, five years (2004-2008) of annual average rainfall, snowfall, and days of frost data were used. Both annual average rainfall and snowfall precipitation were measured in inches.

2.3.2.5 Crash Data

Crash data were collected from the South Dakota Accident Records System Files provided by the South Dakota Department of Public Safety (SDDPS). These files recorded detailed information for each crash that happened on all public roads in South Dakota from 2004 to 2008, including crash location, occurrence time, crash type and severity, vehicle and driver information, and environmental condition.

Considerable care was given to identifying ROR crashes. The key leads to such information can be found from the first harmful event (FHEvent) or the most harmful event (MHEvent) of a crash. The first harmful event refers to the first injury or damage-producing event that characterizes the crash type. The most harmful event refers to the event that resulted in the most severe injury or, if no injury, the greatest property damage involving this motor vehicle. Any harmful event involving a rollover accident or a roadside object (e.g., approaches, bridge piers or supports, bridge rails, concrete traffic barriers, culverts, delineator posts, ditches, embankments, fences, guardrail ends, guardrail faces, traffic signs, luminary supports, other posts, poles or supports, other traffic barriers, utility poles or snow banks) was considered an ROR crash. The crash data also included further descriptions such as "run off road right," "run off road left," "hit bridge rail," and "hit fence."

A vehicle was identified as a truck if the "vehicle configuration description" was light truck (two axles, four tires), single-unit truck (two axles, six tires and gross vehicle weight rating 10,000 pounds or less), single-unit truck (two axles, six tires and gross vehicle weight rating 10,000 pounds or more), single-unit truck (three or more axles), tractor/doubles, tractor/semitrailer, truck pulling trailer(s), and gross vehicle weight rating 10,000 pounds or more, or truck tractor only (bobtail).

2.3.3 Data Processing

Considerable effort was made to integrate data from different data sources. ArcGIS software was used to join bridge dimension and configuration information to the corresponding highway segments by using the "Spatial Join" feature, after setting the buffer as 100 feet. Similarly, each year's crash data were joined to the corresponding highway segments by using "Spatial Join" after setting the buffer as 30 feet. Then, the merge function was used to combine five years (2004-2008) of crash data into each highway segment. From 2004 to 2008, there were a total of 887 ROR crashes involving trucks that occurred on 1,342 miles of roadway on I-29, I-90, I-229, I-190, and other miscellaneous roads in South Dakota. The truck ROR crash frequency is listed in Table 2.2.

Table 2.2 Truck ROR Crash Frequency

Crash Count	Frequency	Percent	Cumulative Frequency	Cumulative Percent
0	742	58.79	742	58.79
1	326	25.84	1068	84.62
2	103	8.16	1171	92.79
3	54	4.28	1225	97.07
4	22	1.74	1247	98.81
5	7	0.55	1254	99.36
>5	8	0.64	1262	100

In addition to the roadway characteristics data, for the roadway segments not associated with any weather station, the weather information needed to be interpolated. The Inverse Distance Weighting (IDW) method was used to interpolate weather data for the corresponding highway segments. IDW is a deterministic spatial interpolation method that computes the value for unknown points as the weighted mean of known points. The statistical software R (https://www.r-project.org) was used to do the IDW interpolation (see Section I.1 of Appendix I). Equation 4 was used:

$$z_j = \frac{\sum_{i=1}^{m} w_{ij} z_i}{\sum_{i=1}^{m} w_{ij}} \text{ and } w_{ij} = \frac{1}{d_{ij}^{k}} \qquad \text{Equation 4}$$

Where:

z_j, z_i = the value for unknown point j and known point i, respectively
w_{ij} = the weight for the influence of point i on point j
d_{ij} = distance between point i and point j

In this study, the weather conditions for each segment were interpolated using the data from all 21 weather stations, i.e., m = 21. The power parameter k was determined based on the minimum root mean square error (RMSE) of the values predicted by the IDW model.

The additional road user costs were calculated from the increased distance caused by the detour route that vehicles had to travel after the bridge collapsed. ArcGIS was used to obtain the detour distance by setting "Point Barriers" in the "Network Analyst" to locate the shortest detour route. Figure 2.7 shows an example of the shortest detour route using ArcGIS.

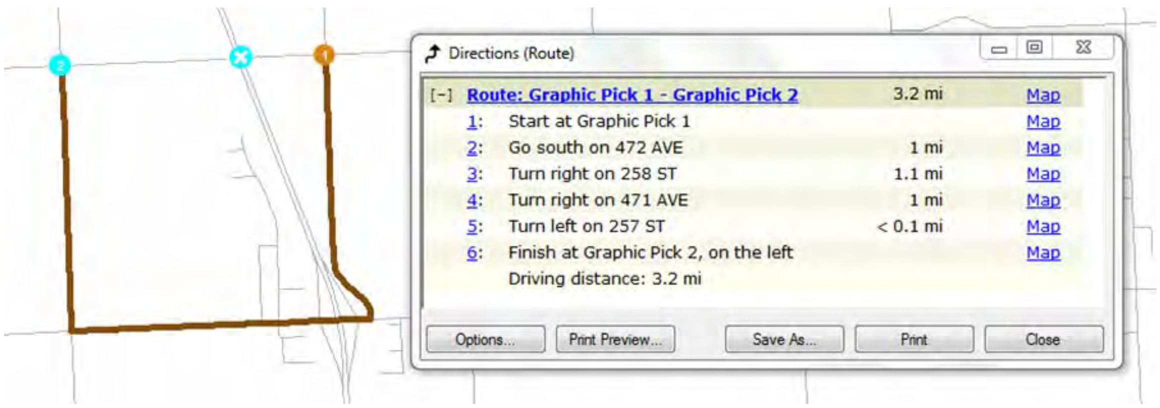

Figure 2.7 The Shortest Detour Route Using ArcGIS

2.3.4 Summary

According to the literature review, crash frequency is mainly influenced by traffic exposure, roadway and roadside characteristics, and weather conditions. In this study, data collection focused mainly on bridge dimension and configuration, roadway characteristics, traffic volume, weather conditions, crash count, and detour distance. Table 2.3 shows the descriptive statistics for key variables used in the estimation of crash frequency.

Traffic volume, weather conditions, and the majority of the roadway characteristics data were collected from SDDOT. Staff and students from the SDSU Civil and Environmental Engineering Department conducted field surveys to verify the bridge, and roadway and roadside conditions, including the clear zone. Some information collected in the survey or from other data sources was not used for further analysis because these parameters are difficult to define and verify. For instance, the distance between the bridge barrier and the bridge column cannot be completely and correctly collected through a windshield survey. The bridge barrier system type was not included in the analysis because most of the current bridge barrier systems on highways in South Dakota are unable to protect bridge bents from being hit by heavy trucks. The clear zone conditions are generally good, which means the trucks are unlikely to collide with roadside obstacles.

Table 2.3 Summary Statistics of Explanatory Variables of Freeway Segments

Continuous Variable	Description	Range	Mean	Std. Dev.
Crash counts	Number of ROR crashes during 2004-2008	[0,8]	0.704	1.096
Median shoulder width	Width of shoulder on the left of the travel direction (in feet)	[4,10]	4.607	1.081
Right shoulder width	Width of shoulder on the right of the travel direction (in feet)	[4,10]	9.602	0.798
Median width	Width of median grass or sod (in feet)	[16,75]	26.311	9.261
Length	Length of segment (in miles)	[0.062,38.108]	2.126	3.479
Truck ADT	Annual average daily truck traffic	[78,5603]	2373.095	868.84
Horizontal Curve	Degree of horizontal curve of segment	[0,36.9]	5.174	4.269
Vertical Curve	K value of vertical curve of segment	[0,110000]	1722.111	7631.683
Annual rainfall	Average annually rainfall 2004-2008 (in inches)	[17.56,27.02]	23.45	2.5
Annual snowfall	Average annually snowfall 2004-2008 (in inches)	[29.32,52.93]	38.67	3.35
Number of frost days	Average number of annual frost days 2004-2008	[168,175]	171	1.15

Categorical Variable	Description	Category	Frequency of Segments	Percent
Number of lanes	Total number of lanes in segment	2	1150	91.13%
		3	100	7.92%
		4	12	0.95%
Lane width	Average width of each lane (in feet)	12	926	73.38%
		13	336	26.62%
Surface type	Pavement type of lanes	Asphalt	240	19.02%
		Concrete	1022	80.98%
Shoulder type	Pavement type of shoulders	Asphalt	1012	80.19%
		Concrete	250	19.81%
Rumble strips	Presence of rumble strips	Exist	694	54.99%
		None	568	45.01%

2.4 Methodology

The procedure of developing a bridge collision risk index has been described in the Study Design section. Detailed information about development of the truck ROR crash prediction model, the truck-bridge collision risk analysis, the calculation of road user costs, and the ranking strategies will be introduced in this section.

Different regression models were applied to explore the relationship between the truck ROR crash frequency and various risk factors. Road user costs were calculated by estimating vehicle operating costs, the value of road users' time, and accident costs. Finally, multi-criteria decision analysis methods were used to prioritize the overpass bridges included in this study.

2.4.1 Truck Run-Off-the-Road Crash Prediction Model

The dependent variable in the crash prediction model is the number of crashes, which is a non-negative integer. Probabilistic distributions for a discrete variable are usually considered for such count models. Assuming crash data have equal mean value and variance, the probability of having y_i truck ROR crashes for a highway segment i can be estimated by a Poisson distribution shown in Equation 5.

$$P(y_i) = \frac{exp(-\lambda_i){\lambda_i}^{y_i}}{y_i!} \qquad \text{Equation 5}$$

where λ_i is the Poisson mean that can be canonically specified by a log-normal function in Equation 6.

$$\lambda_i = exp(\beta X_i) \qquad \text{Equation 6}$$

where X_i denotes a vector of geometric, weather and traffic-related variables on segment i and β is the vector of unknown coefficients for X_i. The probability that a vehicle will run off the road can be attributed to various factors, including the driver's experience, attentiveness, and reaction time. Buth et al (2010) stated that the complexity of the transportation network may also influence crash probabilities. These unobserved or unmeasured factors can easily lead to data overdispersion, or extra variability (statistical dispersion) in a data set than would be expected. Overdispersion is commonly encountered in crash count data. When the equality of the mean and variance of the crash data for a Poisson distribution is violated, a negative binomial (NB) distribution is preferred by defining λ_i as shown in Equation 7:

$$\lambda_i = exp(\beta X_i + \varepsilon_i) \qquad \text{Equation 7}$$

where $exp(\varepsilon_i)$ is a gamma-distributed error term with mean 1 and variance α. The variance-mean function for the NB distribution becomes Equation 8:

$$Var(y_i) = E(y_i) + \alpha E(y_i)^2 \qquad \text{Equation 8}$$

Thus, when α equals zero, the NB model collapses to a Poisson model. If the value of α is statistically different from zero, the NB model is more appropriate for estimating crash counts.

2.4.2 Bridge Hazard Envelope Estimation

According to *RSAP* (Mak and Sicking, 2003), at a vehicle speed of 70 miles per hour, the extreme values and the most likely values of vehicle encroachment angle θ and vehicle orientation angle φ can be determined, as shown in Table 2.4.

Table 2.4 Distribution of Vehicle Encroachment Angle and Orientation Angle

	minimum value	most likely value	maximum value
Vehicle encroachment angle (degrees)	2.5	10	32.5
Vehicle orientation angle (degrees)	-180	0	180

Due to limited data, all the encroachment angles θ were assumed to be 10 degrees and the orientation angles φ were assumed to be 7.5 degrees, based on the impact speed and angle distributions provided by NCHRP Report 492. In terms of the size and lateral offset of the hazard, the length of hazard, L_h, was assumed to be equal to the bridge deck width. The width of hazard, W_h, was assumed to be equal to the bridge bent width. Obviously, the bridge hazard envelope is proportional to the size of the vehicle and bridge structure.

2.4.3 Road User Costs Evaluation

RUCs quantify impacts that road construction activities have on the mobility and safety of travelers, and economics and environment in the local community. The components that are included are value of time (VOT), vehicle operating costs (VOC), and accident costs (AC) (Qin and Cutler, 2013). RUC is formulated as shown in Equation 9:

$$RUC = VOT + VOC + AC \qquad \text{Equation 9}$$

Where:

VOT = value of road user's time
VOC = vehicle operating costs
AV = accident costs

VOT is estimated on the basis of wage rates and delays because of the length of a trip on a detour route or an alternative route(s). The formulation is as shown in Equation 10:

$$VOT = \left(\frac{detour\ distance}{speed}\right) * 60 * volume * unit\ cost * vehicle\ occupancy\ factor \qquad \text{Equation 10}$$

The calculation of the detour distance has been introduced previously. The default values used were as follows: the speed for local roads was 55 mph, the unit cost was \$0.19/minute, and the vehicle occupancy factor was 1.67 (Qin and Cutler, 2013).

VOC is a composite of the costs associated with operation and ownership of the vehicle over the analysis period. Vehicle operating costs include the costs associated with fuel, oil, tire wear, vehicle maintenance, and repairs. Ownership costs include the costs of insurance, license and registration fee, and taxes, economic depreciation, and finance charges. The default value of the unit cost was \$0.6 per automobile per mile. The formulation is shown in Equation 11:

$$VOC = detour\ distance * unit\ cost * volume \qquad \text{Equation 11}$$

AC is measured from changes in the total annual cost of crashes as a result of a highway project. It takes potential accidents on the detour route into consideration. The formulation is as shown in Equation 12:

$$AC = (\text{detour distance} * \text{volume} * \text{accident rate} * \text{unit cost})/1{,}000{,}000 \qquad \text{Equation 12}$$

The accident rate for South Dakota local roads was 1.9 accidents per million vehicle miles of travel (SDDOT, 2012), and the default value of the unit cost was $7,400 per accident. The ADT volume traveled on a specific bridge was collected from the SDDOT. A summary of the calculated RUC for the overpass bridges on I-90, I-29, I-229, I-190, and other miscellaneous roads is presented in Appendix C.

2.4.4 Ranking Strategies

The multi-criteria decision analysis ranking strategy was used to prioritize the overpass bridges. In most cases, the MCDA divides the decision into smaller components, analyzes each component, and finally integrates the components to produce a meaningful solution. The MCDA method used in this study is the weighted sum model that calculates the sum of weighted Z-scores of collision risk and bridge RUC.

2.4.4.1 Weighted Sum Model

The weighted sum model is one of the simplest MCDA methods for evaluating alternatives in terms of decision criteria. Suppose that a given MCDA problem is defined on m alternatives and n decision criteria. Then the weighted sum score (WSS) of alternative A_i, denoted as A_i^{WSS} is defined as shown in Equation 13:

$$A_i^{WSS} = \sum_{j=1}^{n} w_i a_{ij} \text{ , for } i = 1, 2, 3, \ldots \text{ m} \qquad \text{Equation 13}$$

Where

w_{ij}= the relative weight of importance of the criteria c_j

a_{ij}= the performance value of alternative A_i when it is evaluated in terms of criteria c_j

The method of ranking was by the calculation of the sum of weighted Z-scores of the bridge collision risk (CR) and the additional RUC for the collapse of a bridge. The collision risk for a bridge bent was obtained by multiplying the truck ROR crash density by its hazard envelope. The collision risk for a bridge was calculated as the maximum value of all bridge bents. The Z-score is an effective way to compare a sample to a standard normal deviate. The Z-scores were calculated as shown in Equation 14 and Equation 15.

$$\mathrm{Z}(CR_i) = \frac{CR_i - mean\ value}{standard\ deviation} \qquad \text{Equation 14}$$

$$\mathrm{Z}(RUC_i) = \frac{RUC_i - mean\ value}{standard\ deviation} \qquad \text{Equation 15}$$

Transportation agencies may weigh CR and RUC differently. Three different weights were considered to calculate the sum of weighted Z-scores for bridge collision risk and bridge RUC, i.e., 1:1, 1:3, 3:1.

2.5 Analysis of Results

Truck ROR crashes were evaluated by the aforementioned methodologies. It was assumed that the probability that a truck will run off a homogeneous segment is uniform. A ranking of collision indexes for overpass bridges in South Dakota was created.

2.5.1 Truck ROR Crash Prediction Model Results

The Poisson and NB models were considered in this study. Results showed that the dispersion parameter α is statistically different from zero, indicating that the crash data have unequal mean value and standard deviation. Therefore, the NB model is preferred. SAS statistical software was used (see Section I.2 of Appendix I) to calculate the coefficients of the NB model. The results are presented in Table 2.5.

Table 2.5 Negative Binomial Estimation

Variable	Coefficient	P-value
Intercept	-13.2392	<.0001
Truck ADT	1.3696	<.0001
Surface type (0 if asphalt, 1 if concrete)	0.3670	0.0011
Rumble strips (0 if exist, 1 if none)	0.2355	0.0042
Horizontal curve	0.0602	<.0001
Snowfall	0.0370	0.0027
Dispersion	0.2475	

A number of variables, such as the number of lanes, lane width, median width, shoulder width, annual rainfall, and number of frost days, are not listed in Table 2.5 because they were not statistically significant (P-value ≥ 0.05). This indicates that those factors do not significantly influence the truck ROR crash frequency on the Interstate highway system.

According to the NB model results, the truck ADT coefficient is positive, which is consistent with the expectation of higher crash frequencies with higher truck ADTs. Additionally, a higher degree of horizontal curve results in an increased number of ROR crashes. Therefore, vehicles are more likely to run off the road on the segments with sharp horizontal curves, especially for trucks that have a higher center of gravity and off-tracking problems (Miaou et al., 2001). Similarly, increased annual snowfall is also found to increase ROR crashes. It is obvious that inclement weather conditions have adverse effects on trucks and that the installation of rumble strips can effectively reduce the probability of vehicle running off the roads. Most variables seem to behave as expected, except for avement type. It is difficult to explain why the concrete surface type is positively correlated with truck ROR crashes.

2.5.2 Ranking Results

Figure 2.8 presents the results ranked by quartile value. In this Figure, the X-axis represents the collision risk between trucks and overpass bridges. The unit is the number of crashes per year. The Y-axis represents the additional RUC caused by the collision with a bridge. Different symbols represent the right-side, left-side and median bents of a bridge. The three horizontal lines denote the 25, 50, and 75 percent values for RUCs and the three vertical lines denote the 25, 50, and 75 percent values for bridge collision risk, respectively. Thus, the bridge bents are distributed more than 16 clusters. Figure 2.9 shows a schematic of those clusters.

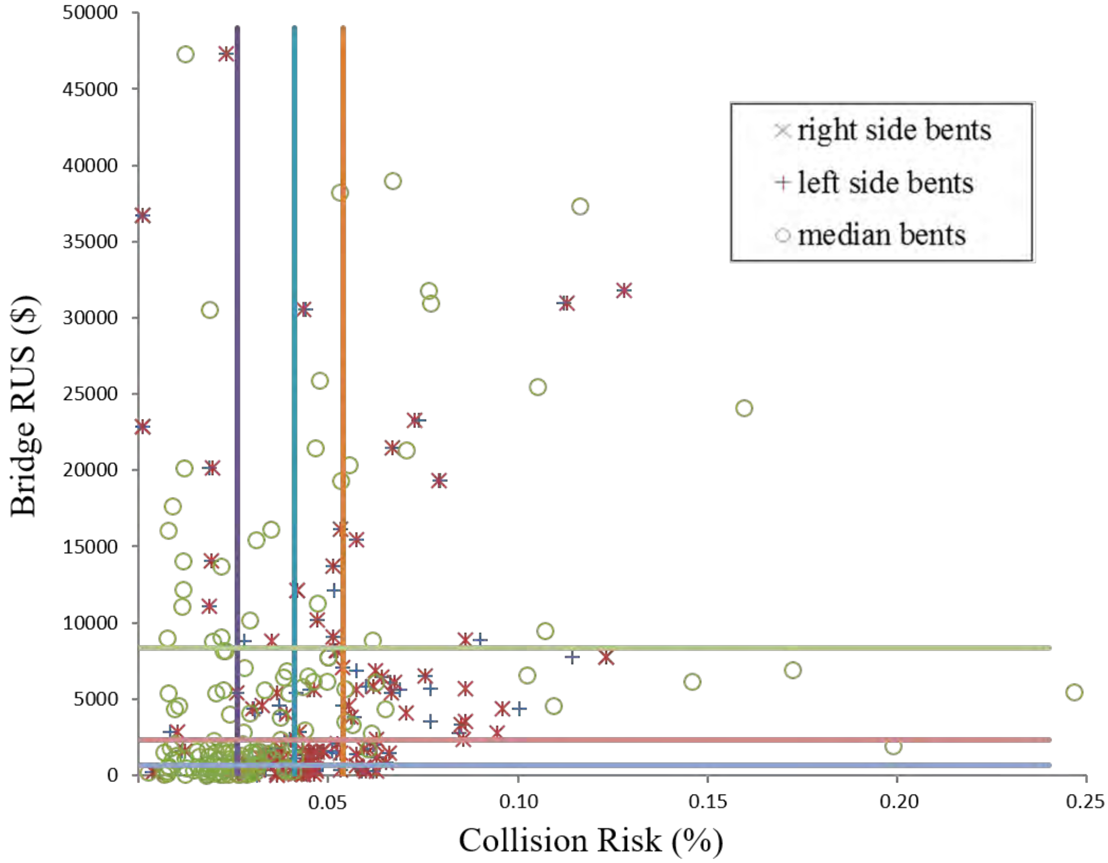

Figure 2.8 Bridge Collision Risk Profile

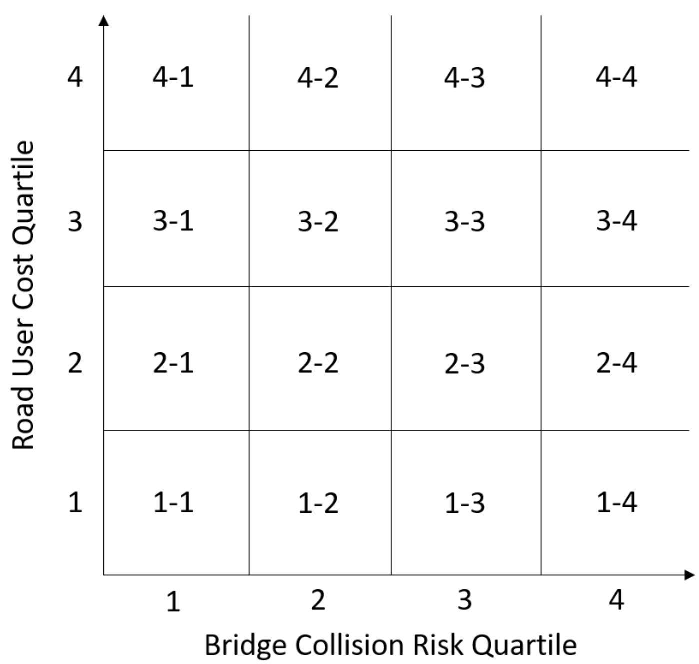

Figure 2.9 Bridge Collision Risk/RUC Clusters

Bridge bents located in Cluster 1-1 have the lowest 25 percent collision risk and the lowest 25 percent additional RUCs, while the bridge bents located in Cluster 1-2 have 25-50 percent mean values for collision risk and the lowest 25 percent additional RUCs. Following this pattern, the bridge bents located in Cluster 4-4 have the top 25 percent collision risk and the top 25 percent additional RUCs among all the bridge bents being considered in the bridge inventory included in this study. A summary of the quartile values ranking is shown in Appendix D.

Figure 2.10 through Figure 2.12 show bridge ranking by the sum of weighted Z-scores (1:1, 1:3, and 3:1) of collision risk and bridge RUC for the overpass bridges considered in this study. Length of the bar chart denotes the value of the sum of weighted Z-scores and the size of the bridge symbol denotes the total collision cost, which is calculated as the product of the truck-bridge collision risk and the bridge RUC.

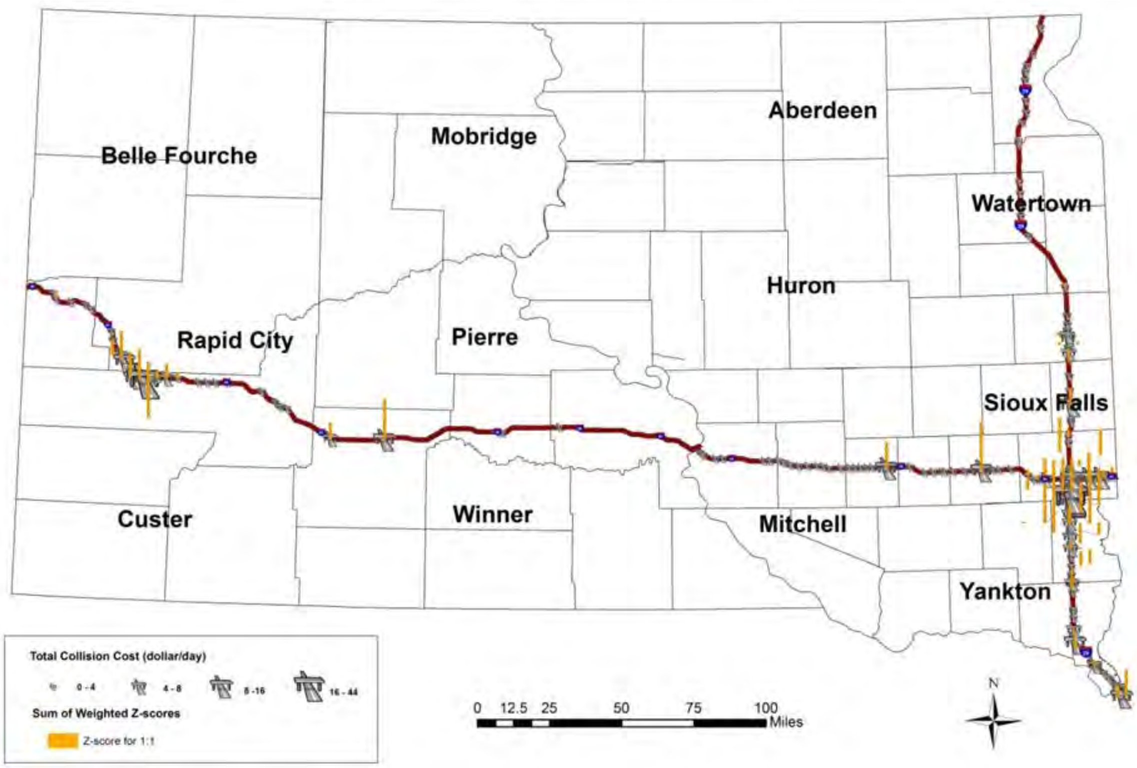

Figure 2.10 Bridge Ranking by Weighted Sum Z-scores (1:1)

Figure 2.11 Bridge Ranking by Weighted Sum Z-scores (1:3)

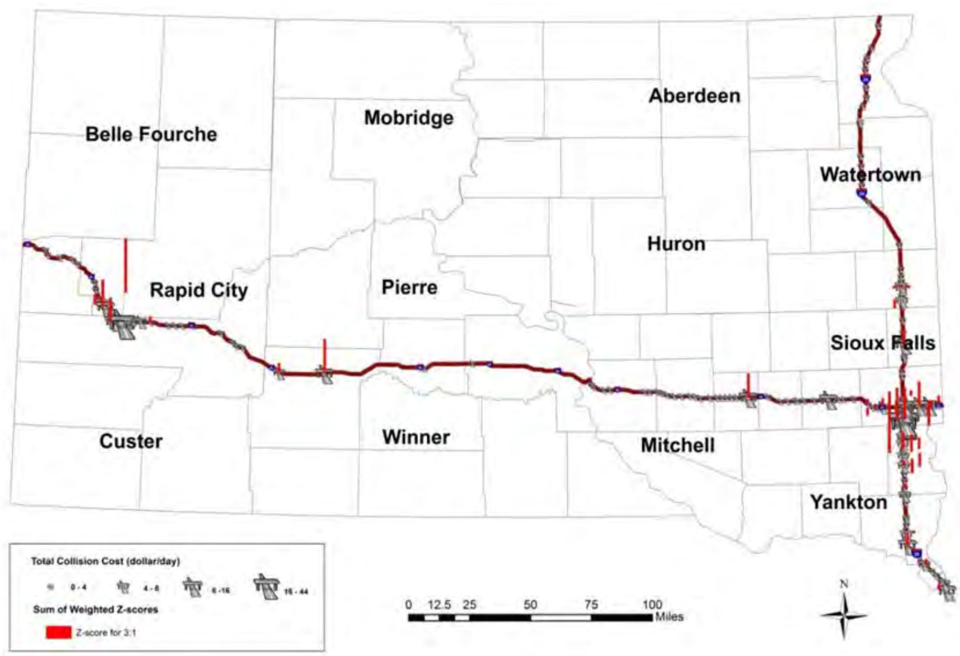

Figure 2.12 Bridge Ranking by Weighted Sum Z-scores (3:1)

According to the above figures, the ranking results by the sum of different weighted Z-scores are similar. As mentioned earlier, a larger number of high collision risk bridges are located in urban areas, which is logical because of the high truck volume and additional RUC resulting from a bridge collapse. Thus, the pattern shows a higher concentration of high collision risk bridges around Rapid City and Sioux Falls. Furthermore, the overpass bridges located on I-29 between Brookings and Sioux City show higher collision risk compared to the bridges located in other sections.

2.6 Summary

Accelerated economic development has substantially increased freight activities on the South Dakota highway system. A large amount of increased traffic is from heavy vehicles, which escalates the probability of a collision between trucks and bridges. In spite of the extremely low odds, this type of collision can be catastrophic because many overpass bridges on South Dakota's interstate highways were designed and constructed prior to development of the collision load design requirements. A collision of this kind can cause partial or total collapse of a highway bridge, and can potentially lead to major road closure. If such an event were to take place, the social and economic impacts could be enormous. Therefore, it is crucial to identify vulnerable highway infrastructure to the transportation agencies that are charged with preventing these accidents.

Crashes are random events, as they may be affected by several factors that are unknown or observable. The unobserved elements are the main contributor to data heterogeneity. To factor the data heterogeneities into the crash risk analysis of this study, random parameter count models were employed. The model output reveals that high truck traffic exposure, sharp horizontal curves, high annual snowfall precipitation, and concrete pavement increase truck ROR crash frequency. Effects vary across highway segments, due to varying roadway conditions and other factors.

A bridge collision occurs if the bridge bent happens to be located in the erratic vehicle's trajectory path. This physical exposure of a bridge to the collision can be measured by the hazard envelope, which is determined by the bridge size, vehicle dimension, encroachment angle, and orientation angle (Mak and Sicking, 2003). In this study, the hazard envelope of each bridge bent has been calculated. Coupled with the unit crash counts, the collision risk can be estimated for each bridge bent, and therefore, the collision risk for a bridge can be determined by the maximum risk of all the bridge bents.

The importance of a bridge reflects the socioeconomic impact that would result from a bridge collapse. It is calculated as the RUC because of the additional distance that would need to be traveled. When collision risk and the economic importance of a bridge were combined, two multi-criteria decision analysis methods were applied to create a bridge collision risk index and to rank overpass bridges on I-29 and I-90 in South Dakota. The method can be transferred and applied to other state DOTs with similar concerns about their bridges. It is expected that the calculated collision risk index can be used to form a prioritization policy for risk mitigation.

3. EVALUATION AND COLLAPSE MITIGATION OF VULNERABLE OVERPASSES

This section covers structural evaluation of bridge columns supporting all overpass bridges on I-90 and I-29 in South Dakota in addition to a few other highway bridges selected by SDDOT. Literature review on cases of bridge collapse under truck collision forces, development of code specifications, and previous studies on vehicle collision loads was conducted and is reported in this section. Elastic structural analysis was performed using the AASHTO-LRFD Extreme Event II load combination (AASHTO, 2012), which includes the vehicular collision force (*CT*), to determine shear and flexural demands in the bridge bents. Shear and flexural capacities were determined using the AASHTO-LRFD specifications (2012). Thus, columns having inadequate shear and/or flexural capacities were identified.

This section also covers experimental and analytical work on two scaled specimens representing an as-built and a retrofitted bent of an overpass identified as high risk for collision and vulnerable to collapse under the AASHTO vehicular collision force. A lateral load representing the AASHTO prescribed vehicular collision force was applied to the column of each specimen until failure. Conclusions and recommendations for retrofitting vulnerable bridges are presented at the end of this section.

3.1 Introduction

According to AASHTO-LRFD Bridge Design Specifications (2012), a bridge column that (1) is within 30.0 feet of the edge of the roadway, (2) lacks adequate protection for collision, and (3) does not qualify for exemption based on the annual frequency of impact must be designed for a collision load of 600 kips applied laterally at five feet above ground. This requirement is set to prevent bridge collapse under the extreme event of a tractor-semitrailer collision with the bridge column. Most overpass bridges on the interstate system and other major highways in the United States were designed and constructed prior to development of the collision force design requirements. In non-seismic regions where the lateral seismic loads on bridge columns are negligible, and in the absence of other significant lateral load requirements such as ice or collision loads on bridge piers, bridge columns were designed for low lateral load demands that did not govern the design of the columns. Therefore, the confinement and shear reinforcement in such columns was kept close to the minimum transverse steel requirements specified in the prevailing codes at the time. During a heavy truck collision incident, columns that lack sufficient shear strength and ductility due to inadequate transverse reinforcement would be vulnerable to catastrophic failure and could consequently lead to bridge collapse.

A risk assessment and mitigation strategy for protecting critical and economically essential bridges against collapse under collision loads involves ranking the bridge inventory for crash risk and identifying bridge structures that are vulnerable to collapse should a truck collision occurs. Bridges that are considered at high crash risk and vulnerable to collapse would be the top candidates for retrofit as shown in Figure 3.1.

A retrofit measure may be accomplished by either adding a protective device against collision as described in AASHTO (2012) or strengthening the bent structure to increase its capacity and meet the demand imposed by the design collision force. Protective devices can be installed only where there is adequate space around a bent such as in wide medians. The majority of existing bridges have bents located close to the roadway and do not permit for the installation of protective devices. Therefore, this study was limited to investigating retrofit measures that enhance structural capacity of inadequate bents.

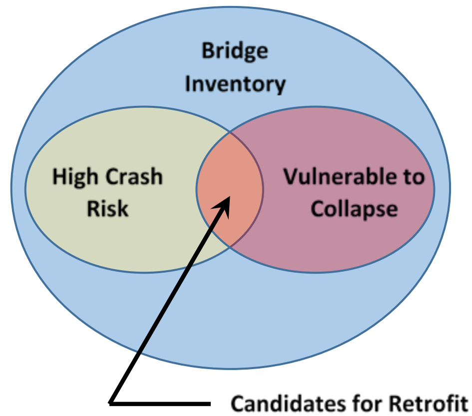

Figure 3.1 Collision Risk Assessment and Mitigation Strategy

3.2 Literature Review

The literature review covered in this section includes notable cases of truck collisions with bridge columns, progression of code specifications for collision loads, previous analytical work on collision loads, and design of a crash strut for mitigating bridge collapse under collision loads.

3.2.1 Recent Cases of Bridge Collapse under Truck Collision Loads

Although tractor-trailer collisions with bridge columns are rare, some have led to collapse of or severe damage to bridges. Three notable cases occurred near Big Springs, Nebraska (May 23, 2003), near Big Springs, Texas (November 6, 2013), and near Worthington, Minnesota (June 2, 2003).

The collision near Big Springs, Nebraska, occurred on I-80 with an overpass bridge that did not have access to the interstate and was only used by local traffic. Impact speed, and the ensuing explosion resulting from the collision, caused a complete collapse of the two interior spans of the bridge (NDOR, 2013). A second truck traveling in the opposite direction was also hit by the falling bridge.

Since there were no on/off ramps to detour traffic around the collapsed bridge, traffic on I-80 was detoured on a 10-mile route around the crash site (AP News, 2003). In addition to the expected socio-economic issues involved with the bridge being out of operation during the reconstruction phase, this accident occurred Friday evening of Memorial Day weekend. Crews were forced to work through the night in an effort to reopen I-80 as quickly as possible to reduce the effect on Memorial Day weekend traffic. Traffic on I-80 resumed on Sunday morning for the westbound lanes and late Sunday night for the eastbound lanes (NDOR, 2013). Figure 3.2 shows photos of the collapsed bridge. A second truck traveling in the opposite direction was also hit by the falling bridge.

(a) Arial View **(b)** Fallen Span on Passing Truck

Figure 3.2 I-80 Bridge Collapse near Big Springs, NE (NDOR, 2013)

The Big Springs, Texas, bridge collapse occurred on I-20 when a westbound 18-wheeler loaded with pipes for the West Texas oil fields collided with a bridge column. The collision occurred close to midnight when the truck driver overcorrected after hitting the guardrail, causing the trailer to swing around and hit a column. The collision caused two spans of the bridge to collapse. Additionally, a second 18-wheeler crashed into the collapsed superstructure. According to Texas DOT (Waltrip, 2013), the cleanup of the collapsed bridge took approximately 24 hours to get the westbound lanes of I-20 reopened to traffic. Estimated cost to repair the bridge was in the range of $5-8 million. Figure 3.3 shows the collapsed bridge near Big Springs, Texas.

Figure 3.3 I-80 Bridge Collapse near Big Springs, TX
(Midland Reporter Telegram, 2013)

On June 2, 2003, a truck collided with a bridge column on I-90 near Worthington, MN. The collision occurred in rainy weather conditions at approximately 3:00 a.m. and was the result of a blown tire which steered the truck towards the column (Haltvick, 2013). This collision bears particular relevance to the state of South Dakota as the bridge design and traffic conditions are similar to those on the South Dakota Interstate system. Although this accident did not result in collapse of the bridge deck, the impacted column failed in shear at the bent cap and a total bent replacement was needed. An item of interest is that the truck appears to have hit the guardrail and ridden along the top of the rail into the column, as can be observed in Figure 3.4.

Figure 3.4 I-90 Bridge Collision near Worthington, MN
(Courtesy MnDOT)

3.2.2 Progression of Code Specifications on Vehicular Collision Force

The majority of bridges investigated in this study were built between the 1950s and the 1970s. The governing design code during that time was the Standard Specifications for Highway Bridges, which went through several updates over the years. The last edition was published in 2002 (AASHTO, 2002). The Standard Specifications did not specify any vehicular collision forces. Therefore, bridge columns built according to the Standard Specifications were not required to be designed for vehicular collision load.

In 1994, AASHTO published the first edition of the LRFD Bridge Design Specifications (AASHTO, 1994) where vehicular collision force was first introduced. Section 3.6.5.2 of the 1994 AASHTO LRFD Bridge Design Specifications (AASHTO, 1994) stated that bridge columns should be designed for "an equivalent static force of 400 kips, assumed to act in any direction in a horizontal plane, at a distance of 4 ft above ground." The vehicular collision force is applied to the column as a point load. The 400-kip equivalent static force represented the collision force resulting from an 80-kip tractor-trailer travelling at 50 mph. The equivalent static force was based on experimental results from full-scale crash tests on barriers impacted by 80-kip tractor-trailers (AASHTO, 1994).

According to the 1994 Bridge Design Specifications, columns need not be considered at risk of collision if they are protected by "a structurally independent, crashworthy ground-mounted 54-in. high barrier, located within 10 feet from the component being protected" or "a 42 in. high barrier located at more than 10 feet from the component being protected" (AASHTO, 1994). The barrier must be capable of withstanding a Test Level 3 impact for the risk of collision to be neglected. In the second edition of the Bridge Design Specifications (AASHTO, 1998), the requirement for the loading capacity of the crash barrier was increased so that the barrier must be capable of withstanding a Test Level 5 impact. This requirement was still in effect in the 2012 version of the code (AASHTO, 2012). Test Level 3 incorporates three crash tests of two small-size passenger cars and a 2,000-kg (4,400 lb) pickup truck traveling at 100 km/h (63 mph) and impacting the crash barrier at approach angles of 20 and 25 degrees, respectively. Test Level 5 incorporates all three crash tests in Test Level 3 in addition to a crash test of a 36,000-kg (79,400 lb.) tractor-trailer vehicle travelling at 80 km/h (50 mph) and an approach angle of 15 degrees (Ross et al., 1993). The bridges included in this study were not protected by any such crash barriers.

Apart from the increase in barrier requirements, no changes were made in the vehicular collision load requirements until the sixth edition of AASHTO-LRFD (AASHTO, 2012). In the sixth edition, the vehicular collision equivalent static load was increased to 600 kips and the height of impact was increased to 5 feet above the ground. Additionally, the direction of loading was changed from "any direction" to "zero to 15 degrees with the edge of the pavement." This increase to 600 kips is based on a study performed by Buth et al. (2010), which found that a 600-kip load applied at 5 feet above the ground surface was a more appropriate load. Buth et al. (2011) performed full-scale testing of 80,000-lb. tractor-trailers crashing with bridge columns to determine the impact force and location.

3.2.3 Previous Analytical Work on Vehicular Collision Loads

3.2.3.1 Tsang and Lam (2008)

The AASHTO code (AASHTO, 2012) specifies a 600-kip static load to be used in lieu of the dynamic impact load resulting from an 80,000-lb. tractor-semitrailer traveling at 50 mph. Tsang and Lam (2008) analyzed concrete columns using quasi-static and dynamic analysis to evaluate collision forces at failure. Dynamic loading is time-dependent, where the inertial effects must be accounted for. Quasi-static loading is time dependen,t but occurs slowly enough that inertial effects can be neglected. Tsang and Lam described collapse of the column as the displacement of the column at the point of instability under imposed dead loads. Using a non-linear static (push-over) analysis, the force-displacement (P-δ) relationship was determined to calculate the column's energy absorption capacity. The total energy resulting from the impact is represented in Equation 16.

$$KE = \frac{1}{2} G V^2 \qquad \text{Equation 16}$$

where KE is kinetic energy, G is the mass of the vehicle, and V is the initial frontal impact velocity. Initially, all of the energy is absorbed by the vehicle (approximately the first 1-2 ms) as the front of the vehicle starts to crush. After this initial phase, the impact energy is partially absorbed by the column and partially by the vehicle. The absorption of energy by the vehicle, particularly at the beginning of the impact, reduces the force that is imparted to the column. Tsang and Lam found that the velocity required to cause collapse using dynamic analysis was approximately 40% higher than the velocity that would cause collapse based on quasi-static analysis. Thus, Lam et al. concluded that quasi-static analysis underestimates the energy absorbed by the column.

3.2.3.2 El-Tawil et al. (2005)

El-Tawil et al. (2005) used finite element analysis to evaluate the validity of using an equivalent static load rather than using dynamic analysis to analyze concrete columns for impact. Finite element models were created for a circular and rectangular column bridge pier and analysis was performed using a 14-kN (3147-lb) and a 66-kN (14,837-lb) truck (note that both of these trucks are significantly smaller than the 80,000-lb. truck on which the AASHTO code is based). Analyses were performed on the vehicles for a range of impact velocities from 55-135 km/h (approximately 35-85 mph). El-Tawil et al. used the equivalent static force (ESF) to compare the results to the code requirements. The ESF was the static force that resulted in the same deflection as dynamic impact force. It was found that at an impact velocity of 90 km/h (56.25 mph, which is approximately the basis of the AASHTO code requirement), the ESF for the 66-kN truck was more than 5000 kN (1125 kips). The tractor-trailers specified in the code are almost six times heavier than the 66-kN truck but the code only specifies a 600-kip static load. This indicates that current code specifications might significantly underestimate the imposed load in the event of a tractor-semitrailer collision with a bridge column.

3.2.4 MnDOT Crash Strut Retrofit

To mitigate column or bent failure due to truck collision loads, the Minnesota Department of Transportation (MnDOT) developed a retrofitting technique that can be applied to bridges not designed for collision loads. This retrofit technique, referred to as a “crash strut,” involves the construction of a partial-height wall that spans between and is attached to the bent columns. The crash strut acts as a shear wall at the portion below the point of impact and couples the columns to which it is attached.

MnDOT’s preferred method of protection is to provide sufficient barriers to prevent collision. For newly constructed one- and two-column bents where collision protection cannot be provided, the individual columns are designed to withstand a 400-kip collision load. For bents with three-or-more columns where collision protection cannot be provided, the preferred method is to design the structure for the 400-kip collision load using the crash strut (MnDOT, 2007). The philosophy behind this design approach is that one- and two-column bents are non-redundant and, consequently, the columns in those bents should be designed for the full collision force. At the time this study was started, AASHTO’s vehicular collision force had not yet been increased to 600 kips.

Per MnDOT Memo to Designers (2007), the strut is to extend a minimum of 4 ft. 6 in. above the ground surface while extending into the ground all the way to the top of the footing. The strut thickness should be a minimum of 3 ft. and should extend at least 2 in. on each side wider than the column. The strut should be doweled to the footing using a minimum of #6 bars and should be designed as a horizontal beam able to resist a 400-kip collision load between the columns. A summary of the steps for the MnDOT design of a crash strut can be found in Appendix E.

3.3 Description of the Bridge Inventory

This section presents a description of the bridges included in this study.

3.3.1 Introduction

A total of 175 overpass bridges from the South Dakota Interstate system and several other SDDOT-selected bridges throughout the state were analyzed. Table 3.1 shows the distribution of these bridges based on the roads they cross. A detailed inventory showing the bridge identification number, location, and other bridge-specific details is provided in Appendix B.

Table 3.1 Distribution of Bridges by Road

Road	Number of Overpass Bridges
I-90	81
I-29	72
I-229	11
I-190	1
Hwy 14 (Near Brookings)	1
Hwy 50 (Near Vermillion)	2
Madison St. (Sioux Falls)	2
12^{th} St. (Sioux Falls)	2
Mt. Rushmore Rd. (Rapid City)	1
Haines Ave. (Rapid City)	2

The overpass bridges analyzed were mostly two- and four-span bridges, with a small number of three- and five-span bridges. The bent can be either integral with the bridge deck or non-integral. An integral bent is one where the columns of that bent are monolithic with the bridge deck. For bridges that do not have bent caps, the girders rest directly on the columns. In integral abutments, the bridge girders are considered to have fixed support at the abutments. In non-integral abutments, the bridge girders are simply supported at the abutment sill. Most of the bridges analyzed in this study were simply-supported at the abutments. Figure 3.5 shows a typical four-span bridge with simple supports at the abutments.

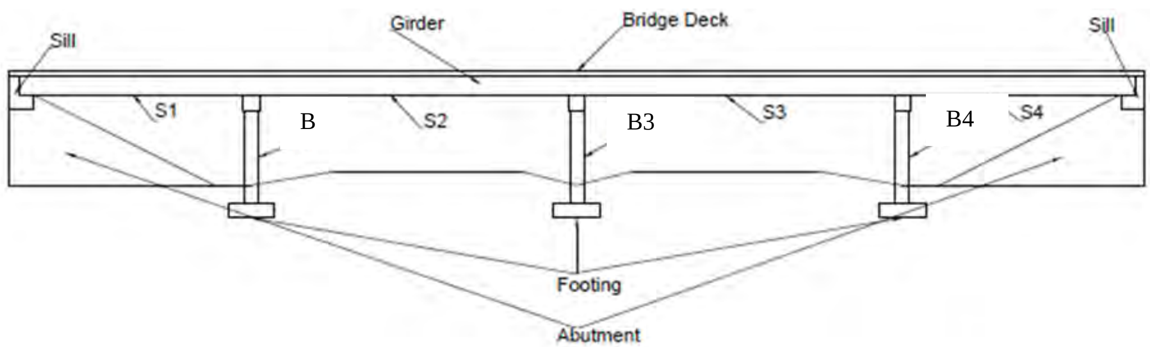

Figure 3.5 I-90 Diagram of Typical Four-Span Bridge

3.3.2 Column Types

The columns of the analyzed bridges can be grouped into seven different types: circular, square, flared, hammerhead, tee, rectangular, and octagonal. Figure 3.6 shows the different column types. The bridge type distribution is shown in Figure 3.7. Bridges with circular columns represented the vast majority of the bridges in this study (77%). Flared column bridges were the second highest in number (14%).

(a) Single Circular Column with Integral Cap

(b) Multi-Circular Columns

(c) Square Columns

(d) Flared Columns

(e) Tee Column

(f) Hammerhead Column

(g) Octagonal Column

(h) Rectangular Column

Figure 3.6 Column Types

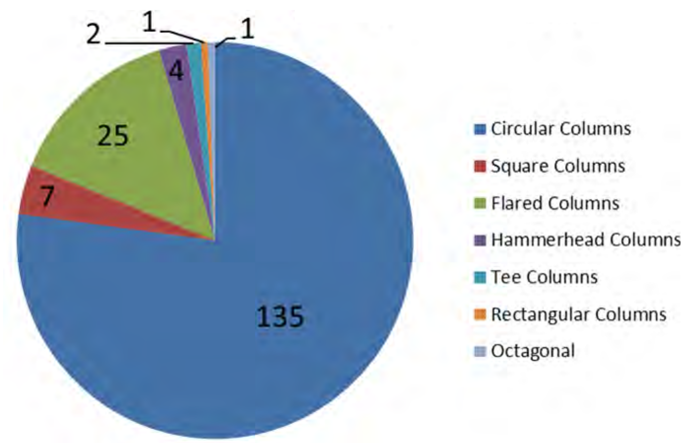

Figure 3.7 Number of Bridges by Column Type

The circular columns can be split into two groups, single-column and multi-column bents. The single-circular columns were much larger in diameter than the multi-circular columns. The single- circular columns were either 60 in. or 72 in. in diameter and were integral with the bridge deck or with box girders. Bents with multiple-circular columns had smaller diameter columns ranging between 27 in. and 42 in. Except for two bridges where girders were supported directly by the columns, the multi-circular column bridges had bent caps that supported the girders. Of the multi-circular column bridges, 69 had two-column bents. Figure 3.8 shows the distribution of bridges with circular columns based on the number of columns per bent.

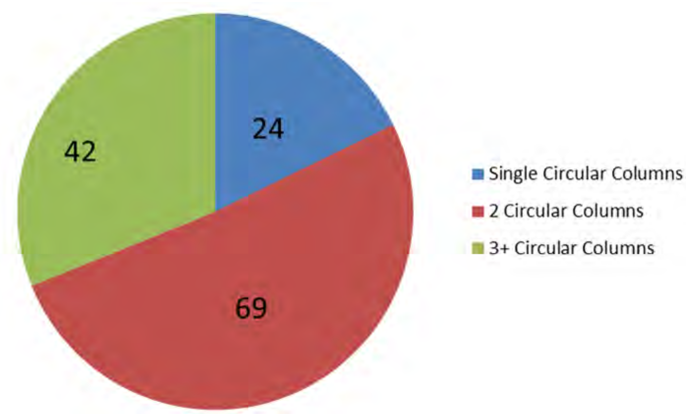

Figure 3.8 Number of Bridges with Circular Columns

All square-column bridges had at least three columns per bent. The cross-sectional dimensions of the columns ranged between 28 in. and 36 in. square.

The majority of the flared columns had a rectangular cross section widened in the direction perpendicular to the bridge longitudinal axis. Flares were either partial over the top segment of the column or full over the entire column height. Figure 3.9 shows partially-flared and fully-flared columns. There were five bridges with flared columns that also had varying depth perpendicular and parallel to the bridge longitudinal axis. All of the five bridges were located on I-29 and had no bent caps. Figure 3.10 shows flared columns with no bent caps.

(a) Partially-Flared Columns **(b)** Fully-Flared Columns

Figure 3.9 Partially- and Fully-Flared Columns

Figure 3.10 Flared Columns with No Bent Cap

Two bridges in this study were fitted with tee columns. These bridges spanned over Haines Avenue in Rapid City and carried the westbound and eastbound traffic on I-90.

The hammerhead columns were similar to the tee columns except that there were two hammerhead columns per bent. The four bridges with hammerhead columns spanned Madison Street and 12th Street in Sioux Falls and carried northbound and southbound traffic on I-29.

One bridge in this study had octagonal columns. The bridge was located west of Rapid City on I-90 and consisted of a four-span bridge with one-column bents. The column was 72 in. wide and had a 36 in. diameter hollow core that extended over the entire column height.

Only one bridge had rectangular columns with inverted flares. The cross section at the top of the column was 36-in. square. The section flared outward perpendicular to the bridge along the column length. This flare was different from the flared columns discussed earlier where the column's section flares outward towards the top of the column. The bridge with rectangular columns is a two-span bridge with a two-column bent.

3.3.3 Bridge Types

In general, there were five types of bridge superstructures on the Interstate system in South Dakota: plate girder, prestressed concrete girder, slab, square-haunch, and concrete box girder. Figure 3.11 shows the different bridge types. At the time the bridge inventory was inspected by the researchers, the most common type was the plate girder bridge (62%), followed by the prestressed girder bridge (23%). Figure 3.12 shows a chart of bridge distribution by superstructure type.

(a) Parabolic Plate Girder

(b) Unit Plate Girder

(c) Prestressed Concrete Girder

(d) Slab

(e) Square Haunch

(f) Box Girder

Figure 3.11 Bridge Superstructure Types

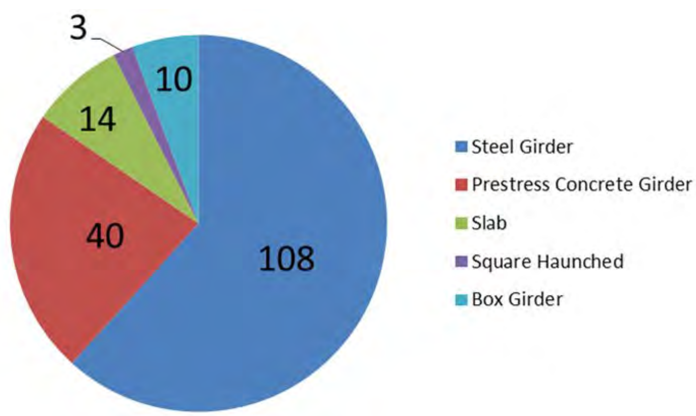

Figure 3.12 Number of Bridges by Superstructure Type

Plate girders were either “unit” or “parabolic.” A unit plate girder has a constant depth over the entire length of the girder. A parabolic plate girder is deeper at the bents and shallower at mid-span.
For the prestressed concrete girder bridge type, individual prestressed concrete girders spanned between the supports. At the interior supports, the girders were made continuous for live load.

In slab bridges, the superstructure was a slab without any supporting girders. All slab bridges were four spans with single circular column at the interior supports. The columns were integral with the superstructure. Therefore, upon collision the entire bridge would be engaged in resisting the impact. A square haunch bridge superstructure consisted of a continuous slab that was supported by multi-column bents with integral bent caps. Slab thickening was provided in the vicinity of the bent cap. The bent cap connection to the deck slab was detailed so as to provide only translational restraint to the superstructure; therefore, the entire bridge would be engaged in the event of a collision, but no moment could be transmitted between the superstructure (deck) and the substructure (bent). One of the square haunch bridges had integral abutments, while the other two were simply-supported at the abutments. Upon inspection, the middle bent of the square haunch bridges was deemed not to be in danger of collision due to the elevated concrete median which prevents a direct hit to the bent columns (see Figure 3.11 (e)). Therefore, the middle bent on the square haunch bridges was not analyzed for collision forces.

The box girder bridges were multi-cell reinforced concrete box girders with integral bent caps. Of the 10 box girder bridges included in this study, seven were four-cell and three were three-cell box girders. All of the box girder bridges were four-span bridges with single circular column bents. The columns were six feet in diameter.

3.3.4 Foundation Types

Except for two bridges that were supported by drilled pier foundations, all of the bridge columns in this study were supported by spread footings or pile caps. Figure 3.13 shows the bridge distribution by foundation type.

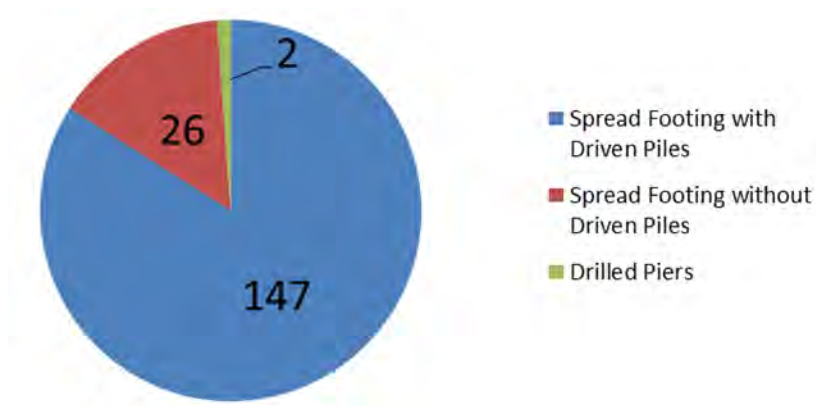

Figure 3.13 Number of Bridges by Foundation Type

3.3.5 Redundancy

A bent structure was considered redundant if it provided a path for load redistribution without losing stability in the event of a column collapse under a vehicular collision force. In this study, a bent was assumed to be redundant if it had three-or-more columns. Of the bridges included in this study, only 38% were redundant. Almost 40% of the bridges in the inventory were non-redundant two-column bents with circular columns. Figure 3.14 shows the bridge distribution by redundancy classification.

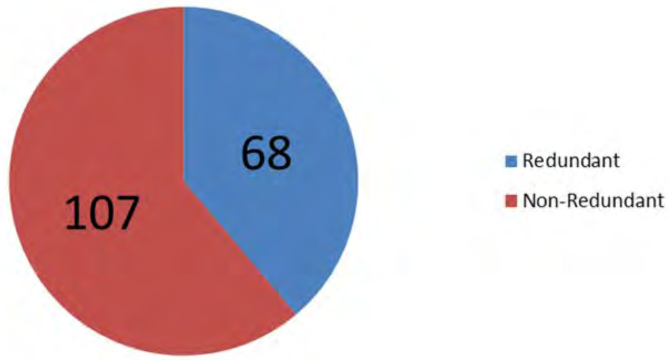

Figure 3.14 Number of Bridges by Redundancy Classification

3.4 Evaluation of South Dakota Bridge Structures for Vehicular Collision Force

Elastic structural analysis was performed to determine flexural and shear demands in the bridge columns when subjected to the vehicular collision force. The flexural and shear capacities were determined from code equations. They were compared to the demands to identify the structures that did not have adequate capacity to carry the vehicular collision force specified by AASHTO (2012). No strength reduction factors were applied to the nominal capacities since the analysis was performed for the purpose of identifying deficient bridge columns and prioritizing mitigation needs.

3.4.1 Dead Load Carried by the Columns

The shear and flexural capacities of columns are dependent on the axial load carried by the columns. Since the shear and flexural capacities of bridge columns increase with an increase in the axial load, the live load was neglected to obtain conservative lower-bound estimates for the shear and flexural capacities. Thus, the analysis was performed under an axial load that accounted for the dead load only. The axial loads in the columns were determined using the self-weight of the superstructure tributary to the columns. The unit weights were assumed to be 150 pcf for normal weight reinforced concrete, 115 pcf for light-weight concrete, and 490 pcf for structural steel. The weight of any railing along the bridge roadway was neglected due to the absence of sufficient information on the sets of plans that were available to the research team. Neglecting the railing weight reduced the axial loads in the columns and, consequently, resulted in conservative estimates for the shear and flexural capacities. A spreadsheet was created to perform the necessary calculations using input values given in the construction plan sets. A summary of the axial dead loads in the columns is given Appendix F.

3.4.2 Column Shear Capacity

The shear capacity of the columns was calculated based on AASHTO Guide Specifications for LRFD Seismic Bridge Design, 2nd Ed. (2011). A column's overall shear capacity is the result of the shear capacity of the concrete and the shear capacity of the reinforcement steel. The overall shear capacity is the summation of both shear capacity components, as shown in Equation 17.

$$V_n = V_c + V_s \quad \text{Equation 17}$$

where V_n is the nominal shear capacity, V_c is the concrete shear capacity, and V_s is the reinforcing steel shear capacity. In design, a reduction factor, ϕ, would be applied to the nominal shear capacity to obtain the design shear strength. Since the purpose of this study was to identify critical bridges that may require retrofitting rather than design new bridges, a strength reduction factor was not applied to the calculated nominal strengths.

The concrete shear capacity was determined using Equation 18:

$$V_c = v_c A_e \qquad \text{Equation 18}$$

where v_c is the unit shear strength and A_e is the effective shear area.

The unit shear strength is determined using Equation 19:

$$v_c = 0.032\,\alpha'\left(1+\frac{P_u}{2A_g}\right)\sqrt{f'_c} \quad \le \quad \min\begin{cases} 0.11\sqrt{f'_c} \\ 0.047\,\alpha'\sqrt{f'_c}\end{cases} \qquad \text{Equation 19}$$

where α' is a concrete shear stress adjustment factor, which accounts for concrete deterioration due to plastic hinging, P_u is the factored compressive force in kips acting on the section, A_g is the gross area of the member cross-section in in^2, and f'_c is the nominal concrete compressive strength in ksi. The concrete shear stress adjustment factor should not be greater than 3 and need not be less than 0.3 (AASHTO, 2011). The structural demand and capacity approach used in this analysis was based on a strength design approach without consideration of plastic response. Therefore, no shear capacity reduction for plastic hinging was adopted. Thus, the concrete shear stress adjustment factor was taken as the maximum allowable value of 3. The concrete compressive strength specified in the plan sets was used. All of the bridges included in this study had concrete compressive strength of either 4.0 or 4.5 ksi.

The flared, hammerhead, tee, and rectangular columns had dimensions that varied with height. Except for the rectangular columns, the reinforced core concrete area was constant throughout the column. The concrete area outside of the core was for architectural purposes only. Therefore, the concrete gross area was taken equal to the core area. The reinforcement in the rectangular columns flared with the columns outer dimensions. As a result, the concrete gross area varied with height; thus, the shear capacity also varied with height. Since the imposed shear on the column was constant below the impact point, the shear capacity at the most critical section was used. The critical section was at the point of application of the collision force. The effective shear area was calculated using Equation 20:

$$A_e = 0.8A_g \qquad \text{Equation 20}$$

For columns with spiral reinforcement, the shear capacity of the shear reinforcement was determined using Equation 21:

$$V_s = \frac{\pi}{2}\left(\frac{nA_{sp}f_{yh}D'}{s}\right) \qquad \text{Equation 21}$$

where n is the number of interlocking spirals or hoops, A_{sp} is the area of the spiral or hoop reinforcing bar (in^2), f_{yh} is the yield stress of reinforcing bar (ksi), D' is the core diameter of the column (in.), and s is the pitch of the spiral or the spacing of the hoop reinforcement (in.). None of the columns had interlocking spirals or hoops, so n was taken as 1. For columns with rectilinear shear reinforcement, the shear capacity of the shear reinforcement was determined using Equation 22:

$$V_s = \frac{A_v f_{yh} d}{s}$$ Equation 22

where A_v is the cross-sectional area of shear reinforcement in the direction of the shear force (in.^{2}), d is the effective depth of section (in.), and s is the spacing of the tie sets (in.). The yield strength of the reinforcing bar was given in the plan set specifications.

The shear capacity of all of the columns included in this study is summarized in Section G.1 of Appendix G.

3.4.3 Column Flexural Capacity

The flexural capacity of a column is dependent on the column geometry, reinforcement, material properties, and axial load carried by the column. The flexural capacity of a column section corresponds to an ultimate concrete compressive strain, ε_u, of 0.003 as required by AASHTO (2012). Bridge columns are seldom slender. Therefore, the slenderness effect was not considered in determining the flexural capacity of the columns.

The circular and square columns were prismatic and were reinforced with uniform main reinforcement along their entire length; thus, the flexural capacity was the same throughout the length of a column. As a result, the critical section was at the bottom of the columns where the flexural demand is highest. Except for the rectangular columns with inverted flares, the critical section of non-prismatic columns was located at the bottom of the column where the flexural demand is highest and the cross section is smallest. For the rectangular columns with inverted flares, the flexural capacity and demand were both highest at the bottom of the column and decreased with height. However, the critical section happened to be at the bottom of the column because the flexural demand decreased at a rate higher than that for the flexural capacity. Therefore, the maximum bending moment controlled the critical section.

The analytical flexural capacity was determined using the computer program spColumn (StructurePoint, 2011). The strength reduction factor was not applied to the nominal flexural capacity since the purpose of this exercise was to assess the capacity of existing rather than design new bridges. The flexural capacity of all columns included in this study is summarized in Section G.1 of Appendix G.

3.4.4 Shear and Flexural Demands

Elastic structural analysis was performed on all 175 bridge structures included in this study to identify bridge columns that would be deficient under collision loads. The structural analysis was performed to determine the flexural and shear demands in the columns under AASHTO's Extreme Event II load combination (AASHTO, 2012). This load case provides the factored load combination for dead load (DL), live load (LL) plus impact (I) due to the dynamic motion of the live load, and vehicular collision force (CV) as shown in Equation 23:

$$\textit{Factored Load} = \gamma_p\ (DL) + 0.5\ (LL + I) + 1.0\ (CV)$$ Equation 23

where γ_p is a dead load multiplier that can be varied between 0.90 and 1.25. Bridge columns are normally subjected to relatively low axial loads and are designed for axial load and bending combinations that fall below the balance points of the respective axial load-moment interaction diagrams. Thus, as the axial load increases, the column's flexural capacity increases. An increase in the axial load also increases the shear capacity of the column. The structural analysis in this study was performed assuming absence of the live load and impact since such an assumption would correspond to the most critical loading combination. Although the lowest dead load multiplier of 0.90 would be the most critical case, γ_p was taken as 1.00 since the self-weight of the columns was not added to the dead load in the analysis.

The analysis was done using SAP2000 finite element software (CSI 2012). The following assumptions were adopted to simplify the analysis: (1) under the vehicular collision force the soil was assumed to provide sufficient resistance against footing translation, (2) the column-footing connection was assumed to be a moment-resisting connection, and (3) the soil lateral pressure on the buried portion of the column was neglected. Neglecting the lateral soil pressure yielded conservative estimates for the shear and moment demands.

For the two bridges that had drilled pier foundations, the Equivalent Cantilever Method (PoLam et al., 1998) was used to model soil-structure interaction. The Equivalent Cantilever Method replaces the drilled pier with a fictitious cantilever beam fixed at its lower end and has a flexural stiffness equivalent to that of the combined pile and surrounding soil. The depth of the fixed end of the equivalent cantilever can be determined using Equation 24.

$$L_c = N_o\ D \qquad \text{Equation 24}$$

where L_c is the equivalent cantilever length (or depth below the ground surface of the equivalent cantilever), N_o is the number of diameter lengths to effective fixity, and D is the diameter of the drilled pier. The number of diameter lengths to effective fixity can be determined from the Standard Penetration Index (SPT) of the soil as shown in Figure 3.15. The soil at the bridge sites was a brown silt-clay as described in the construction plans. In the absence of a graph for silty-clays in Figure 3.15, the graph for clay soils was used. The SPT blow count was given in the plan sets and was greater than 50 blows per foot throughout the soil profile.

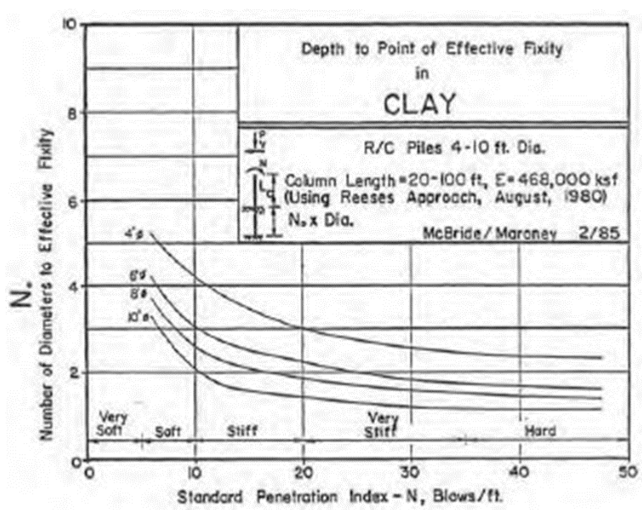

Figure 3.15 SPT Blow Count vs. Depth to Effective Fixity in Clay (Caltrans, 1990)

Prismatic columns with uniform cross-sectional reinforcement were modeled with the overall dimensions and material properties given in the plan sets. For columns that did not have constant cross-sections, average cross sectional properties were used. For example, a flared column was modeled as a prismatic column with a rectangular section based on averaging the properties of the sections at the top and the bottom of the column. A more accurate model could have been obtained by dividing the column into multiple segments and using the average cross sectional properties of each segment. Because the difference in the results of the two models was minimal, it was decided to model the columns as single elements with uniform cross sections.

The superstructure of a bridge with integral bent caps would be mobilized under a vehicular collision load applied to one of the bent columns. However, the superstructure provides little or no resistance to a vehicular collision force when the bent caps are non-integral. Therefore, when performing structural analysis, the entire bridge (superstructure and substructure) was modeled for integral bent cap bridges, while only the bent structure was modeled for non-integral bent cap bridges. Extruded views and line element models for a non-integral and integral bent cap bridges are shown in Figure 3.16 and Figure 3.17, respectively.

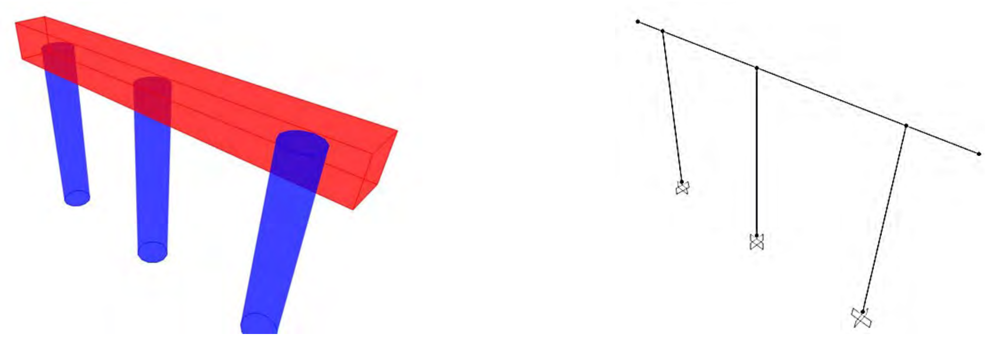

(a) Extruded View **(b)** Line Element Model

Figure 3.16 Model of a Non-Integral Bent

(a) Extruded View **(b)** Line Element Model

Figure 3.17 Model of an Integral Bent Bridge

A 600-kip load was applied horizontally at a height of five feet above the ground surface, as specified by AASHTO (2012). For each bridge, two different loading patterns were used in the analysis, one where the load was applied parallel to the roadway and the other where the load was applied at an angle 15° to the roadway. The higher shear and bending moment demands were selected to assess the adequacy of the columns for the vehicular impact force. A summary of shear and flexural demands is presented in Section G.2 of Appendix G.

3.4.5 Assessment of Bridge Vulnerability under a Vehicular Collision Force

The shear and flexural demand-to-capacity ratios (D/C) for the columns were calculated using the analytical shear and flexural capacity and demand values. Thus, a D/C ratio of greater than one indicates that a column is inadequate (insufficient) under the applied 600-kip vehicle collision force. A summary of the D/C values is presented in Section G.3 of Appendix G. Only 35 bridges had columns classified as "Sufficient" in shear and flexure. The columns of the remaining bridges were classified as "Insufficient."

Of the 175 bridges considered in this study, the columns of 140 bridges were found to be structurally inadequate in flexure, shear, or both. In the event that a bridge has "Insufficient" columns, the redundancy of the structure becomes an important factor when considering potential collapse of the superstructure. If a bridge column fails under a collision force and the gravity load from the superstructure gets safely redistributed to the remaining columns, then collapse of the superstructure will not occur. Therefore, bridges that are non-redundant and have columns that are "Insufficient" would be considered most vulnerable to collapse under a vehicular collision force. Of the 140 "Insufficient" bridges, 87 bridges were found to be also non-redundant. The bridge distribution based on sufficiency and redundancy is shown in Figure 3.18.

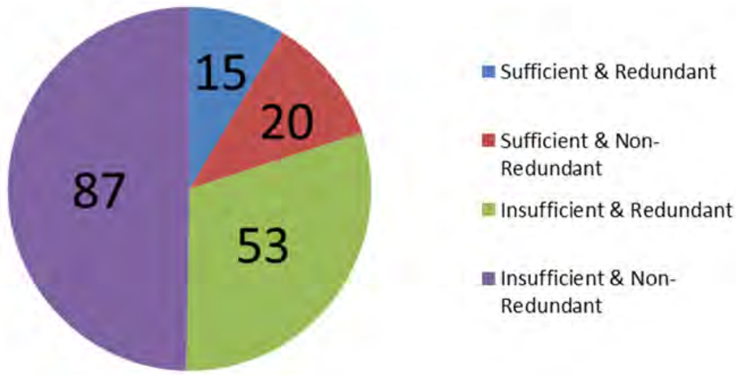

Figure 3.18 Number of Bridges Based on Sufficiency and Redundancy

All two-column bents with circular columns were non-redundant and had "Insufficient" columns. The square haunch bridge was considered "Sufficient" because of the collision protection provided by the concrete median wall. The circular columns of the single-column bents were "Sufficient" in shear, but half of these columns were "Insufficient" in flexure. Of the 25 flared-column bridges, 15 were "Sufficient" and one-half of the "Insufficient" flared column bridges were bridges without bent caps.

3.4.6 Prioritization of Vulnerable Bridge Bents for Collapse Mitigation

The collision risk and the collapse vulnerability analyses were combined to identify high-risk deficient bridge bents and prioritize mitigation needs. Results are presented in Appendix D. Each bent listed in the 16 clusters of the quartile risk ranking is labeled with a string of alpha-numeric characters to indicate bridge identification, road crossed by the bridge (**I-90**, **I-29**, etc.), mile marker, bent location (**L**eft, **M**edian, **R**ight) relative to the bridge, bent redundancy (Redundant: **R**; Non-Redundant: **NR**), and column strength adequacy (**S**ufficient; **I**nsufficient). The bent location identification (L, M, R) is based on bent location on the construction plans. Bent structures with inadequate column strength are labeled with red font.

The collapse of inadequate bents vulnerable to vehicular collision forces could be mitigated through installing protective devices or implementing retrofit measures to enhance the bent's strength. However, retrofitting all inadequate bents is cost prohibitive. One strategy to prioritize bridge bents for collapse mitigation retrofit would be to consider the pool of bridge bents that fall in clusters 4-4, 3-4, and 4-3. This pool of bridge bents includes 35 single-circular column bents, 35 two-circular column bents, 22 three-or-more-circular column bents, and 16 two-or-more-flared column bents. Of those bents, almost all the two-or-more-circular column bents, eight of the single-circular column bents, and five of the flared-column bents were inadequate under a vehicular collision force. Table 3.2 presents a summary of the bridge bent types in the high-risk collision pool (clusters 4-4, 3-4, and 4-3). Figure 3.19 shows pictures of typical bridge bents in the high collision risk pool. By considering the vulnerable bents in the high collision risk pool, a priority list for protection or retrofit can be generated by SDDOT engineers and planners, depending on additional factors including the remaining useful life of the bridge, availability of resources, and cost effectiveness of implementing the same retrofit method for a group of bents that share the same features.

Table 3.2 High Collision Risk Bents

	Bent Type			
	Single-Circular	**Two-Circular**	**Three+-Circular**	**Flared**
Total Number of Bents in Collision Risk Clusters 4-4, 3-4, and 4-3	35	35	22	16
Number of Inadequate Bents in Collision Risk Clusters 4-4, 3-4, and 4-3	8	35	21	5

(a) Single-Circular Column Bent

(b) Two-Circular Column Bent

(c) Three-Circular Column Bent

(d) Flared-Column Bent

Figure 3.19 Typical Bridge Bents in Collision Risk Quadrants 4-4, 3-4, and 4-3

3.5 Proof Tests of As-Built and Retrofitted Two-Circular Column Bents

This section presents the experimental work conducted in this study to evaluate structural performance of an as-built bent and a retrofitted bent when subjected to AASHTO’s vehicular collision force. The experimental work involved load tests of two 1/3-scale specimens at the Lohr Structures Laboratory at South Dakota State University. One specimen represented a two-circular column bent of a prototype I-29 overpass that was determined by analysis to be inadequate for the vehicular collision force. The other specimen represented a similar bent, but retrofitted with a crash strut to resist the collision force. The main objectives for the laboratory tests were to evaluate the performance of the as-built condition of the bent and verify the effectiveness of the crash strut when the bent specimen is subjected to combined gravity loads at the bent cap and in-plane lateral force at the middle of one column.

3.5.1 Selection and Description of the Prototype Bridge

The prioritization analysis indicated that the two-circular column bent type represented the vast majority of the structurally inadequate bents in the high-risk collision pool (clusters 4-4, 3-4, and 4-3) and all of the 35 two-circular bents in the high-risk collision pool were also structurally inadequate. Moreover, two-column bents are non-redundant and represent worst case scenario for catastrophic collapse under a vehicular collision force. In a meeting that was held on June 14, 2013, the research team and the technical panel agreed to select one of the high-risk two-circular column bents as the prototype structure for experimental investigation. The selected prototype overpass was Structure No. 51-065-150 which carries Highway 34 over I-29 at milepost 109. The bents of this bridge fell within collision risk cluster 4-4. A view of the prototype bridge is shown in Figure 3.20 and the details of the bent are shown in Figure 3.21.

Figure 3.20 The Prototype Bridge

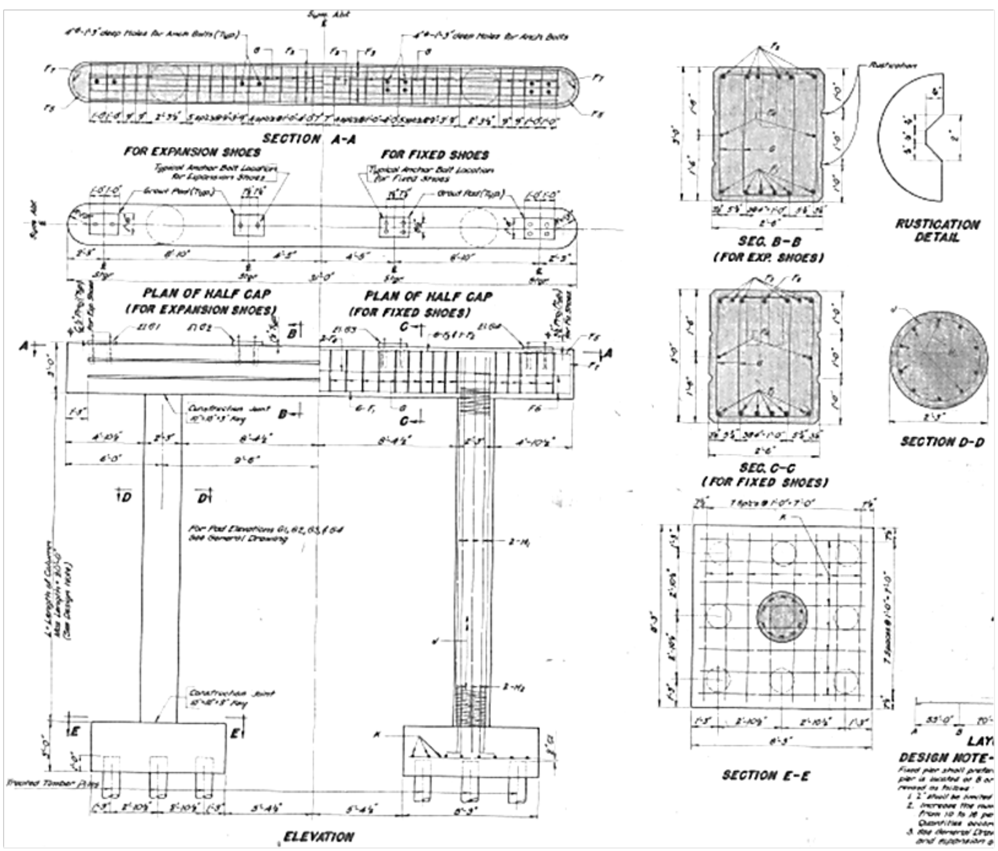

Figure 3.21 Details of the Prototype Bridge Bent (Courtesy SDDOT)

The bridge superstructure consisted of a concrete deck supported by four steel plate girders. The girders were supported at the bent cap by roller supports, with two girders located between the columns and one girder located at each bent cap overhang. Each column was 27 in. in diameter and was reinforced with 10 #11 longitudinal bars and #4 spiral at 2 in. pitch. The bent cap was 36 in. deep, 30 in. wide, and 372 in. long, and was reinforced with six #11 top and six #11 bottom bars. The shear reinforcement consisted of two #5 overlapping ties spaced at 9 in. in the column region and at 12 in. elsewhere, as is shown in Figure 3.21. The clear cover for the columns and the bent cap was 2 in. Each column was supported by a 36 in. deep by 99 in. square footing supported by nine piles. The footing was reinforced with eight #8 bottom bars in each direction. The specified yield strength of the steel reinforcement was 50 ksi and the specified concrete strength was 4000 psi.

3.5.2 Selection and Description of the Retrofit Method

The research team and the technical panel agreed to test effectiveness of the MnDOT crash strut as a retrofit measure for the inadequate bridge bents in South Dakota. The crash strut is simply a partial height wall that spans between the bent columns and is anchored to the top of the footings. The crash strut would resist the collision load through development of shear stresses in the strut wall. An early version of a crash strut retrofit is shown in Figure 3.22. The crash strut in Figure 3.22 does not wrap around the columns, but the recent MnDOT detailing requires the strut to extend 6 in. past each column. A slightly modified version of the MnDOT crash strut was adopted for the retrofitted test specimen.

Figure 3.22 Crash Strut Retrofit (Courtesy MnDOT)

3.5.3 Design and Construction of the Test Specimens

The two test specimens were identical except for the addition of a crash strut to the retrofitted specimen. The as-built specimen was labeled NCS (No Crash Strut) and the retrofitted specimen was labeled CSR (Crash Strut Retrofit).

The columns were 9 in. in diameter and were reinforced with 8-#4 longitudinal bars and W5 smooth wire spiral at 1.75 in. pitch. The column clear height between the top of the footing and the bent cap soffit was 80 in. The clear concrete cover was 5/8 in. Since the only steel reinforcement available for the construction of the specimens was Grade 60, the provided steel reinforcement was slightly lower than what would be required based on Grade 50. The reduced steel amount was selected to maintain the target flexural and shear strengths of the scaled specimens. Figure 3.23 shows details of the columns of the test specimens. The bent cap was 10 in. wide by 12 in. deep and was reinforced with three #3 top and bottom bars. The shear reinforcement consisted of #3 ties spaced at 5.25 in. in zone Z1 and 7.25 in. in zone Z2 as shown in Figure 3.24. The longitudinal and transverse steel were fitted with strain gages at the column's mid-height and the column-footing interface.

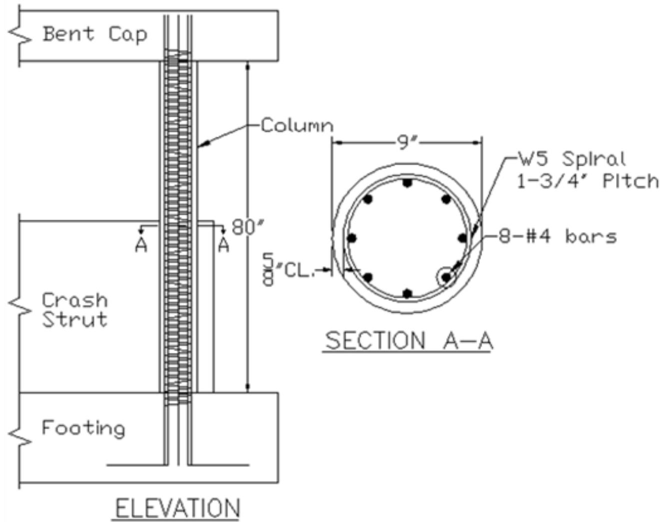

Figure 3.23 Details of the Test Specimen Columns

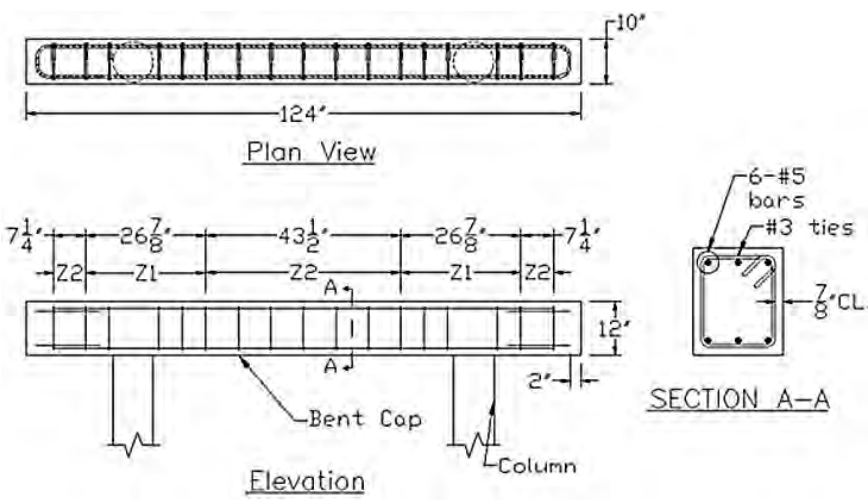

Figure 3.24 Details of the Test Specimen Bent Cap

Minnesota DOT crash strut design requires the strut to be extend vertically from the top of the footing to a minimum distance of 4.5 ft. above the ground level. In this study, the crash strut of the prototype was considered to extend to 5 ft. above ground level to match the collision force application point specified by AASHTO. MnDOT also specifies that the crash strut should extend horizontally a minimum of 6 in. past each column in the longitudinal direction and a minimum of 2 in. on each side of each column in the transverse direction. The 6-in. extension on the prototype would be a 2-in. extension on the ⅓-scaled specimen. However, 4-in. extension was provided in the specimen to allow for placement of the strut reinforcement.

The MnDOT design method for the crash strut is based on assuming the strut to behave as a flexural member subjected to a collision force between the column supports. Based upon the design of the prototype crash strut, the specimen crash strut was 12 in. wide by 41.5 in. high. The length of the strut was 92 in. on one side and 95.25 in. on the other side as shown in Figure 3.25. The different lengths were needed to form a chamfered vertical face that would allow for lateral load application at 15˚ to the bent plane. The longitudinal reinforcement consisted of 10-#3 bars and the shear reinforcement consisted of #3 stirrups placed at a spacing of 9.75 in. on center. The crash strut was anchored to the footing at each column by means of 7-#3 dowel bars on each side of the column. The dowel bar was 11.5 in. long with 4.5 in embedment length into the footing.

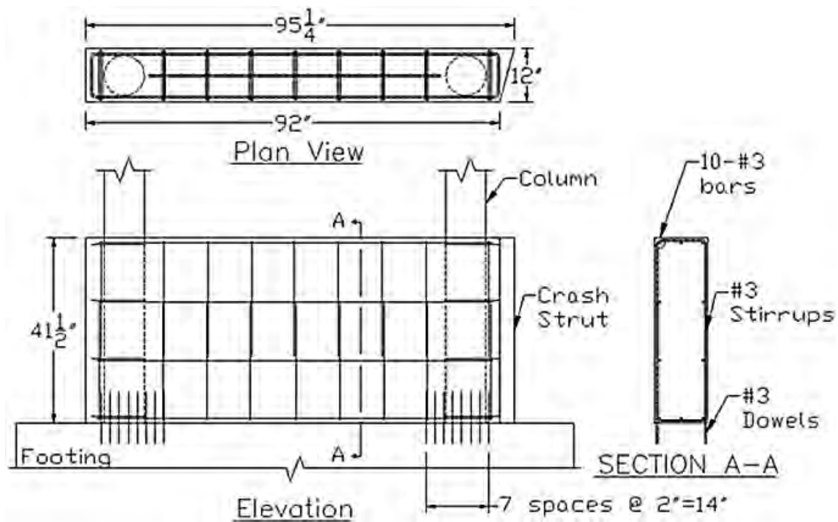

Figure 3.25 Details of the Test Specimen Crash Strut

Design of the test specimen footing did not follow the prototype footing. Instead of a single footing under each column, one continuous footing was designed to support both columns of each specimen. The continuous footing was needed to facilitate moving the test specimens inside the laboratory. Since uplift of the footing during the test was retrained by tie-downs, the footing needed to be designed for both a positive and negative bending moment. To simplify the construction of the footing, identical reinforcement was used in the top and bottom of the footing. Five #9 longitudinal bars and seven #5 bars in both the top and bottom of the footing were used to provide the flexural reinforcement. The concrete clear cover was 2 inches on all sides. Figure 3.16 shows the details of the footing.

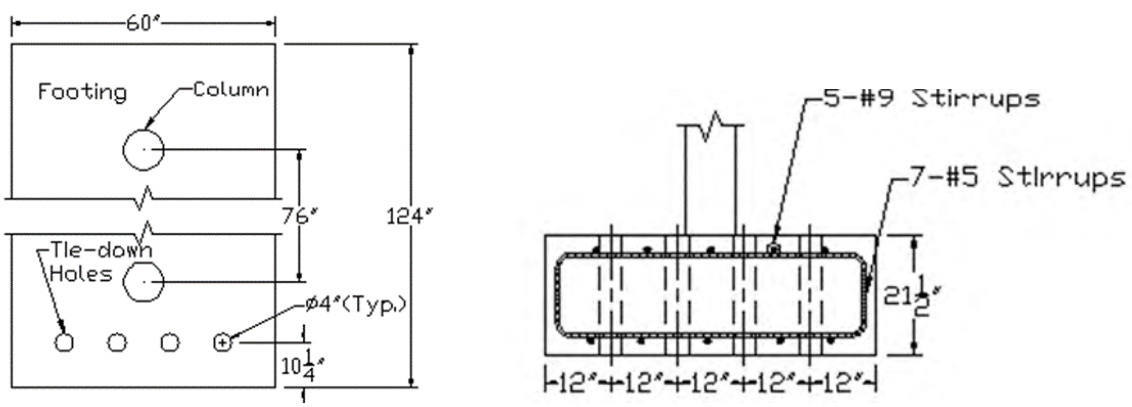

(a) Plan View **(b)** Transverse Section

Figure 3.26 Details of the Test Specimen Footing

The specimens were cast using ready-mixed concrete. The measured concrete strengths on the day of testing were 4890 psi and 5450 psi for the NCS specimen and the CSR specimen columns, respectively, and 5700 psi for the crash strut. Figure 3.27 shows the test specimens during construction.

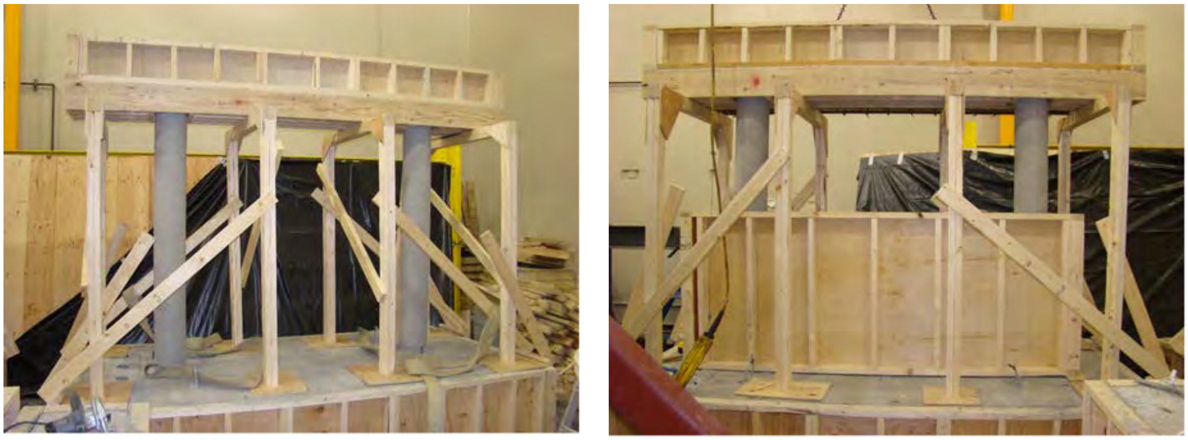

(a) Specimen NCS **(b)** Specimen CSR

Figure 3.27 Test Specimens during Construction

3.5.4 Instrumentation

The specimens were instrumented using a combination of strain gages to determine stress in the reinforcement and cable-extension transducers to measure the displacement of the bent cap. A total of sixteen strain gages and four cable-extension transducers were used in each test.

All strain gages were installed in the front (South) column. Twelve strain gages were installed on the longitudinal bars—six on the front (South) bar and six on the back (North) bar as shown in Figure 3.28. The gages were placed at the base of the column and at the location of the lateral load. The longitudinal bar gages were labeled N for North (back bar) or S for South (front bar), followed by a number (1 to 6) that corresponded to the vertical location of the gage. Four strain gages were installed on the spiral reinforcement at approximately 9.25 in. above and 9.25 in. below the point of application of the lateral load. The gages were placed at 15° to the plane of the bent to align with direction of the lateral load. Figure 3.28 shows a schematic of the spiral reinforcement strain gage locations. The spiral bar gages were labeled E or W, followed by a number (1 or 2) that corresponded to the vertical location of the gage.

Two cable-extension transducers were attached to each end of the bent cap to measure the end displacement in two directions. This allowed for determining the displaced location of the bent cap under the applied out-of-plane lateral load and the potential for unseating of the outer girders. A schematic view of the transducers arrangement is shown in Figure 3.28.

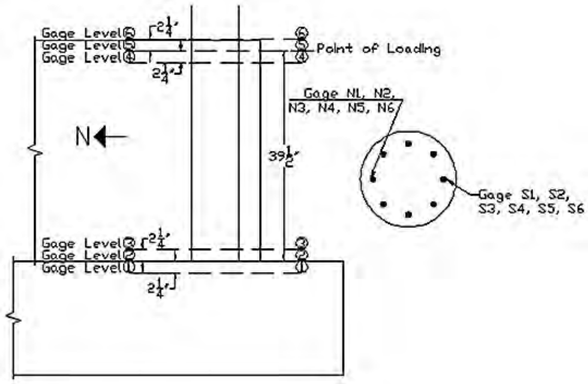

(a) Strain Gages on Main Reinforcement

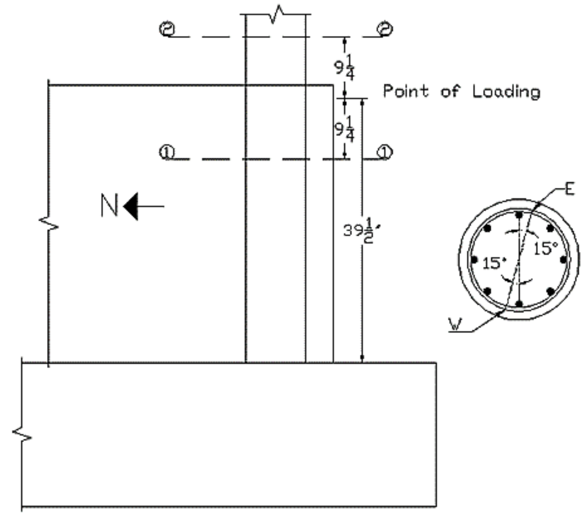

(b) Strain Gages on Transverse Reinforcement

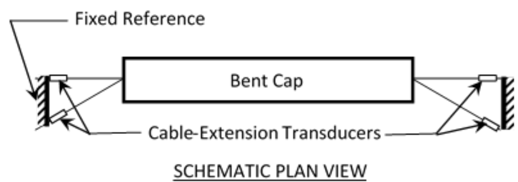

(c) Cable-Extension Transducers

Figure 3.28 Instrumentation of the Test Specimens

3.5.5 Test Set Up

Each specimen was subjected to four static vertical loads along the bent cap length and an increasing lateral load. The lateral load was applied to the column at 39.5 in. above the footing and at an angle of 15˚ to the bent plane since the out-of-plane lateral load was determined to be more critical than the in-plane load. The vertical loads represented the dead load from the superstructure while the horizontal load represented the vehicular collision force. Figure 3.29 shows the test set up.

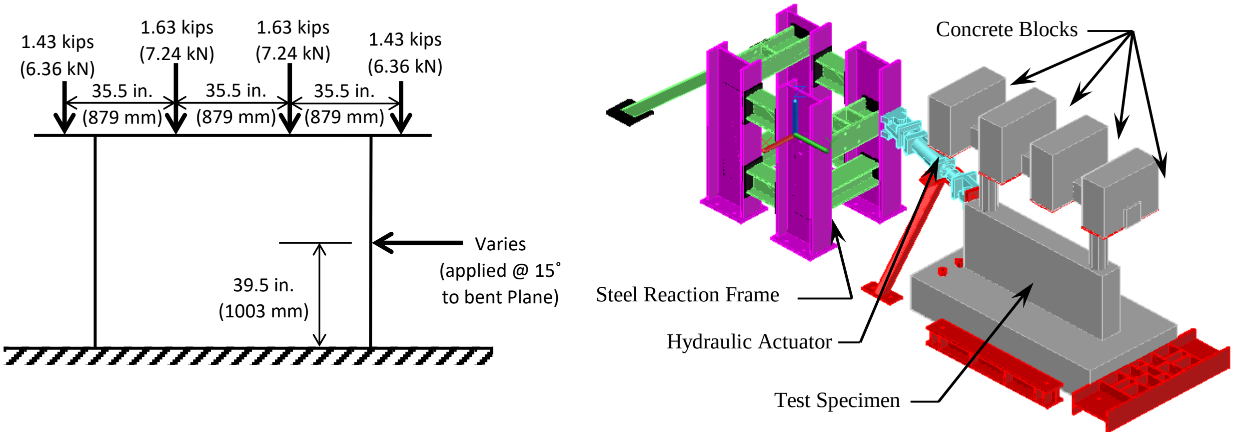

(a) Schematic diagram **(b)** Isometric view

Figure 3.29 Test Set Up

Vertical loads were applied by means of four concrete blocks mounted on top of the bent cap. The horizontal load was applied by means of a 146 kip hydraulic actuator that reacted against a steel frame anchored to the strong floor. To prevent overturning and sliding of the specimen, the footing was tied down to the floor by means of four post tensioning rods and was held in place by means of steel beams anchored to the floor. The lateral loading was applied under displacement-controlled protocol. The loading was quasi-static with displacement increments ranging between 0.02 in. during the initial elastic response and 0.1 in. after significant yielding had occurred. Figure 3.30 shows specimen NCS in place prior to the test.

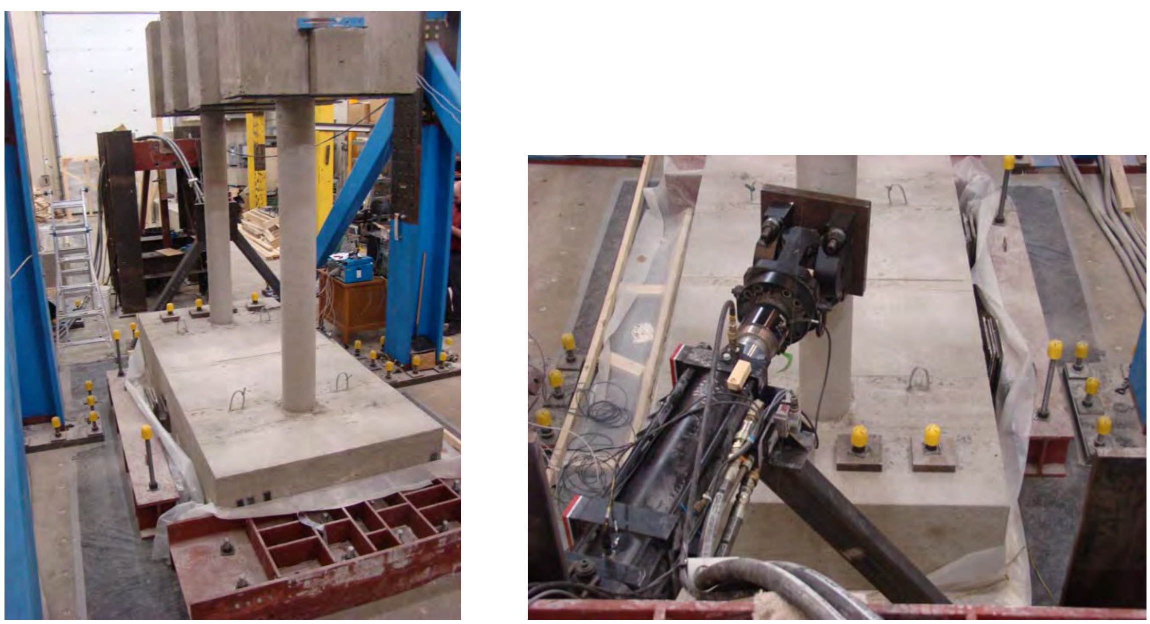

(a) Specimen NCS Set Up **(b)** Actuator Set Up (15° Out-of-Plane)

Figure 3.30 Specimen NCS after Set Up

3.7.6 Experimental Results

Prior to testing, an elastic structural analysis was performed for test specimens to compare the internal forces during the elastic response phase. The analysis was performed using structural analysis software

SAP2000 (CSI, 2012). Figure 3.31 shows plots of the shear and bending moments for the two specimens. All bending moment values are shown relative to the maximum bending moment M for a given lateral load. The maximum bending moment occurs at the bottom of the loaded column, and the bending moment values in the retrofitted bent are negligible.

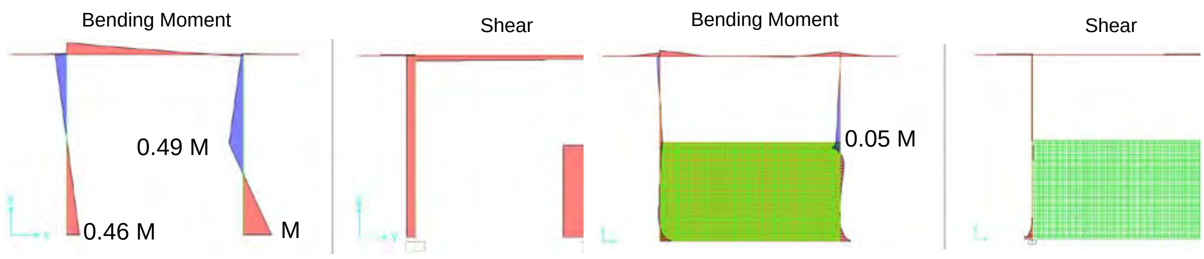

(a) Specimen NCR **(b)** Specimen CSR

Figure 3.31 Elastic Analysis Shear and Bending Moment Diagrams

3.5.6.1 Specimen NCS

Specimen NCS was tested first. The measured actuator load versus the actuator displacement is shown in Figure 3.32.

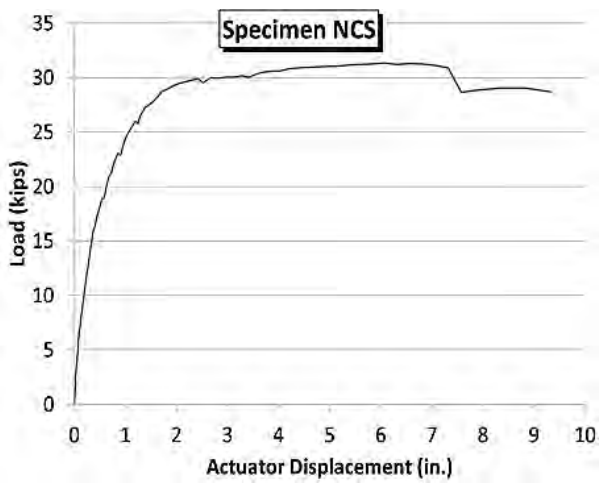

Figure 3.32 Measured Actuator Load-Displacement – Specimen NCS

The first flexural cracks started to form at the bottom of the loaded column at a lateral load of 7.97 kips and a corresponding actuator displacement of 0.13 in. At a displacement of 0.25 in. and a corresponding lateral of 12.14 kips, flexural cracks were visible at the mid-height of the loaded column and at the top and bottom ends of the unloaded column (back column). As the load increased, the loaded column started to exhibit inclined shear cracks at its base and distributed flexural cracks along its height. At approximately 30 kips and a corresponding displacement of 2.30 in., the lateral load started to plateau. The maximum recorded lateral load was 31.3 kips at a displacement of 6.06 in. At a displacement of 9.33 in. two longitudinal bars ruptured in tension at the base of the loaded column. The bar rupture was followed immediately by a drop in the lateral load to 20 kips. At this stage, the specimen was considered to have failed. Figure 3.33 shows specimen NCS at different stages of the test. The 600 kip vehicular collision force specified by AASHTO is equivalent to 66.7 kips for the scaled specimen. Thus, specimen NCS could only sustain 47% of the required design collision load.

Strain measurements obtained from the strain gauges attached to the reinforcing steel showed that yielding of the tension steel in the loaded column started at the base at approximately 15 kips and at the mid-height of the column at approximately 20 kips. The transverse reinforcement remained essentially elastic throughout the test. Plots of the strain measurements are presented in Appendix H. At the end of the test, it was visually observed that significant inelastic deformations had also occurred at the top and bottom of the back column. Thus, the development of four plastic hinges (two hinges in each column) resulted in the formation of a frame mechanism. Figure 3.34 shows locations of the plastic hinges in specimen NCS after the test was completed.

(a) Start of Testing

(b) Cracking in the Loaded Column

(c) Cracking in the Back Column

(d) Plastic Deformation in the Loaded Column

Figure 3.33 Specimen NCS at Different Stages of the Test

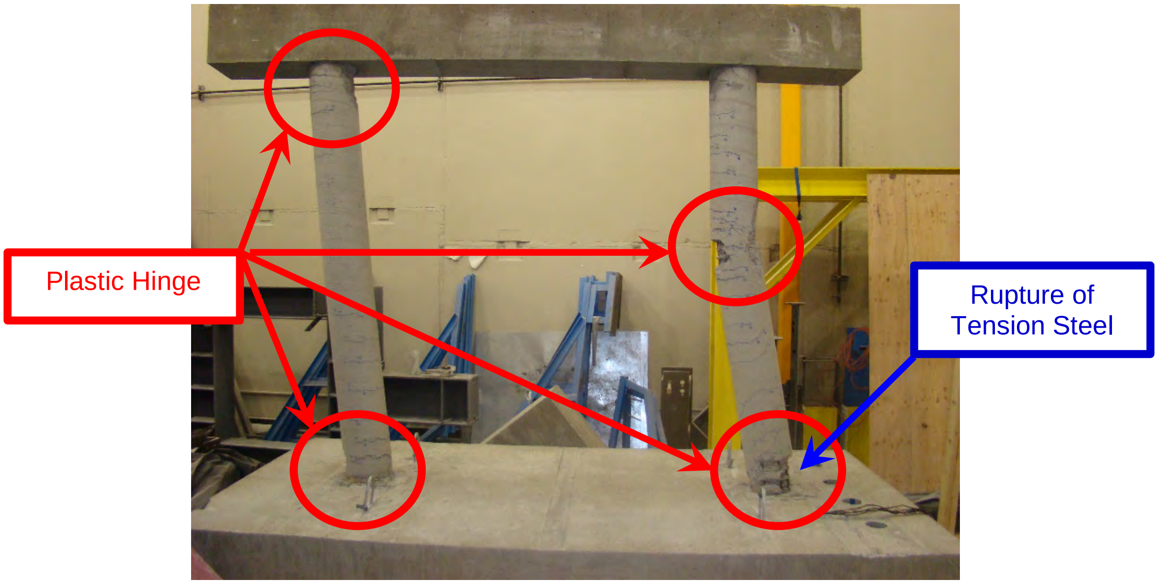

Figure 3.34 Plastic Hinging in Specimen NCS

Figure 3.35 shows a plot of the displaced location of the bent cap centerline at progressively increasing lateral load. The Y- and X directions in the plot represent the bent's in-plane and out-of-plane directions, respectively. The displaced location was determined from the measured displacements at the bent cap ends. The rotation experienced by the bent was the result of the out-of-plane lateral load. Excessive out-of-plane displacement of the bent cap could result in unseating of the edge girder at the collision force side. The maximum out-of-plane displacement at the edge girder location (on the loaded columns side) of specimen NCS was 8.5 in. This displacement is equivalent to 25.5 in. on the prototype. The girder seat in the prototype structure was 24 in. long in the longitudinal direction by 18 in. wide in the transverse direction. A 25.5 in. transverse displacement of the cap centerline would result in unseating of the edge girder.

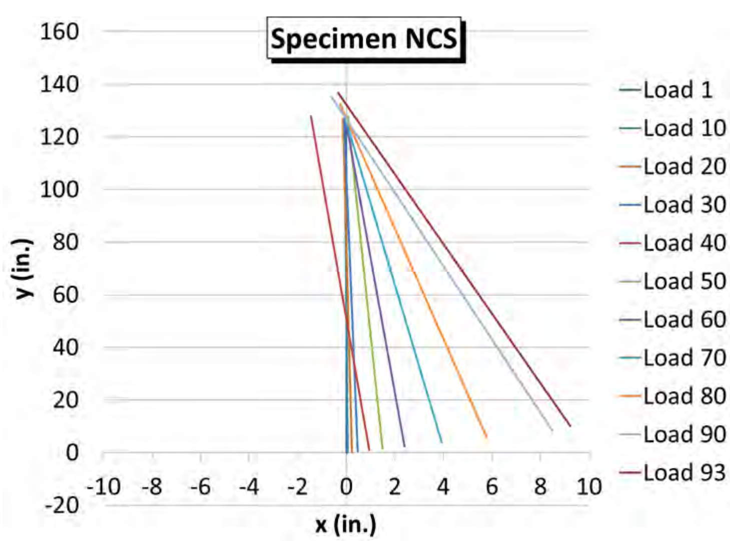

Figure 3.35 Displacement of the Bent Cap Centerline – Specimen NCS

3.5.6.2 Specimen CSR

Specimen CSR was tested under the same conditions applied to specimen NCS. However, the actuator head was aligned with the top of the crash strut. Thus, the load was applied to the top of strut instead of the column. The measured actuator load versus the actuator displacement is shown in Figure 3.36.

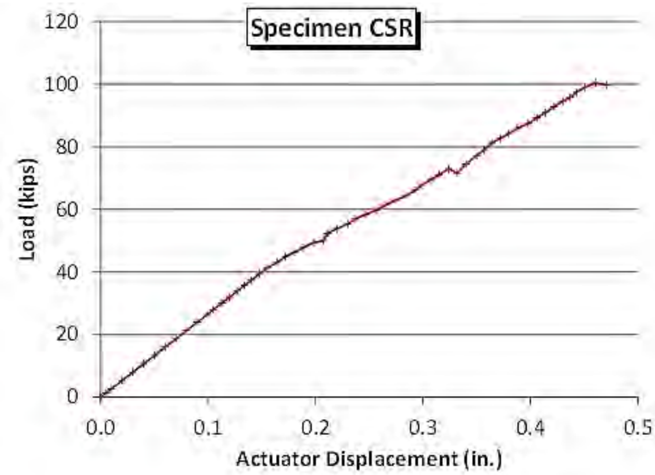

Figure 3.36 Measured Actuator Load-Displacement – Specimen CSR

The crash strut increased the elastic stiffness of specimen CSR by approximately 7.5 times that of specimen NCS. The response was essentially elastic throughout the test. At a load of 71.2 kips and a corresponding displacement of 0.38 in., a horizontal crack initiated at the top of the crash strut. It was observed that the crack had formed in the cover concrete as a result of the direct horizontal loading at the top of the strut. Failure occurred in the footing at a load of 100 kips and a corresponding displacement of 0.56 in. The failure was the result of an inclined crack that formed at the bottom corner of the footing and extended between front vertical surface and the bottom side of the footing. Figure 3.37 and Figure 3.38 show specimen CSR at different stages of the test and at footing failure, respectively. A 100 kip force on the specimen is equivalent to 900 kips on the prototype. Thus, the retrofitted specimen was capable of carrying 1.5 times the AASHTO vehicular collision force before a failure occurred in the footing.

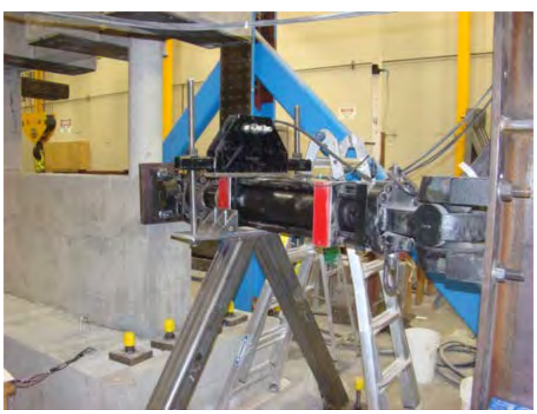

(a) Specimen CSR at the Start of the Test

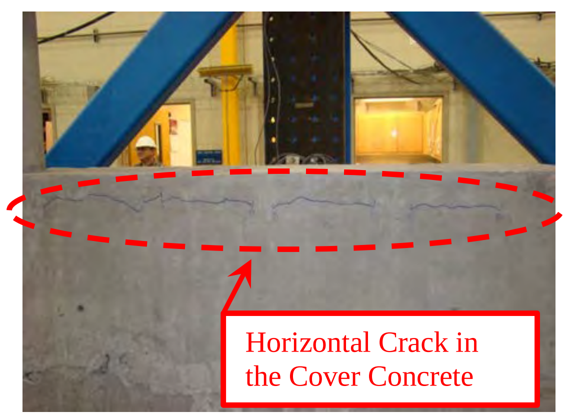

(b) Horizontal Crack at the Top of the Strut

Figure 3.37 Specimen CSR Different Stages of the Test

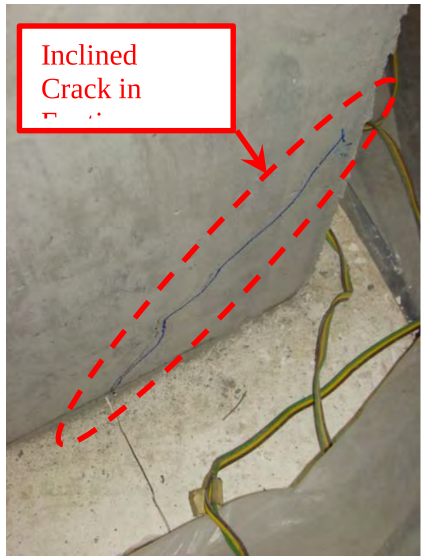

Figure 3.38 Footing Failure in Specimen CSR

Strain measurements obtained from the steel strain gages indicated that the strains remained significantly below yield throughout the entire test. Plots of the measured strains are shown in Appendix H. Strain gages S3 and W2 malfunctioned during the test.

Figure 3.39 shows the displacement of the bent cap's centerline. Maximum displacement at locations of the girders was less than a 0.5 in. On the full-scale prototype, the corresponding displacement would be less than 1.5 in. Therefore none of the girders in the prototype structure would be at risk of unseating.

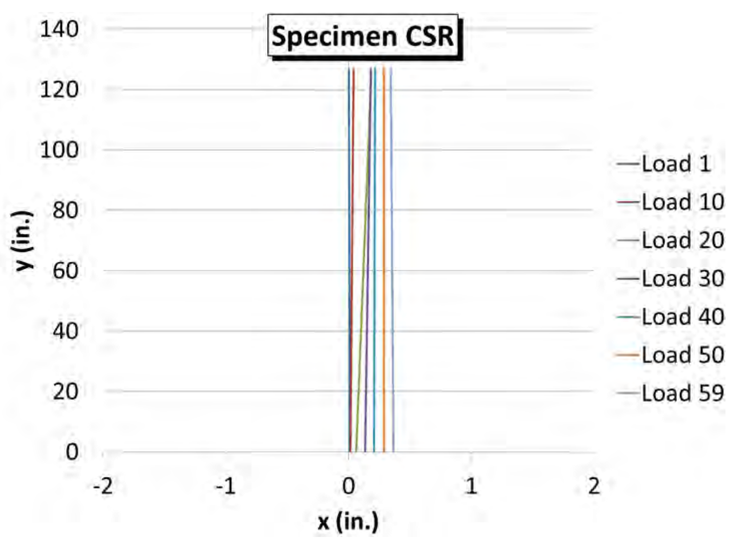

Figure 3.39 Displacement of the Bent Cap Centerline – Specimen CSR

3.6 Summary

Elastic structural analysis was performed on 175 overpass bridges on I-29, I-90, I-229, I-190, and other roads in South Dakota. The analysis' purpose was to assess vulnerability of those bridges to vehicular collision forces. The collision risk assessment and the vulnerability assessment were used to develop a retrofit prioritization list for mitigating collapse of bridge bents of the bridges included in this study.

Based on collision risk assessment and collapse vulnerability under vehicular collision force of 175 bridges in South Dakota, a high collision risk and vulnerable two-column bent prototype was selected for an experimental study. The study was designed to examine structural performance under design collision loads of as-built and retrofitted cases. Two ⅓-scale bridge bents were tested in the laboratory. One specimen represented the vulnerable prototype bent. The other specimen was retrofitted with a MnDOT "crash strut" to prevent bridge collapse under collision loads. Test results were analyzed and effectiveness of the crash strut was evaluated. Test results indicated that the as-built bent is severely inadequate if subjected to the design collision force. The specimen failed at less than one-half the scaled design load and the bent cap underwent excessive displacement that could cause unseating of the superstructure's girders. Addition of a concrete crash strut between the columns increased the bent collision load capacity to at least 1.5 times the collision force demand. Thus, the collision strut would be an effective retrofit measure for bent structures that are vulnerable to collapse under the vehicular collision force.

4. ESTIMATION OF THE COLLISION FORCE USING COMPUTATIONAL MODELS

This section covers the finite element analysis performed in this study to simulate trucks crashing into the column of the prototype bent. Comparison between the analytical results and the AASHTO vehicular collision force are also presented.

4.1 Introduction

Many researchers have used finite element (FE) simulation to determine collision forces on bridge piers and crash barriers resulting from truck crashes (Buth et al., 2010; El-Tawil et al., 2005; Sharma et al., 2011; Itoh et al., 2007). The 600-kip vehicular collision force specified by AASHTO (2012) was based on recommendations by Buth et al (2010, 2011) who performed FE simulation and full-scale testing of an 80-kip tractor-semitrailer crashing into a concrete column. Since collision force is dependent on stiffness of the structure and approach speed of the crashing truck, FE analysis was performed in this study to evaluate the collision forces resulting from two different truck sizes crashing into the prototype bridge bent at three different approach speeds (55 mph, 65 mph, 75 mph). The FE simulation was performed using the computer software LS-DYNA (LSTC, 2013).

4.2 Vehicle Finite Element Models

Two vehicle models were used in the FE analysis, the 15,000 lb Single Unit Truck (SUT) and the 80,000 lb Tractor-Trailer (TT). The FE models for the two vehicles were developed at George Washington University and were downloaded from the National Crash Analysis Center website (www.ncac.gwu.edu). Figure 4.1 and Figure 4.2 show the FE models for the SUT and the TT vehicles, respectively. The models take into account the stiffness of the engine block and drive train parts. The SUT model represents a medium-weight vehicle, while the TT model corresponds to the truck size for which the AASHTO vehicle collision force was developed. Although the impact load resulting from an SUT model is less critical than that of a TT model, the SUT model was included in the FE analysis to assess the response of the bent elements when a light vehicle collides with the bent column.

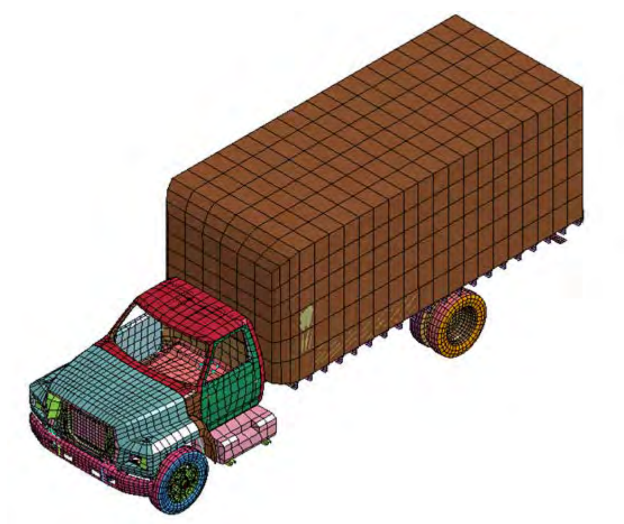

Figure 4.1 15,000 lb Single Unit Truck FE Model

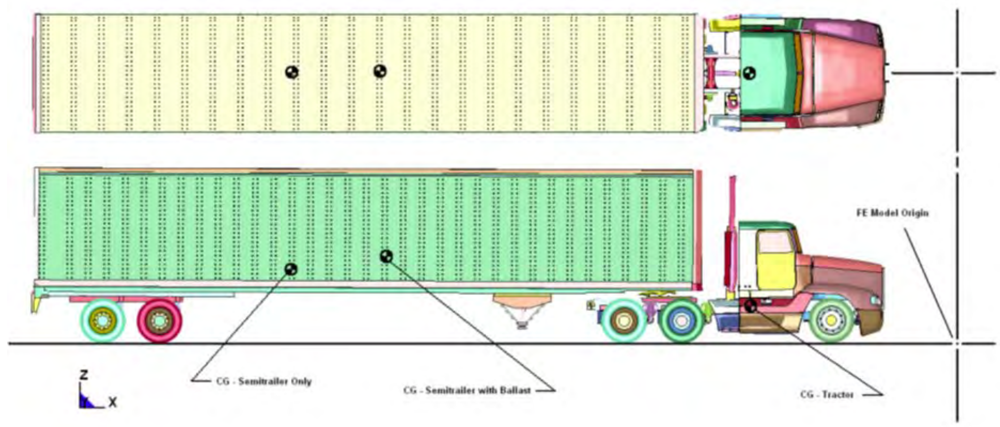

Figure 4.2 80,000 lb Truck-Trailer FE Model

4.3 Structure Finite Element Model

The FE model for the structure was based on the two-column bent of the prototype bridge. LS-DYNA provides a variety of material types that can be used to represent the concrete behavior. In this study, MAT_CSCM_CONC (MAT 159 in LS-DYNA) was selected to model the concrete material since it factors in the effect of strain rate on the performance of the concrete and can model concrete in tension and compression based on strain limits. The failure criteria were set to erode the concrete at 6% compressive strain. The unconfined compressive strength was set at 4,000 psi. The strain at concrete strength was set at 0.0022 in/in and the crushing strain was set at 0.0047 in/in. Figure 4.3 shows the stress-strain model for the 4-ksi strength concrete.

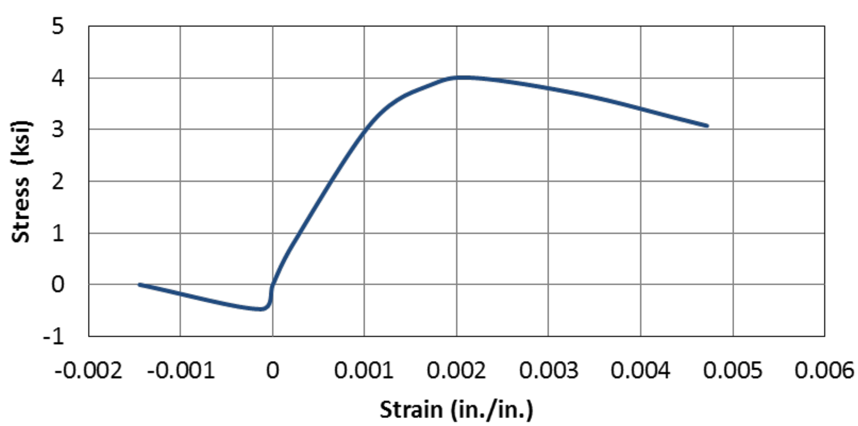

Figure 4.3 Concrete Stress-Strain Model

The reinforcing steel material was modeled using MAT_PIECEWISE_LINEAR_PLASTICITY (MAT 24 in LS-DYNA). This material incorporates effects of the strain rate and can model the inelastic behavior of steel after yielding. Steel grade 50 with modulus of elasticity of 29,000 ksi and ultimate stress of 64 ksi was used to model the material for all of steel reinforcement. The strain at the beginning of strain hardening and at ultimate strain were set at 0.0017 in./in and 0.17 in./in., respectively. Figure 4.4 shows the stress-strain model for the grade 50 steel.

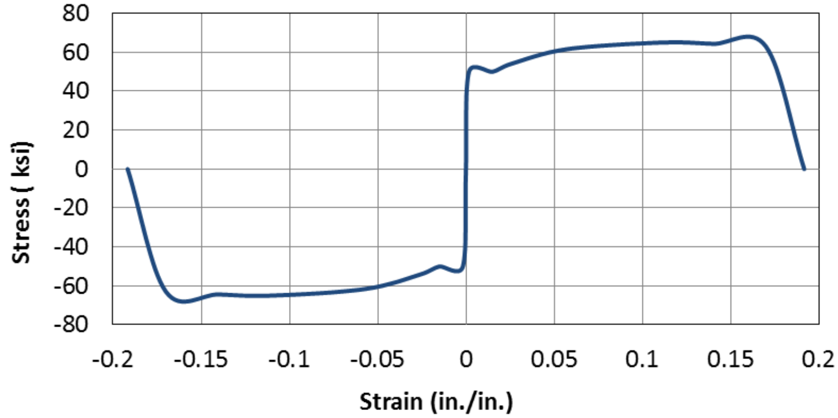

Figure 4.4 Reinforcing Steel Stress-Strain Model

Fully integrated solid elements were used to model all concrete members. An AUTOMATIC_SURFACE_TO_SURFACE contact was assigned between all of the concrete elements. The Lagrangian coupling method was used to model the contact between the steel bars and the concrete. The translational and rotational degrees of freedom at the footings were restrained since the footings were supported by piles. Figure 4.5 shows the FE model for the bent.

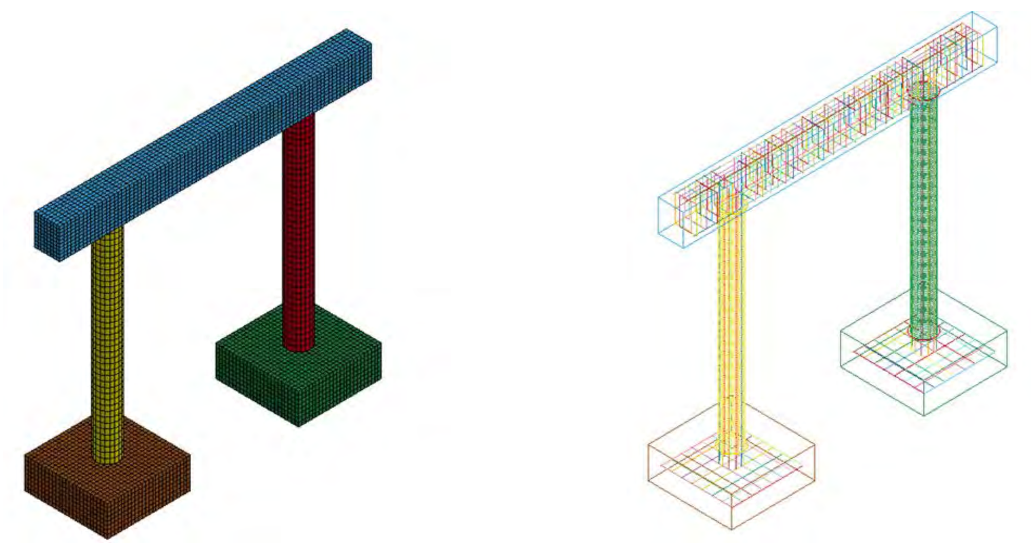

(a) Concrete Elements Mesh **(b)** Reinforcing Steel Elements Mesh

Figure 4.5 FE Model of the Bent Structure

4.4 Simulation Cases and Results

Finite element dynamic analysis was performed for the SUT and the TT truck models. The approach angle was set at 15° and the truck placement was configured such that impact with the column was at five feet above ground level. For each truck, dynamic analysis was conducted at speeds of 55 mph, 65 mph, and 75 mph. Figure 4.6 shows computer-generated images of the trucks at impact. The total simulation time was set to 200 ms for the SUT model and 300 ms for the TT model to capture the significant collision events and optimize the computer program run time. Figure 4.7 shows the trucks and the bent after impact for the 55 mph run.

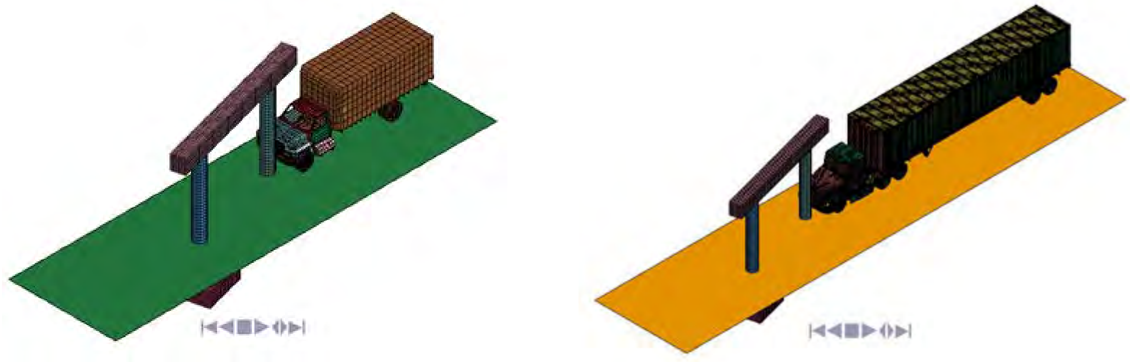

(a) SUT at Impact **(b)** TT at Impact

Figure 4.6 Isometric Views of the Trucks at Impact

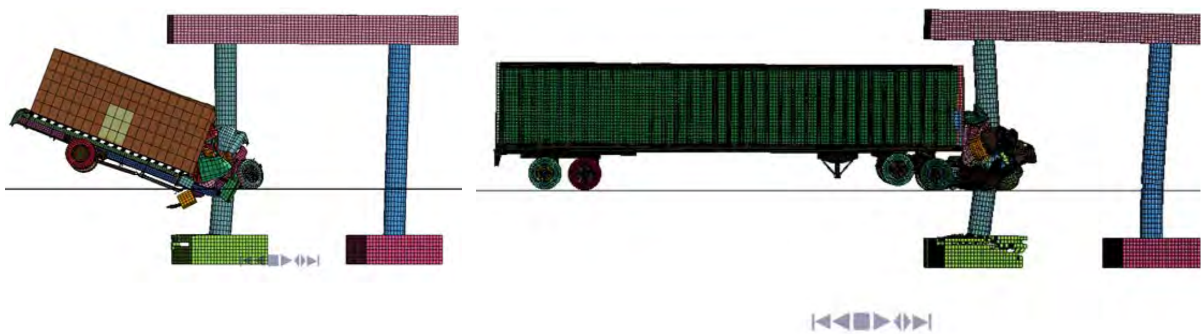

(a) SUT after Impact **(b)** TT after Impact

Figure 4.7 Isometric Views after Impact – 55 mph Approach Speed

For each run, the collision dynamic force was plotted versus the time after initial contact. The collision dynamic force is defined as the force corresponding to 1 ms moving average. Figure 4.8 and Figure 4.9 show the collision dynamic force at approach speeds of 55 mph, 65 mph, and 75 mph versus time after initial impact for the SUT and the TT models, respectively.

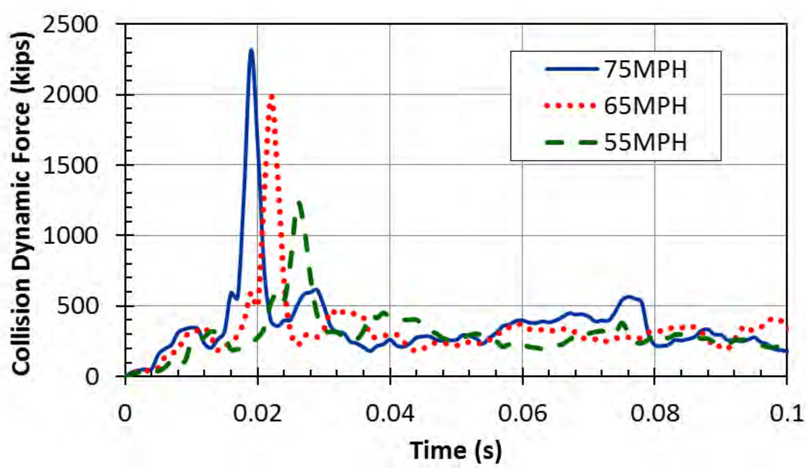

Figure 4.8 Collision Dynamic Force – SUT Simulation

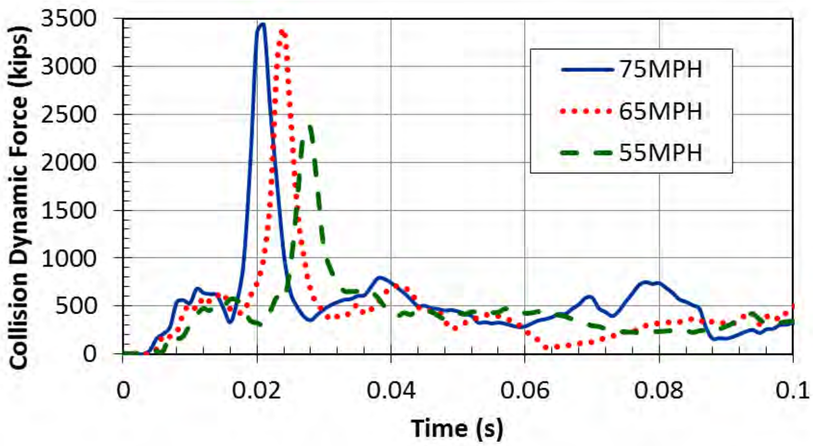

Figure 4.9 Collision Dynamic Force – TT Simulation

The peaks in Figure 4.8 and Figure 4.9 correspond to the impact of the engine block with the column. For the SUT simulation, the peak collision dynamic forces were 1,229 kips, 1,988 kips, and 2,312 kips at approach speeds of 55 mph, 65 mph, and 75 mph, respectively. For the TT simulation, the peak collision dynamic forces were 2,359 kips, 3,384 kips, and 3,433 kips at approach speeds of 55 mph, 65 mph, and 75 mph, respectively. The results indicate that higher approach speeds result in higher peak collision dynamic forces, but the rate of increase in the peak collision dynamic force reduces with increased speed. The results also indicate that the TT vehicle induced significantly higher peak collision dynamic forces than the SUT vehicle. At 55 mph approach speed, the peak dynamic collision force induced by the TT vehicle was almost twice that of the SUT vehicle.

The simulation results also revealed effects of the approach speed and vehicle size on the damage caused to the bent structure. Figure 4.10 and Figure 4.11 how computer-generated images of the damage to the bent structure inflicted by the SUT and TT vehicles, respectively. The SUT collision events resulted in localized damage to the impacted column and did not lead to global failure of the bent structure. On the other hand, the TT collision events resulted in severe damage to the substructure (columns, footings, and bent cap) which could cause loss of stability and subsequent failure of the superstructure.

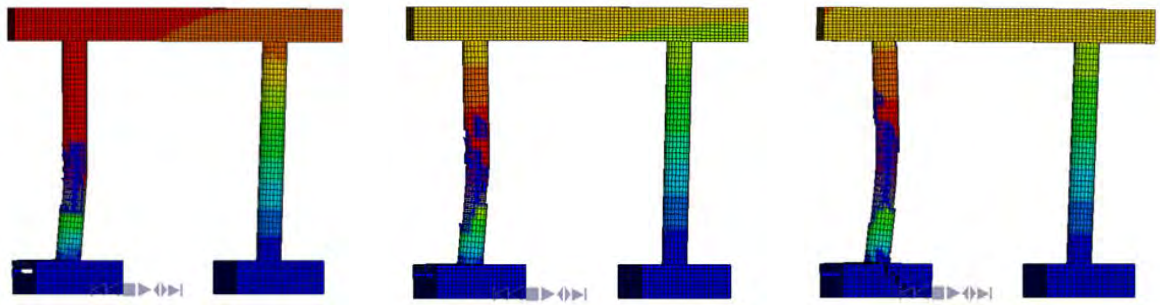

(a) Speed = 55 mph **(b)** Speed = 65 mph **(c)** Speed = 75 mph

Figure 4.10 Damaged Bent after Collision – SUT Simulation

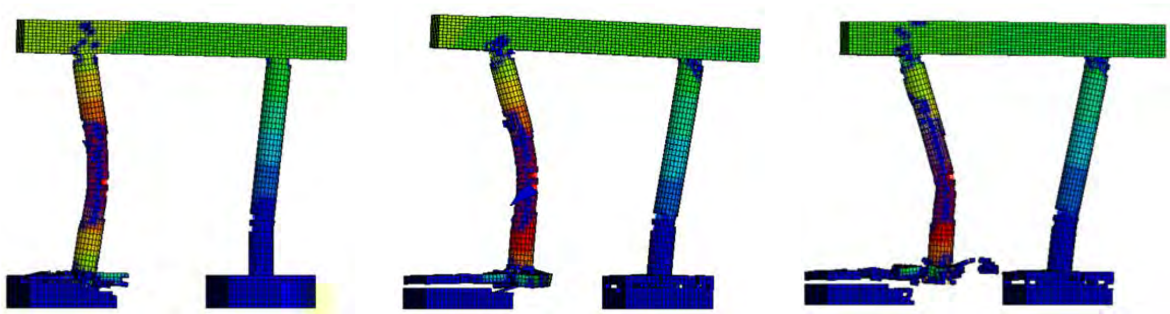

(a) Speed = 55 mph **(b)** Speed = 65 mph **(c)** Speed = 75 mph

Figure 4.11 Damaged Bent after Collision – TT Simulation

4.5 Analysis of the Simulation Results

The peak collision dynamic force is a short-duration event that does not allow sufficient time for the structure to respond in proportion to magnitude of the applied force. Thus, the peak collision dynamic force should not be used for determining load demand on a structure. In this study, the collision force was determined at 1 ms, 10 ms, and 50 ms moving averages. Figuer 4.12 and Figure 4.13 show results for the SUT and TT vehicles, respectively. A summary of the peak forces at the 1ms, 10 ms, and 50 ms moving averages are summarized in Table 4.1.

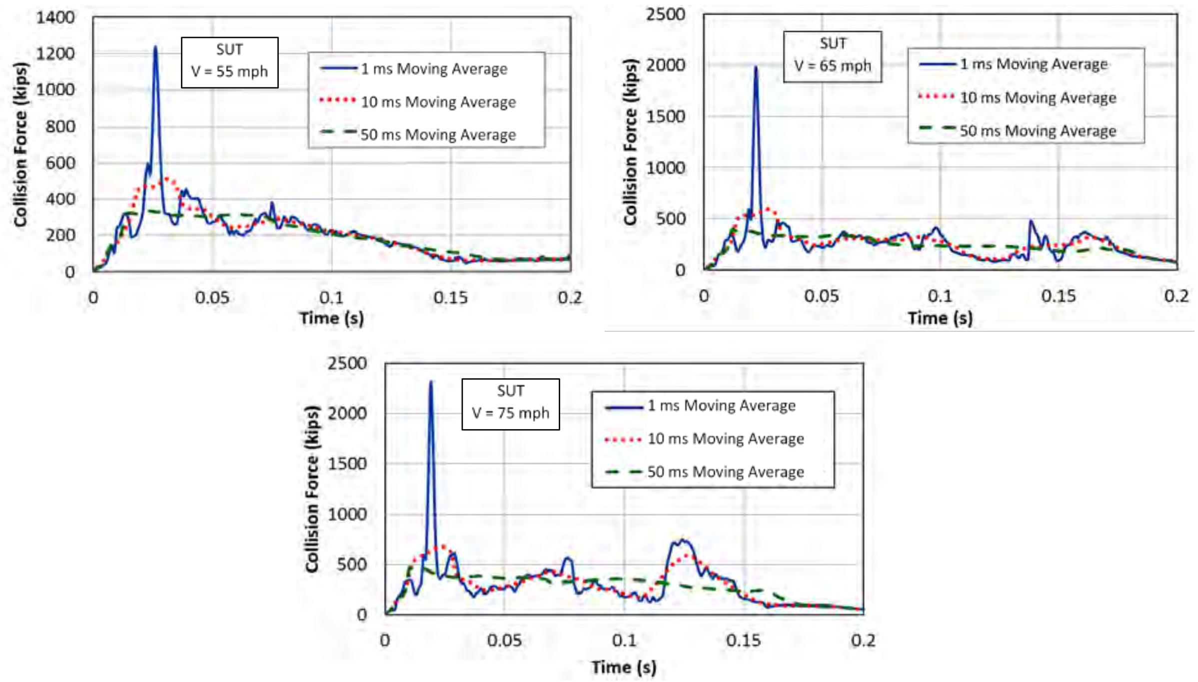

Figure 4.12 1 ms, 10 ms, and 50 ms Moving Average Collision Force – SUT Simulation

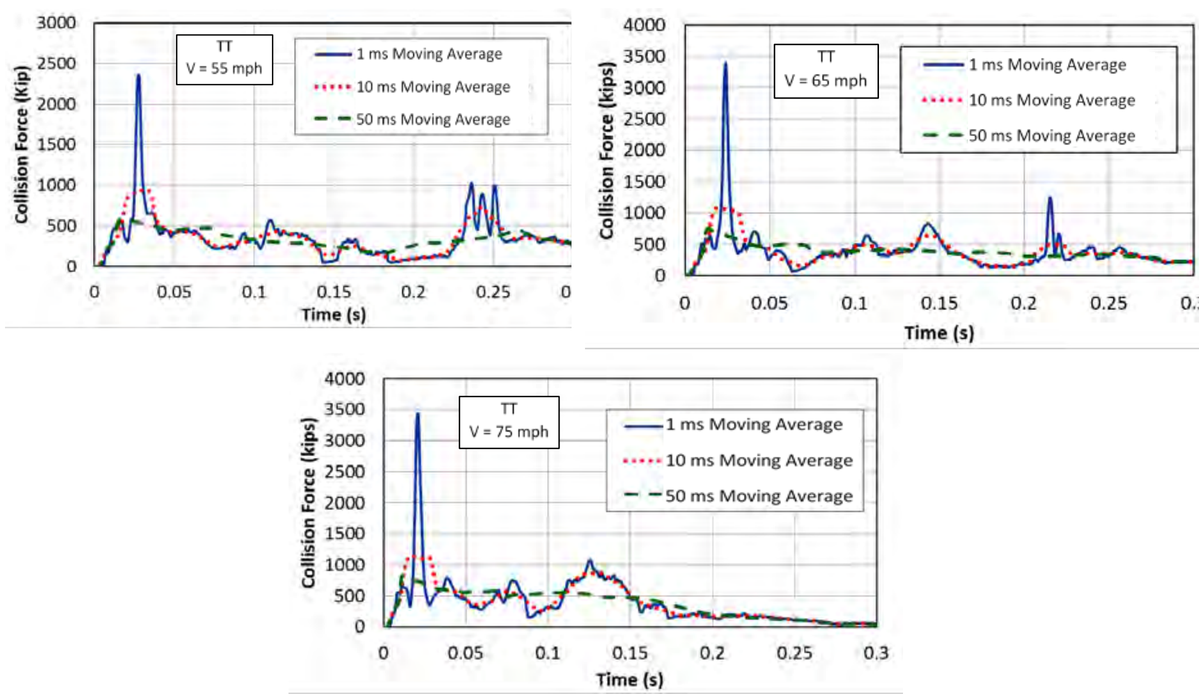

Figure 4.13 1 ms, 10 ms, and 50 ms Moving Average Collision Force – TT Simulation

Table 4.1 Peak Collision Force at 1 ms, 10 ms, and 50 ms Moving Average

Case	Peak Load (Kip) 1 ms Moving Average	10 ms Moving Average	50 ms Moving Average
SUT V = 55 mph	1229	512	335
SUT V = 65 mph	1988	593	402
SUT V = 75 mph	2312	680	475
TT V = 55 mph	2359	949	585
TT V = 65 mph	3384	1091	751
TT V = 75 mph	3433	1145	853

It is customary in the automotive industry to use the collision force obtained from the 50 ms moving average for determining equivalent static design force (El-Tawil et al., 2005). The 50 ms moving average method also has been evaluated by researchers for determining equivalent static collision forces on bridge piers (Buth et al., 2010; El-Tawil et al., 2005). The peak forces at 1 ms and 50 ms moving averages are plotted in Figure 4.14 and Figure 4.15 for the SUT and TT vehicles. Also shown on the plots are lines representing the AASHTO 600-kip vehicle collision force and the lateral load capacity obtained from the experimental work. Based on the 50 ms peak force, the results indicate that the AASHTO 600-kip design force would be adequate for the SUT vehicle at all approach speeds, but would be adequate for the TT vehicle only at or below an approach speed of 55 mph. At 55 mph, the 50 ms peak force is 585 kips, or 97.5% of the AASHTO vehicular collision force. For speeds higher than 55 mph, the 50 ms peak load exceeds the AASHTO vehicular collision force. Since the AASHTO vehicular collision force was based on the load imparted by an 80,000 lb. tractor-semitrailer traveling at an approach speed of 50 mph, it can be concluded that a collision static design load of 600 kips is reasonable for the prototype bent considered in this study.

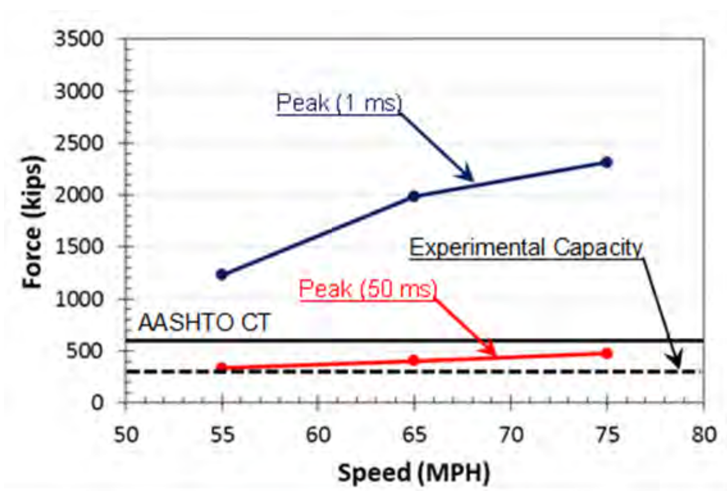

Figure 4.14 1 ms and 50 ms Moving Average Peak Forces – SUT Simulation

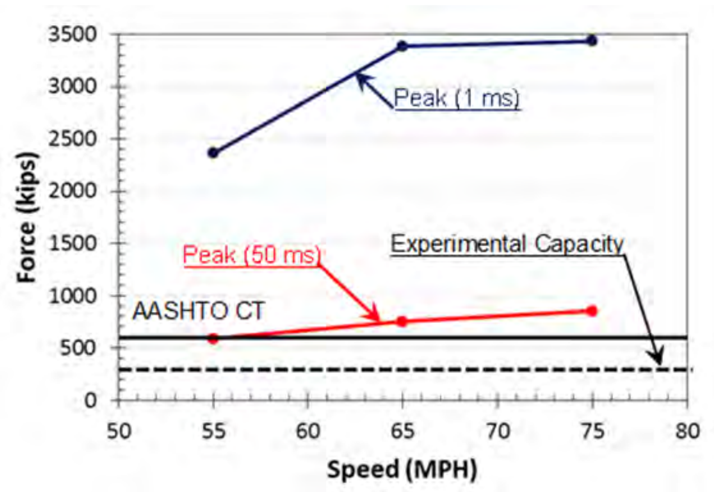

Figure 4.15 1 ms and 50 ms Moving Average Peak Forces – TT Simulation

5. FINDINGS AND CONCLUSIONS

Crashes of heavy trucks with bridge columns are random events with low probability of occurrence. In spite of the low odds, previous collision events in other states have resulted in catastrophic partial or full collapse of bridges. Increased truck traffic on South Dakota highways escalates the probability of collision. Collapse of an important bridge may result in significant negative socioeconomic impact at the local, state, and national levels. Therefore, a risk evaluation and mitigation plan is needed to reduce the risk of bridge collapse below a threshold that would be acceptable to stakeholders in South Dakota. This study was performed to develop a risk evaluation and mitigation plan for truck collision with columns of 175 overpasses located on I-29, I-90, I-229, I-190, and a few other roads in South Dakota.

5.1 Findings

Based on results obtained from this study, the following findings were identified.

- The uncertainties involved in truck collision events lead to a range of outcomes for calculating the hazard envelope, a physical exposure of a bridge to the collision. Therefore, statistical models have been developed to identify statistically significant collision contributing factors as well as their impacts. The model results show that high truck traffic exposure, sharp horizontal curves, high annual snowfall precipitation, and concrete pavement surfaces all increase the truck ROR crash frequency. The hazard envelope of each bridge bent was calculated based on measured bent dimensions and default values recommended in NCHRP Report 492. Coupled with the unit crash counts, the collision risk can be estimated for each bridge bent, and thereby, the collision risk for a bridge can be determined by the maximum risk of all the bridge bents.
- The importance of a bridge reflects severity of the socioeconomic impact that would result from a bridge collapse. It is calculated as the RUC because of the additional distance that would need to be traveled.
- When the collision risk and economic importance of a bridge were combined, a decision analysis method was applied to rank the overpass bridges. The quartile distribution, based on collision risk and RUC, resulted in 16 clusters of bridges that can be used to form a prioritization policy for the implementation of risk mitigation procedures. The highest risk cluster (quartile 4-4, i.e. RUC 4 and Collision Risk 4) contained 24 bridge bents. Quartiles 3-4 and 4-3 contained 49 and 25 bridge bents, respectively.
- AASHTO’s Standard Specifications for Highway Bridges did not include provisions for truck collision with bridge columns and abutments. The vehicular collision force requirements first appeared in AASHTO’s LRFD Bridge Design Specifications first edition in 1994.
- In the early editions of AASHTO-LRFD, the vehicular collision force requirements for bridges without adequate protection for collision consisted of a 400-kip static force applied horizontally to a bridge column at four feet above ground level. In 2012, the vehicular collision force was increased to 600 kips and the point of application was changed to five feet above ground level.
- The vast majority of the 175 bridges included in this study were designed and constructed prior to the development and implementation of the vehicular collision force requirements for unprotected bridge columns. Using elastic structural analysis and code methods for determining structural capacity, the columns of 140 bridges were found to be structurally inadequate in flexure, shear, or both.

- Bents with less than three columns were considered non-redundant. Of the 175 bridges included in this study, 107 had non-redundant bents (61%).
- Bridges with circular columns represented the vast majority of the bridge inventory in this study (77%). Flared column bridges were the second highest in number (14%). Almost 40% of the bridges in the inventory were non-redundant two-column bents with circular columns.
- Of the 98 bridge bents that fell in quartiles 4-4, 3-4, and 4-3, 59 bents were both non-redundant and structurally inadequate for the design collision load.
- Laboratory testing of 1/3-scale of a vulnerable two-circular column bent indicated structural failure at less than one-half the design collision force and potential for unseating of the edge girder. A similar specimen, but with a crash strut retrofit, was capable of resisting 1.5 times the design collision force.
- The finite element dynamic analysis performed in this study showed that for the prototype bridge considered in the analysis, the 600-kip vehicle collision force specified by AASHTO is a reasonable estimate for the load demand induced by the collision with the bridge column of an 80,000 lb. tractor-trailer travelling at 55 mph.

5.2 Conclusions

Following are the conclusions of this study.

- Crashes are random events, as they may be affected by several factors that are unknown or observable. Unobserved elements are the main contributor to data dispersion. To account for data dispersion in the crash risk analysis of this study, the NB count models can be employed. The model output reveals that high truck traffic exposure, sharp horizontal curves, high annual snowfall precipitation as well as the concrete pavement surface all increase the truck ROR crash frequency.
- By considering vulnerable bents in the high collision risk pool, a priority list for protection or retrofit can be generated by SDDOT engineers and planners. The prioritization should take into consideration additional factors such as the remaining useful life of the bridge, bridge replacement schedule, availability of resources, and cost effectiveness of implementing the same retrofit method for a group of bents that share the same features.
- Columns of the vast majority of two- and three-circular column bents are inadequate in shear, flexure, or both under the 600-kip vehicular collision force.
- The crash strut used in this study provides an effective measure for retrofitting high risk and vulnerable bridge bents. The MnDOT method for designing the crash strut yielded adequate results.

6. RECOMMENDATIONS

Based on the findings of this study, the research team offer the following recommendations.

6.1 Recommendation 1

The South Dakota Department of Transportation should adopt the prioritization list generated in this study, coupled with other factors, such as the remaining useful life of the bridge, bridge replacement schedule, availability of resources, and cost effectiveness of using the same retrofit method for a group of bents that share the same features, for implementing protection or retrofit measures for vehicular collision forces.

The collapse risk of inadequate bents vulnerable to vehicular collision forces could be mitigated through implementing retrofit measures to enhance strength of the bent. However, retrofitting all inadequate bents is cost prohibitive. One strategy to prioritize bridge bents for collapse mitigation retrofit would be to consider the pool of bridge bents that fall in the high risk quartiles (4-4, 3-4, and 4-3) and are vulnerable to collapse under the vehicular collision force. A priority list for retrofit can be generated by SDDOT engineers and planners considering additional factors such as the remaining useful life of the bridge, bridge replacement schedule, availability of resources, and cost effectiveness of implementing the same retrofit method for a group of bents that share the same features.

6.2 Recommendation 2

The South Dakota Department of Transportation should adopt a crash strut, similar to the one tested in this study, for retrofit of two- and three-column bents.

Test results of the 1/3-scaled two-column bent indicated that the as-built bent is severely inadequate if subjected to the design collision force. The as-built specimen failed at less than one-half the scaled design load and the bent cap underwent excessive displacement that could cause unseating of the superstructure's girders. The addition of a concrete crash strut between the columns increased the bent collision load capacity to at least 1.5 times the collision force demand. Thus, the collision strut provides an effective retrofit measure for bent structures that are vulnerable to collapse under the vehicular collision force.

7. REFERENCES

American Association of State and Highway Officials (AASHTO). (2012). "AASHTO-LRFD Bridge Design Specifications, Fifth Edition." Washington, D.C.

American Association of State and Highway Officials (AASHTO). (2011). "AASHTO Guide Specifications for LRFD Seismic Bridge Design, Second Edition." Washington, D.C.

American Association of State Highway and Transportation Officials (AASHTO). (2011). "Roadside Design Guide", Washington, D.C.

American Association of State and Highway Officials (AASHTO) (2002). "Standard Specifications for Highway Bridges, 17th Edition." Washington, D.C.

American Association of State and Highway Officials (AASHTO) (1998). "AASHTO-LRFD Bridge Design Specifications, Second Edition." Washington, D.C.

American Association of State and Highway Officials (AASHTO). (1994). "AASHTO-LRFD Bridge Design Specifications, First Edition." Washington, D.C.

AP News, "AP News Archive." Accessed December 10, 2013. http://www.apnewsarchive.com/2003/Fatal-Crash-Causes-I-80-Bridge-Collapse/id-241431bd969779343b699abfeb8e6156.

Bligh, R. P., Arrington, D. and Meza, R. (2013). "MASH Tl-2 Guardrail-to-Bridge-Rail Transition Compatible with 31-in. Guardrail." Transportation Research Board 92nd Annual Meeting. Compendium of Papers, Paper No. 13-5298.

Buth, C. E., Brackin, M. S., Williams, W. F. and Fry, G. T. (2011). "Collision Loads on Bridge Piers: Phase 2. Report of Guidelines for Designing Bridge Piers and Abutments for Vehicle Collisions." 9-4973-2. Texas Transportation Institute, College Station, TX.

Buth, C. E., Williams, W. F., Brackin, M. S., Lord, D., Geedipally, S. R. and Abu-Odeh, A. Y. (2010). "Analysis of Large Truck Collisions with Bridge Piers: Phase 1. Report of Guidelines for Designing Bridge Piers and Abutments for Vehicle Collisions." 9-4973-1. Texas Transportation Institute, College Station.

California Department of Transportation (Caltrans) (1990). "Seismic Design References." Sacramento, CA.

Chan, A., Keoleian, G. and Gabler, E. (2008). "Evaluation of life-cycle cost analysis practices used by the Michigan Department of Transportation." Journal of transportation engineering, Vol. 134, No. 6. pp. 236-245.

Collura, J., Heaslip, K. P., Moriarty, K., Wu, F., Khanta, R. and Berthaume, A. (2010). "Simulation models for assessment of the impacts of strategies for highway work zones." Transportation Research Record: Journal of the Transportation Research Board, Vol. 2169, No. 1. pp. 62-69.

Computers and Structures, Inc. (2012). "SAP2000, Version 14." Berkeley, CA.

Daily, K., Hughes, W. E. and McGee, H. W. (1997). "Experimental Plans for Accident Studies of Highway Design Elements: Encroachment Accident Study." No. FHWA-RD-96-081. Federal Highway Administration, Washington, D.C.

Daniels, G., Ellis, D.R. and Stockton, W.R. (1999). “Techniques for Manually Estimating RUC Associated with Construction Projects.” Texas Transportation Institute, College Station, TX.

El-Tawil, S., Severino, E. and Fonseca, P. (2005). “Vehicle Collision with Bridge Piers.” Journal of Bridge Engineering, No. 3. pp 345-353.

Engineering News Record (2003). “Nebraska overpass will be rebuilt with fewer piers.” June 9, 2003.

Haltvick, N. (MnDOT) (2013), personal communication by Nadim Wehbe, email, March 22, 2013.

Jiang, X. and Adeli, H. (2003). “Freeway Work Zone Traffic Delay and Cost Optimization Model.” Journal of Transportation Engineering, Vol. 129, No. 3. pp. 230-241.

Jiang, Y. (1999). “A Model for Estimating Excess User Costs at Highway Work Zones. (1999). “Transportation Research Record: Journal of the Transportation Research Board, Vol. 1657, No. 1. pp. 31-41.

Livermore Software Technology Corporation (2013). “LS-DYNA Keyword User's Manual, Version R7.0.” Livermore, CA.

Mak, K. K. and Sicking, D. (2003). “Roadside Safety Analysis Program (RSAP): Engineer's Manual.” Transportation Research Board. Washington, D.C.

Manuel, L., Kallivokas, L. F., Williamson, E. B., Bomba, M., Berlin, K. B., Cryer, A. and Henderson, W. R. (2006). “A probabilistic analysis of the frequency of bridge collapses due to vessel impact.” No. FHWA/TX-07/0-4650-1. Federal Highway Administration. Washington, D.C.

Miaou, S. P. (2001). “Another Look at the Relationship between Accident-and Encroachment-Based Approaches to Run-Off-the-Road Accidents Modeling.” No. ORNL/CP--94364; CONF-980112--. Oak Ridge National Lab., TN.

Miaou, S. P. (1997). “Estimating Vehicle Roadside Encroachment Frequencies by Using Accident Prediction Models.” Transportation Research Record: Journal of the Transportation Research Board, No. 1599. Transportation Research Board of the National Academies, Washington, D.C. pp. 64-71.

Midland Reporter-Telegram, “Photo Gallery: Big Spring Bridge Collapse.” Accessed December 5, 2013. http://www.mrt.com/editors_picks/collection_5ebd5c68-4734-11e3-a65d-001a4bcf887a.html

Minnesota Department of Transportation (2007). “Memo to Designers (2007-01): Bridge Office Substructure Protection.” Oakdale, MN.

National Transportation Safety Board (NTSB) (1995). “Propane truck collision with bridge column and fire, White Plains, New York. July 27, 1994.” Highway Accident Report. Washington, D.C.

National Transportation Safety Board (NTSB) (1993). “Tractor-semitrailer collision with bridge columns on Interstate 65. Evergreen, Alabama.” NTSB Number HAR-94-2. Washington, D.C.

Nebraska Department of Roads, “I-80 Overpass Collapse & Repair.” Accessed December 3, 2013. http://www.transportation.nebraska.gov/big-springs/.

Neuman, T., Prefer, R., Slack, K., Hardy, K., Council, F., McGee, H., Prothe, L. and Eccles, K. (2003). “NCHRP Report 500. Volume 6: A Guide for Addressing Run-Off-Road Collisions.” Transportation Research Board. Washington, D.C.

Polam, I., Kapuskar, M. and Chaudhuri, D. (1998). "Modeling Pile Footings and Drilled Shafts for Seismic Design." Technical Report MCEER-98-0018.

Ross, H. E., Sicking, D. L., Zimmer, R. A., and Michie, J.D. (1993). "Recommended Procedures for the Safety Performance Evaluation of Highway Features." NCHRP Report 350. Transportation Research Board, Washington, D.C.

Shankar, V., Milton, J. and Mannering, F. (1997). "Modeling Accident Frequencies as Zero-Altered Probability Processes: an Empirical Inquiry." Accident Analysis & Prevention, Vol. 29, No. 6. pp. 829-837.

South Dakota Department of Transportation. (SDDOT) (2012). "Highway Needs and Project Analysis Report." Pierre, SD.

StructurePoint. (2011). "spColumn, Version 4.8." Skokie, IL.

Tsang, H. and Lam, N. (2008). "Collapse of Reinforced Concrete Columns by Vehicle Impact." Computer-Aided Civil and Infrastructure Engineering. pp 427-436.

Waltrip, D. (TxDOT) (2013). Personal communication by Brett Tigges, Phone, November 22, 2013.

Wardhana K. and Hadipriono F.C. (2003). "Analysis of recent bridge failures in the United States." Journal of Performance of Construction Facilities. 17(3):144-50.

Western, K. (2007). "Mn/DOT Bridge Office Substructure Protection Policy." Minnesota Department of Transportation.

Xiao, Q. and Cutler, C. (2013). "Review of Road User Costs and Methods." MPC-13-254. North Dakota State University - Upper Great Plains Transportation Institute. Fargo, ND.

Zegeer, C. V., Reinfurt, D. W., Hummer, J., Herf, L. and Hunter, W. (1988). "Safety Effects of Cross-Section Design for Two-Lane Roads." Transportation Research Record: Journal of the Transportation Research Board, No. 1195. Transportation Research Board of the National Academies, Washington, D.C. pp. 20-32.

APPENDIX A: MEETING NOTES

A.1: Kickoff Meeting

Kickoff Meeting
Pierre – September 27, 2012

Evaluation and Mitigation of Vehicle Impact Hazards for Overpasses

Nadim Wehbe
Shiling Pei
Xiao Qin

Motivation

- Economic growth in the upper mid-western states will result in increased heavy truck traffic on SD highways
- Increased potential for truck collision with bridge columns – Extreme Event (low probability, high impact)
- Majority of bridges in SD were designed prior to current AASHTO truck collision load requirements
- Need to develop risk assessment and management

September 27, 2012 Evaluation and Mitigation of Vehicle Impact Hazards for Overpasses

---

Objectives

1. Develop risk assessment method for truck collision with highway overpass columns
2. Evaluate risk of overpass collapse under truck impact
3. Develop mitigation measures for locations of high risk

September 27, 2012 Evaluation and Mitigation of Vehicle Impact Hazards for Overpasses

---

Research Plan

- **Task 1.** Kick-off meeting; review scope and plan
- **Task 2.** Literature review on related studies
  - Collision risk
  - Collapse analysis
- **Task 3.** Site visit and data collection (risk factors)
  - 866 Bridges identified by SDDOT; 402 bridges are overcrossings, 220 overcrossings are on I90, I29, and I229
  - Data collection method (will discuss in detail later)
- **Task 4.** Develop collision risk assessment process
- **Task 5.** Meeting to review risk assessment
- **Task 6.** Develop collision risk index and identify critical bridges

September 27, 2012 Evaluation and Mitigation of Vehicle Impact Hazards for Overpasses

---

Research Plan

- **Task 7.** Meeting to review high risk bridges, select columns for testing
- **Task 8.** Construction of the specimen
- **Task 9.** Lateral load testing
- **Task 10.** Meeting to review test results
- **Task 11.** Develop recommendations based on analysis and test results
- **Task 12.** Final report
- **Task 13.** Executive presentation to RRB

September 27, 2012 Evaluation and Mitigation of Vehicle Impact Hazards for Overpasses

---

Schedule

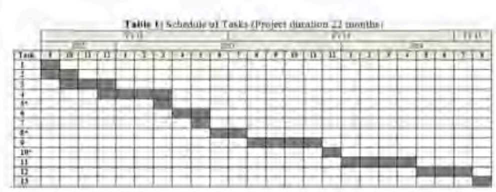

September 27, 2012 Evaluation and Mitigation of Vehicle Impact Hazards for Overpasses

Risk Assessment and Mitigation

Collision Risk

Important Literature:

1. NCHRP 500: Volume 6: A Guide for Addressing Run-Off-Road Collisions
2. AASHTO Roadside Design Guide, 2002
3. Highway Safety Manual
4. More…

Collision Risk

Brief Summary for Risk Factors:

- *Shoulder Width*

The beneficial effect of allowing for the safe recovery of stray vehicles, and the detrimental tendencies of inviting some voluntary shoulder stops, faster travel, the possibility of steeper roadside slopes, and shoulder use for travel. (NCHRP 17-27 project team, 2009)

- *Roadside Hazard Rating (RHR)*

The Roadside Hazard Rating (RHR) system considers the clear zone in conjunction with the roadside slope, roadside surface roughness, recoverability of the roadside, and other elements beyond the clear zone such as barriers or trees. (NCHRP 17-27 project team, 2009)

- *Sight Distance on Horizontal Curves*

A minimum sight distance, and anything less may restrict the safe operation of the intersection at the intended design speed.(Mark A Marek, 2010)

Illustration of Data Collection

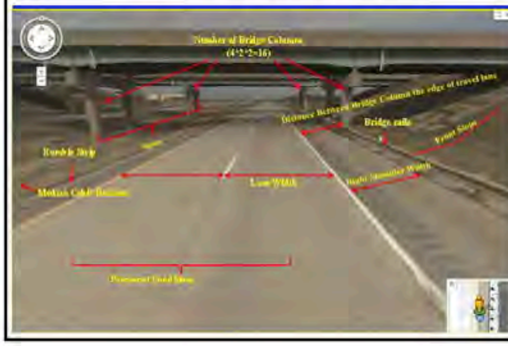

Collision Risk

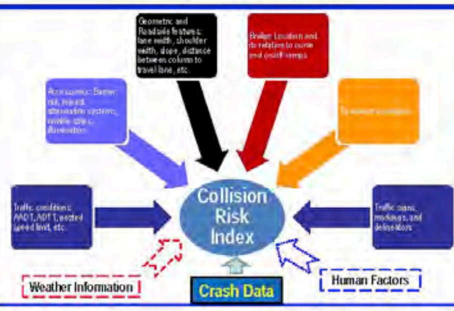

Bridge Inventory

Count of bridge_id	on_under				
facility	2	A	B	C	Grand Total
I029 P	1				1
I029 L	1				1
I029 N	25	4	3	2	34
I029 S	25	4	3	2	34
I090		1			1
I090 P	1				1
I090 E	78	3	1	1	83
I090 W	78	3	1	1	83
I090 WB OFF RAMP	1	1			2
I090 WB ON RAMP	1				1
I090 WF	1				1
I190	1				1
I190 N	1				1
I190 S	1				1
I229	1				1
I229 N	2	2			4
I229 S	2	2			4
Grand Total	220	20	8	6	234

Crash Data

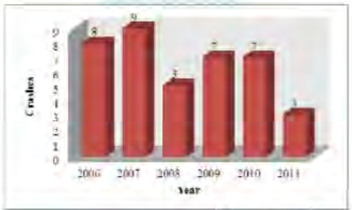

freeways)

Collapse Risk

- Evaluation of collision load
  - ➢ AASHTO LRFD Bridge Design Specifications, 5th Ed., 2010, § 3.6.5.1: Protection of Structures
    - ▪ Equivalent static force of 400 kip assumed to be acting at a distance of 4.0 ft above ground.
    - ▪ Based off of crash tests of 80 kip tractor-trailers
  - ➢ AASHTO LRFD BDS 6th Ed., 2012?
  - ➢ Research articles in the literature

Collapse Risk

- Evaluation of column Capacity
  - Shear capacity
  - Flexural capacity
  - Ductility
- Structural Redundancy
- Laboratory testing of scaled columns

Mitigation Strategies

- Shear capacity
- Ductility capacity
- Majority of bridges in SD were designed prior to current AASHTO truck collision load requirements
- Need to develop risk assessment and management

A.2: Evaluation of the Risk Assessment Process

Task 5: Evaluate Risk Assessment Process

Evaluation and Mitigation of Vehicle Impact Hazards for Overpasses

Nadim Wehbe, Shiling Pei, Xiao Qin, Zhao Shen, and Brett Tigges

April 5, 2013 — Evaluation and Mitigation of Vehicle Impact Hazards for Overpasses

Outline

- Development of the Bridge Collision Index (BCI)
- Case Study
- Results
  - ➢ Bridges ranked by total risk-significance
  - ➢ Bridges ranked by sum of Z-scores of collision risk and significance
  - ➢ Bridge grouped by quartiles of collision risk and significance
- Structural Analysis

April 5, 2013 — Evaluation and Mitigation of Vehicle Impact Hazards for Overpasses

Bridge Collision Index

- Encroachment Module

Estimate the average truck roadside encroachment frequency based on truck volume and roadway geometric characteristics.

- Crash Prediction Module

Given the occurrence of an encroachment, what is the risk for an erratic vehicle to hit bridge substructure?

- Bridge Significance Module

What is the additional road user cost (RUC) due to the detour after the bridge collapses.

- Bridge collision index

The Index is determined by both collision risk and significance.

April 5, 2013 — Evaluation and Mitigation of Vehicle Impact Hazards for Overpasses

Collision Risk Index Flow Chart

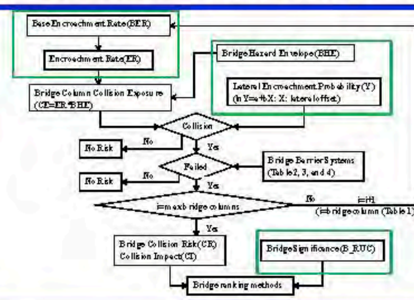

April 5, 2013 — Evaluation and Mitigation of Vehicle Impact Hazards for Overpasses

Reference

Figure 1. Probability of Run-Off-Road (ROR) Crashes at Horizontal Curve
(TTI: Analysis of large truck collisions with bridge piers)

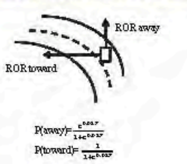

Figure 2. Bridge Hazard Envelope
(NCHRP Report 492: Roadside Safety Analysis Program (RSAP)—Engineer's Manual)

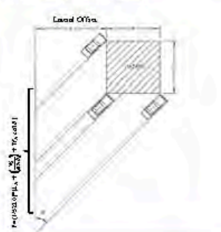

April 5, 2013 — Evaluation and Mitigation of Vehicle Impact Hazards for Overpasses

Reference (cont.)

Table 1. Encroachment Rate by direction & by roadside/median

side of the road \ direction	NB/EB	SB/WB
right_side	ER_1	ER_2
left_side(median)	ER_3	ER_4

Table 2. Vehicle Gross Static Mass Upper and Lower Limits[a]

Test Vehicle Designation and Type	Target Vehicle Weight lb(kg)	Acceptable Variation lb(kg)
1100C (Passenger Car)	2420 (1100)	±55(25)
1500A (Passenger Car)	3300 (1500)	±220(100)
2270P (Pickup Truck)	5000 (2270)	±110(50)
10000S (Single-Unit Truck)	22000 (10000)	±660(300)
36000V (Tractor-Van Trailer)	79300 (36000)	±1100(500)
36000T (Tractor-Tank Trailer)	79300 (36000)	±1100(500)

April 5, 2013 — Evaluation and Mitigation of Vehicle Impact Hazards for Overpasses

Reference (cont.)

Table 3. Roadside Barriers and NCHRP Report 350 Approved Test Levels#

Roadside Barrier System	Test Level	Containment Capacity(kJ)
W-beam(Weak Post)	2	70.5
Three-Strand Cable Barriers	3	144
High-Tension Cable Barriers	3/4	144/193
Thrie-Beam(Strong Post)	3	144
Concrete Barrier	5	548

April 5, 2013 — Evaluation and Mitigation of Vehicle Impact Hazards for Overpasses

Reference (cont.)

Table 4. Recommended Test Matrices for Longitudinal Barriers#

Test Level	Barrier section	Vehicle	Impact Speed, mph(km/h)	Impact Angle, θ,deg	Acceptable IS Range, kip-ft(kJ)
2	Length of need	1100C 2270P	44 (70.0) 44 (70.0)	25 25	≥25 (34.2) ≥52 (70.5)
	Transition	1100C 2270P	44 (70.0) 44 (70.0)	25 25	≥25 (34.2) ≥52 (70.5)
3	Length of need	1100C 2270P	62 (100.0) 62 (100.0)	25 25	≥51 (69.7) ≥106 (144)
	Transition	1100C 2270P	62 (100.0) 62 (100.0)	25 25	≥51 (69.7) ≥106 (144)
4	Length of need	1100C 2270P 10000S	62 (100.0) 62 (100.0) 56 (90.0)	25 25 15	≥51 (69.7) ≥106 (144) ≥142 (193)
	Transition	1100C 2270P 10000S	62 (100.0) 62 (100.0) 56 (90.0)	25 25 15	≥51 (69.7) ≥106 (144) ≥142 (193)
5	Length of need	1100C 2270P 36000V	62 (100.0) 62 (100.0) 50 (80.0)	25 25 16	≥51 (69.7) ≥106 (144) ≥404 (548)
	Transition	1100C 2270P 36000V	62 (100.0) 62 (100.0) 50 (80.0)	25 25 17	≥51 (69.7) ≥106 (144) ≥404 (548)

April 5, 2013 — Evaluation and Mitigation of Vehicle Impact Hazards for Overpasses

Case Study

Table 5. Basic information of bridge 64020220

Bridge ID	Interstate	Mile Marker	Bridge Length(ft)	Deck Width(ft)
64020220	I29	24	254.00	28.00
Bridge Volume	Lane Width(ft)(14,15,34,35)	Curve(degree)	Right Shoulder Width(NB)(ft)(12)	Right Shoulder Width(SB)(ft)(32)
2005	12	0.5	10	10
Median Width(ft)(38)	AADT(NB)	AADT(SB)	The number of trucks(NB)	The number of trucks(SB)
51.9	9760	9760	1250	1250
Roadside Guardrail	Median Cable	Rumble Strip(Right side)	Rumble Strip(Left side)	Bridge Column Width(ft)
W-beam(weak post)	Three-Strand Cable(Weak Post)	Intermittent	Continuous	5

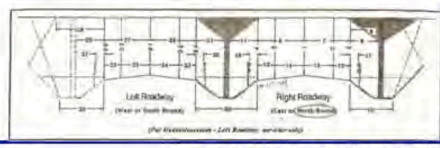

April 5, 2013 — Evaluation and Mitigation of Vehicle Impact Hazards for Overpasses

Case Study

April 5, 2013 — Evaluation and Mitigation of Vehicle Impact Hazards for Overpasses

Case Study (cont.)

Base Encroachment Rate (BER: collision per mile per year)

$\mu_i = e^{\ln\beta_0} * L_i * TADT_i^{\beta_1} * e^{(\sum_i^t \beta_i x_i)}$

Base Encroachment Rate (BER_NB)

$(\frac{\mu_i}{L_i}) = e^{\ln\beta_0} * TADT_i^{\beta_1} * e^{(\sum_i^t \beta_i x_i)} = e^{-8.414} * 1250^{0.943} * e^{-0.02*12-0.076*10} = 0.0679$

Base Encroachment Rate (BER_SB)

$(\frac{\mu_i}{L_i}) = e^{\ln\beta_0} * TADT_i^{\beta_1} * e^{(\sum_i^t \beta_i x_i)} = e^{-8.414} * 1250^{0.943} * e^{-0.02*12-0.076*10} = 0.0679$

Encroachment Rate(ER: collision per mile per year)

Encroachment Rate= Base Encroachment Rate ***SD Calibration Factor** *∏CMFs

ER_1=BER_NB*Calibration Factor*CMF(Horizontal Curve)*P(away)*CMF(Rumble Strip_right)
=0.0679*0.855*1.03*0.51*0.73= 0.0222

ER_2=BER_SB*Calibration Factor*CMF(Horizontal Curve)*P(away)*CMF(Rumble Strip_right)
=0.0679*0.855*1.03*(1- 0.51)*0.73= 0.0214

Median

ER_3=BER_NB*Calibration Factor*CMF(Horizontal Curve)*P(toward)*CMF(Rumble Strip_left)
=0.0679*0.855*1.03*(1-0.51)*0.73= 0.0214

ER_4=BER_SB*Calibration Factor*CMF(Horizontal Curve)*P(toward)*CMF(Rumble Strip_left)
=0.0679*0.855*1.03*0.51*0.73= 0.0222

April 5, 2013 — Evaluation and Mitigation of Vehicle Impact Hazards for Overpasses

Case Study (cont.)

Bridge Hazard Envelope (BHE: mile)

P=(1/5280)*$[L_h + \left(\frac{W_e}{\sin\theta}\right) + W_h \cot\theta]$

For single-unit truck(length:21ft; width: 8.7ft)

$W_e = L_v * \sin\psi + W_v * \cos\psi$=21*sin 7.5+8.7*cos 7.5=64.325(ft)

P=(1/5280)*$[28 + \left(\frac{64.325}{\sin 10}\right) + 5\cot 10]$=0.0229(mile)

For semi-trailor truck(length:53ft;width: 8.7ft)

$W_e = L_v * \sin\psi + W_v * \cos\psi$=53*sin 7.5+8.7*cos 7.5=88.368(ft)

P=(1/5280)*$[28 + \left(\frac{88.368}{\sin 10}\right) + 5\cot 10]$=0.0274(mile)

Lateral Encroachment Probability

lnY=5.235-0.161X

where X= (51.9-5)/2/3.3

Y=31.84% (normalized)

April 5, 2013 — Evaluation and Mitigation of Vehicle Impact Hazards for Overpasses

Case Study (cont.)

Bridge Column Collision Risk (CR=ER*BHE*Y)

CE(NB_right side)= ER_1* 0.0229=0.051%
CE(NB_left_side)= ER_2*0.0229*31.8398% = 0.016%
CE(SB_right side)= ER_3*0.0229= 0.049%
CE(SB_left side)= ER_4*0.0229*31.8398% =0.016%
Collision Risk for Bridge 64020220= ∑CR= 0.131%

Bridge Significance(B_RUC) ($ per day)

VOT = (distance/speed)*60*volume*unit cost*vehicle occupancy factor
= (3/55)*60*7065*0.19*1.67 = $7,336.55
VOC = distance*unit cost*volume = 3*0.6*7065 = $12,717
AC = distance*volume*accident rate*unit cost/1,000,000 = 3*7065*1.9*7400/1,000,000 = $298
RUC = VOT+VOC+AC= $20,352

April 5, 2013 Evaluation and Mitigation of Vehicle Impact Hazards for Overpasses

Bridge Ranking

Table 6. Bridges listed as top 30 in both ranking methods

R1: Bridges ranked by total risk-significance

R2: Bridges ranked by sum of Z-scores of bridge collision risk and bridge significance

Bridge	R1	R2
I-29 MM76.5	1	2
I-90 MM59	2	1
I-29 MM78	3	[illegible]
I-90 MM55	4	3
I-90 MM131	[illegible]	6
I-90 MM330	6	7
I-90 MM150	7	4
I-29 MM77	8	10
I-29 MM26	9	15
I-29 MM109	10	16
I-29 MM34	11	8
I-29 MM84	12	9
I-29 MM71	13	11
I-29 MM127	14	22
I-29 MM83	15	17
I-29 MM62	17	20
I-29 MM81	18	19
I-29 MM4	19	24
I-29 MM47	20	[illegible]
I-29 MM1	21	23
I-29 MM1	23	29
I-29 MM59	24	28
I-90 MM14	25	27
I-90 MM364	29	12

April 5, 2013 Evaluation and Mitigation of Vehicle Impact Hazards for Overpasses

Bridge Ranking (cont.)

Scatter Plot by collision risk (CR) and significance (B_RUC)

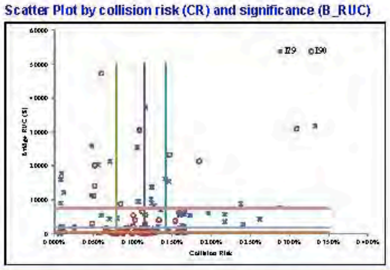

April 5, 2013 Evaluation and Mitigation of Vehicle Impact Hazards for Overpasses

Bridge Ranking (cont.)

Table 7. Bridges listed as top 25% by collision risk (CR) and significance (B_RUC)

RUC \ Collision risk	<25%	25-50%	50-75%	>75%
>75%	I-90 (4) I-29 (8) Total (12)	I-90 (2) I-29 (2) Total (4)	I-90 (0) I-29 (7) Total (7)	I-90 (3) I-29 (5) Total (8)*
50-75%	I-90 (3) I-29 (4) Total (7)	I-90 (5) I-29 (1) Total (6)	I-90 (3) I-29 (2) Total (5)	I-90 (3) I-29 (12) Total (15)
25-50%	I-90 (6) I-29 (3) Total (9)	I-90 (11) I-29 (0) Total (11)	I-90 (7) I-29 (5) Total (12)	I-90 (0) I-29 (6) Total (6)
<25%	I-90 (3) I-29 (7) Total (8)	I-90 (10) I-29 (8) Total (18)	I-90 (7) I-29 (4) Total (11)	I-90 (0) I-29 (3) Total (3)

*All eight bridges are also in Table 6

April 5, 2013 Evaluation and Mitigation of Vehicle Impact Hazards for Overpasses

Bridge Collision Risk Maps

April 5, 2013 Evaluation and Mitigation of Vehicle Impact Hazards for Overpasses

April 5, 2013 Evaluation and Mitigation of Vehicle Impact Hazards for Overpasses

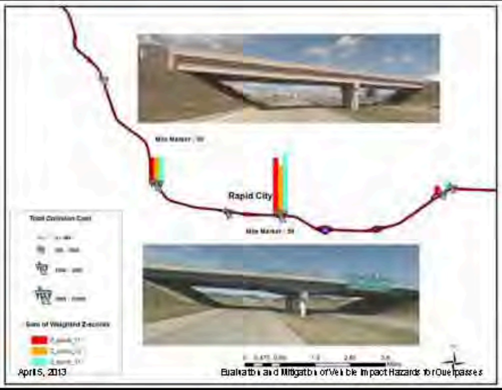

Structural Analysis

- All columns are being analyzed using linear elastic analysis to determine the *Demand/Capacity (D/C) Ratio.*
  - $D/C\ Ratio = \frac{Demand}{Capacity}$
- A D/C Ratio greater than 1 indicates that the column is insufficient.
- Inelastic pushover analysis may be performed if deemed necessary.

Column Capacity

- Shear Capacity
  - Determined as per AASHTO Guide Specifications for LRFD Seismic Bridge Design, 2nd Ed., 2011, Section 8.6.
- Flexural Capacity
  - Determined from the software spColumn

Collision Load

- Structural analysis was performed using program SAP200
- Load Application:
  - In accordance with AASHTO LRFD Bridge Design Specifications, 6th Ed., 2012, Section 3.6.5-Vehicular Collision Force: CT
  - A 600 kip lateral force applied to the column at 5 feet above the ground surface
  - Load was applied at 0° and 15° from the plane of the bent

SAP2000 Model

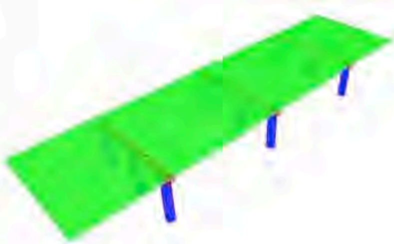

Bridge Types

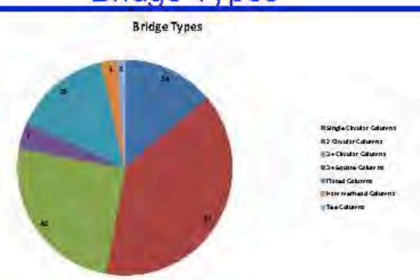

Bridge Types

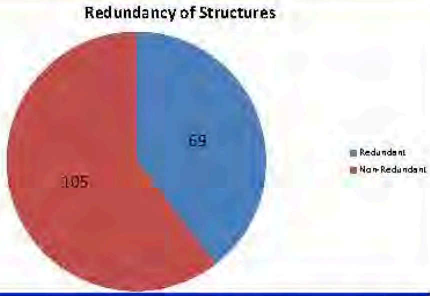

April 5, 2013 — Evaluation and Mitigation of Vehicle Impact Hazards for Overpasses

Bridge Redundancy Distribution

Collision Risk / RUC	<25%	25-50%	50-75%	>75%
>75%	Redundant (11) Non-Red. (1) Total (12)	Redundant (4) Non-Red. (0) Total (4)	Redundant (1) Non-Red. (6) Total (7)	Redundant (6) Non-Red. (2) Total (8)
50-75%	Redundant (5) Non-Red. (2) Total (7)	Redundant (4) Non-Red. (2) Total (6)	Redundant (0) Non-Red. (5) Total (5)	Redundant (2) Non-Red. (13)* Total (15)
25-50%	Redundant (3) Non-Red. (2) Total (5)	Redundant (2) Non-Red. (9) Total (11)	Redundant (0) Non-Red. (12) Total (12)	Redundant (0) Non-Red. (6) Total (6)
<25%	Redundant (3) Non-Red. (5) Total (8)	Redundant (1) Non-Red. (9) Total (10)	Redundant (0) Non-Red. (11) Total (11)	Redundant (0) Non-Red. (3) Total (3)

* 3 of these bridges have adequate capacity

April 5, 2013 — Evaluation and Mitigation of Vehicle Impact Hazards for Overpasses

Preliminary Results

- The Single Circular Column, 2 Circular Column Bents, and Square Column bridges have been analyzed so far.

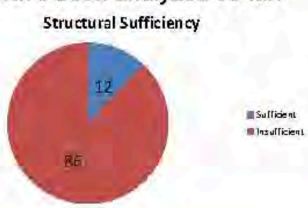

April 5, 2013 — Evaluation and Mitigation of Vehicle Impact Hazards for Overpasses

Preliminary Results

- The Single Circular Column, 2 Circular Column Bents, and Square Column bridges have been analyzed so far.

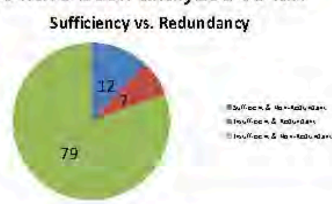

April 5, 2013 — Evaluation and Mitigation of Vehicle Impact Hazards for Overpasses

Moving Forward

- Further pushover analysis on high risk bridges will be done to determine if mitigation is required.
- High risk bridges may be:
  - Bridges with a high collision risk
  - Bridges with non-redundant structures

April 5, 2013 — Evaluation and Mitigation of Vehicle Impact Hazards for Overpasses

A.3: Review of High Risk Bridges

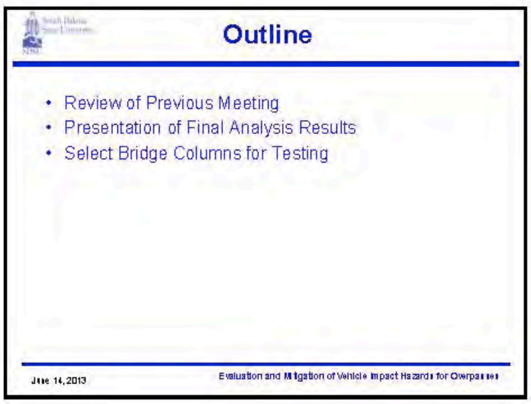

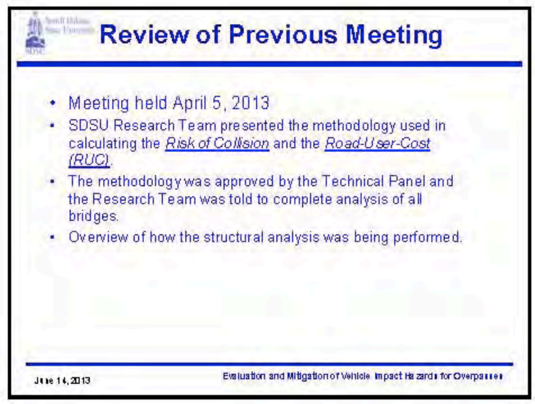

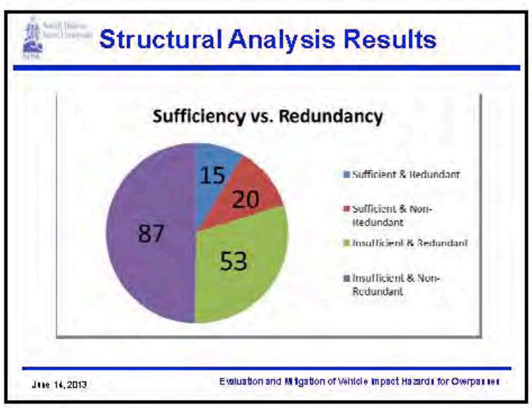

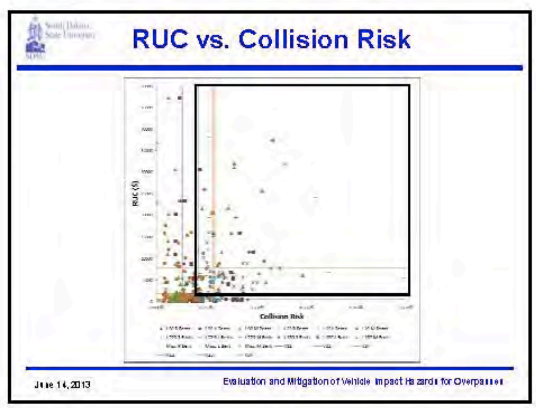

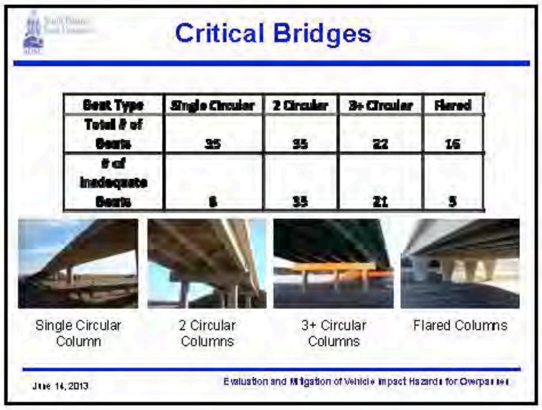
Critical Bridges
Bent Type | Single Circular | 2 Circular | 3+ Circular | Flared
Total # of Bents | 35 | 35 | 22 | 16
# of Inadequate Bents | 8 | 35 | 21 | 5
Single Circular Column
2 Circular Columns
3+ Circular Columns
Flared Columns
June 14, 2013
Evaluation and Mitigation of Vehicle Impact Hazards for Overpasses

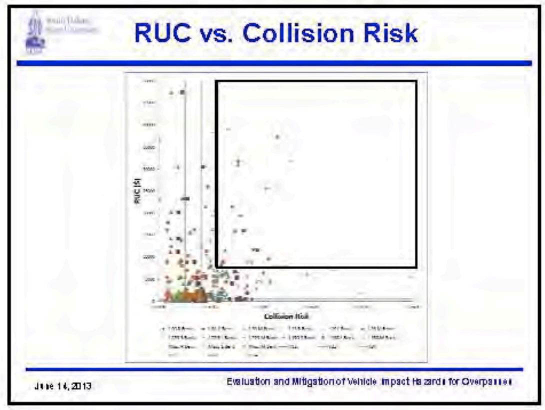
RUC vs. Collision Risk
Collision Risk
June 14, 2013
Evaluation and Mitigation of Vehicle Impact Hazards for Overpasses

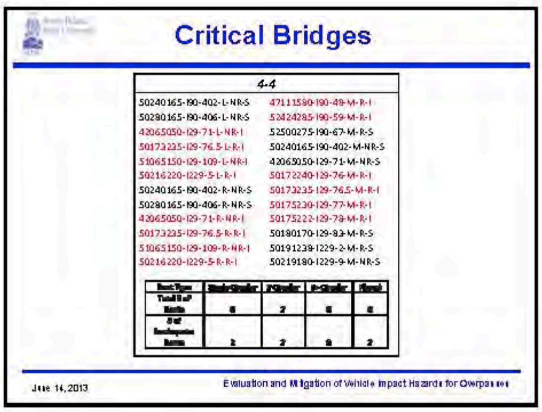
Critical Bridges
4-4
50240165-I90-402-L-NR-S
50280165-I90-406-L-NR-S
42065050-I29-71-L-NR-I
50173235-I29-76.5-L-R-I
51065150-I29-109-L-NR-I
50216220-I229-5-L-R-I
50240165-I90-402-R-NR-S
50280165-I90-406-R-NR-S
42065050-I29-71-R-NR-I
50173235-I29-76.5-R-R-I
51065150-I29-109-R-NR-I
50216220-I229-5-R-R-I
47111590-I90-49-M-R-I
52424285-I90-59-M-R-I
52500275-I90-67-M-R-S
50240165-I90-402-M-NR-S
42065050-I29-71-M-NR-S
50172240-I29-76-M-R-I
50173235-I29-76.5-M-R-I
50175230-I29-77-M-R-I
50175222-I29-78-M-R-I
50180170-I29-83-M-R-S
50191238-I229-2-M-R-S
50219180-I229-9-M-NR-S
June 14, 2013
Evaluation and Mitigation of Vehicle Impact Hazards for Overpasses

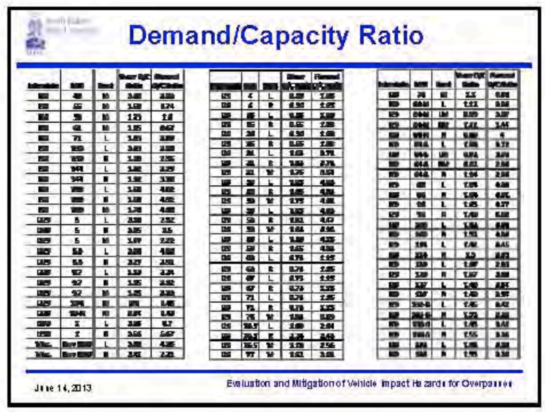
Demand/Capacity Ratio
June 14, 2013
Evaluation and Mitigation of Vehicle Impact Hazards for Overpasses

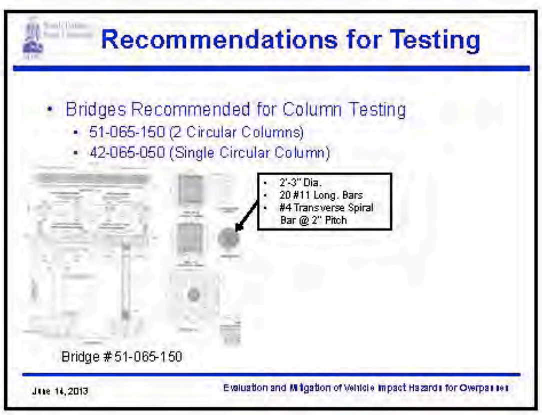
Recommendations for Testing
• Bridges Recommended for Column Testing
• 51-065-150 (2 Circular Columns)
• 42-065-050 (Single Circular Column)
• 2'-3" Dia.
• 20 #11 Long. Bars
• #4 Transverse Spiral Bar @ 2" Pitch
Bridge # 51-065-150
June 14, 2013
Evaluation and Mitigation of Vehicle Impact Hazards for Overpasses

A.4: Proposed Test Specimens

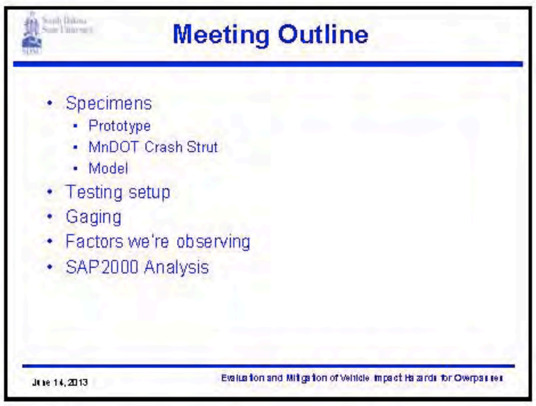

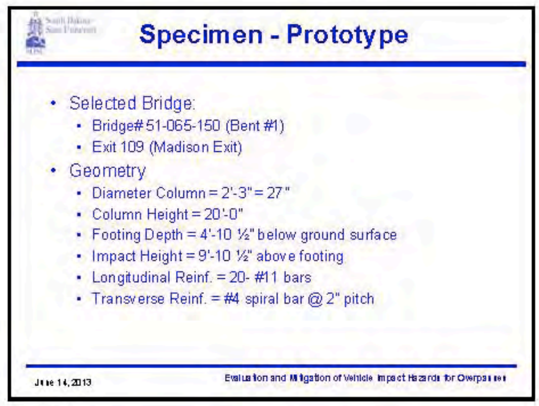

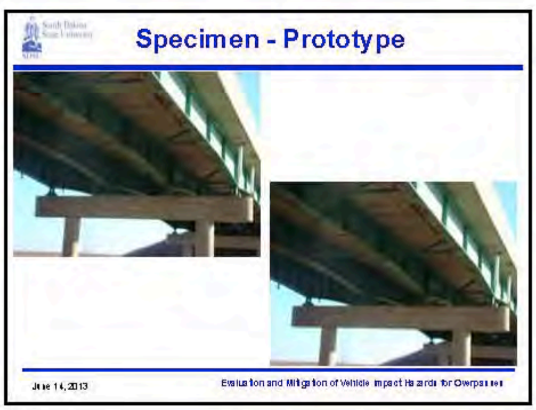

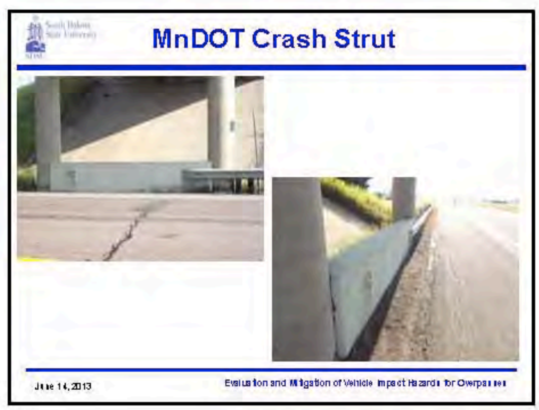

MnDOT Crash Strut

- **Height** = Minimum of 4'-6" above ground surface
  - 2012 AASHTO Specifications increased impact height from 4' to 5' above ground surface.
  - Thus, we recommend increasing minimum height to 5'-6"
- **Width** = Minimum of 3'
- **Length** = Typically extend strut to 6" from outside of footing
- **Reinforcement**
  - **Horizontal Bars** = Minimum #6 bars at 12" spacing
  - **Transverse** = No specifications (Design I reviewed used #6 stirrups at 12" spacing between columns and spaced with dowels on end region)
  - **Dowels** = #6 bars at 6" spacing over minimum distance of 7' per column/footing

June 14, 2013 — Evaluation and Mitigation of Vehicle Impact Hazards for Overpasses

MnDOT Crash Strut

- Design Procedure (Design strut region between the columns as a horizontal beam)
- P_{crash} = 400 kips
  - 2012 Specifications increased this load to 600 kips
- θ_{max} = 30°

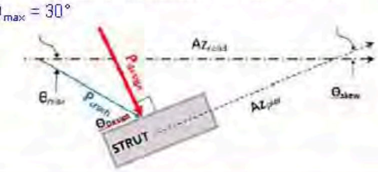

June 14, 2013 — Evaluation and Mitigation of Vehicle Impact Hazards for Overpasses

Test Specimen - Model

- Test specimen is to be a one-third scale model of the prototype.
  - **Linear Dimensions** = 1/3(Prototype)
  - **Area Dimensions** = 1/9(Prototype)
  - **Loads** = 1/9(Prototype)
- One specimen will be a scaled model of the as-built prototype and the other will include the crash strut retrofit.

June 14, 2013 — Evaluation and Mitigation of Vehicle Impact Hazards for Overpasses

Test Specimen – Column

		Prototype	Model	Scale
Geometry	D (in)	27	9	3.0
	A_c (in²)	572.6	63.6	9.0
	H (in)	240	80	3.0
Longitudinal Reinforcement	# of Bars	10	8	
	Bar Size (#)	11	4	
	A_s (in²)	15.6	1.6	8.1
Transverse Reinforcement	Bar Size (#)	4	W5	
	A'_{sp} (in²)	0.2	0.0499	
	S (in)	2	1.75	
	c_c (in)*	2	0.667	* Clear to transverse bars
Shear Capacity	V_n (k)	268.08	30.07	8.9
Moment Capacity	M_n (k-ft)	607.3	23.2	26.2

June 14, 2013 — Evaluation and Mitigation of Vehicle Impact Hazards for Overpasses

Test Specimen – Bent Cap

		Prototype	Model
Geometry	b (in)	30	10
	h (in)	36	12
	A (in²)	1080.0	120.0
	L (in)	372	124
Longitudinal Reinforcement (Top/Bottom)	# of Bars	12	6
	Bar Size (#)	11	5
	A'_s (in²)	1.56	0.31
	A_s (in²)	18.72	1.86
Transverse Reinforcement (12" Spacing Region)	Bar Size (#)	6	3
	# Ties	3	2
	S (in)	12	7.25
	c_c (in)*	2	0.667
Transverse Reinforcement (6" Spacing Region)	Bar Size (#)	6	3
	# Ties	3	2
	S (in)	[illegible]	3.25
	c_c (in)*	2	0.667

June 14, 2013 — Evaluation and Mitigation of Vehicle Impact Hazards for Overpasses

Test Specimen – Strut

		Prototype	Model	Scale
Geometry	b (in)	36	12	[illegible]
	h (in)	124.56	41.5	[illegible]
	A (in²)	3961.4	498.0	[illegible]
	L (in)	379	95	3.0
Longitudinal Reinforcement (Sides)	# of Bars	20	5	
	Bar Size (#)	6	3	
	A_s (in²)	8.8	0.55	16.0
Longitudinal Reinforcement (Top/Bottom)	# of Bars	4	2	
	Bar Size (#)	6	3	
	A_s (in²)	1.76	0.22	8.0
Transverse Reinforcement	Bar Size (#)	6	3	
	S (in)	12	9.75	
	c_c (in)*	2	0.480	
Dowels (End Region)	Bar Size (#)	6	3	
	S (in)	6	2	
	Projection (in)	52.24	7	
	Embedment (in)	6	4.5	

June 14, 2013 — Evaluation and Mitigation of Vehicle Impact Hazards for Overpasses

Test Specimen - Model

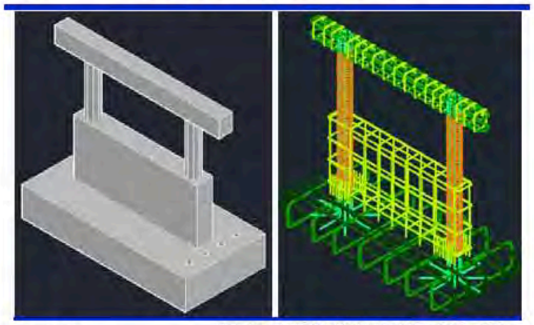

June 14, 2013 — Evaluation and Mitigation of Vehicle Impact Hazards for Overpasses

Test Setup

- A lateral load of 66.7 kips will be applied at a height of 39.5" from the top of the footing using the 146 kip capacity actuator.
- Dead loads representing the weight of the superstructure will be applied.
  - **Exterior Girders** = 1.44 kips
  - **Interior Girders** = 1.61 kips
  - This will be applied using yet to be determined steel beams or weights of some kind

June 14, 2013 — Evaluation and Mitigation of Vehicle Impact Hazards for Overpasses

Test Setup

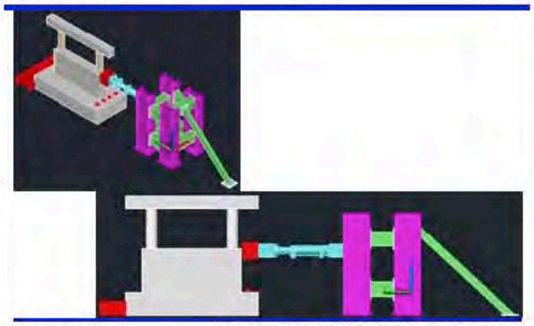

June 14, 2013 — Evaluation and Mitigation of Vehicle Impact Hazards for Overpasses

Gaging

- Strain gages will be applied on the **longitudinal** bars at:
  - The base of the column (top of the footing)
  - The point of load application/top of strut
- Strain gages will be applied on the **transverse** (spiral) bars:
  - Above the strut
  - Just below the point of loading

June 14, 2013 — Evaluation and Mitigation of Vehicle Impact Hazards for Overpasses

Factors to Evaluate

- During the experimental testing, we will be looking at and evaluating the:
  - Imposed Shear
  - Imposed Moment
  - Stress in the Column Longitudinal Bars
  - Stress in the Column Shear Reinforcement
  - Displacement

June 14, 2013 — Evaluation and Mitigation of Vehicle Impact Hazards for Overpasses

SAP2000 Analysis

- A finite element analysis was performed using SAP2000 to determine predicted results for the experimental testing.
- Model was created assuming fixed connections at the bottom of the columns.
- Strut modeled as beam element and divided into multiple elements to increase accuracy.

June 14, 2013 — Evaluation and Mitigation of Vehicle Impact Hazards for Overpasses

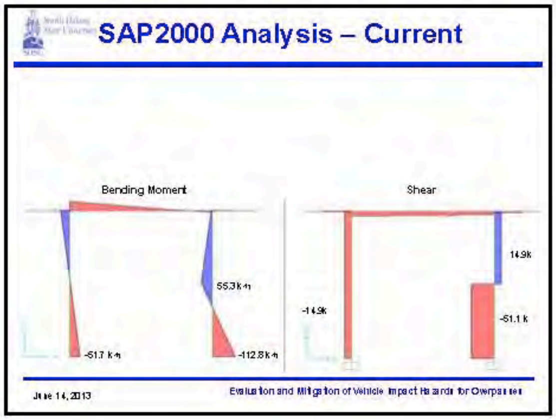
SAP2000 Analysis – Current
Bending Moment
Shear
55.3 k-ft
-51.7 k-ft
-112.8 k-ft
14.9k
-14.9k
-61.1 k
June 14, 2013
Evaluation and Mitigation of Vehicle Impact Hazards for Overpasses

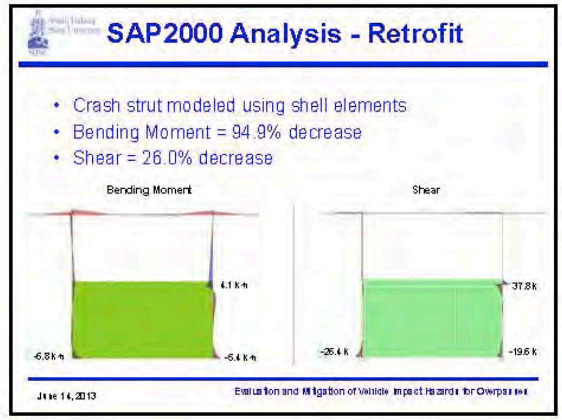
SAP2000 Analysis - Retrofit
• Crash strut modeled using shell elements
• Bending Moment = 94.9% decrease
• Shear = 26.0% decrease
Bending Moment
Shear
4.1 k-ft
-6.8 k-ft
-5.4 k-ft
37.8 k
-26.4 k
-19.6 k
June 14, 2013
Evaluation and Mitigation of Vehicle Impact Hazards for Overpasses

A.5: Report on Test Results

Task 10: Review of Test Results

Evaluation and Mitigation of Vehicle Impact Hazards for Overpasses

Nadim Wehbe, Xiao Qin, and Brett Tigges

March 6, 2014 — Evaluation and Mitigation of Vehicle Impact Hazards for Overpasses

Outline

- Review of Tasks 7: Selection of Test Specimens
- Task 8: Construction of Test Specimens
- Task 9: Perform Load Testing
- Task 10: Meet with Technical Pane lto Review test Results

March 6, 2014 — Evaluation and Mitigation of Vehicle Impact Hazards for Overpasses

Review of Tasks 7

- Task 7: *Meet with technical panel and finalize selection of test specimens*
  - Completed on June 14, 2013
  - Selected prototype: Bridge #51-065-150 (Bent #1); I-29 Exit 109 (Madison Exit)
  - Two specimens: as-built and retrofitted with crash strut
    - Diameter Column = 2'-3" = 27"
    - Column Height = 20'-0"
    - Footing Depth = 4'-10 ½" below ground surface
    - Impact Height = 9'-10 ½" above footing
    - Longitudinal Reinf. = 20 #11 bars
    - Transverse Reinf. = #4 spiral bar @ 2" pitch

March 6, 2014 — Evaluation and Mitigation of Vehicle Impact Hazards for Overpasses

Review of Tasks 7

MnDOT Crash Strut:

- Height = Minimum of 4'-6" above ground surface
- 2012 AASHTO Specifications changed location of collision load from 4' to 5' above ground surface
- We recommended increasing minimum height to 5'-6" (extend 6" above point of collision load application)
- Width = Minimum of 3'
- Length = Typically extend strut to 6" from outside of footing
- Reinforcement:
  - Horizontal Bars: Minimum #6 bars at 12" spacing
  - Transverse: No specifications (one design shows #6 stirrups at 12" spacing)
  - Dowels: #6 bars at 6" spacing over minimum distance of 7' per column/footing

March 6, 2014 — Evaluation and Mitigation of Vehicle Impact Hazards for Overpasses

Review of Tasks 7

MnDOT Crash Strut:

- Design Procedure (Design strut region between the columns as a horizontal beam)
- Pcrash = 400 kips
- 2012 Specifications increased this load to 600 kips
- θ_{max} = 30°

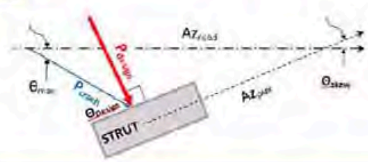

March 6, 2014 — Evaluation and Mitigation of Vehicle Impact Hazards for Overpasses

Task 8

- Task 8: *Construct Test Specimens*
  - Design of test specimens was approved by the technical panel on August 13, 2013
  - Test specimen is one-third scale of the prototype
    - Linear Dimensions = 1/3 of Prototype
    - Area Dimensions = 1/9 of Prototype
    - Loads = 1/9 of Prototype (600 kips prototype ≡ 66.7 kips model)

March 6, 2014 — Evaluation and Mitigation of Vehicle Impact Hazards for Overpasses

Task 8

- Column Scaling:

		Prototype	Model	Scale
Geometry	D (in)	27	9	3.0
	A_g (in²)	572.5	63.6	9.0
	H (in)	240	60	3.0
Longitudinal Reinforcement	# of Bars	10	8	
	Bar Size (#)	11	4	
	A_s (in²)	15.6	1.6	8.1
Transverse Reinforcement	Bar Size (#)	4	W5	
	A'_s (in²)	0.2	0.0499	
	S (in)	3	1.75	
	c_c (in)*	2	0.667	
Shear Capacity	V_n (k)	265.05	30.07	8.9
Moment Capacity	M_n (k-ft)	607.5	23.2	26.2

* Clear to transverse bars

Task 8

- Bent Cap Scaling:

		Prototype	Model
Geometry	h (in)	36	12
	b (in)	36	12
	A (in²)	1080.0	120.0
	L (in)	372	124
Longitudinal Reinforcement (Top/Bottom)	# of Bars	12	6
	Bar Size (#)	11	5
	A'_s (in²)	1.56	0.31
	A_s (in²)	18.72	1.86
Transverse Reinforcement (12" Spacing Region)	Bar Size (#)	6	3
	# Ties	2	2
	S (in)	12	7.25
	c_c (in)*	2	0.667
Transverse Reinforcement (3" Spacing Region)	Bar Size (#)	6	3
	# Ties	3	2
	S (in)	2	1.25
	c_c (in)*	2	0.667

Task 8

- Model

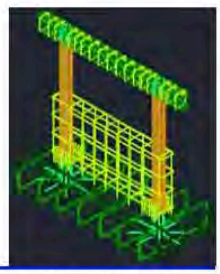

Task 8

- Strain gages on **longitudinal** bars at:
  - The base of the column (top of the footing)
  - The point of load application/top of strut
- Strain gages on **transverse** (spiral) bars:
  - Just above the point of loading/strut
  - Just below the point of loading

Task 8

- Construction

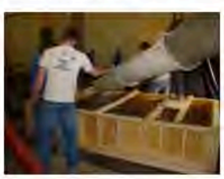

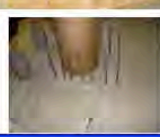

Task 8

- Construction

Task 9

- Task 9: *Perform Load Testing*
- Test Set Up
  - Lateral load was applied at a height of 39.5" from the top of the footing and at 15° to bent plane
  - Dead loads (representing superstructure weight) were applied to the bent cap
    - **Exterior Girders** = 1.44 kips (two loads)
    - **Interior Girders** = 1.61 kips (two loads)

March 6, 2014 Evaluation and Mitigation of Vehicle Impact Hazards for Overpasses

Task 9

- Test Set Up

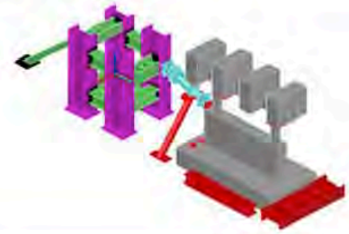

March 6, 2014 Evaluation and Mitigation of Vehicle Impact Hazards for Overpasses

Task 9

- Test Set Up

March 6, 2014 Evaluation and Mitigation of Vehicle Impact Hazards for Overpasses

Task 9

- Elastic Analysis of As-Built Bent

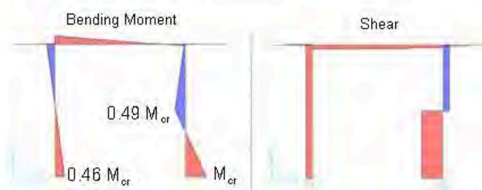

March 6, 2014 Evaluation and Mitigation of Vehicle Impact Hazards for Overpasses

Task 9

- Elastic Analysis of Retrofitted Bent

March 6, 2014 Evaluation and Mitigation of Vehicle Impact Hazards for Overpasses

Task 10

- Task 10: Review Test Results with Technical Panel
- Testing was conducted in late December 2013 and early January 2014
- Specimens behaved as expected – no surprises

March 6, 2014 Evaluation and Mitigation of Vehicle Impact Hazards for Overpasses

Task 10

- **As-Built Specimen**

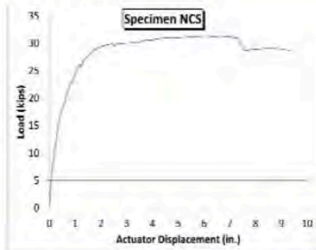

Task 10

- **As-Built Specimen**
  - ➢ First hinge formed at bottom of front column (loaded column)
  - ➢ Second hinge formed at point of lateral load application in the front column
  - ➢ Third and fourth hinges formed at top and bottom of back column
  - ➢ Failure occurred by rupture of tension steel at bottom of front column
  - ➢ Load at failure is approximately ½ AASHTO prescribed load

Task 10

- **As-Built Specimen**

Task 10

- **As-Built Specimen**

Task 10

- **Retrofitted Specimen**

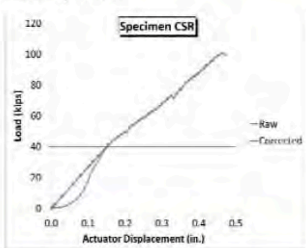

Task 10

- **Retrofitted Specimen**
  - ➢ Reached a lateral load of 1.5 times the AASHTO prescribed load
  - ➢ No hinging or yielding of reinforcement
  - ➢ Horizontal crack at the top of crash strut (cover concrete) at a load = 73 kips
  - ➢ Failure occurred in footing

Task 10

- Retrofitted Specimen

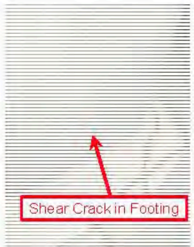

March 6, 2014 Evaluation and Mitigation of Vehicle Impact Hazards for Overpasses

Task 10

Questions?

March 6, 2014 Evaluation and Mitigation of Vehicle Impact Hazards for Overpasses

APPENDIX B: BRIDGE INVENTORY

The following material code is for use with the next tabulated inventory.

Material Code

9	ALUMINUM
8	CONCRETE, PRESTRESSED
7	COMP STEEL AND CONCRETE
6	TIMBER AND CONCRETE
5	TIMBER AND STEEL
4	STEEL AND CONCRETE
3	STEEL
2	CONCRETE, NOT PS
1	MASONRY
0	TIMBER

I-29 Bridge Inventory

					Superstructure					Substructure		
Bridge ID	Mile Marker	Location	Exit Ramp	Speed Limit (mph)	No. of Spans	Span Type	No. of Girders	Material	Comments	No. of Bents	Column Type	Columns per Bent
64158399	1	1.6 S NSCITY INTERCHANGE	Y	65	2	Girder	7	7	PLATE GIRDER 250' UNIT	1	Circular	3
64149367	4	1.9 N NSCITY INTERCHANGE	Y	65	4	Girder	4 Cell	2	STANDARD CONCRETE BOX GIRDER	3	Circular	3
64140355	6	3.4 NW N SCITY INTERCH	N	75	4	Girder	4 Cell	2	STANDARD CONCRETE BOX GIRDER	3	Circular	3
64120336	8.5	0.5 SE JEFFERSON INTERCH	N	75	4	Girder	3 Cell	2	STANDARD CONCRETE BOX GIRDER	3	Circular	3
64115330	9	JEFFERSON INTERCHANGE	Y	75	4	Girder	4 Cell	2	STANDARD CONCRETE BOX GIRDER	3	Circular	3
64100315	11	2.2 NW JEFFERSON INTERCH	N	75	4	Girder	3 Cell	2	STANDARD CONCRETE BOX GIRDER	3	Circular	2
64080296	13	1.3 SE OF ELK POINT	N	75	4	Girder	3 Cell	2	STANDARD CONCRETE BOX GIRDER	3	Circular	2
64070287	15	E ELK POINT INTERCHANGE	Y	75	4	Girder	4 Cell	2	STANDARD CONCRETE BOX GIRDER	3	Circular	3
64050250	20	6.2 SE SD 50 INTERCH	N	75	4	Slab	NA	2	UMBRELLA	3	Circular	2
64020220	24	2.2 SE SD 50 INTERCH	N	75	4	Slab	NA	2	UMBRELLA	3	Circular	2
64008205	26	SD 50 INTERCHANGE	Y	75	4	Girder	4 Cell	2	STANDARD CONCRETE BOX GIRDER	3	Circular	1
64006160	31	SD 48 INTERCHANGE	Y	75	4	Girder	4	7	PLATE GIRDER 252' PARABOLIC	3	Circular	3
64006120	35	4 N SD 48 INTERCH	N	75	4	Girder	4	7	PLATE GIRDER 252' PARABOLIC	3	Circular	3
64006100	37	10 S SD 46 INTERCH	N	75	4	Girder	4	7	PLATE GIRDER 252' PARABOLIC	3	Circular	4
64006090	38	9.0 S SD 46 INTERCHANGE	Y	75	4	Girder	4	7	PLATE GIRDER 250.4' PARABOLIC	3	Circular	3
64006030	44	3 S SD 46 INTERCH	N	75	4	Girder	4	7	PLATE GIRDER 252' PARABOLIC	3	Circular	4
64006010	46	1 S SD 46 INTERCH	N	75	4	Girder	4	7	PLATE GIRDER 252' PARABOLIC	3	Circular	10
64006000	47	SD 46 INTERCHANGE	Y	75	2	Girder	8	8	GIRDERS 8 PER SPAN TYPE 72	1	Flared	4
42065260	50	3 N SD 46 INTERCHANGE	Y	75	4	Girder	4	7	PLATE GIRDER 252' PARABOLIC	3	Circular	3
42065230	53	6 N SD 46 INTERCHANGE	Y	75	4	Girder	4	7	PLATE GIRDER 252' PARABOLIC	3	Circular	3
42065200	56	3.5 US 18 W INTERCHANGE	Y	75	4	Girder	4	7	PLATE GIRDER 252' PARABOLIC	3	Circular	2
42065170	59	US 18 W INTERCHANGE	Y	75	4	Girder	4	7	PLATE GIRDER 252' PARABOLIC	3	Circular	1
42065140	62	US 18 E INTERCHANGE	Y	75	4	Girder	4B	2	STANDARD CONCRETE BOX GIRDER	3	Circular	1
42065141	62	US 18 E INTERCHANGE	Y	75	4	Girder	4B	2	STANDARD CONCRETE BOX GIRDER	3	Circular	1
42065130	63	1 N US 18 E INTERCH	N	75	4	Slab	NA	2	UMBRELLA	3	Circular	1
42065120	64	SD 44 INTERCHANGE	Y	75	4	Slab	NA	2	UMBRELLA	3	Circular	2
42065100	65	2 N SD 44 INTERCH	N	75	4	Slab	NA	2	UMBRELLA	3	Circular	3
42065080	68	4.0 N SD 44 INTERCHANGE	Y	75	2	Girder	7	8	GIRDERS 7 PER SPAN TYPE 72	1	Flared	4
42065050	71	4.1 S I229 INTERCHANGE	Y	75	4	Slab	NA	2	UMBRELLA	3	Circular	2
50172240	76	INTERSECTION 57TH & I029	Y	65	2	Girder	7	8	Concrete Girder - Continuous Span	1	Flared	3
50173235	76.5	0.5 SW 41ST INTERCH	N	65	4	Girder	7	8	GIRDERS 7 PER SPAN TYPE IV	3	Circular	3
50175230	77	41ST INTERCHANGE	Y	65	2	Girder	11	7	PLATE GIRDER 240' PARABOLIC	1	Circular	3
50175222	78	26TH ST INTERCHANGE	Y	65	2	Girder	15	8	GIRDERS 15 PER SPAN TYPE 72	1	Flared	2
50178191	81	RUSSEL STR INTERCH	Y	65	2	Girder	13	8		1	Flared	4
50180170	83	W 60TH ST N INTERCHANGE	Y	65	4	Girder	12	8	GIRDERS 12 PER SPAN TYPE 72	1	Flared	3
50180162	84	I 90 & I 29 INTERCHANGE	Y	65	5	Girder	6	7	PLATE GIRDER 316' UNIT	4	Circular	4
50180163	84	I 90 & I 29 INTERCHANGE	Y	65	5	Girder	6	7	PLATE GIRDER 316' UNIT	4	Circular	4
50180140	86	2.2 N I 90 INTERCHANGE	Y	75	4	Girder	4	7	PLATE GIRDER 250' PARABOLIC	3	Circular	5
50177130	87	3.3 N I 90 INTERCH	N	75	4	Girder	4	7	PLATE GIRDER 252' PARABOLIC	3	Circular	2
50175040	96	2 S SD 115 INTERCH	N	75	4	Girder	4	7	PLATE GIRDER 250' PARABOLIC	3	Circular	2

I-29 Bridge Inventory

					Superstructure					Substructure		
Bridge ID	Mile Marker	Location	Exit Ramp	Speed Limit (mph)	No. of Spans	Span Type	No. of Girders	Material	Comments	No. of Bents	Column Type	Columns per Bent
50175020	98	SD 115 & I29 INTERCHANGE	Y	75	4	Girder	4	7	PLATE GIRDER 250' PARABOLIC	3	Circular	3
51065210	103	3.2 N MINNEHAHA CO LINE	N	75	4	Girder	4	7	PLATE GIRDER 252' PARABOLIC	3	Circular	2
51065200	104	5 S SD 34 INTERCHANGE	Y	75	4	Girder	4	7	PLATE GIRDER 252' PARABOLIC	3	Circular	2
51065150	109	SD 34 INTERCHANGE	Y	75	4	Girder	4	7	PLATE GIRDER 250' PARABOLIC	3	Circular	4
51066100	114	SD 32 INTERCHANGE	Y	75	4	Girder	4	7	PLATE GIRDER 252' PARABOLIC	3	Circular	2
51065050	120	5 S BROOKINGS CO LINE	N	75	4	Girder	4	8	GIRDERS 4 PER SPAN TYPE III	3	Circular	2
06185230	125	1 N MOODY CO LINE	N	75	4	Girder	4	7	PLATE GIRDER 252' PARABOLIC	3	Circular	2
06185210	127	SD 324 INTERCHANGE	Y	75	4	Girder	4	7	PLATE GIRDER 252' PARABOLIC	3	Circular	2
06185190	129	3 S US 14 INTERCH	N	75	4	Girder	4	8	GIRDERS 4 PER SPAN TYPE III	3	Circular	2
06185159	132	US 14 & I 29 INTERCHANGE	Y	75	4	Girder	4	7	PLATE GIRDER 252' PARABOLIC	3	Circular	2
06185160	132	US 14 & I 29 INTERCHANGE	Y	75	4	Girder	4	7	PLATE GIRDER 252' PARABOLIC	3	Circular	2
06185150	133	US14 BY-PASS INTERCHANGE	Y	75	4	Girder	4	7	PLATE GIRDER 252' PARABOLIC	3	Circular	2
06185130	135	2 N US14 BY PASS	N	75	2	Girder	4	7	PLATE GIRDER 210' PARABOLIC	1	Circular	2
06185110	137	3 S SD 30 INTERCH	N	75	2	Girder	5	7	PLATE GIRDER 210' PARABOLIC	1	Circular	2
06185080	140	SD 30 INTERCHANGE	Y	75	2	Girder	6	7	PLATE GIRDER 210' PARABOLIC	1	Circular	2
20061280	150	SD 28 INTERCHANGE	Y	75	2	Girder	6	7	PLATE GIRDER 224' PARABOLIC	1	Circular	2
29280020	167	2.8 NW SD 22 INTERCH	N	75	4	Girder	4	7	PLATE GIRDER 420' PARABOLIC	3	Circular	2
15240220	173	2.9 N HAMLIN CO LINE	N	75	4	Girder	4	7	PLATE GIRDER 412' PARABOLIC	3	Circular	3
15215150	180	3 N US 212 INTERCHANGE	N	75	2	Girder	6	7	PLATE GIRDER 222' PARABOLIC	1	Square	2
15215120	183	6 N US 212 INTERCH	N	75	2	Girder	4	7	PLATE GIRDER 224' PARABOLIC	1	Square	2
15215070	189	4 S SD 20 INTERCH	N	75	2	Girder	4	7	PLATE GIRDER 224' PARABOLIC	1	Square	2
15215030	193	I 29 & SD 20 INTERCHANGE	Y	75	2	Girder	6	7	PLATE GIRDER 222' PARABOLIC	1	Square	2
55085440	206	GRANT CO LINE	N	75	2	Girder	4	7	PLATE GIRDER 224' PARABOLIC	1	Flared (NC)	2
55085429	207	US 12 & I 29 INTERCHANGE	Y	75	4	Girder	5	7	PLATE GIRDER 356' UNIT	3	Circular	2
55100367	213	I 29 & SD 15 INTERCHANGE	Y	75	4	Girder	5	7	PLATE GIRDER 476' PARABOLIC	3	Circular (NC)	2
55115330	218	4 N SD 15 INTERCH	N	75	2	Girder	4	7	PLATE GIRDER 224' PARABOLIC	1	Flared (NC)	2
55115290	222	2 S PEEVER INTERCH	N	75	2	Girder	4	7	PLATE GIRDER 224' PARABOLIC	1	Flared (NC)	2
55115220	229	3 S SD 10 INTERCH	N	75	2	Girder	4	7	PLATE GIRDER 224' PARABOLIC	1	Flared (NC)	2
55116190	232	SD 10 & I29 INTERCHANGE	Y	75	4	Girder	5	7	PLATE GIRDER 340' UNIT	3	Circular	2
55124170	234	2.0 N SD 10 & I29 INTERCH	N	75	4	Girder	4	7	PLATE GIRDER 328' PARABOLIC	3	Circular	2
55144130	239	6.5 NE SD 10 INTERCH	N	75	4	Girder	4	7	PLATE GIRDER 352' PARABOLIC	3	Circular	4
55175040	248	2.0 N SD 127 INTERCH	N	75	2	Girder	4	7	PLATE GIRDER 224' PARABOLIC	1	Flared (NC)	2

I-90 Bridge Inventory

					Superstructure					Substructure		
Bridge ID	Mile Marker	Location	Exit Ramp	Speed Limit (mph)	No. of Spans	Span Type	No. of Girders	Material	Comments	No. of Bents	Column Type	Columns per Bent
41095059	10	US 85 INTERCHANGE	Y	75	4	Girder	5	7	PLATE GIRDER 330' UNIT	3	Circular	3
41116088	14	US 14A INTERCHANGE	Y	75	4	Girder	6	8	GIRDERS 6 PER SPAN	3	Circular	3
41101077	14	SPEARFISH INTERCHANGE	Y	75	4	Girder	6	8	GIRDERS 6 PER SPAN	3	Circular	3
41154087	17	US 85 S INTERCHANGE	Y	75	4	Girder	6	8	GIRDERS 6 PER SPAN	3	Circular	3
41155087	17	US 85 S INTERCHANGE	Y	75	4	Girder	6	8	GIRDERS 6 PER SPAN	3	Circular	3
41185086	19	2.2 W SD 34 N INTERCH	N	75	4	Girder	4	7	PLATE GIRDER 250' PARABOLIC	3	Circular	2
41207092	23	SD 34 W INTERCHANGE	Y	75	4	Girder	4	7	PLATE GIRDER 264' PARABOLIC	3	Circular	2
41226107	26	2.4 SE SD 34 N INTERCH	N	75	4	Girder	5	8	GIRDERS 5 PER SPAN TYPE III	3	Circular	3
47061480	37	3.2NW TILFORD INTERCHANGE	Y	75	4	Girder	4	7	PLATE GIRDER 253.6' PARABOLIC	3	Circular	2
47069510	40	TILFORD INTERCHANGE	Y	75	4	Girder	4	7	PLATE GIRDER 223' PARABOLIC	3	Circular	2
47098563	46	S PIEDMONT INTERCHANGE	Y	75	4	Girder	4	7	PLATE GIRDER 203.7' PARABOLIC	3	Octagonal	1
47111580	48	3.1 NW SD 231 INTERCHANGE	Y	75	2	Girder	6	7	PLATE GIRDER 232' PARABOLIC	1	Circular	3
47135609	52	1.0 MILE NW PENN CO LINE	Y	75	2	Girder	8	8		1	Top Flare	3
52390278	55	DEADWOOD AVE INTERCHANGE	Y	65	2	Girder	6	8	GIRDERS 6 PER SPAN TYPE 72	1	Circular	4
52410285	57	I 90 & I 190 INTERCHANGE	Y (Loop)	65	2	Girder	7	7	PLATE GIRDER 265' UNIT	1	Top Flare	3
52424285	59	LACROSSE ST INTERCHANGE	Y	65	2	Girder	9	7	PLATE GIRDER 220.5' PARABOLIC	1	Circular	4
52450287	61	US16 B INTERCHANGE	Y	65	2	Girder	23	8		1	Top Flare	10
52467276	62	2.0 E US 16 B INTERCHANGE	Y	65	4	Girder	4	7	PLATE GIRDER 351' PARABOLIC	3	Circular	4
52470276	62.5	2.3 E US 16 B INTERCHANGE	N	65	2	Girder	4	8		1	Flared	3
52500275	67	EXIT 67	Y	75	2	Girder	8	8		1	Top Flare	3
52540275	71	4.0 E BOX ELDER INTERCH	N	75	2	Girder	4	7	PLATE GIRDER 252' PARABOLIC	3	Circular	2
52610285	78	NEW UNDERWOOD INTERCHANGE	Y	75	4	Slab	NA	2	UMBRELLA (SCS)	3	Circular	1
52640285	81	3.0 E NEW UNDRWD INTERCH	N	75	4	Slab	NA	2	UMBRELLA (HSCS)	3	Circular	1
52670285	84	6.0 E NEW UND INTERCHANGE	Y	75	4	Slab	NA	2	UMBRELLA (SCS)	3	Circular	1
52710283	88	10 E NEW UND INTERCHANGE	Y	75	4	Slab	NA	2	UMBRELLA (HSCS)	3	Circular	1
52830310	101	3.1 E WASTA INTERCHANGE	Y	75	4	Girder	6	8	GIRDERS 6 SPAN #1, 7 SPAN #2 #3, 5 SPAN #4	3	Circular	2
52880346	107	1.9 NW W WALL INTERCHANGE	Y	75	4	Girder	4	7	PLATE GIRDER 400' PARABOLIC	3	Circular	3
52900360	109	WEST WALL INTERCHANGE	Y	75	4	Girder	6	7	PLATE GIRDER 405' PARABOLIC	3	Circular	4
52925365	112	US 14 & I 90 INTERCHANGE	Y	75	4	Girder	4	7	PLATE GIRDER 356' UNIT	3	Circular	2
52926366	112.1	US 14 & I 90 INTERCHANGE	Y	75	4	Girder	6	7	PLATE GIRDER 358' UNIT	3	Circular	3
36120107	131	CACTUS FLAT INTERCHANGE	Y	75	4	Girder	5	7	PLATE GIRDER 302' UNIT	3	Circular	3
36309106	150	SD 73 S INTERCHANGE	Y	75	4	Girder	4	8	GIRDERS 4 PER SPAN TYPE III	3	Circular	2
38030185	177	6.2 W OKATON INTERCHANGE	Y	75	2	Girder	4	7	PLATE GIRDER 210' PARABOLIC	1	Rvse. Flare	2
38166196	191	MURDO INTERCHANGE	Y	75	4	Girder	5	7	PLATE GIRDER 426' PARABOLIC	3	Circular	4
38180198	192	US 83 S INTERCHANGE	Y	75	2	Girder	5	7	PLATE GIRDER 224' PARABOLIC	1	Circular	3
43026195	212	US 83 N INTERCHANGE	Y	75	4	Girder	5	7	PLATE GIRDER 370' PARABOLIC	3	Circular	4
08069103	264	0.9 SE CHAMB INTERCHANGE	Y	75	2	Girder	6	7	PLATE GIRDER 204' PARABOLIC	1	Square	4
08080112	265	E CHAMBERLAIN INTERCHANGE	Y	75	4	Girder	7	8	GIRDERS 7 PER SPAN TYPE III	3	Circular	5
08120125	269	2.5 W SD 50 INTERCH	N	75	4	Girder	4	7	PLATE GIRDER 252' PARABOLIC	3	Circular	2
08145124	272	PUKWANA INTERCHANGE	Y	75	4	Girder	4	7	PLATE GIRDER 250' PARABOLIC	3	Circular	2
08290135	286	2.0 W SD 45S INTERCH	N	75	4	Girder	5	8	GIRDERS 5 PER SPAN TYPE III	3	Circular	3

I-90 Bridge Inventory

					Superstructure					Substructure		
Bridge ID	Mile Marker	Location	Exit Ramp	Speed Limit (mph)	No. of Spans	Span Type	No. of Girders	Material	Comments	No. of Bents	Column Type	Columns per Bent
08310135	289	SD 45 SOUTH INTERCHANGE	Y	75	4	Girder	4	7	PLATE GIRDER 250' PARABOLIC	3	Circular	2
02000135	291	AURORA & BRULE CO LINE	N	75	4	Girder	4	7	PLATE GIRDER 252' PARABOLIC	3	Circular	2
02018140	294	2.6 W WHITE LAKE INTERCH	N	75	4	Girder	4	7	PLATE GIRDER 348' PARABOLIC	3	Circular	4
02040149	296	WHITE LAKE INTERCHANGE	Y	75	4	Girder	4	7	PLATE GIRDER 250' PARABOLIC	3	Circular	2
02070155	299	3.0 E WHITE LAKE INTERCH	N	75	4	Girder	4	8	GIRDERS 4 PER SPAN TYPE III	3	Circular	2
02100155	302	6.0 E WHITE LAKE INTERCH	N	75	4	Girder	4	8	GIRDERS 4 PER SPAN TYPE III	3	Circular	2
02140155	306	2.0 W PLANKINTON INTERCH	N	75	4	Girder	4	8	GIRDERS 4 PER SPAN TYPE III	3	Circular	2
0215C158	308	PLANKINTON INTERCHANGE	Y	75	4	Girder	4	7	PLATE GIRDER 264' PARABOLIC	3	Circular	2
02180165	310	US 281 INTERCHANGE	Y	75	4	Girder	4	7	PLATE GIRDER 252' PARABOLIC	3	Circular	2
02220165	312	2 W EAST CO LINE	N	75	4	Girder	4	8	GIRDERS 4 PER SPAN TYPE III	3	Circular	2
18010105	317	1.0 E AURORA CO LINE	N	75	4	Girder	4	8	GIRDERS 4 PER SPAN TYPE III	3	Circular	2
18030105	319	MT VERNON INTERCHANGE	Y	75	4	Girder	4	7	PLATE GIRDER 252' PARABOLIC	3	Circular	2
18050105	321	2.0 E MT VERNON INTERCH	N	75	4	Girder	4	8	GIRDERS 4 PER SPAN TYPE III	3	Circular	2
18070105	323	4.0 E MT VERNON INTERCH	N	75	4	Girder	4	8	GIRDERS 4 PER SPAN TYPE III	3	Circular	2
18090105	325	6 E MT VERNON INTERCHANGE	Y	75	4	Girder	4	7	PLATE GIRDER 252' PARABOLIC	3	Circular	2
18120105	328	2.3 W SD 37 N INTERCH	N	75	4	Girder	4	8	GIRDERS 4 PER SPAN TYPE III	3	Circular	2
18140107	330	SD 37 N INTERCHANGE	Y	75	4	Girder	6	7	PLATE GIRDER 252' PARABOLIC	3	Circular	3
31040105	338	4 E DAVISON CO LINE	N	75	4	Girder	4	8	GIRDERS 4 PER SPAN TYPE III	3	Circular	2
31090126	344	SD 262 INTERCHANGE	Y	75	4	Girder	4	7	PLATE GIRDER 252' PARABOLIC	3	Circular	2
31120126	347	3 E SD 262 INTERCH	N	75	4	Girder	4	8	GIRDERS 4 PER SPAN TYPE III	3	Circular	2
31150125	350	SD 25 INTERCHANGE	Y	75	4	Girder	4	7	PLATE GIRDER 252' PARABOLIC	3	Circular	2
31160125	351	1 E SD 25 INTERCH	N	75	4	Girder	4	8	GIRDERS 4 PER SPAN TYPE III	3	Circular	2
44010126	353	4.0 E SD 25 INTERCHANGE	Y	75	4	Girder	4	7	PLATE GIRDER 252' PARABOLIC	3	Circular	2
44050127	358	6.0 W US 81 INTERCHANGE	Y	75	4	Girder	4	7	PLATE GIRDER 252' PARABOLIC	3	Circular	2
44080125	361	3.0 W US 81 INTERCH	N	75	4	Girder	4	7	PLATE GIRDER 252' PARABOLIC	3	Circular	2
44110125	364	US 81 INTERCHANGE	Y	75	2	Girder	6	8	GIRDERS 6 PER SPAN TYPE 72	1	Flared	2
44150126	368	4 E US 81 INTERCHANGE	Y	75	4	Girder	4	7	PLATE GIRDER 252' PARABOLIC	3	Circular	2
44170126	370	6 E US 81 INTERCH	Y	75	4	Girder	4	7	PLATE GIRDER 252' PARABOLIC	3	Circular	2
44210126	374	MONTROSE INTERCHANGE	Y	75	4	Girder	4	7	PLATE GIRDER 252' PARABOLIC	3	Circular	2
50030149	381	1.2 E SD 19 INTERCH	N	75	4	Girder	4	7	PLATE GIRDER 292' PARABOLIC	3	Circular	4
50050164	384	3.8 E SD 19 INTERCH	N	75	4	Girder	4	7	PLATE GIRDER 244' PARABOLIC	3	Circular	2
50070165	386	4.8 W SD 38 INTERCH	N	75	4	Girder	4	7	PLATE GIRDER 252' PARABOLIC	3	Circular	2
50090165	388	2.8 W SD 38 INTERCHANGE	Y	75	4	Girder	4	7	PLATE GIRDER 252' PARABOLIC	3	Circular	2
50160166	394	2.1 W I 29 INTERCH	N	75	4	Girder	4	7	PLATE GIRDER 252' PARABOLIC	3	Circular	2
50170164	395	1.1 W I 29 INTERCH	Y (Loop)	75	2	Girder	12	8		1	Flared	4
50185163	396.5	0.5 E I 29 INTERCH	N	65	4	Girder	4	7	PLATE GIRDER 212' UNIT	3	Circular	3
50240165	402	2 E I 229 INTERCHANGE	Y	75	4	Slab	NA	2	UMBRELLA (SCS-30-00-254)	3	Circular	1
50280165	406	SD 11 & I 90 INTERCHANGE	Y	75	4	Slab	NA	2	UMBRELLA (SCS-30-00-254)	3	Circular	1
50300166	408	2 E SD 11 INTERCH	N	75	4	Slab	NA	2	UMBRELLA (SCS)	3	Circular	1
50320166	410	4.0 E SD 11 INTERCHANGE	Y	75	4	Slab	NA	2	UMBRELLA (SCS)	3	Circular	1

I-229 Bridge Inventory

Bridge ID	Mile Marker	Location	Exit Ramp	Speed Limit (mph)	Superstructure: No. of Spans	Span Type	No. of Girders	Material	Comments	Substructure: No. of Bents	Column Type	Columns per Bent
42079004	1	LOUISE AVE INTERCHANGE	Y	65	2	Girder	10	8	GIRDERS 10 PER SPAN TYPE 81	1	Flared	3
50191238	2	WESTERN AVE INTERCHANGE	Y	65	2	Girder	10	7	PLATE GIRDER 247' UNIT	1	Flared	3
50216220	5	26TH ST INTERCHANGE	Y	65	4	Girder	6	7	PLATE GIRDER 320' PARABOLIC	3	Circular	4
50219215	5.5	18TH ST OVERHEAD	N	65	4	Slab	NA	2	SQUARE HAUNCHED	3	Square	3
50219210	5.75	12TH ST OVERHEAD	N	65	2	Girder	7	7	W33X118 W33X141	1	Flared	3
50219206	6	10TH & I229 INTERCHANGE	Y	65	2	Slab	NA	2	SQUARE HAUNCHED	1	Circular	7
50219205	6.25	6TH ST OVERHEAD	N	65	2	Girder	8	8	GIRDERS 8 PER SPAN TYPE IV	1	Flared	3
50219180	9	BENSON RD. INTERCHANGE	Y	65	2	Girder	9	8	GIRDERS 9 PER SPAN TYPE 72	1	MegaFlare	1
50221170	9.7	0.3 S I 90 INTERCH	N	65	4	Girder	7	8	GIRDERS 4 42' & 38' SPAN TYPE III	3	Circular	3
50221167	10	I 90 & I 229 INTERCHANGE	Y	65	2	Girder	7	7	PLATE GIRDERS PARABOLIC	1	Top Flare	3
50221166	10.1	I 90 & I 229 INTERCHANGE	Y	65	2	Girder	8	7	PLATE GIRDERS PARABOLIC	1	Top Flare	3

I-190 Bridge Inventory

Bridge ID	Mile Marker	Location	Exit Ramp	Speed Limit (mph)	Superstructure: No. of Spans	Span Type	No. of Girders	Material	Comments	Substructure: No. of Bents	Column Type	Columns per Bent
52410290	1	0.5 S I 90 INTERCH	N	65	4	Slab	NA	2	Square Haunch	3	Square	3

Miscellaneous Inventory

Bridge ID	Mile Marker	Location	Exit Ramp	Speed Limit (mph)	Superstructure: No. of Spans	Span Type	No. of Girders	Material	Comments	Substructure: No. of Bents	Column Type	Columns per Bent
6154150		14 - 14 Bypass W. of Brookings	NA	55	4	Girder	5	7	PLATE GIRDER 367' UNIT	3	Circular	3
14092199		50 - 50L W. of Vermillion	NA	55	4	Girder	8	7	PLATE GIRDER 393' UNIT	3	Circ. (NC on 2 bents)	3
14131205		50 - 50L E. of Vermillion	NA	55	3	Girder	4	7	PLATE GIRDER 326' UNIT	2	Circular	4
50175210	80	Under I29 in Sioux Falls	NA	40	3	Girder	7	7	PLATE GIRDER 374' UNIT	2	Hammerhead	3
50176210	80	Under I29 in Sioux Falls	NA	40	3	Girder	7	7	PLATE GIRDER 374' UNIT	2	Hammerhead	3
50177199	79	Under I29 in Sioux Falls	NA	40	3	Girder	7	7	PLATE GIRDER 374' UNIT	2	Hammerhead	7
50178199	79	Under I29 in Sioux Falls	NA	40	3	Girder	7	7	PLATE GIRDER 374' UNIT	2	Hammerhead	3
52410318		Viaduct SW Rapid City	N	35	5	Girder	4	7	PLATE GIRDER 294' UNIT	4	Circular	1
52415285	58	Under I90 in Rapid City	NA	35	3	Girder	5	7	PLATE GIRDER 374' UNIT	2	Tee	3
52415286	58	Under I90 in Rapid City	NA	35	3	Girder	5	7	PLATE GIRDER 374' UNIT	2	Tee	3

APPENDIX C: COLLISION RISK ANALYSIS RESULTS

C.1: Calculated Bridge Collision Risk, RUC, and Quartile

Table C.1-1 Bridge Collision Risk, RUC, and Quartile – I-29 Overpass Bridges

I-29								
Bridge ID	**Mile Marker**	***Risk of Collision***			***RUC (S)***	***Quartiles***		
		Right	**Left**	**Median**		**L**	**M**	**R**
64158399	1			0.056%	20352	NA	4-3	NA
64149367	4	0.066%	0.067%	0.062%	6116	3-4	3-4	3-4
64140355	6	0.062%	0.063%	0.041%	270.874	1-4	1-2	1-4
64120336	8	0.059%	0.060%	0.039%	267	1-4	1-2	1-4
64115330	9	0.062%	0.062%	0.041%	1988	3-4	3-2	3-4
64100315	11	0.059%	0.059%	0.039%	579	1-4	1-2	1-4
64080296	14	0.059%	0.059%	0.039%	402	1-4	1-2	1-4
64070287	15	0.057%	0.062%	0.039%	6872	3-4	3-2	3-4
64050250	20	0.048%	0.048%	0.031%	1562	2-3	2-2	2-3
64020220	24	0.051%	0.049%	0.032%	1562	2-3	2-2	2-3
64008205	26	0.053%	0.053%	0.035%	16166	4-3	4-2	4-3
64006160	31	0.047%	0.047%	0.029%	10189	4-3	4-2	4-3
64006120	35	0.044%	0.044%	0.028%	622	2-3	2-2	2-3
64006100	37	0.044%	0.044%	0.028%	434	1-3	1-2	1-3
64006090	38	0.048%	0.047%	0.029%	1517	2-3	2-2	2-3
64006030	44	0.047%	0.047%	0.030%	261	1-3	1-2	1-3
64006010	46	0.047%	0.047%	0.029%	426	1-3	1-2	1-3
64006000	47			0.047%	11292	NA	4-3	NA
42065260	50	0.060%	0.062%	0.043%	5848	3-4	3-3	3-4
42065230	53	0.063%	0.063%	0.037%	2362	3-4	3-2	3-4
42065200	56	0.063%	0.063%	0.041%	1152	2-4	2-2	2-4
42065170	59	0.064%	0.064%	0.038%	6453	3-4	3-2	3-4
42065140	62	0.077%	0.086%	0.054%	5704	3-4	3-3	3-4
42065141	62	0.077%	0.086%	0.054%	5704	3-4	3-3	3-4
42065130	63	0.084%	0.095%	0.061%	2804	3-4	3-4	3-4
42065120	64	0.077%	0.086%	0.054%	3534	3-4	3-3	3-4
42065100	67	0.100%	0.096%	0.065%	4394	3-4	3-4	3-4
42065080	68			0.053%	910	NA	2-3	NA
42065050	71	0.090%	0.086%	0.062%	8834	4-4	4-4	4-4
50172240	76			0.107%	9506	NA	4-4	NA
50173235	76.5	0.128%	0.128%	0.077%	31802	4-4	4-4	4-4
50175230	77			0.105%	25493	NA	4-4	NA
50175222	78			0.116%	37333	NA	4-4	NA
50178191	81			0.048%	25926	NA	4-3	NA
50180170	83			0.071%	21345	NA	4-4	NA
50180162	84	0.114%	0.123%	0.050%	7739	3-4	3-3	3-4
50180163	84	0.114%	0.123%	0.050%	7739	3-4	3-3	3-4
50180140	86	0.067%	0.067%	0.040%	5409	3-4	3-2	3-4
50177130	87	0.066%	0.066%	0.034%	1479	2-4	2-2	2-4
50175040	96	0.065%	0.065%	0.032%	864	2-4	2-2	2-4

I-29								
Bridge ID	**Mile Marker**	***Risk of Collision***			***RUC (S)***	***Quartiles***		
		Right	**Left**	**Median**		**L**	**M**	**R**
50175020	98	0.069%	0.057%	0.033%	5608	3-4	3-2	3-4
51065210	102	0.057%	0.057%	0.031%	622	2-4	2-2	2-4
51065200	104	0.057%	0.057%	0.031%	1354	2-4	2-2	2-4
51065150	109	0.057%	0.057%	0.031%	15421	4-4	4-2	4-4
51066100	114	0.054%	0.054%	0.028%	7048	3-3	3-2	3-3
51065050	120	0.052%	0.052%	0.027%	2105	3-3	3-2	3-3
06185230	126	0.053%	0.053%	0.023%	380	1-3	1-1	1-3
06185210	127	0.051%	0.051%	0.022%	13750	4-3	4-1	4-3
06185190	129	0.052%	0.053%	0.023%	1456	2-3	2-1	2-3
06185159	132	0.052%	0.052%	0.023%	8162	4-3	4-1	4-3
06185160	132	0.052%	0.052%	0.022%	8162	4-3	4-1	4-3
06185150	133	0.051%	0.051%	0.022%	9064	4-3	4-1	4-3
06185130	135			0.012%	1142	NA	2-1	NA
06185110	137			0.013%	511	NA	1-1	NA
06185080	140			0.012%	12185	NA	4-1	NA
20061280	150			0.009%	17689	NA	4-1	NA
29280020	167	0.078%	0.081%	0.026%	674	2-4	2-2	2-4
15240220	173	0.028%	0.028%	0.009%	1060	2-2	2-1	2-2
15215150	180			0.008%	8988	NA	4-1	NA
15215120	183			0.007%	1536	NA	2-1	NA
15215070	189			0.007%	98	NA	1-1	NA
15215030	193			0.008%	16055	NA	4-1	NA
55085440	206			0.009%	2106	NA	3-1	NA
55085429	207	0.037%	0.033%	0.011%	4597.	3-2	3-1	3-2
55100367	213	0.030%	0.030%	0.009%	4379	3-2	3-1	3-2
55115330	218			0.008%	452	NA	1-1	NA
55115290	222			0.008%	1821	NA	2-1	NA
55115220	229			0.008%	637	NA	2-1	NA
55116190	232	0.026%	0.026%	0.008%	5435	3-2	3-1	3-2
55124170	234	0.025%	0.024%	0.007%	159	1-1	1-1	1-1
55144130	239	0.024%	0.024%	0.008%	253	1-1	1-1	1-1
55175040	248			0.010%	1330	NA	2-1	NA

Table C.1-2 Bridge Collision Risk, RUC, and Quartile – I-90 Overpass Bridges

I-90								
Bridge ID	**Mile Marker**	***Risk of Collision***			***RUC ($)***	***Quartiles***		
		Right	**Left**	**Median**		**L**	**M**	**R**
41095059	10	0.028%	0.035%	0.020%	8795.482	4-2	4-1	4-2
41116088	12	0.019%	0.019%	0.011%	11099.98	4-1	4-1	4-1
41101077	14	0.019%	0.019%	0.012%	20193.12	4-1	4-1	4-1
41154087	17	0.019%	0.019%	0.012%	14086.21	4-1	4-1	4-1
41155087	17	0.019%	0.019%	0.012%	14086.21	4-1	4-1	4-1
41185086	21	0.032%	0.033%	0.021%	1125.361	2-2	2-1	2-2
41207092	23	0.037%	0.039%	0.024%	4032.863	3-2	3-1	3-2
41226107	25.5	0.034%	0.034%	0.020%	756.1618	2-2	2-1	2-2
47061480	36.5	0.035%	0.038%	0.031%	1142.644	2-2	2-2	2-2
47069510	40	0.046%	0.041%	0.035%	1075.43	2-2	2-2	2-3
47098563	46	0.074%	0.074%	0.065%	6867.101	3-4	3-4	3-4
47111580	48			0.074%	16045.03	NA	4-4	NA
47135609	52			0.044%	3013.125	NA	3-3	NA
52390278	55			0.046%	21441.39	NA	4-3	NA
52410285	57			0.102%	6548.601	NA	3-4	NA
52424285	59			0.077%	30985.83	NA	4-4	NA
52450287	61			0.045%	5746.83	NA	3-3	NA
52467276	63	0.060%	0.059%	0.037%	1755.256	2-4	2-2	2-4
52470276	63.5			0.060%	1755.256	NA	2-4	NA
52500275	67			0.060%	8502.619	NA	4-4	NA
52540275	71	0.031%	0.071%	0.029%	4101.998	3-4	3-2	3-2
52610285	78	0.042%	0.042%	0.028%	2866.213	3-3	3-2	3-3
52640285	81	0.043%	0.041%	0.028%	51.85109	1-2	1-2	1-3
52670285	84	0.045%	0.045%	0.031%	259.2555	1-3	1-2	1-3
52710283	88	0.043%	0.042%	0.029%	115.2247	1-3	1-2	1-3
52830310	101	0.033%	0.032%	0.019%	374.4801	1-2	1-1	1-2
52880346	107	0.036%	0.038%	0.018%	1766.778	2-2	2-1	2-2
52900360	109	0.038%	0.040%	0.020%	2314.095	3-2	3-1	3-2
52925365	112	0.031%	0.038%	0.017%	504.1079	1-2	1-1	1-2
52926366	112	0.031%	0.038%	0.017%	504.1079	1-2	1-1	1-2
36120107	131	0.024%	0.028%	0.022%	23260.98	4-2	4-1	4-1
36309106	150	0.023%	0.023%	0.012%	47342.93	4-1	4-1	4-1
38030185	177			0.016%	148.8318	NA	1-1	NA
38166196	191	0.069%	0.069%	0.026%	552.1181	1-4	1-1	1-4
38180198	192			0.026%	2971.836	NA	3-2	NA
43026195	212	0.058%	0.058%	0.022%	46.08986	1-4	1-1	1-4
08069103	264			0.023%	1854.157	NA	2-1	NA
08080112	265	0.033%	0.033%	0.020%	1541.13	2-2	2-1	2-2
08120125	269	0.028%	0.028%	0.014%	337.0321	1-2	1-1	1-2
08145124	272	0.030%	0.032%	0.018%	748.9603	2-2	2-1	2-2
08290135	286	0.031%	0.030%	0.012%	80.65726	1-2	1-1	1-2
08310135	289	0.030%	0.029%	0.017%	288.0616	1-2	1-1	1-2

I-90								
Bridge ID	**Mile Marker**	***Risk of Collision***			***RUC ($)***	***Quartiles***		
		Right	**Left**	**Median**		**L**	**M**	**R**
02000135	291	0.028%	0.028%	0.021%	44.16945	1-2	1-1	1-2
02018140	293	0.031%	0.031%	0.016%	469	1-2	1-1	1-2
02040149	296	0.032%	0.032%	0.016%	1239	2-2	2-1	2-2
02070155	299	0.031%	0.036%	0.018%	81	1-2	1-1	1-2
02100155	302	0.031%	0.036%	0.018%	35	1-2	1-1	1-2
02140155	306	0.031%	0.036%	0.018%	200	1-2	1-1	1-2
0215C158	308	0.034%	0.037%	0.018%	1258	2-2	2-1	2-2
02180165	310	0.041%	0.037%	0.020%	5396	3-2	3-1	3-2
02220165	312	0.041%	0.036%	0.020%	196	1-2	1-1	1-2
18010105	317	0.041%	0.036%	0.024%	780	2-2	2-1	2-2
18030105	319	0.041%	0.037%	0.024%	1123	2-2	2-1	2-2
18050105	321	0.043%	0.043%	0.026%	67	1-3	1-2	1-3
18070105	323	0.043%	0.043%	0.026%	67	1-3	1-2	1-3
18090105	325	0.044%	0.045%	0.027%	1296	2-3	2-2	2-3
18120105	328	0.043%	0.044%	0.024%	1940	2-3	2-1	2-3
18140107	330	0.044%	0.043%	0.019%	30559	4-3	4-1	4-3
31040105	337	0.045%	0.045%	0.024%	1532	2-3	2-1	2-3
31090126	344	0.045%	0.046%	0.022%	5617	3-3	3-1	3-3
31120126	347	0.046%	0.046%	0.025%	1512	2-3	2-1	2-3
31150125	350	0.046%	0.046%	0.024%	471	1-3	1-1	1-3
31160125	351	0.044%	0.046%	0.024%	49	1-3	1-1	1-3
44010126	354	0.046%	0.046%	0.025%	847	2-3	2-1	2-3
44050127	358	0.046%	0.046%	0.024%	565	1-3	1-1	1-3
44080125	361	0.043%	0.043%	0.022%	104	1-3	1-1	1-3
44110125	364			0.146%	6179	NA	3-4	NA
44150126	368	0.041%	0.041%	0.021%	595	1-2	1-1	1-2
44170126	370	0.038%	0.038%	0.020%	119	1-2	1-1	1-2
44210126	374	0.043%	0.043%	0.022%	1671	2-3	2-1	2-3
50030149	381	0.079%	0.079%	0.042%	657	2-4	2-3	2-4
50050164	384	0.091%	0.085%	0.043%	438	1-4	1-3	1-4
50070165	386	0.076%	0.076%	0.045%	438	1-4	1-3	1-4
50090165	388	0.076%	0.076%	0.045%	5385	3-4	3-3	3-4
50160166	394	0.045%	0.044%	0.027%	1009	2-3	2-2	2-3
50170164	395			0.037%	3799	NA	3-2	NA
50185163	396.5	0.050%	0.052%	0.034%	1152	2-3	2-2	2-3
50240165	402	0.092%	0.096%	0.064%	11542	4-4	4-4	4-4
50280165	406	0.083%	0.083%	0.056%	15920	4-4	4-3	4-4
50300166	408	0.081%	0.080%	0.055%	365	1-4	1-3	1-4
50320166	410	0.086%	0.086%	0.059%	1815	2-4	2-4	2-4

Table C.1-3 Bridge Collision Risk, RUC, and Quartile – I-229 Overpass Bridges

I-229

Bridge ID	Mile Marker	Risk of Collision Right	Risk of Collision Left	Risk of Collision Median	RUC ($)	Quartiles L	Quartiles M	Quartiles R
42079004	1			0.053%	38255	NA	4-3	NA
50191238	2			0.067%	39023	NA	4-4	NA
50216220	5	0.079%	0.079%	0.053%	19306	4-4	4-3	4-4
50219215	5.5	0.085%	0.085%	0.056%	3299	3-4	3-3	3-4
50219210	5.75			0.199%	1959	NA	2-4	NA
50219208	6			0.247%	5504	NA	3-4	NA
50219205	6.25			0.172%	6924	NA	3-4	NA
50219180	9			0.159%	24095	NA	4-4	NA
50221170	9.7	0.076%	0.076%	0.044%	6505	3-4	3-3	3-4
50221167	10			0.046%	6136	NA	3-3	NA
50221166	10.1			0.050%	6136	NA	3-3	NA

Table C.1-4 Bridge Collision Risk, RUC, and Quartile – I-190 Bridges

I-190

Bridge ID	Mile Marker	Risk of Collision Right	Risk of Collision Left	Risk of Collision Median	RUC ($)	Quartiles L	Quartiles M	Quartiles R
52410290	1	0.054%	0.055%	0.109%	4600	NA	4-3	NA

Table C.1-5 Bridge Collision Risk, RUC, and Quartile – Miscellaneous Roads

Miscellaneous Roads

Bridge ID	Mile Marker	Risk of Collision Right	Risk of Collision Left	Risk of Collision Median	RUC ($)	Quartiles L	Quartiles M	Quartiles R
06154150 Hwy 14 Bypass		0.004%	0.004%	0.002%	209	1-1	1-1	1-1
14092199 Hwy 50W		0.040%	0.086%		2379	3-4	NA	3-2
14131205 Hwy 50E		0.008%	0.010%		2839	3-1	NA	3-1
50175210 Madison St		0.001%	0.001%		22885	4-1	NA	4-1
50176210 Madison St		0.001%	0.001%		22885	4-1	NA	4-1
50177199 12th St		0.001%	0.001%		36721	4-1	NA	4-1
50178199 12th St		0.001%	0.001%		36721	4-1	NA	4-1
52410318 Mt. Rushmore Rd.		0.011%	0.012%	0.015%	1567	2-1	2-1	2-1
52415285 Haines Ave.		0.052%	0.042%		12105	4-3	NA	4-3
52415286 Haines Ave.		0.052%	0.042%		12105	4-3	NA	4-3

APPENDIX D: PRIORITIZATION OF BRIDGE BENTS FOR COLLAPSE MITIGATION

Interpretation of the alpha-numeric characters:

1st String: Bridge identification
2nd String: Road crossed by the bridge (**I-90**, **I-29**, etc.)
3rd String: Mile marker
4th String: Bent location (**L**eft, **M**edian, **R**ight) as shown on the construction plans
5th String: Bent redundancy (Redundant: **R**; Non-Redundant: **NR**)
6th String: Column strength adequacy (**S**ufficient; **I**nsufficient). Bent structures with inadequate column strength are labeled with red font.

Quartile cluster 4-4

50240165-I90-402-L-NR-S	50173235-I29-76.5-M-R-I
50280165-I90-406-L-NR-S	50175230-I29-77-M-R-I
42065050-I29-71-L-NR-I	50175222-I29-78-M-R-I
50173235-I29-76.5-L-R-I	50180170-I29-83-M-R-S
51065150-I29-109-L-NR-I	50191238-I229-2-M-R-S
50216220-I229-5-L-R-I	50219180-I229-9-M-NR-S
50240165-I90-402-R-NR-S	47111580-I90-48-M-R-I
50280165-I90-406-R-NR-S	52424285-I90-59-M-R-I
42065050-I29-71-R-NR-I	52500275-I90-67-M-R-S
50173235-I29-76.5-R-R-I	50240165-I90-402-M-NR-S
51065150-I29-109-R-NR-I	42065050-I29-71-M-NR-S
50216220-I229-5-R-R-I	50172240-I29-76-M-R-I

Quartile cluster 4-3

18140107-I90-330-L-NR-I	52390278-I90-55-M-R-I
64008205-I29-26-L-NR-I	50280165-I90-406-M-NR-S
64006160-I29-31-L-NR-I	64158399-I29-1-M-R-I
06185210-I29-127-L-NR-I	64006000-I29-47-M-R-S
06185159-I29-132-L-NR-I	50178191-I29-81-M-R-S
06185160-I29-132-L-NR-I	42079004-I229-1-M-R-S
06185150-I29-133-L-NR-I	50216220-I229-5-M-R-I
52415285-Misc.-Haines Ave.-L-NR-S	06185159-I29-132-R-NR-I
52415286-Misc.-Haines Ave.-L-NR-S	06185160-I29-132-R-NR-I
18140107-I90-330-R-NR-I	06185150-I29-133-R-NR-I
64008205-I29-26-R-NR-I	52415285-Misc.-Haines Ave.-R-NR-S
64006160-I29-31-R-NR-I	52415286-Misc.-Haines Ave.-R-NR-S
06185210-I29-127-R-NR-I	

Quartile cluster 4-2

41095059-I90-10-L-R-I	64008205-I29-26-M-NR-S
36120107-I90-131-L-R-I	64006160-I29-31-M-NR-I
41095059-I90-10-R-R-I	51065150-I29-109-M-NR-I

Quartile cluster 4-1

41116088-I90-12-L-R-I	50178199-Misc.-12th St-R-NR-S
41101077-I90-14-L-R-I	41095059-I90-10-M-R-I
41154087-I90-17-L-R-I	41116088-I90-12-M-R-I
41155087-I90-17-L-R-I	41101077-I90-14-M-R-I
36309106-I90-150-L-NR-I	41154087-I90-17-M-R-I
50175210-Misc.-Madison St-L-NR-S	41155087-I90-17-M-R-I
50176210-Misc.-Madison St-L-NR-S	36120107-I90-131-M-R-I
50177199-Misc.-12th St-L-NR-S	36309106-I90-150-M-NR-I
50178199-Misc.-12th St-L-NR-S	18140107-I90-330-M-NR-I
41116088-I90-12-R-R-I	06185210-I29-127-M-NR-I
41101077-I90-14-R-R-I	06185159-I29-132-M-NR-I
41154087-I90-17-R-R-I	06185160-I29-132-M-NR-I
41155087-I90-17-R-R-I	06185150-I29-133-M-NR-I
36120107-I90-131-R-R-I	06185080-I29-140-M-R-I
36309106-I90-150-R-NR-I	20061280-I29-150-M-R-I
50175210-Misc.-Madison St-R-NR-S	15215150-I29-180-M-R-I
50176210-Misc.-Madison St-R-NR-S	15215030-I29-193-M-R-I
50177199-Misc.-12th St-R-NR-S	

Quartile cluster 3-4

47098563-I90-46-L-NR-S
52540275-I90-71-L-NR-I
50090165-I90-388-L-NR-I
64149367-I29-4-L-NR-I
64115330-I29-9-L-NR-S
64070287-I29-15-L-NR-I
42065260-I29-50-L-NR-I
42065230-I29-53-L-NR-I
42065170-I29-59-L-NR-I
42065140-I29-62-L-NR-S
42065141-I29-62-L-NR-S
42065130-I29-63-L-NR-I
42065120-I29-64-L-NR-S
42065100-I29-67-L-NR-I
50180162-I29-84-L-R-I
50180163-I29-84-L-R-I
50180140-I29-86-L-NR-I
50175020-I29-98-L-NR-I
50219215-I229-5.5-L-R-I
50221170-I229-9.7-L-R-I
14092199-Misc.-Hwy 50W-L-R-I
47098563-I90-46-R-NR-S
50090165-I90-388-R-NR-I
64149367-I29-4-R-NR-I
64115330-I29-9-R-NR-S
64070287-I29-15-R-NR-I
42065260-I29-50-R-NR-I
42065230-I29-53-R-NR-I
42065170-I29-59-R-NR-I
42065140-I29-62-R-NR-S
42065141-I29-62-R-NR-S
42065130-I29-63-R-NR-I
42065120-I29-64-R-NR-S
42065100-I29-67-R-NR-I
50180162-I29-84-R-R-I
50180163-I29-84-R-R-I
50180140-I29-86-R-NR-I
50175020-I29-98-R-NR-I
50219215-I229-5.5-R-R-I
50221170-I229-9.7-R-R-I
47098563-I90-46-M-NR-S
52410285-I90-57-M-R-S
44110125-I90-364-M-R-S
64149367-I29-4-M-NR-S
42065130-I29-63-M-NR-S
42065100-I29-67-M-NR-S
50219208-I229-6-M-R-S
50219205-I229-6.25-M-R-S
52410290-I190-1-M-R-S

Quartile cluster 3-3

52610285-I90-78-L-NR-S
31090126-I90-344-L-NR-I
51066100-I29-114-L-NR-I
51065050-I29-120-L-NR-I
52410290-I190-1-L-R-I
52610285-I90-78-R-NR-S
31090126-I90-344-R-NR-I
51066100-I29-114-R-NR-I
51065050-I29-120-R-NR-I
52410290-I190-1-R-R-I
47135609-I90-52-M-R-S
52450287-I90-61-M-R-I
50090165-I90-388-M-NR-I
42065260-I29-50-M-NR-I
42065140-I29-62-M-NR-S
42065141-I29-62-M-NR-S
42065120-I29-64-M-NR-S
50180162-I29-84-M-R-I
50180163-I29-84-M-R-I
50219215-I229-5.5-M-R-S
50221170-I229-9.7-M-R-I
50221167-I229-10-M-R-I
50221166-I229-10-M-R-I

Quartile cluster 3-2

41207092-I90-23-L-NR-I	52540275-I90-71-M-NR-I
52900360-I90-109-L-R-I	52610285-I90-78-M-NR-S
02180165-I90-310-L-NR-I	50170164-I90-395-M-R-S
55085429-I29-207-L-R-I	64115330-I29-9-M-NR-S
55100367-I29-213-L-R-I	64070287-I29-15-M-NR-S
41207092-I90-23-R-NR-I	42065230-I29-53-M-NR-I
52540275-I90-71-R-NR-I	42065170-I29-59-M-NR-I
52900360-I90-109-R-R-I	50180140-I29-86-M-NR-I
02180165-I90-310-R-NR-I	50175020-I29-98-M-NR-I
55085429-I29-207-R-R-I	51066100-I29-114-M-NR-I
55100367-I29-213-R-R-I	51065050-I29-120-M-NR-I
14092199-Misc.-Hwy 50W-R-R-I	

Quartile cluster 3-1

55116190-I29-232-L-R-I	02180165-I90-310-M-NR-I
14131205-Misc.-Hwy 50E-L-R-I	31090126-I90-344-M-NR-I
55116190-I29-232-R-R-I	55085440-I29-206-M-NR-I
14131205-Misc.-Hwy 50E-R-R-I	55085429-I29-207-M-R-I
41207092-I90-23-M-NR-I	55100367-I29-213-M-R-I
52900360-I90-109-M-R-I	55116190-I29-232-M-R-I
38180198-I90-192-M-R-I	

Quartile cluster 2-4

52467276-I90-63-L-R-I	50320166-I90-410-R-NR-S
50030149-I90-381-L-R-I	42065200-I29-56-R-NR-I
50320166-I90-410-L-NR-S	50177130-I29-87-R-NR-I
42065200-I29-56-L-NR-I	50175040-I29-96-R-NR-I
50177130-I29-87-L-NR-I	51065210-I29-102-R-NR-I
50175040-I29-96-L-NR-I	51065200-I29-104-R-NR-I
51065210-I29-102-L-NR-I	29280020-I29-167-R-R-I
51065200-I29-104-L-NR-I	52470276-I90-63.5-M-R-S
29280020-I29-167-L-R-I	50320166-I90-410-M-NR-S
52467276-I90-63-R-R-I	50219210-I229-5.75-M-R-S
50030149-I90-381-R-R-I	

Quartile cluster 2-3

18090105-I90-325-L-NR-I	18090105-I90-325-R-NR-I
18120105-I90-328-L-NR-I	18120105-I90-328-R-NR-I
31040105-I90-337-L-NR-I	31040105-I90-337-R-NR-I
31120126-I90-347-L-NR-I	31120126-I90-347-R-NR-I
44010126-I90-354-L-NR-I	44010126-I90-354-R-NR-I
44210126-I90-374-L-NR-I	44210126-I90-374-R-NR-I
50160166-I90-394-L-NR-I	50160166-I90-394-R-NR-I
50185163-I90-396.5-L-R-I	50185163-I90-396.5-R-R-I
64050250-I29-20-L-NR-I	64050250-I29-20-R-NR-I
64020220-I29-24-L-NR-I	64020220-I29-24-R-NR-I
64006120-I29-35-L-NR-I	64006120-I29-35-R-NR-I
64006090-I29-38-L-NR-I	64006090-I29-38-R-NR-I
06185190-I29-129-L-NR-I	06185190-I29-129-R-NR-I
47069510-I90-40-R-NR-I	42065080-I29-68-M-R-S

Quartile cluster 2-2

41185086-I90-21-L-NR-I	18010105-I90-317-R-NR-I
41226107-I90-25.5-L-R-I	18030105-I90-319-R-NR-I
47061480-I90-36.5-L-NR-I	15240220-I29-173-R-R-I
47069510-I90-40-L-NR-I	47061480-I90-36.5-M-NR-I
52880346-I90-107-L-R-I	47069510-I90-40-M-NR-I
08080112-I90-265-L-R-I	52467276-I90-63-M-R-I
08145124-I90-272-L-NR-I	18090105-I90-325-M-NR-I
02040149-I90-296-L-NR-I	50030149-I90-381-M-R-I
0215C158-I90-308-L-NR-I	50160166-I90-394-M-NR-I
18010105-I90-317-L-NR-I	50185163-I90-396.5-M-R-I
18030105-I90-319-L-NR-I	64050250-I29-20-M-NR-S
15240220-I29-173-L-R-I	64020220-I29-24-M-NR-S
41185086-I90-21-R-NR-I	64006120-I29-35-M-NR-I
41226107-I90-25.5-R-R-I	64006090-I29-38-M-NR-I
47061480-I90-36.5-R-NR-I	42065200-I29-56-M-NR-I
52880346-I90-107-R-R-I	50177130-I29-87-M-NR-I
08080112-I90-265-R-R-I	50175040-I29-96-M-NR-I
08145124-I90-272-R-NR-I	51065210-I29-102-M-NR-I
02040149-I90-296-R-NR-I	51065200-I29-104-M-NR-I
0215C158-I90-308-R-NR-I	

Quartile cluster 2-1

52410318-Misc.-Mt. Rushmore Rd.-L-NR-I	31040105-I90-337-M-NR-I
52410318-Misc.-Mt. Rushmore Rd.-R-NR-I	31120126-I90-347-M-NR-I
41185086-I90-21-M-NR-I	44010126-I90-354-M-NR-I
41226107-I90-25.5-M-R-I	44210126-I90-374-M-NR-I
52880346-I90-107-M-R-I	06185190-I29-129-M-NR-I
08069103-I90-264-M-R-I	06185130-I29-135-M-R-I
08080112-I90-265-M-R-I	29280020-I29-167-M-R-I
08145124-I90-272-M-NR-I	15240220-I29-173-M-R-I
02040149-I90-296-M-NR-I	15215120-I29-183-M-R-I
0215C158-I90-308-M-NR-I	55115290-I29-222-M-NR-I
18010105-I90-317-M-NR-I	55115220-I29-229-M-NR-I
18030105-I90-319-M-NR-I	55175040-I29-248-M-NR-I
18120105-I90-328-M-NR-I	52410318-Misc.-Mt. Rushmore Rd.-M-NR-I

Quartile cluster 1-4

38166196-I90-191-L-R-I	38166196-I90-191-R-R-I
43026195-I90-212-L-R-I	43026195-I90-212-R-R-I
50050164-I90-384-L-NR-I	50050164-I90-384-R-NR-I
50070165-I90-386-L-NR-I	50070165-I90-386-R-NR-I
50300166-I90-408-L-NR-S	50300166-I90-408-R-NR-S
64140355-I29-6-L-NR-S	64140355-I29-6-R-NR-S
64120336-I29-8-L-NR-I	64120336-I29-8-R-NR-I
64100315-I29-11-L-NR-S	64100315-I29-11-R-NR-S
64080296-I29-14-L-NR-I	64080296-I29-14-R-NR-I

1-3

52670285-I90-84-L-NR-S
52710283-I90-88-L-NR-I
18050105-I90-321-L-NR-I
18070105-I90-323-L-NR-I
31150125-I90-350-L-NR-I
31160125-I90-351-L-NR-I
44050127-I90-358-L-NR-I
44080125-I90-361-L-NR-I
64006100-I29-37-L-NR-I
64006030-I29-44-L-NR-I
64006010-I29-46-L-NR-I
06185230-I29-126-L-NR-I
52640285-I90-81-R-NR-I
52670285-I90-84-R-NR-S
52710283-I90-88-R-NR-I
18050105-I90-321-R-NR-I
18070105-I90-323-R-NR-I
31150125-I90-350-R-NR-I
31160125-I90-351-R-NR-I
44050127-I90-358-R-NR-I
44080125-I90-361-R-NR-I
64006100-I29-37-R-NR-I
64006030-I29-44-R-NR-I
64006010-I29-46-R-NR-I
06185230-I29-126-R-NR-I
50050164-I90-384-M-NR-I
50070165-I90-386-M-NR-I
50300166-I90-408-M-NR-S

1-2

52640285-I90-81-L-NR-I
52830310-I90-101-L-NR-I
52925365-I90-112-L-NR-I
52926366-I90-112-L-R-I
08120125-I90-269-L-NR-I
08290135-I90-286-L-R-I
08310135-I90-289-L-NR-I
02000135-I90-291-L-NR-I
02018140-I90-293-L-R-I
02070155-I90-299-L-NR-I
02100155-I90-302-L-NR-I
02140155-I90-306-L-NR-I
02220165-I90-312-L-NR-I
44150126-I90-368-L-NR-I
44170126-I90-370-L-NR-I
52830310-I90-101-R-NR-I
52925365-I90-112-R-NR-I
52926366-I90-112-R-R-I
08120125-I90-269-R-NR-I
08290135-I90-286-R-R-I
08310135-I90-289-R-NR-I
02000135-I90-291-R-NR-I
02018140-I90-293-R-R-I
02070155-I90-299-R-NR-I
02100155-I90-302-R-NR-I
02140155-I90-306-R-NR-I
02220165-I90-312-R-NR-I
44150126-I90-368-R-NR-I
44170126-I90-370-R-NR-I
52640285-I90-81-M-NR-S
52670285-I90-84-M-NR-S
52710283-I90-88-M-NR-S
64140355-I29-6-M-NR-S
64120336-I29-8-M-NR-S
64100315-I29-11-M-NR-S
64080296-I29-14-M-NR-S
64006100-I29-37-M-NR-I
64006030-I29-44-M-NR-I
64006010-I29-46-M-NR-I

1-1

55124170-I29-234-L-NR-I	02100155-I90-302-M-NR-I
55144130-I29-239-L-NR-I	02140155-I90-306-M-NR-I
06154150-Misc.-Hwy 14 Bypass-L-R-I	02220165-I90-312-M-NR-I
55124170-I29-234-R-NR-I	18050105-I90-321-M-NR-I
55144130-I29-239-R-NR-I	18070105-I90-323-M-NR-I
06154150-Misc.-Hwy 14 Bypass-R-R-I	31150125-I90-350-M-NR-I
52830310-I90-101-M-NR-I	31160125-I90-351-M-NR-I
52925365-I90-112-M-NR-I	44050127-I90-358-M-NR-I
52926366-I90-112-M-R-I	44080125-I90-361-M-NR-I
38030185-I90-177-M-NR-I	44150126-I90-368-M-NR-I
38166196-I90-191-M-R-I	44170126-I90-370-M-NR-I
43026195-I90-212-M-R-I	06185230-I29-126-M-NR-I
08120125-I90-269-M-NR-I	06185110-I29-137-M-R-I
08290135-I90-286-M-R-I	15215070-I29-189-M-R-I
08310135-I90-289-M-NR-I	55115330-I29-218-M-NR-I
02000135-I90-291-M-NR-I	55124170-I29-234-M-NR-I
02018140-I90-293-M-R-I	55144130-I29-239-M-NR-I
02070155-I90-299-M-NR-I	06154150-Misc.-Hwy 14 Bypass-M-R-I

APPENDIX E: MNDOT CRASH STRUT DESIGN PROCEDURE

1. Determine Design Loads
    a. Determine the skew of the bent from the roadway (typically parallel)
    b. Givens:
        i. $P_{crash} = 400$ k
            1. Note: This is now 600 k
        ii. $\Theta_{max} = 30°$
        iii. $L_t = 5'$ (impact width if designing as distributed crash load instead of point load)
        iv. $L_{top} = 6''$ (conservative distance to top of the strut)
    c. Design Loads:
        i. $\theta_{design} = \theta_{\max} + \theta_{skew}$
        ii. $P_u = P_{crash} \sin(\theta_{design})$
        iii. $w_u = \dfrac{P_u}{L_t}$
    d. Resistance Factors:
        i. $\phi_{EE} = 1$ *(for extreme events)*
        ii. $\phi_{STR} = 0.90$ *(for strength)*

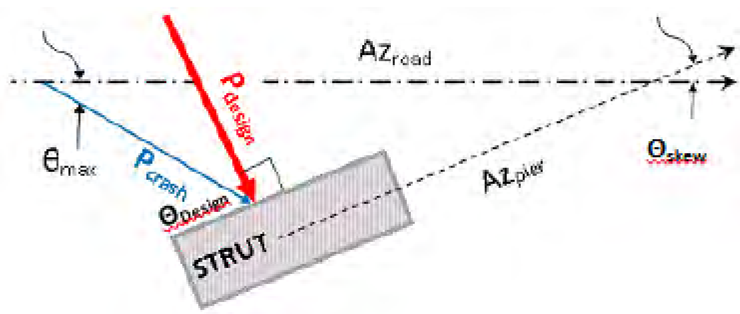

2. Determine Strut Dimensions
    a. Height
        i. *H = 4.5′ + depth to footing*
            1. Note: 4.5′ increased to 5.5′
            2. Note: Round height up
    b. Length
        i. Typically extend strut to 6″ from outside of footings (End Offset)
        ii. Minimum of 1′ extension past columns
    c. Width
        i. *$b = b_{col}$ + 2″ min. each side*
            1. Can increase by more than 2″ each side to ease constructability
        ii. *$b_{min} = 3'$*

3. Design Strut Reinforcement
    a. Select reinforcement
        i. Shear Stirrups
            1. Approximately #6 bars @ 12″ spacing (in interior region – bars spaced with dowels in end regions)
            2. Clear to stirrups = 2″
        ii. Horizontal Bars
            1. Minimum #6 bars @ approximately 12″ spacing
        iii. Dowel Bars
            1. #6 bars @ TBD spacing
    b. Determine dowel bar spacing
        i. End clearance
            1. $clr_{end} = clr + dia_v$ *(rounded to nearest inch)*
        ii. Dowel Spacing
            1. #6 bar @ 6″ spacing over a minimum length of 7′
            2. $Dowel\ Spacing = \dfrac{L_{footing} - clr_{end} - 2EndOffset - dia_D}{n_D - 1}$
            3. If footing is continuous, install anchorage over entire length of footings.
    c. Determine development length of dowels
        i. Calculate required projection of dowel into the strut.
        ii. Determine embedment of dowel into the footing.

APPENDIX F: DEAD LOAD

I-90		*Dead Load (kips)*			
Bridge ID	**Mile Marker**	**Bent 2**	**Bent 3**	**Bent 4**	**Bent 5**
41095059	10	65	76	67	NA
41116088	12	114	134	114	NA
41101077	14	113	133	113	NA
41154087	17	113	133	113	NA
41155087	17	113	133	113	NA
41185086	21	40	42	40	NA
41207092	23	57	61	57	NA
41226107	25.5	76	86	76	NA
47061480	36.5	50	55	50	NA
47069510	40	42	45	42	NA
47098563	44	128	154	124	NA
47111580	46	96	NA	NA	NA
47135609	52	364	NA	NA	NA
52390278	55	176	NA	NA	NA
52410285	57	125	NA	NA	NA
52424285	59	97	NA	NA	NA
52450287	61	185	NA	NA	NA
52467276	63	33	36	33	NA
52470276	63.5	317	NA	NA	NA
52500275	67	341	NA	NA	NA
52540275	71	35	37	35	NA
52610285	78	617	686	617	NA
52640285	81	479	532	479	NA
52670285	84	617	686	617	NA
52710283	88	455	506	455	NA
52830310	101	237	298	274	NA
52880346	107	59	63	59	NA
52900360	109	59	63	59	NA
52925365	112	61	66	61	NA
52926366	112	64	66	59	NA
36120107	131	54	57	54	NA
36309106	150	113	122	113	NA
38030185	177	84	NA	NA	NA
38166196	191	55	59	55	NA
38180198	192	76	NA	NA	NA
43026195	212	50	54	50	NA
08069103	264	156	NA	NA	NA
08080112	265	79	90	79	NA
08120125	269	36	38	36	NA
08145124	272	45	48	45	NA
08290135	286	71	81	71	NA
08310135	289	45	48	45	NA
02000135	291	36	38	36	NA
02018140	293	29	33	29	NA

I-90		*Dead Load (kips)*			
Bridge ID	**Mile Marker**	**Bent 2**	**Bent 3**	**Bent 4**	**Bent 5**
02040149	296	49	52	49	NA
02070155	299	111	120	111	NA
02100155	302	111	120	111	NA
02140155	306	111	120	111	NA
0215C158	308	54	57	54	NA
02180165	310	49	52	49	NA
02220165	312	111	120	111	NA
18010105	317	111	120	111	NA
18030105	319	49	52	49	NA
18050105	321	111	120	111	NA
18070105	323	111	120	111	NA
18090105	325	49	52	49	NA
18120105	328	111	120	111	NA
18140107	330	49	52	51	NA
31040105	337	111	120	111	NA
31090126	344	49	52	49	NA
31120126	347	111	120	111	NA
31150125	350	49	52	49	NA
31160125	351	111	120	111	NA
44010126	354	45	48	45	NA
44050127	358	45	48	45	NA
44080125	361	36	38	36	NA
44110125	364	359	NA	NA	NA
44150126	368	45	48	45	NA
44170126	370	36	38	36	NA
44210126	374	45	48	45	NA
50030149	381	32	36	32	NA
50050164	384	48	54	48	NA
50070165	386	45	48	45	NA
50090165	388	45	48	45	NA
50160166	394	44	47	44	NA
50170164	395	387	NA	NA	NA
50185163	396.5	28	31	28	NA
50240165	402	617	686	617	NA
50280165	406	617	686	617	NA
50300166	408	617	686	617	NA
50320166	410	617	686	617	NA

I-29		*Dead Load (kips)*			
Bridge ID	**Mile Marker**	**Bent 2**	**Bent 3**	**Bent 4**	**Bent 5**
64158399	1	108	NA	NA	NA
64149367	4	582	639	582	NA
64140355	6	773	851	773	NA
64120336	8	611	673	611	NA
64115330	9	772	851	772	NA
64100315	11	578	642	578	NA
64080296	14	578	642	578	NA
64070287	15	582	639	582	NA
64050250	20	479	532	479	NA
64020220	24	479	532	479	NA
64008205	26	582	639	582	NA
64006160	31	34	36	34	NA
64006120	35	34	36	34	NA
64006100	37	34	36	34	NA
64006090	38	43	46	43	NA
64006030	44	43	46	43	NA
64006010	46	43	46	43	NA
64006000	47	322	NA	NA	NA
42065260	50	44	46	44	NA
42065230	53	43	46	43	NA
42065200	56	43	46	43	NA
42065170	59	43	46	43	NA
42065140	62	1163	1278	1163	NA
42065141	62	1163	1278	1163	NA
42065130	63	477	530	477	NA
42065120	64	617	686	617	NA
42065100	67	477	530	477	NA
42065080	68	271	NA	NA	NA
42065050	71	478	531	478	NA
50172240	76	278	NA	NA	NA
50173235	76.5	146	167	146	NA
50175230	77	81	NA	NA	NA
50175222	78	490	NA	NA	NA
50178191	81	255	NA	NA	NA
50180170	83	359	NA	NA	NA
50180162	84	32	38	38	32
50180163	84	32	38	38	32
50180140	86	45	47	45	NA
50177130	87	48	51	48	NA
50175040	96	45	48	45	NA
50175020	98	45	48	45	NA
51065210	102	45	48	45	NA
51065200	104	45	48	45	NA
51065150	109	45	48	45	NA
51066100	114	49	52	49	NA
51065050	120	111	120	111	NA

I-29		Dead Load (kips)			
Bridge ID	**Mile Marker**	**Bent 2**	**Bent 3**	**Bent 4**	**Bent 5**
64158399	1	108	NA	NA	NA
06185230	126	49	52	49	NA
06185210	127	49	52	49	NA
06185190	129	111	120	111	NA
06185159	132	49	52	49	NA
06185160	132	49	52	49	NA
06185150	133	49	52	49	NA
06185130	135	57	NA	NA	NA
06185110	137	66	NA	NA	NA
06185080	140	80	NA	NA	NA
20061280	150	89	NA	NA	NA
29280020	167	64	71	64	NA
15240220	173	59	64	59	NA
15215150	180	256	NA	NA	NA
15215120	183	193	NA	NA	NA
15215070	189	193	NA	NA	NA
15215030	193	256	NA	NA	NA
55085440	206	73	NA	NA	NA
55085429	207	76	86	76	NA
55100367	213	37	44	37	NA
55115330	218	69	NA	NA	NA
55115290	222	69	NA	NA	NA
55115220	229	61	NA	NA	NA
55116190	232	61	69	61	NA
55124170	234	66	74	66	NA
55144130	239	71	79	71	NA
55175040	248	72	NA	NA	NA

I-229		Dead Load (kips)			
Bridge ID	**Mile Marker**	**Bent 2**	**Bent 3**	**Bent 4**	**Bent 5**
42079004	1	543	NA	NA	NA
50191238	2	201	NA	NA	NA
50216220	5	57	68	57	NA
50219215	5.5	115	141	115	NA
50219210	5.75	56	NA	NA	NA
50219208	6	84	NA	NA	NA
50219205	6.25	249	NA	NA	NA
50219180	9	1125	NA	NA	NA
50221170	9.7	72	108	71	NA
50221167	10	65	NA	NA	NA
50221166	10	80	NA	NA	NA

I-190		*Dead Load (kips)*			
Bridge ID	**Mile Marker**	**Bent 2**	**Bent 3**	**Bent 4**	**Bent 5**
52410290	1	115	141	115	NA

Miscellaneous Roads		*Dead Load (kips)*			
Bridge ID	**Location**	**Bent 2**	**Bent 3**	**Bent 4**	**Bent 5**
06154150	Hwy 14 Bypass	77	82	73	NA
14092199	Hwy 50W	30	59	29	NA
14131205	Hwy 50E	52	56	NA	NA
50175210	Madison St	250	250	NA	NA
50176210	Madison St	254	254	NA	NA
50177199	12th St	250	250	NA	NA
50178199	12th St	254	254	NA	NA
52410318	Mt. Rushmore Rd.	32	36	40	36
52415285	Haines Ave.	346	346	NA	NA
52415286	Haines Ave.	346	346	NA	NA

APPENDIX G: SHEAR AND FLEXURAL CAPACITIES AND DEMANDS

G.1: Shear and Flexural Capacities

I-90		*Column Shear Capacity (kips)*				*Column Flexural Capacity (kip-ft)*			
Bridge ID	**Mile Marker**	**Bent 2**	**Bent 3**	**Bent 4**	**Bent 5**	**Bent 2**	**Bent 3**	**Bent 4**	**Bent 5**
41095059	10	311	312	312	NA	2132	2140	2133	NA
41116088	12	430	431	430	NA	924	942	924	NA
41101077	14	430	431	430	NA	923	941	923	NA
41154087	17	250	299	250	NA	771	941	771	NA
41155087	17	250	299	250	NA	771	941	771	NA
41185086	21	212	212	212	NA	708	709	708	NA
41207092	23	376	377	376	NA	868	871	868	NA
41226107	25.5	378	378	378	NA	700	708	700	NA
47061480	36.5	321	321	321	NA	522	526	522	NA
47069510	40	276	276	276	NA	623	624	623	NA
47098563	44	898	900	898	NA	9870	9916	9863	NA
47111580	46	230	NA	NA	NA	839	NA	NA	NA
47135609	52	727	NA	NA	NA	11521	NA	NA	NA
52390278	55	306	NA	NA	NA	1468	NA	NA	NA
52410285	57	759	NA	NA	NA	9771	NA	NA	NA
52424285	59	267	NA	NA	NA	1382	NA	NA	NA
52450287	61	534	NA	NA	NA	6074	NA	NA	NA
52467276	63	403	404	403	NA	721	1538	721	NA
52470276	63.5	546	NA	NA	NA	6146	NA	NA	NA
52500275	67	815	NA	NA	NA	9189	NA	NA	NA
52540275	71	281	281	281	NA	737	738	737	NA
52610285	78	1022	1027	1022	NA	6999	7125	6999	NA
52640285	81	792	796	792	NA	4249	4329	4249	NA
52670285	84	1022	1027	1022	NA	6999	7125	6999	NA
52710283	88	790	794	790	NA	4212	4289	4212	NA
52830310	101	372	372	372	NA	1078	1114	1100	NA
52880346	107	395	395	395	NA	949	952	949	NA
52900360	109	405	406	405	NA	1188	1191	1188	NA
52925365	112	220	221	220	NA	972	976	972	NA
52926366	112	227	227	227	NA	1255	1257	1251	NA
36120107	131	169	170	169	NA	480	482	480	NA
36309106	150	430	431	430	NA	1147	1155	1147	NA
38030185	177	530	NA	NA	NA	1958	NA	NA	NA
38166196	191	405	405	405	NA	1062	1066	1062	NA
38180198	192	247	NA	NA	NA	730	NA	NA	NA
43026195	212	405	405	405	NA	1057	1061	1057	NA
08069103	264	248	NA	NA	NA	786	NA	NA	NA
08080112	265	378	379	378	NA	703	712	703	NA
08120125	269	275	275	275	NA	728	729	728	NA
08145124	272	276	276	276	NA	624	626	624	NA
08290135	286	377	378	377	NA	696	704	696	NA
08310135	289	282	282	282	NA	636	637	636	NA
02000135	291	275	275	275	NA	728	729	728	NA

I-90		*Column Shear Capacity (kips)*				*Column Flexural Capacity (kip-ft)*			
Bridge ID	**Mile Marker**	**Bent 2**	**Bent 3**	**Bent 4**	**Bent 5**	**Bent 2**	**Bent 3**	**Bent 4**	**Bent 5**
02018140	293	308	308	308	NA	864	867	864	NA
02040149	296	312	312	312	NA	964	966	964	NA
02070155	299	430	430	430	NA	1146	1153	1146	NA
02100155	302	430	430	430	NA	1146	1153	1146	NA
02140155	306	430	430	430	NA	1146	1153	1146	NA
0215C158	308	357	358	357	NA	683	685	683	NA
02180165	310	312	312	312	NA	964	966	964	NA
02220165	312	430	430	430	NA	1146	1153	1146	NA
18010105	317	430	430	430	NA	1146	1153	1146	NA
18030105	319	312	312	312	NA	964	966	964	NA
18050105	321	430	430	430	NA	1146	1153	1146	NA
18070105	323	430	430	430	NA	1146	1153	1146	NA
18090105	325	312	312	312	NA	964	966	964	NA
18120105	328	430	430	430	NA	1146	1153	1146	NA
18140107	330	177	178	304	NA	912	915	953	NA
31040105	337	430	430	430	NA	1146	1153	1146	NA
31090126	344	312	312	312	NA	964	966	964	NA
31120126	347	430	430	430	NA	1146	1153	1146	NA
31150125	350	312	312	312	NA	964	966	964	NA
31160125	351	430	430	430	NA	1146	1153	1146	NA
44010126	354	282	282	282	NA	636	637	636	NA
44050127	358	282	282	282	NA	636	637	636	NA
44080125	361	281	281	281	NA	738	739	738	NA
44110125	364	599	NA	NA	NA	6713	NA	NA	NA
44150126	368	282	282	282	NA	636	637	636	NA
44170126	370	281	281	281	NA	738	739	738	NA
44210126	374	282	282	282	NA	636	637	636	NA
50030149	381	424	424	424	NA	720	1538	720	NA
50050164	384	320	321	320	NA	520	525	520	NA
50070165	386	282	282	282	NA	636	637	636	NA
50090165	388	282	282	282	NA	636	637	636	NA
50160166	394	281	282	281	NA	635	637	635	NA
50170164	395	611	NA	NA	NA	8184	NA	NA	NA
50185163	396.5	403	403	403	NA	718	721	718	NA
50240165	402	1022	1027	1022	NA	6999	7125	6999	NA
50280165	406	1022	1027	1022	NA	6999	7125	6999	NA
50300166	408	1022	1027	1022	NA	6999	7125	6999	NA
50320166	410	1022	1027	1022	NA	6999	7125	6999	NA

I-29		*Column Shear Capacity (kips)*				*Column Flexural Capacity (kip-ft)*			
Bridge ID	**Mile Marker**	**Bent 2**	**Bent 3**	**Bent 4**	**Bent 5**	**Bent 2**	**Bent 3**	**Bent 4**	**Bent 5**
64158399	1	278	NA	NA	NA	970	NA	NA	NA
64149367	4	1038	1042	1038	NA	5409	5523	5409	NA
64140355	6	1052	1058	1052	NA	5787	5938	5787	NA
64120336	8	1040	1045	1040	NA	5615	5736	5615	NA
64115330	9	1052	1058	1052	NA	5787	5938	5787	NA
64100315	11	1038	1042	1038	NA	5550	5675	5550	NA
64080296	14	1038	1042	1038	NA	5550	5675	5550	NA
64070287	15	1038	1042	1038	NA	5409	5523	5409	NA
64050250	20	792	796	792	NA	4249	4329	4249	NA
64020220	24	792	796	792	NA	4249	4329	4249	NA
64008205	26	1038	1042	1038	NA	5409	5523	5409	NA
64006160	31	281	281	281	NA	737	738	737	NA
64006120	35	281	281	281	NA	737	738	737	NA
64006100	37	281	281	281	NA	737	738	737	NA
64006090	38	281	282	281	NA	635	636	635	NA
64006030	44	281	282	281	NA	635	636	635	NA
64006010	46	281	282	281	NA	635	636	635	NA
64006000	47	669	NA	NA	NA	11373	NA	NA	NA
42065260	50	281	282	281	NA	635	636	635	NA
42065230	53	281	282	281	NA	635	636	635	NA
42065200	56	281	282	281	NA	635	636	635	NA
42065170	59	281	282	281	NA	635	636	635	NA
42065140	62	1082	1084	1082	NA	6527	6729	6527	NA
42065141	62	1082	1084	1082	NA	6527	6729	6527	NA
42065130	63	792	796	792	NA	4249	4329	4249	NA
42065120	64	1022	1027	1022	NA	6999	7125	6999	NA
42065100	67	792	796	792	NA	4249	4329	4249	NA
42065080	68	651	NA	NA	NA	5892	NA	NA	NA
42065050	71	792	796	792	NA	4249	4329	4249	NA
50172240	76	539	NA	NA	NA	4111	NA	NA	NA
50173235	76.5	234	235	234	NA	980	999	980	NA
50175230	77	247	NA	NA	NA	1173	NA	NA	NA
50175222	78	530	NA	NA	NA	4184	NA	NA	NA
50178191	81	715	NA	NA	NA	11652	NA	NA	NA
50180170	83	550	NA	NA	NA	6104	NA	NA	NA
50180162	84	403	404	404	403	720	1540	1540	720
50180163	84	403	404	404	403	720	1540	1540	720
50180140	86	282	282	282	NA	636	637	636	NA
50177130	87	327	327	327	NA	527	529	527	NA
50175040	96	282	282	282	NA	636	637	636	NA
50175020	98	282	282	282	NA	636	637	636	NA
51065210	102	282	282	282	NA	636	637	636	NA
51065200	104	282	282	282	NA	636	637	636	NA
51065150	109	282	282	282	NA	636	637	636	NA
51066100	114	304	304	304	NA	951	953	951	NA

I-29		*Column Shear Capacity (kips)*				*Column Flexural Capacity (kip-ft)*			
Bridge ID	**Mile Marker**	**Bent 2**	**Bent 3**	**Bent 4**	**Bent 5**	**Bent 2**	**Bent 3**	**Bent 4**	**Bent 5**
51065050	120	430	430	430	NA	1146	1153	1146	NA
6185230	126	304	304	304	NA	951	953	951	NA
6185210	127	304	304	304	NA	951	953	951	NA
6185190	129	430	430	430	NA	1146	1153	1146	NA
6185159	132	304	304	304	NA	951	953	951	NA
6185160	132	304	304	304	NA	951	953	951	NA
6185150	133	304	304	304	NA	951	953	951	NA
6185130	135	207	NA	NA	NA	771	NA	NA	NA
6185110	137	208	NA	NA	NA	779	NA	NA	NA
6185080	140	209	NA	NA	NA	792	NA	NA	NA
20061280	150	248	NA	NA	NA	840	NA	NA	NA
29280020	167	199	199	199	NA	1179	1184	1179	NA
15240220	173	229	229	229	NA	1092	905	1092	NA
15215150	180	233	NA	NA	NA	877	NA	NA	NA
15215120	183	228	NA	NA	NA	624	NA	NA	NA
15215070	189	228	NA	NA	NA	624	NA	NA	NA
15215030	193	233	NA	NA	NA	877	NA	NA	NA
55085440	206	511	NA	NA	NA	1498	NA	NA	NA
55085429	207	228	229	228	NA	1279	1287	1279	NA
55100367	213	197	197	197	NA	977	983	977	NA
55115330	218	511	NA	NA	NA	1491	NA	NA	NA
55115290	222	511	NA	NA	NA	1491	NA	NA	NA
55115220	229	1041	NA	NA	NA	3727	NA	NA	NA
55116190	232	227	227	227	NA	1389	1395	1389	NA
55124170	234	196	196	196	NA	1486	1017	1486	NA
55144130	239	196	197	196	NA	1489	1231	1489	NA
55175040	248	511	NA	NA	NA	1496	NA	NA	NA

I-229		*Column Shear Capacity (kips)*				*Column Flexural Capacity (kip-ft)*			
Bridge ID	**Mile Marker**	**Bent 2**	**Bent 3**	**Bent 4**	**Bent 5**	**Bent 2**	**Bent 3**	**Bent 4**	**Bent 5**
42079004	1	1311	NA	NA	NA	7453	NA	NA	NA
50191238	2	1817	NA	NA	NA	13047	NA	NA	NA
50216220	5	207	208	207	NA	1064	1074	1064	NA
50219215	5.5	158	160	158	NA	521	545	521	NA
50219210	5.75	768	NA	NA	NA	6643	NA	NA	NA
50219208	6	229	NA	NA	NA	1395	NA	NA	NA
50219205	6.25	764	NA	NA	NA	7732	NA	NA	NA
50219180	9	2113	NA	NA	NA	11525	NA	NA	NA
50221170	9.7	406	409	406	NA	681	716	680	NA
50221167	10	507	NA	NA	NA	3736	NA	NA	NA
50221166	10	508	NA	NA	NA	3749	NA	NA	NA

I-90		*Column Shear Capacity (kips)*				*Column Flexural Capacity (kip-ft)*			
Bridge ID	**Mile Marker**	**Bent 2**	**Bent 3**	**Bent 4**	**Bent 5**	**B1**	**B2**	**B3**	**B4**
52410290	1	158	160	158	NA	440	465	440	NA

Miscellaneous Roads		*Column Shear Capacity (kips)*				*Column Flexural Capacity (kip-ft)*			
Bridge ID	**Location**	**Bent 2**	**Bent 3**	**Bent 4**	**Bent 5**	**Bent 2**	**Bent 3**	**Bent 4**	**Bent 5**
06154150	Hwy 14 Bypass	456	457	456	NA	1244	1249	1241	NA
14092199	Hwy 50W	224	227	224	NA	1065	1251	1064	NA
14131205	Hwy 50E	207	207	NA	NA	1071	1075	NA	NA
50175210	Madison St	838	838	NA	NA	16107	16107	NA	NA
50176210	Madison St	838	838	NA	NA	16112	16112	NA	NA
50177199	12th St	838	838	NA	NA	16107	16107	NA	NA
50178199	12th St	838	838	NA	NA	16112	16112	NA	NA
52410318	Mt. Rushmore Rd.	327	327	328	327	743	495	498	746
52415285	Haines Ave.	760	760	NA	NA	18272	18272	NA	NA
52415286	Haines Ave.	760	760	NA	NA	18272	18272	NA	NA

G.2: Shear and Flexural Demands

I-90		Column Shear Demand (kips)				Column Flexural Demand (kip-ft)			
Bridge ID	**Mile Marker**	**Bent 2**	**Bent 3**	**Bent 4**	**Bent 5**	**Bent 2**	**Bent 3**	**Bent 4**	**Bent 5**
41095059	10	480	537	513	NA	3518	3140	2878	NA
41116088	12	486	489	499	NA	2868	2645	2734	NA
41101077	14	506	487	473	NA	3206	3016	2880	NA
41154087	17	501	451	486	NA	3428	2931	2809	NA
41155087	17	518	486	461	NA	3312	2969	3057	NA
41185086	21	473	522	522	NA	2715	3175	3175	NA
41207092	23	492	492	517	NA	2935	2935	2708	NA
41226107	25.5	515	518	486	NA	3605	2897	3274	NA
47061480	36.5	486	498	518	NA	2673	3064	2976	NA
47069510	40	444	517	444	NA	3029	2644	3029	NA
47098563	44	600	600	600	NA	5020	5753	7771	NA
47111580	46	547	NA	NA	NA	2546	NA	NA	NA
47135609	52	518	NA	NA	NA	11521	NA	NA	NA
52390278	55	483	NA	NA	NA	2551	NA	NA	NA
52410285	57	512	NA	NA	NA	9771	NA	NA	NA
52424285	59	462	NA	NA	NA	2217	NA	NA	NA
52450287	61	563	NA	NA	NA	6074	NA	NA	NA
52467276	63	425	488	425	NA	2499	2322	2499	NA
52470276	63.5	488	NA	NA	NA	6146	NA	NA	NA
52500275	67	452	NA	NA	NA	9189	NA	NA	NA
52540275	71	513	519	478	NA	2943	2480	3092	NA
52610285	78	584	558	579	NA	4545	3200	5327	NA
52640285	81	569	541	575	NA	5997	3447	5323	NA
52670285	84	574	550	575	NA	5675	3374	5720	NA
52710283	88	576	566	576	NA	5633	3056	5633	NA
52830310	101	439	484	501	NA	4051	4664	4040	NA
52880346	107	431	517	431	NA	3396	2914	3396	NA
52900360	109	400	454	400	NA	2781	2699	2781	NA
52925365	112	446	528	450	NA	4769	3940	4576	NA
52926366	112	497	522	543	NA	3804	3434	2961	NA
36120107	131	497	497	497	NA	2537	2537	2537	NA
36309106	150	533	546	483	NA	2778	2570	3288	NA
38030185	177	491	NA	NA	NA	3405	NA	NA	NA
38166196	191	333	410	346	NA	2824	2512	2499	NA
38180198	192	419	NA	NA	NA	3031	NA	NA	NA
43026195	212	430	480	363	NA	2353	2454	2601	NA
08069103	264	421	NA	NA	NA	3161	NA	NA	NA
08080112	265	485	502	485	NA	2429	2569	2429	NA
08120125	269	439	495	439	NA	3126	2822	3126	NA
08145124	272	397	496	397	NA	3174	2830	3174	NA
08290135	286	448	502	448	NA	2802	2553	2802	NA
08310135	289	465	496	465	NA	3032	2830	3032	NA
02000135	291	431	495	431	NA	3153	2822	3153	NA
02018140	293	422	466	422	NA	2242	2158	2242	NA

I-90		Column Shear Demand (kips)				Column Flexural Demand (kip-ft)			
Bridge ID	**Mile Marker**	**Bent 2**	**Bent 3**	**Bent 4**	**Bent 5**	**Bent 2**	**Bent 3**	**Bent 4**	**Bent 5**
02040149	296	445	493	445	NA	3071	2804	3071	NA
02070155	299	461	520	477	NA	3246	2781	3156	NA
02100155	302	492	534	492	NA	3050	2614	3050	NA
02140155	306	471	539	486	NA	3344	2664	3246	NA
0215C158	308	490	521	490	NA	2771	2502	2771	NA
02180165	310	456	486	456	NA	3183	2860	3183	NA
02220165	312	461	506	461	NA	3246	2926	3246	NA
18010105	317	461	506	461	NA	3246	2926	3246	NA
18030105	319	456	487	472	NA	3183	3001	3100	NA
18050105	321	477	506	477	NA	3156	2926	3156	NA
18070105	323	477	520	477	NA	3156	2781	3156	NA
18090105	325	456	509	487	NA	3183	2818	3001	NA
18120105	328	461	520	461	NA	3246	2781	3246	NA
18140107	330	412	484	390	NA	2805	2588	2820	NA
31040105	337	447	506	447	NA	3319	2926	3319	NA
31090126	344	412	486	412	NA	3173	2860	3173	NA
31120126	347	447	506	447	NA	3319	2926	3319	NA
31150125	350	453	517	453	NA	3037	2605	3037	NA
31160125	351	447	506	447	NA	3319	2926	3319	NA
44010126	354	458	522	465	NA	2962	2507	3032	NA
44050127	358	458	522	458	NA	2962	2507	2962	NA
44080125	361	435	519	452	NA	2979	2480	2916	NA
44110125	364	540	NA	NA	NA	6713	NA	NA	NA
44150126	368	424	498	424	NA	3084	2717	3084	NA
44170126	370	447	525	463	NA	3094	2541	3021	NA
44210126	374	513	551	513	NA	3358	2760	3358	NA
50030149	381	334	418	334	NA	2225	2243	2225	NA
50050164	384	486	524	470	NA	2651	2613	2743	NA
50070165	386	474	518	474	NA	3129	2765	3129	NA
50090165	388	474	496	474	NA	3129	2970	3129	NA
50160166	394	474	503	448	NA	3129	2767	3108	NA
50170164	395	520	NA	NA	NA	8184	NA	NA	NA
50185163	396.5	466	499	466	NA	2370	2458	2370	NA
50240165	402	566	557	571	NA	6247	3161	5875	NA
50280165	406	580	549	570	NA	4994	3426	6113	NA
50300166	408	578	553	569	NA	5033	3404	6319	NA
50320166	410	580	549	573	NA	4944	3426	5825	NA

I-29		Column Shear Demand (kips)				Column Flexural Demand (kip-ft)			
Bridge ID	**Mile Marker**	**Bent 2**	**Bent 3**	**Bent 4**	**Bent 5**	**Bent 2**	**Bent 3**	**Bent 4**	**Bent 5**
64158399	1	521	NA	NA	NA	2086	NA	NA	NA
64149367	4	578	551	578	NA	5697	3660	5697	NA
64140355	6	589	569	589	NA	4417	3403	4417	NA
64120336	8	585	579	585	NA	5996	3545	5996	NA
64115330	9	585	563	585	NA	5159	3625	5159	NA
64100315	11	590	574	590	NA	5126	3811	5126	NA
64080296	14	587	579	587	NA	5594	3529	5594	NA
64070287	15	575	561	575	NA	5864	3335	5864	NA
64050250	20	575	550	575	NA	5275	3270	5275	NA
64020220	24	577	547	572	NA	5127	3334	5614	NA
64008205	26	576	563	576	NA	5868	3347	5868	NA
64006160	31	458	494	458	NA	2735	2683	2735	NA
64006120	35	458	494	458	NA	2735	2683	2735	NA
64006100	37	454	518	489	NA	2912	2621	3018	NA
64006090	38	465	504	465	NA	2560	2627	2560	NA
64006030	44	465	494	465	NA	2560	2550	2560	NA
64006010	46	465	494	465	NA	2560	2550	2560	NA
64006000	47	518	NA	NA	NA	11373	NA	NA	NA
42065260	50	465	494	465	NA	2560	2550	2560	NA
42065230	53	465	517	511	NA	2560	2644	2839	NA
42065200	56	446	494	446	NA	2636	2550	2636	NA
42065170	59	446	494	465	NA	2636	2550	2560	NA
42065140	62	580	553	587	NA	5444	3635	4463	NA
42065141	62	581	557	588	NA	5342	3499	4253	NA
42065130	63	578	565	578	NA	4885	2738	4885	NA
42065120	64	567	536	567	NA	6103	3535	6103	NA
42065100	67	578	565	578	NA	4885	2738	4885	NA
42065080	68	517	NA	NA	NA	5892	NA	NA	NA
42065050	71	578	560	578	NA	4885	2918	4885	NA
50172240	76	553	NA	NA	NA	4111	NA	NA	NA
50173235	76.5	489	514	522	NA	2786	2558	2384	NA
50175230	77	474	NA	NA	NA	3408	NA	NA	NA
50175222	78	534	NA	NA	NA	4184	NA	NA	NA
50178191	81	545	NA	NA	NA	11652	NA	NA	NA
50180170	83	536	NA	NA	NA	6104	NA	NA	NA
50180162	84	450	359	450	359	2216	3193	2216	3193
50180163	84	434	371	371	458	2246	3204	3204	2198
50180140	86	518	518	463	NA	2756	2756	2548	NA
50177130	87	463	524	453	NA	3090	2613	2983	NA
50175040	96	439	532	465	NA	3141	2602	3032	NA
50175020	98	465	503	416	NA	3032	2767	3217	NA
51065210	102	431	511	465	NA	3169	2699	3032	NA
51065200	104	465	516	465	NA	3032	2650	3032	NA
51065150	109	456	511	431	NA	3072	2699	3169	NA
51066100	114	432	517	456	NA	3279	2745	3183	NA

I-29		*Column Shear Demand (kips)*				*Column Flexural Demand (kip-ft)*			
Bridge ID	**Mile Marker**	**Bent 2**	**Bent 3**	**Bent 4**	**Bent 5**	**Bent 2**	**Bent 3**	**Bent 4**	**Bent 5**
51065050	120	461	520	461	NA	3246	2781	3246	NA
06185230	126	432	502	456	NA	3279	2883	3183	NA
06185210	127	451	510	451	NA	3365	2957	3365	NA
06185190	129	447	506	447	NA	3319	2926	3319	NA
06185159	132	440	509	472	NA	3249	2818	3100	NA
06185160	132	440	509	472	NA	3249	2818	3100	NA
06185150	133	487	524	472	NA	3001	2668	3100	NA
06185130	135	479	NA	NA	NA	2331	NA	NA	NA
06185110	137	394	NA	NA	NA	3444	NA	NA	NA
06185080	140	502	NA	NA	NA	2240	NA	NA	NA
20061280	150	456	NA	NA	NA	2561	NA	NA	NA
29280020	167	396	486	396	NA	2885	2632	2885	NA
15240220	173	464	494	464	NA	2293	2284	2293	NA
15215150	180	425	NA	NA	NA	3503	NA	NA	NA
15215120	183	448	NA	NA	NA	3419	NA	NA	NA
15215070	189	501	NA	NA	NA	3800	NA	NA	NA
15215030	193	437	NA	NA	NA	3603	NA	NA	NA
55085440	206	600	NA	NA	NA	4633	NA	NA	NA
55085429	207	477	495	477	NA	3310	3193	3310	NA
55100367	213	600	600	600	NA	5478	5253	5703	NA
55115330	218	600	NA	NA	NA	4633	NA	NA	NA
55115290	222	600	NA	NA	NA	4650	NA	NA	NA
55115220	229	600	NA	NA	NA	4895	NA	NA	NA
55116190	232	511	511	501	NA	3101	3101	3188	NA
55124170	234	505	496	505	NA	2758	2532	2758	NA
55144130	239	478	477	478	NA	2964	2666	2964	NA
55175040	248	600	NA	NA	NA	4633	NA	NA	NA

I-229		*Column Shear Demand (kips)*				*Column Flexural Demand (k-ft)*			
Bridge ID	**Mile Marker**	**Bent 2**	**Bent 3**	**Bent 4**	**Bent 5**	**Bent 2**	**Bent 3**	**Bent 4**	**Bent 5**
42079004	1	500	NA	NA	NA	7453	NA	NA	NA
50191238	2	521	NA	NA	NA	13047	NA	NA	NA
50216220	5	449	410	425	NA	2678	2384	2664	NA
50219215	5.5	325	NA	359	NA	2533	NA	2035	NA
50219210	5.75	501	NA	NA	NA	6643	NA	NA	NA
50219208	6	459	NA	NA	NA	2795	NA	NA	NA
50219205	6.25	503	NA	NA	NA	7732	NA	NA	NA
50219180	9	600	NA	NA	NA	6787	NA	NA	NA
50221170	9.7	459	510	466	NA	2204	2384	2123	NA
50221167	10	403	NA	NA	NA	3736	NA	NA	NA
50221166	10	425	NA	NA	NA	3749	NA	NA	NA

I-190		*Column Shear Demand (kips)*				*Column Flexural Demand (k-ft)*			
Bridge ID	**Mile Marker**	**Bent 2**	**Bent 3**	**Bent 4**	**Bent 5**	**Bent 2**	**Bent 3**	**Bent 4**	**Bent 5**
52410290	1	451	NA	404	NA	2947	NA	2494	NA

		Column Shear Demand (kips)				*Column Flexural Demand (k-ft)*			
Bridge ID	**Location**	**Bent 2**	**Bent 3**	**Bent 4**	**Bent 5**	**Bent 2**	**Bent 3**	**Bent 4**	**Bent 5**
06154150	Hwy 14 Bypass	463	465	416	NA	3803	3718	3675	NA
14092199	Hwy 50W	600	547	NA	NA	4635	2893	NA	NA
14131205	Hwy 50E	432	459	NA	NA	2749	2990	NA	NA
50175210	Madison St	446	446	NA	NA	2674	2674	NA	NA
50176210	Madison St	430	430	NA	NA	2788	2788	NA	NA
50177199	12th St	426	459	NA	NA	3489	2579	NA	NA
50178199	12th St	416	445	NA	NA	3836	2894	NA	NA
52410318	Mt. Rushmore Rd.	503	570	558	549	3660	3659	3212	3214
52415285	Haines Ave.	600	600	NA	NA	9366	9366	NA	NA
52415286	Haines Ave.	600	600	NA	NA	9366	9366	NA	NA

G.3: Column Demand-to-Capacity Ratios

I-90		Shear D/C Ratio				Bending Moment D/C Ratio			
Bridge ID	Mile Marker	Bent 2	Bent 3	Bent 4	Bent 5	Bent 2	Bent 3	Bent 4	Bent 5
41095059	10	1.54	1.72	1.65	NA	1.65	1.47	1.35	NA
41116088	12	1.13	1.13	1.16	NA	3.10	2.81	2.96	NA
41101077	14	1.18	1.13	1.10	NA	3.47	3.21	3.12	NA
41154087	17	2.00	1.51	1.95	NA	4.45	3.12	3.64	NA
41155087	17	2.07	1.62	1.84	NA	4.30	3.15	3.96	NA
41185086	21	2.24	2.46	2.47	NA	3.83	4.48	4.49	NA
41207092	23	1.31	1.31	1.37	NA	3.38	3.37	3.12	NA
41226107	25.5	1.36	1.37	1.29	NA	5.15	4.09	4.68	NA
47061480	36.5	1.52	1.55	1.62	NA	5.12	5.83	5.70	NA
47069510	40	1.61	1.87	1.61	NA	4.86	4.24	4.86	NA
47098563	44	0.67	0.67	0.67	NA	0.51	0.58	0.79	NA
47111580	46	2.38	NA	NA	NA	3.03	NA	NA	NA
47135609	52	0.71	NA	NA	NA	0.42	NA	NA	NA
52390278	55	1.58	NA	NA	NA	1.74	NA	NA	NA
52410285	57	0.67	NA	NA	NA	0.59	NA	NA	NA
52424285	59	1.73	NA	NA	NA	1.60	NA	NA	NA
52450287	61	1.05	NA	NA	NA	0.67	NA	NA	NA
52467276	63	1.05	1.21	1.05	NA	3.47	1.51	3.47	NA
52470276	63.5	0.89	NA	NA	NA	0.78	NA	NA	NA
52500275	67	0.55	NA	NA	NA	0.68	NA	NA	NA
52540275	71	1.83	1.85	1.70	NA	3.99	3.36	4.20	NA
52610285	78	0.57	0.54	0.57	NA	0.65	0.45	0.76	NA
52640285	81	0.72	0.68	0.73	NA	1.41	0.80	1.25	NA
52670285	84	0.56	0.54	0.56	NA	0.81	0.47	0.82	NA
52710283	88	0.73	0.71	0.73	NA	1.34	0.71	1.34	NA
52830310	101	1.18	1.30	1.35	NA	3.76	4.19	3.67	NA
52880346	107	1.09	1.31	1.09	NA	3.58	3.06	3.58	NA
52900360	109	0.99	1.12	0.99	NA	2.34	2.27	2.34	NA
52925365	112	2.02	2.39	2.04	NA	4.91	4.04	4.71	NA
52926366	112	2.19	2.30	2.40	NA	3.03	2.73	2.37	NA
36120107	131	2.93	2.93	2.93	NA	5.29	5.26	5.29	NA
36309106	150	1.24	1.27	1.12	NA	2.42	2.23	2.87	NA
38030185	177	0.93	NA	NA	NA	1.74	NA	NA	NA
38166196	191	0.82	1.01	0.85	NA	2.66	2.36	2.35	NA
38180198	192	1.70	NA	NA	NA	4.15	NA	NA	NA
43026195	212	1.06	1.19	0.90	NA	2.23	2.31	2.46	NA
08069103	264	1.70	NA	NA	NA	4.02	NA	NA	NA
08080112	265	1.28	1.33	1.28	NA	3.45	3.61	3.45	NA
08120125	269	1.59	1.80	1.59	NA	4.29	3.87	4.29	NA
08145124	272	1.44	1.79	1.44	NA	5.09	4.52	5.09	NA
08290135	286	1.19	1.33	1.19	NA	4.03	3.63	4.03	NA
08310135	289	1.65	1.76	1.65	NA	4.77	4.44	4.77	NA
02000135	291	1.57	1.80	1.57	NA	4.33	3.87	4.33	NA
02018140	293	1.37	1.51	1.37	NA	2.59	2.49	2.59	NA

I-90		*Shear D/C Ratio*				*Bending Moment D/C Ratio*			
Bridge ID	**Mile Marker**	**Bent 2**	**Bent 3**	**Bent 4**	**Bent 5**	**Bent 2**	**Bent 3**	**Bent 4**	**Bent 5**
02040149	296	1.43	1.58	1.43	NA	3.19	2.90	3.19	NA
02070155	299	1.07	1.21	1.11	NA	2.83	2.41	2.75	NA
02100155	302	1.14	1.24	1.14	NA	2.66	2.27	2.66	NA
02140155	306	1.10	1.25	1.13	NA	2.92	2.31	2.83	NA
0215C158	308	1.37	1.46	1.37	NA	4.06	3.65	4.06	NA
02180165	310	1.46	1.56	1.46	NA	3.30	2.96	3.30	NA
02220165	312	1.07	1.18	1.07	NA	2.83	2.54	2.83	NA
18010105	317	1.07	1.18	1.07	NA	2.83	2.54	2.83	NA
18030105	319	1.46	1.56	1.51	NA	3.30	3.11	3.22	NA
18050105	321	1.11	1.18	1.11	NA	2.75	2.54	2.75	NA
18070105	323	1.11	1.21	1.11	NA	2.75	2.41	2.75	NA
18090105	325	1.46	1.63	1.56	NA	3.30	2.92	3.11	NA
18120105	328	1.07	1.21	1.07	NA	2.83	2.41	2.83	NA
18140107	330	2.33	2.72	1.28	NA	3.08	2.83	2.96	NA
31040105	337	1.04	1.18	1.04	NA	2.90	2.54	2.90	NA
31090126	344	1.32	1.56	1.32	NA	3.29	2.96	3.29	NA
31120126	347	1.04	1.18	1.04	NA	2.90	2.54	2.90	NA
31150125	350	1.45	1.66	1.45	NA	3.15	2.70	3.15	NA
31160125	351	1.04	1.18	1.04	NA	2.90	2.54	2.90	NA
44010126	354	1.63	1.85	1.65	NA	4.66	3.94	4.77	NA
44050127	358	1.63	1.85	1.63	NA	4.66	3.94	4.66	NA
44080125	361	1.55	1.85	1.61	NA	4.04	3.36	3.95	NA
44110125	364	0.90	NA	NA	NA	0.88	NA	NA	NA
44150126	368	1.51	1.77	1.51	NA	4.85	4.27	4.85	NA
44170126	370	1.59	1.87	1.65	NA	4.19	3.44	4.09	NA
44210126	374	1.82	1.96	1.82	NA	5.28	4.33	5.28	NA
50030149	381	0.79	0.99	0.79	NA	3.09	1.46	3.09	NA
50050164	384	1.52	1.63	1.47	NA	5.10	4.98	5.27	NA
50070165	386	1.68	1.84	1.68	NA	4.92	4.34	4.92	NA
50090165	388	1.68	1.76	1.68	NA	4.92	4.66	4.92	NA
50160166	394	1.68	1.79	1.59	NA	4.93	4.34	4.89	NA
50170164	395	0.85	NA	NA	NA	0.61	NA	NA	NA
50185163	396.5	1.16	1.24	1.16	NA	3.30	3.41	3.30	NA
50240165	402	0.55	0.54	0.56	NA	0.89	0.44	0.84	NA
50280165	406	0.57	0.53	0.56	NA	0.71	0.48	0.87	NA
50300166	408	0.57	0.54	0.56	NA	0.72	0.48	0.90	NA
50320166	410	0.57	0.53	0.56	NA	0.71	0.48	0.83	NA

I-29		Shear D/C Ratio				Bending Moment D/C Ratio			
Bridge ID	**Mile Marker**	**Bent 2**	**Bent 3**	**Bent 4**	**Bent 5**	**Bent 2**	**Bent 3**	**Bent 4**	**Bent 5**
64158399	1	1.88	NA	NA	NA	2.15	NA	NA	NA
64149367	4	0.56	0.53	0.56	NA	1.05	0.66	1.05	NA
64140355	6	0.56	0.54	0.56	NA	0.76	0.57	0.76	NA
64120336	8	0.56	0.55	0.56	NA	1.07	0.62	1.07	NA
64115330	9	0.56	0.53	0.56	NA	0.89	0.61	0.89	NA
64100315	11	0.57	0.55	0.57	NA	0.92	0.67	0.92	NA
64080296	14	0.57	0.56	0.57	NA	1.01	0.62	1.01	NA
64070287	15	0.55	0.54	0.55	NA	1.08	0.60	1.08	NA
64050250	20	0.73	0.69	0.73	NA	1.24	0.76	1.24	NA
64020220	24	0.73	0.69	0.72	NA	1.21	0.77	1.32	NA
64008205	26	0.56	0.54	0.56	NA	1.08	0.61	1.08	NA
64006160	31	1.63	1.76	1.63	NA	3.71	3.64	3.71	NA
64006120	35	1.63	1.76	1.63	NA	3.71	3.64	3.71	NA
64006100	37	1.62	1.85	1.74	NA	3.95	3.55	4.10	NA
64006090	38	1.65	1.79	1.65	NA	4.03	4.13	4.03	NA
64006030	44	1.65	1.75	1.65	NA	4.03	4.01	4.03	NA
64006010	46	1.65	1.75	1.65	NA	4.03	4.01	4.03	NA
64006000	47	0.77	NA	NA	NA	0.68	NA	NA	NA
42065260	50	1.65	1.75	1.65	NA	4.03	4.01	4.03	NA
42065230	53	1.65	1.84	1.82	NA	4.03	4.16	4.47	NA
42065200	56	1.58	1.75	1.58	NA	4.15	4.01	4.15	NA
42065170	59	1.58	1.75	1.65	NA	4.15	4.01	4.03	NA
42065140	62	0.54	0.51	0.54	NA	0.83	0.54	0.68	NA
42065141	62	0.54	0.51	0.54	NA	0.82	0.52	0.65	NA
42065130	63	0.73	0.71	0.73	NA	1.15	0.63	1.15	NA
42065120	64	0.55	0.52	0.55	NA	0.87	0.50	0.87	NA
42065100	67	0.73	0.71	0.73	NA	1.15	0.63	1.15	NA
42065080	68	0.79	NA	NA	NA	0.85	NA	NA	NA
42065050	71	0.73	0.70	0.73	NA	1.15	0.67	1.15	NA
50172240	76	1.03	NA	NA	NA	0.99	NA	NA	NA
50173235	76.5	2.09	2.18	2.24	NA	2.84	2.56	2.43	NA
50175230	77	1.92	NA	NA	NA	2.91	NA	NA	NA
50175222	78	1.01	NA	NA	NA	0.96	NA	NA	NA
50178191	81	0.76	NA	NA	NA	0.47	NA	NA	NA
50180170	83	0.97	NA	NA	NA	0.90	NA	NA	NA
50180162	84	1.12	0.89	1.12	0.89	3.08	2.07	1.44	4
50180163	84	1.08	0.92	0.92	1.14	3.12	2.08	2.08	3
50180140	86	1.84	1.84	1.64	NA	4.33	4.33	4.01	NA
50177130	87	1.42	1.60	1.38	NA	5.86	4.94	5.66	NA
50175040	96	1.56	1.89	1.65	NA	4.94	4.08	4.77	NA
50175020	98	1.65	1.79	1.48	NA	4.77	4.34	5.06	NA
51065210	102	1.53	1.81	1.65	NA	4.98	4.24	4.77	NA
51065200	104	1.65	1.83	1.65	NA	4.77	4.16	4.77	NA
51065150	109	1.62	1.81	1.53	NA	4.83	4.24	4.98	NA

I-29		*Shear D/C Ratio*				*Bending Moment D/C Ratio*			
Bridge ID	**Mile Marker**	**Bent 2**	**Bent 3**	**Bent 4**	**Bent 5**	**Bent 2**	**Bent 3**	**Bent 4**	**Bent 5**
51066100	114	1.42	1.70	1.50	NA	3.45	2.88	3.35	NA
51065050	120	1.07	1.21	1.07	NA	2.83	2.41	2.83	NA
06185230	126	1.42	1.65	1.50	NA	3.45	3.02	3.35	NA
06185210	127	1.49	1.68	1.49	NA	3.54	3.10	3.54	NA
06185190	129	1.04	1.18	1.04	NA	2.90	2.54	2.90	NA
06185159	132	1.45	1.68	1.55	NA	3.42	2.96	3.26	NA
06185160	132	1.45	1.68	1.55	NA	3.42	2.96	3.26	NA
06185150	133	1.61	1.72	1.55	NA	3.16	2.80	3.26	NA
06185130	135	2.31	NA	NA	NA	3.02	NA	NA	NA
06185110	137	1.89	NA	NA	NA	4.42	NA	NA	NA
06185080	140	2.40	NA	NA	NA	2.83	NA	NA	NA
20061280	150	1.84	NA	NA	NA	3.05	NA	NA	NA
29280020	167	1.99	2.44	1.99	NA	2.45	2.22	2.45	NA
15240220	173	2.03	2.15	2.03	NA	2.10	2.52	2.10	NA
15215150	180	1.83	NA	NA	NA	3.99	NA	NA	NA
15215120	183	1.96	NA	NA	NA	5.48	NA	NA	NA
15215070	189	2.19	NA	NA	NA	6.09	NA	NA	NA
15215030	193	1.88	NA	NA	NA	4.11	NA	NA	NA
55085440	206	1.17	NA	NA	NA	4.08	NA	NA	NA
55085429	207	2.09	2.16	2.09	NA	2.59	2.48	2.59	NA
55100367	213	3.06	3.05	3.06	NA	5.61	5.34	5.84	NA
55115330	218	1.17	NA	NA	NA	4.10	NA	NA	NA
55115290	222	1.17	NA	NA	NA	4.11	NA	NA	NA
55115220	229	0.58	NA	NA	NA	1.86	NA	NA	NA
55116190	232	2.25	2.25	2.21	NA	2.23	2.22	2.30	NA
55124170	234	2.58	2.53	2.58	NA	1.86	2.49	1.86	NA
55144130	239	2.44	2.43	2.44	NA	1.99	2.17	1.99	NA
55175040	248	1.17	NA	NA	NA	4.08	NA	NA	NA

I-229		*Shear D/C Ratio*				*Bending Moment D/C Ratio*			
Bridge ID	**Mile Marker**	**Bent 2**	**Bent 3**	**Bent 4**	**Bent 5**	**Bent 2**	**Bent 3**	**Bent 4**	**Bent 5**
42079004	1	0.38	NA	NA	NA	0.87	NA	NA	NA
50191238	2	0.29	NA	NA	NA	0.54	NA	NA	NA
50216220	5	2.16	1.97	2.05	NA	2.52	2.22	2.50	NA
50219215	5.5	2.06	NA	2.27	NA	4.86	NA	3.91	NA
50219210	5.75	0.65	NA	NA	NA	0.79	NA	NA	NA
50219208	6	NA	NA	NA	NA	NA	NA	NA	NA
50219205	6.25	0.66	NA	NA	NA	0.65	NA	NA	NA
50219180	9	0.28	NA	NA	NA	0.59	NA	NA	NA
50221170	9.7	1.13	1.25	1.15	NA	3.24	3.33	3.12	NA
50221167	10	0.80	NA	NA	NA	1.45	NA	NA	NA
50221166	10	0.84	NA	NA	NA	1.43	NA	NA	NA

I-190		*Shear D/C Ratio*				*Bending Moment D/C Ratio*			
Bridge ID	**Mile Marker**	**Bent 2**	**Bent 3**	**Bent 4**	**Bent 5**	**Bent 2**	**Bent 3**	**Bent 4**	**Bent 5**
52410290	1	2.85	NA	2.56	NA	6.70	NA	5.67	NA

Miscellaneous Roads		*Shear D/C Ratio*				*Bending Moment D/C Ratio*			
Bridge ID	**Location**	**Bent 2**	**Bent 3**	**Bent 4**	**Bent 5**	**Bent 2**	**Bent 3**	**Bent 4**	**Bent 5**
06154150	Hwy 14 Bypass	1.02	1.02	0.91	NA	3.06	2.98	2.96	NA
14092199	Hwy 50W	2.68	2.41	NA	NA	4.35	2.31	NA	NA
14131205	Hwy 50E	2.09	2.22	NA	NA	2.57	2.78	NA	NA
50175210	Madison St	0.53	0.53	NA	NA	0.17	0.17	NA	NA
50176210	Madison St	0.51	0.51	NA	NA	0.17	0.17	NA	NA
50177199	12th St	0.51	0.55	NA	NA	0.22	0.16	NA	NA
50178199	12th St	0.50	0.53	NA	NA	0.24	0.18	NA	NA
52410318	Mt. Rushmore Rd.	1.54	1.74	1.70	1.68	4.93	7.39	6.45	4
52415285	Haines Ave.	0.79	0.79	NA	NA	0.51	0.51	NA	NA
52415286	Haines Ave.	0.79	0.79	NA	NA	0.51	0.51	NA	NA

APPENDIX H: MEASURED STRAIN

G.1: Measured Strain in Specimen NCS

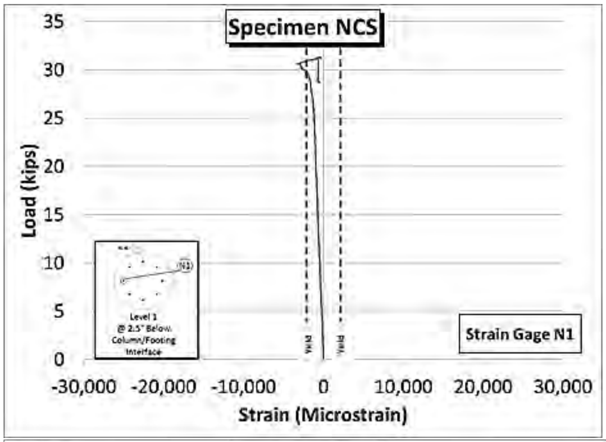

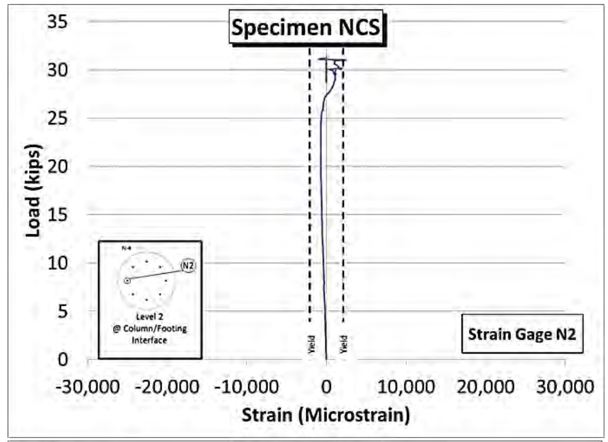

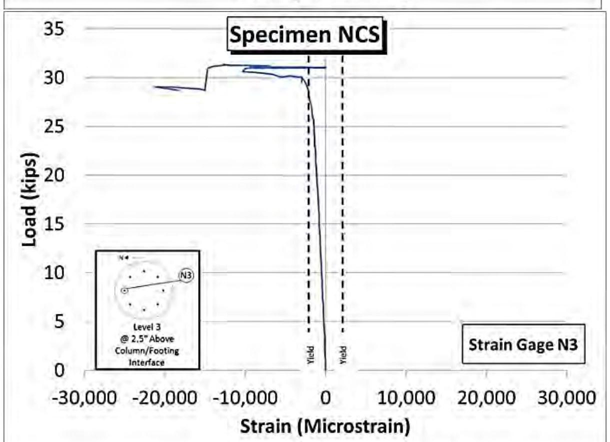

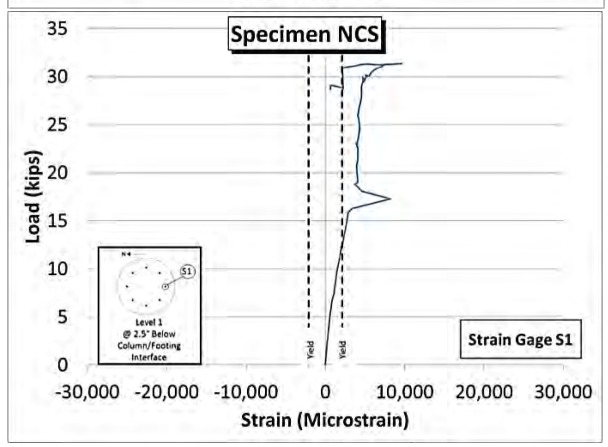

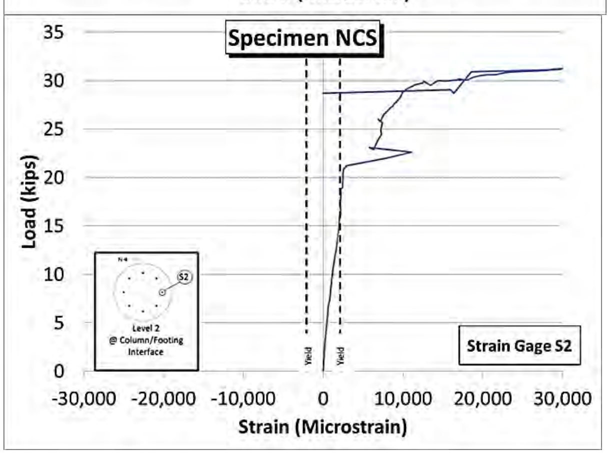

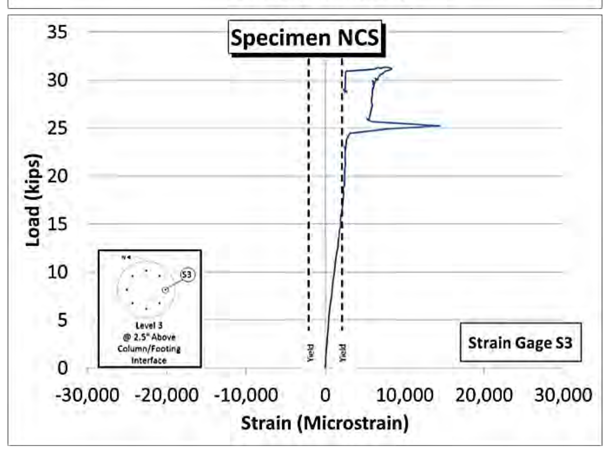

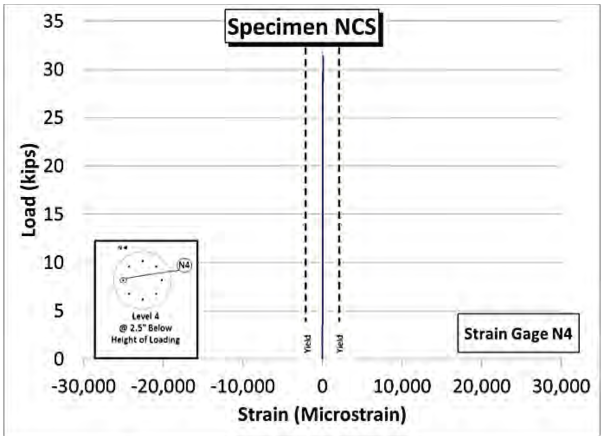
Specimen NCS
Load (kips)
Strain (Microstrain)
35
30
25
20
15
10
5
0
-30,000
-20,000
-10,000
0
10,000
20,000
30,000
Yield
Yield
N4
Level 4
@ 2.5" Below
Height of Loading
Strain Gage N4

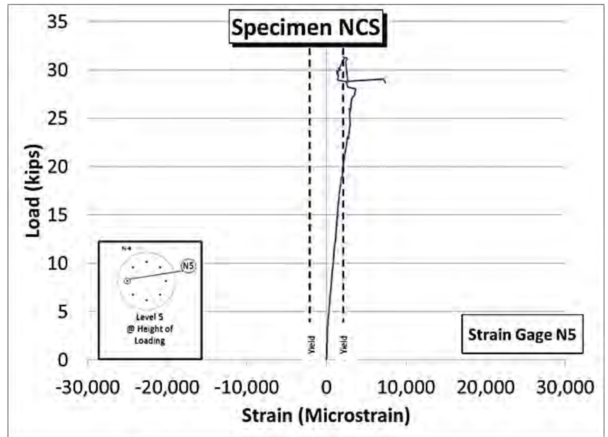
Specimen NCS
Load (kips)
Strain (Microstrain)
35
30
25
20
15
10
5
0
-30,000
-20,000
-10,000
0
10,000
20,000
30,000
Yield
Yield
N5
Level 5
@ Height of
Loading
Strain Gage N5

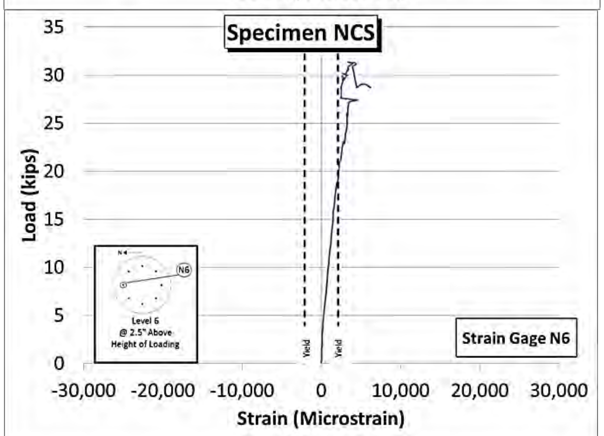
Specimen NCS
Load (kips)
Strain (Microstrain)
35
30
25
20
15
10
5
0
-30,000
-20,000
-10,000
0
10,000
20,000
30,000
Yield
Yield
N6
Level 6
@ 2.5" Above
Height of Loading
Strain Gage N6

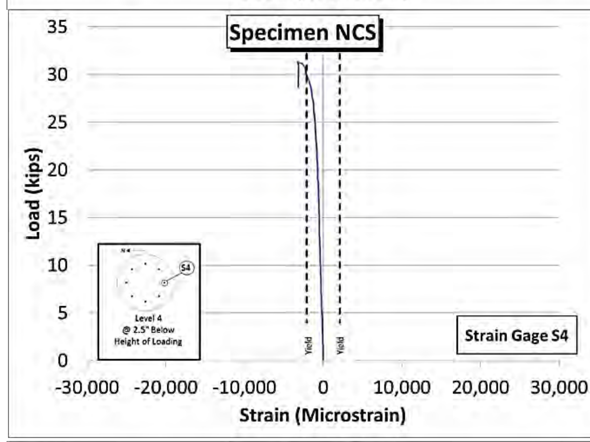
Specimen NCS
Load (kips)
Strain (Microstrain)
35
30
25
20
15
10
5
0
-30,000
-20,000
-10,000
0
10,000
20,000
30,000
Yield
Yield
S4
Level 4
@ 2.5" Below
Height of Loading
Strain Gage S4

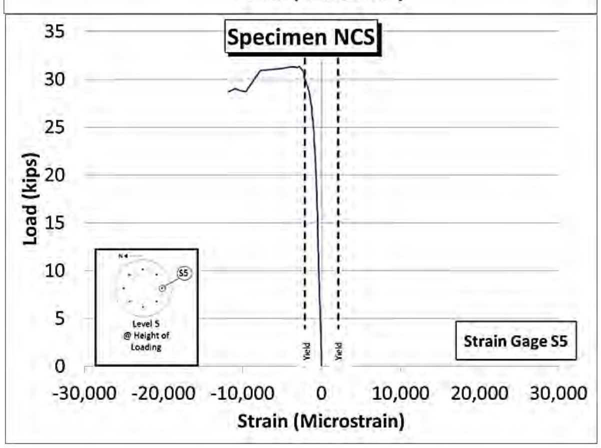
Specimen NCS
Load (kips)
Strain (Microstrain)
35
30
25
20
15
10
5
0
-30,000
-20,000
-10,000
0
10,000
20,000
30,000
Yield
Yield
S5
Level 5
@ Height of
Loading
Strain Gage S5

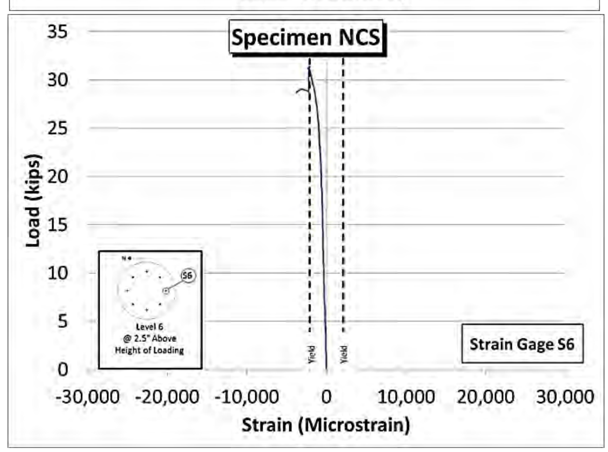
Specimen NCS
Load (kips)
Strain (Microstrain)
35
30
25
20
15
10
5
0
-30,000
-20,000
-10,000
0
10,000
20,000
30,000
Yield
Yield
S6
Level 6
@ 2.5" Above
Height of Loading
Strain Gage S6

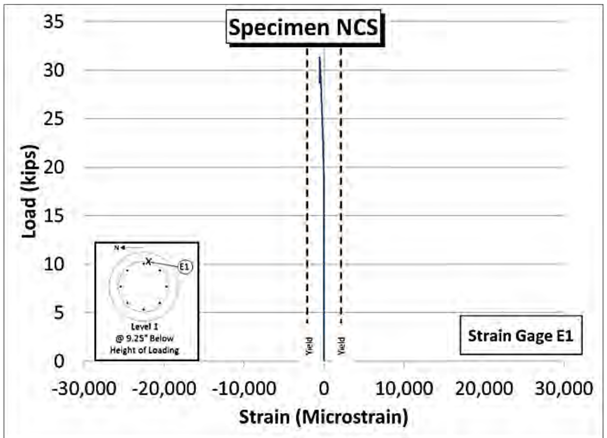

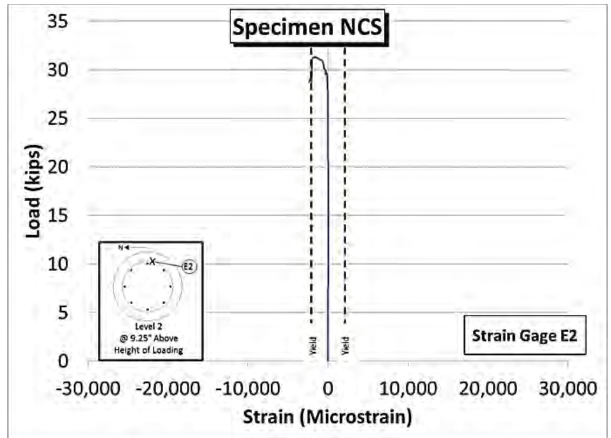

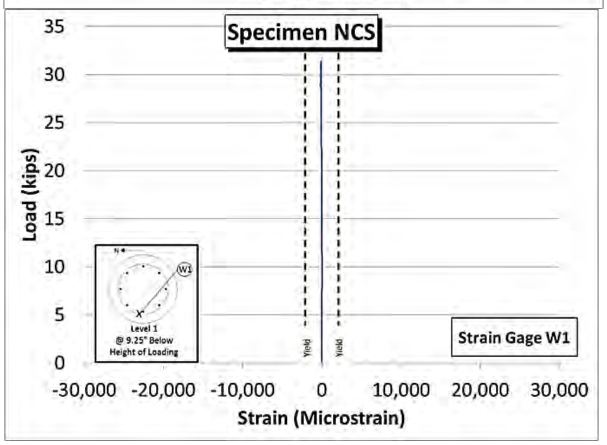

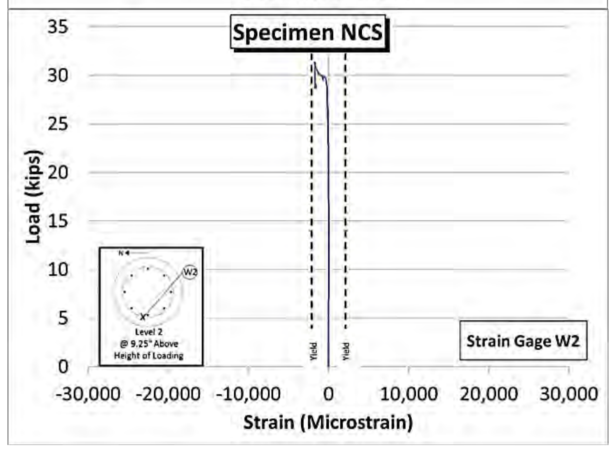

G.2: Measured Strain in Specimen CSR

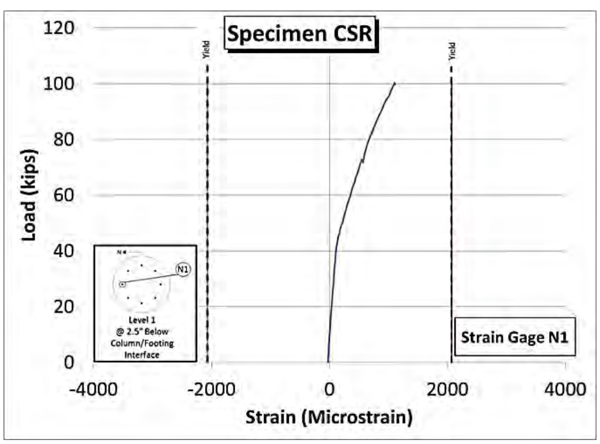

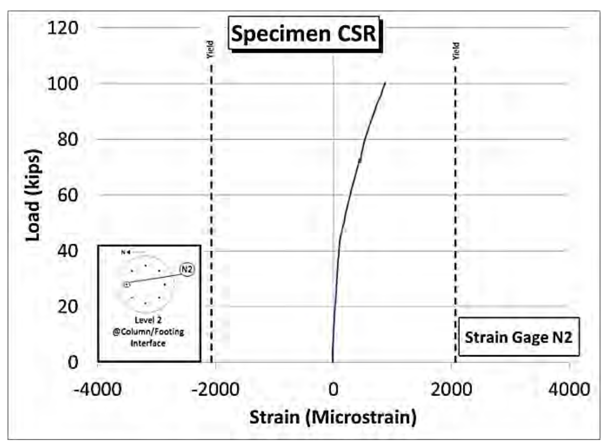

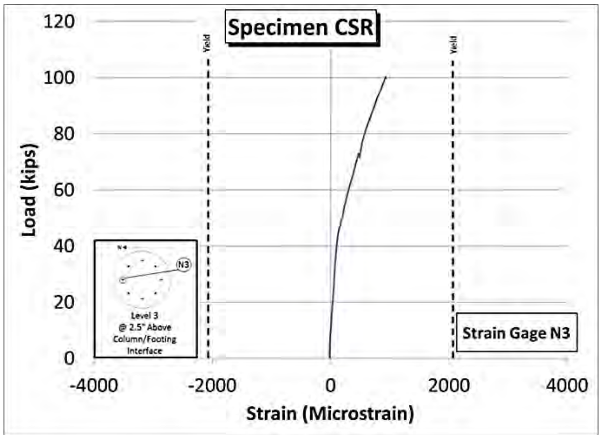
Specimen CSR
Load (kips)
Strain (Microstrain)
Yield
Yield
Level 3
@ 2.5" Above
Column/Footing
Interface
N3
Strain Gage N3

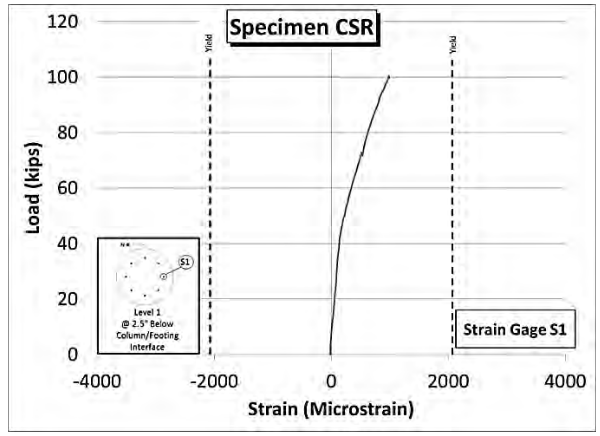
Specimen CSR
Load (kips)
Strain (Microstrain)
Yield
Yield
Level 1
@ 2.5" Below
Column/Footing
Interface
S1
Strain Gage S1

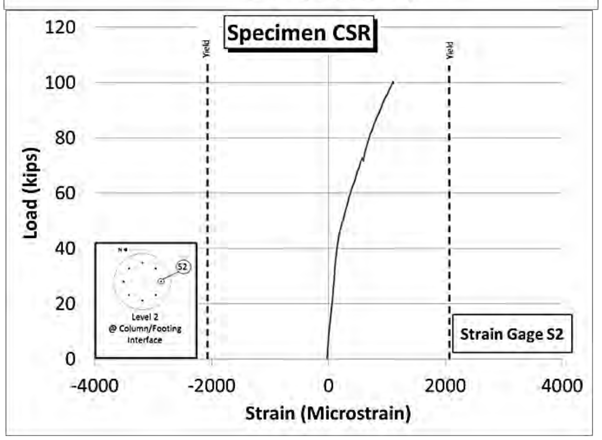
Specimen CSR
Load (kips)
Strain (Microstrain)
Yield
Yield
Level 2
@ Column/Footing
Interface
S2
Strain Gage S2

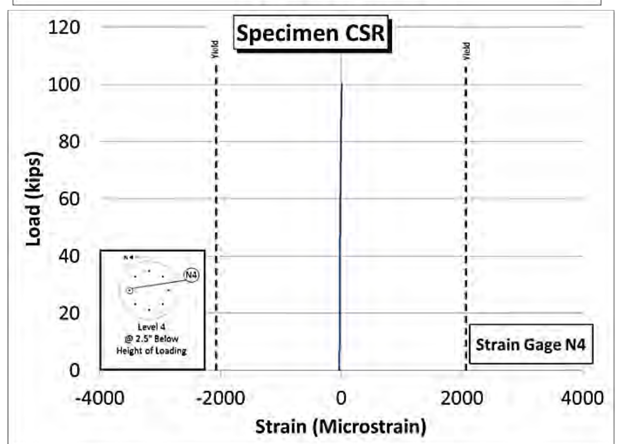
Specimen CSR
Load (kips)
Strain (Microstrain)
Yield
Yield
Level 4
@ 2.5" Below
Height of Loading
N4
Strain Gage N4

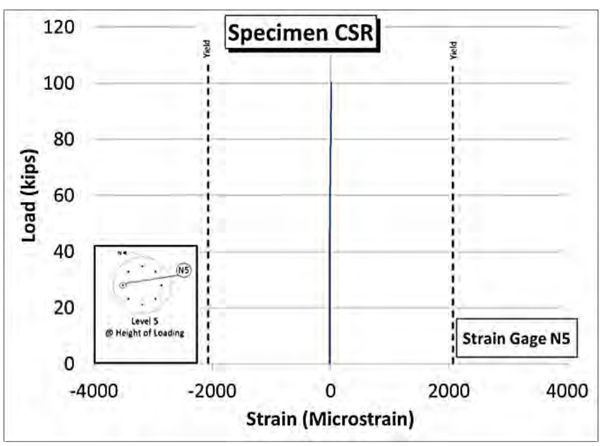
Specimen CSR
Load (kips)
Strain (Microstrain)
Yield
Yield
Level 5
@ Height of Loading
N5
Strain Gage N5

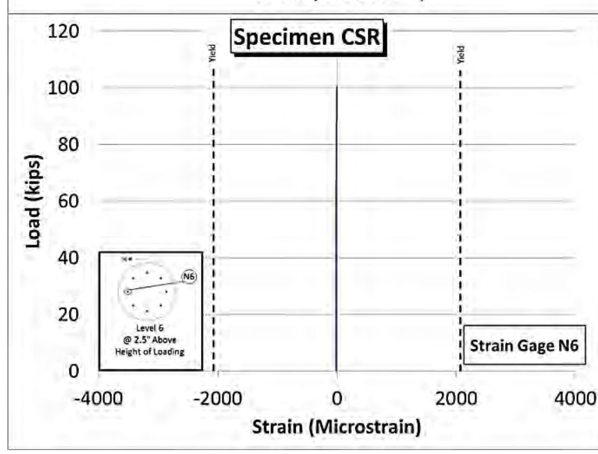
Specimen CSR
Load (kips)
Strain (Microstrain)
Yield
Yield
Level 6
@ 2.5" Above
Height of Loading
N6
Strain Gage N6

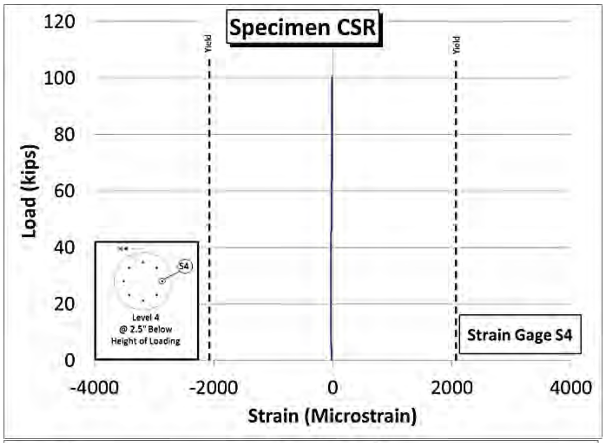
Specimen CSR
Load (kips)
Strain (Microstrain)
Yield
Strain Gage S4
Level 4
@ 2.5" Below
Height of Loading

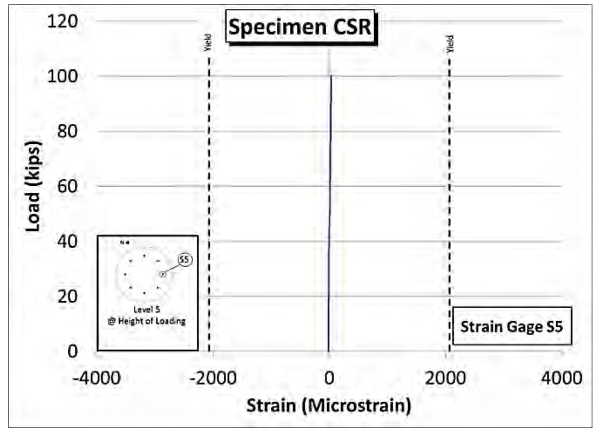
Specimen CSR
Load (kips)
Strain (Microstrain)
Yield
Strain Gage S5
Level 5
@ Height of Loading

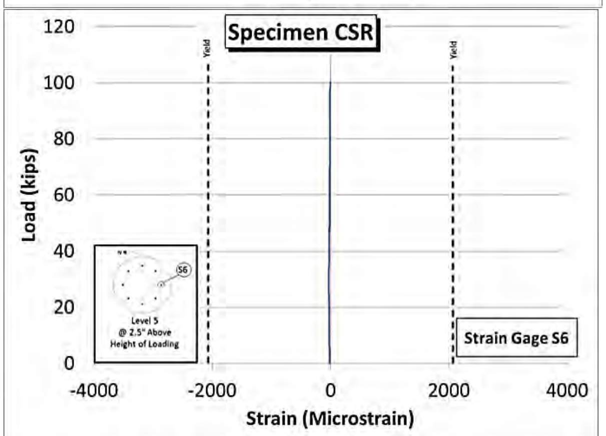
Specimen CSR
Load (kips)
Strain (Microstrain)
Yield
Strain Gage S6
Level 5
@ 2.5" Above
Height of Loading

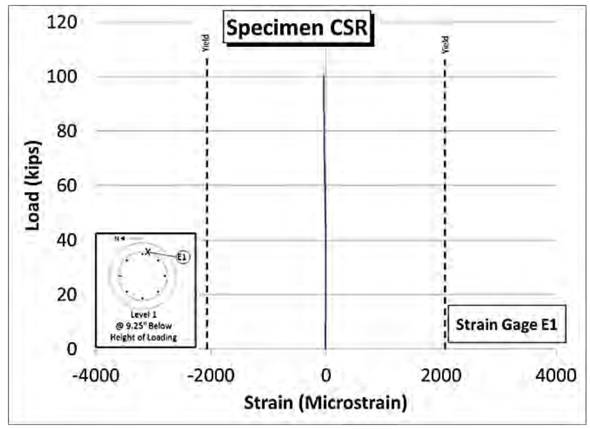
Specimen CSR
Load (kips)
Strain (Microstrain)
Yield
Strain Gage E1
Level 1
@ 9.25" Below
Height of Loading

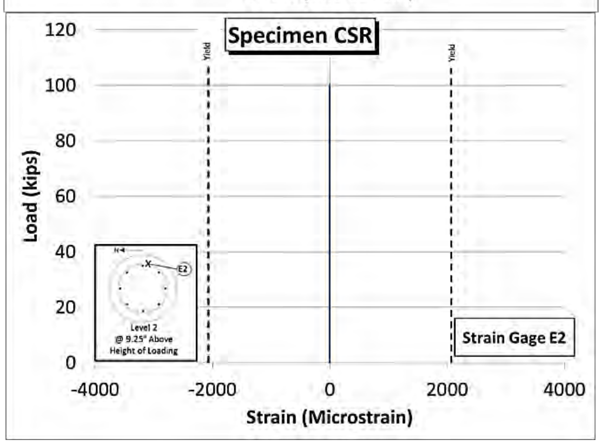
Specimen CSR
Load (kips)
Strain (Microstrain)
Yield
Strain Gage E2
Level 2
@ 9.25" Above
Height of Loading

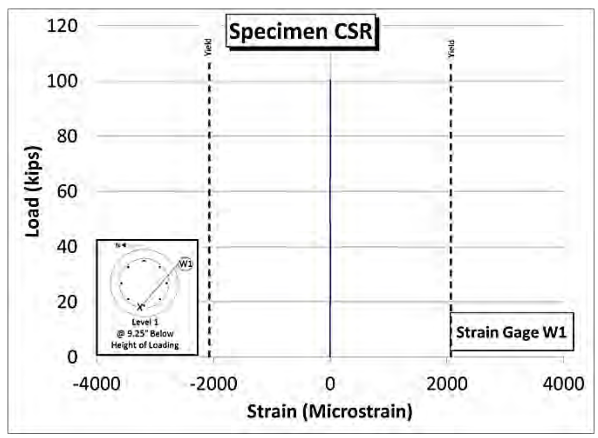
Specimen CSR
Load (kips)
Strain (Microstrain)
Yield
Strain Gage W1
Level 1
@ 9.25" Below
Height of Loading

APPENDIX I: STATISTICAL SOFTWARE CODE

I.1: R Code for Inverse Distance Weighting

```
# Before starting, we need to have both the gstat package loaded
library(gstat)
library(lattice)
library(sp)
library(RColorBrewer)

# Read in two datasets - the sample points and the prediction grid
# These are two gstat sample datasets that can be accessed by typing data(meuse)
# and data(meuse.grid). Here, we read them from text files as an example
weather1 <- read.csv("C:\\Users\\zhao.shen\\Desktop\\R_kriging\\weatherdatasummary.csv")
weather2 <- read.csv("C:\\Users\\zhao.shen\\Desktop\\R_kriging\\NORMALWEATHER.csv")
left <- read.csv("C:\\Users\\zhao.shen\\Desktop\\R_kriging\\0408left.csv")
class(weather1)
names(weather1)

# Make the data frame into a spatial data object for use with gstat
coordinates(weather1) <- c("X", "Y")
class(weather1)
summary(weather1)

#######################
# Spatial Interpolation
#######################

# Examine the prediction grid
class(left)
names(left)
coordinates(left) <- c("X", "Y")
class(left)
summary(left)

############################
# Inverse distance weighting
############################

idw_pow = seq(0.2,2, by = 0.2) # the idwpower values that will be checked
cv_vals = sapply(idw_pow, do_cv) # calculate the rmse
# List of outcomes
print(data.frame(idp = idw_pow, cv_rmse = cv_vals))

# Generate inverse distance weighting prediction for k=0.8
# Call the idw function and specify the idp parameter
predict.idw1 <- idw(rainfall ~ 1, locations=weather1, newdata=left, idp=0.8)

predict.idw1$var1.pred
pre<-data.frame(predict.idw1$var1.pred)
write.csv(pre,"preidwrain.csv")
```

I.2: SAS Codes for Negative Binomial Model

```
proc import out=data
datafile='C:\data.csv'
DBMS=CSV REPLACE;
GETNAMES=YES;
run;
proc genmod data=data;
class LANES LW SUR_TY SH_TY RS;
model crash = TRUCK_ADT SUR_TY RS H_curve SNOWFALL
/ dist=nb link=log offset=SH_LENG;
run;
```